University of Leicester

CJ0700 IS A REMOTE CHEZ ORTHOLOGUE INVOLVED IN *CAMPYLOBACTER JEJUNI* CHEMOTAXIS SIGNAL TRANSDUCTION

Thesis submitted for the degree of

Doctor of Philosophy

At the University of Leicester

By

Abdullahi Said Jama, MSc, BSc.

Department of Genetics

University of Leicester

Leicester, UK

September 2014

Supervised by Professor Julian Ketley

ABSTRACT

The major food borne pathogen *Campylobacter jejuni* utilizes chemotaxis to colonise the chicken gastrointestinal tract. Similar to the *Escherichia coli* chemotaxis system, *C. jejuni* produces a CheA-CheW-CheY backbone that transduces signals from surface chemoreceptors to direct flagellar rotational direction. In contrast to *E. coli*, *C. jejuni* also expresses CheV and CheA has a response regulator domain. The phosphorylation level of CheY in *E. coli* is modulated by the phosphatase CheZ, however until recently *C. jejuni* was thought to lack a CheZ homologue. The Hp0170 protein of *Helicobacter pylori* was shown to be a CheZ remote homologue. As *C. jejuni* Cj0700 has homology with HP0170, it was postulated that Cj0700 acts as a CheZ orthologue in campylobacters. The aim of this project was to characterise the role of Cj0700 in *C. jejuni* chemotaxis and demonstrate the phosphatase activity of the protein on *C. jejuni* CheY, CheV and the response regulator domain of CheA (CheA-RR).

A mutant (Δ*cj0700)* and the cognate complement (Δ*cj0700, Cj0046::cj0700*) were constructed in *C. jejuni* NCTC 11168. No growth differences were seen between Δ*cj0700, ΔcheY* and wild-type. On semi-solid agar the Δ*cj0700* mutant strain showed reduced motility relative to the wild-type and this phenotype was reversed in the complemented strain. The effect of a mutation in *cj0700* was also demonstrated in *C. jejuni* strains 81-176 and 81116. Cj0700 was expressed as a His-tagged protein and was found to dephosphorylate *C. jejuni* CheY protein. Expressed Cj0700 also dephosphorylated CheA-RR-P and CheV-P, but less efficiently than CheY-P. The ability of Cj0700 to interact with CheY, CheA-RR and CheV was investigated using an *in vitro* pull down assay and also in a two hybrid system in *E. coli*. Using these approaches Cj0700 was shown to interact with CheY, CheA-RR and CheV, with the strength of interaction correlating with the observed cognate phosphatase activity. Although attempts to crystallise Cj0700 were not successful, a combination of

bioinformatics, CD and NMR approaches indicated that expressed Cj0700 contains significant levels of disorder.

These findings indicate that *cj0700* has a role in *C. jejuni* chemotaxis and shows that Cj0700 can promote dephosphorylation of CheY and hence is likely to be a CheZ orthologue. Furthermore, Cj0700 also modulates the phosphorylation level of the response regulator domain on CheA and may also affect the related domain in CheV.

ACKNOWLEDGEMENTS

First of all, all praise and glory to be Allah, the Lord of the Worlds, prayer and peace be upon His messenger. Also, I would like to thank my supervisor Professor Julian Ketley for his help with the project and for his endless encouragement and support. In addition, I would like to thank the members of my thesis committee, Dr Bayliss and Dr Morrissey for their helpful suggestions. Likewise, I would like to thank Department of Biochemistry, University of Leicester for their collaboration, specially to Peter Moody's Research group, who helped me the cristallisation and NMR spectrometer of Cj0700 protein and Dr. Renshaw who helped me using CD spectrometer of Cj0700 protein. I would like to thank Dr Haigh for his advice and support and also I wish to thank my colleagues in lab 121 for their team work and their support. Finally I would like to thank my family for their support and encouragement so that I could complete this project.

TABLE OF CONTENTS

LIST OF FIGURES

LIST OF TABLES

ABBREVIATIONS

Aer	Redox potential
AspA	Aspartate-glutamate aminotransferase
bp	Base pair
BSA	Bovine Serum Albumin,
BTCS	Bacterial two component system
BTH/B2H	Bacterial two hybrid
CapA	*Campylobacter* adhesion protein A
CJIE1	*Campylobacter jejuni-integrated elements*
CCW	Counter-clockwise
CDS	Cytolethal distending toxin
CIA	*C. jejuni* invasion antigens
CW	Clockwise
CPS	Capsular polysaccharide
DTT	Dithiothreitol
Fn	Fibronectin
FlpA	Fibronection-like protein
FSA	Food safety agency
GBS	Guillain-Barré syndrome
GlpT	Glycerol-3-phosphate transporter system
GST	Glutathione-S-transferase
HAP	Hard-agar plug
HK	Histidine kinase
IPTG	Isopropyl-β-D-thiogalactopyranoside,
KatA	Hydrogen peroxide and catalase
LOS	Lipooligosaccharide
MCP	Methyl accepting protein
NCTC	National collection of type cultures
OD	Optical density
PBS	Phosphate buffer saline
T**ap**	Dipeptides
Rg	Ribose/galactose
RR	Response regulator
SDS-PAGE	Sodium dodecyl sulphate- Polyacrylamide gel Electrophoresis
SdaA	Serine dehydrogenase
Tar	Aspartate

TCS	Two component system
TEV	Tobacco Etch Virus
TEMED	N,N,N‘,N‘ tetramethylethylenediamine,
Tlp	Transducer-Like proteins
Tsr	Serine
T3SS	Type 3 secretion system
VAIN	Variable atmosphere incubator

Chapter 1 : Introduction

1. Overview

In terms of morphology, under the microscope *Campylobacter jejuni* is a slender (about 1.5-6.0 µm long and 0.2-0.5 µm wide), Gram-negative rod spirally curved with narrowing ends. In addition, the cell has a polar flagellum at one or both ends of the cell which, combined with the spirally curved morphology, provides the cell a high degree of screw-like darting motility. *C. jejuni* grows in micro-aerobic conditions, where O_2 and CO_2 concentrations are required at 3-15% and 3-5% respectively, and grows at an optimum temperature of 42 $^{\circ}$C. These may well reflect that *C. jejuni* has evolved to grow in the conditions found in the guts of warm-blooded animals and birds (Park, 2002, Ketley, 1997). *Campylobacter* spp are considered one of the major causes of human gastroenteritis in the world, where 400-500 million cases have been reported in each year (Fouts et al., 2005). In the UK alone, the Food Standard Agency (FSA) has estimated that each year more than 371,000 *Campylobacter* cases occur in which around 100 people died. Hence *Campylobacter* is considered economically significant due to the important impact on public health. *Campylobacter* is composed of 16 or 17 species, where *C. jejuni* and *C. coli* have mainly been associated with human illness (Fouts et al., 2005, Claudia Matz, 2002, Poly and Guerry, 2008). *C. jejuni* is a commensal of birds and animals such as poultry and cattle respectively. However, the mechanisms by which *C. jejuni* causes disease are not yet known. Nevertheless, certain studies have associated motility, chemotaxis, toxin production and other surface determinants as virulence factors that play a role in the pathogenicity of *C. jejuni* (Hofreuter et al., 2006, Galindo et al., 2001, Young et al., 2007).

1.1. Historical perspective of *Campylobacter*

Campylobacter has probably been a pathogen for centuries; however it was not until 1886 that Escherich for the first time reported the observation of a spiral bacterium under the microscope from stools of children with diarrhoea, referring to it as 'cholera infantum'(Butzler, 2004, Altekruse et al., 1999). Escherich made an effort to culture this bacterium on solid media, but he failed in that attempt. Interestingly, regardless of the increased incidence of this spiral shaped bacteria in diarrhoeal cases he thought this bacterium had no role in causing disease. Unfortunately, because the report was in the German language this finding was not recognised for many years, until Kist highlighted this article in 1985 at the International *Campylobacter* conference in Ottawa (Butzler, 2004).

For more than 40 years, veterinarians considered *Campylobacter* as a veterinary disease. In 1909 McFaydean and Stockman frequently isolated unknown bacteria from the foetal tissue of aborted sheep, but they considered them a *Vibrio*-like organism (Butzler, 2004). In 1919 in the USA, Smith isolated a spiral bacterium from aborted bovines and knew this bacterium was similar to what McFaydean and Stockman isolated (Butzler, 2004). Later, Smith together with Taylor proposed it as *Vibrio fetus* (Butzler, 2004). In 1931, Jones characterised a bacterium from calves with 'winter dysentery' and referred to this as *Vibrio jejuni* (Butzler, 2004). In 1949, Stegenga and Terpstra showed a pathogenic role for *Vibrio fetus* in cows (Butzler, 2004).

The first human infection was reported in 1947; Vinzent and colleagues isolated *V. fetus* from blood from three pregnant women hospitalised with unknown fever (Butzler, 2004). After four weeks in the hospital two of them aborted and an examination showed a large portion of necrotic tissue and inflammation in the placenta. Even before this report, in 1931 in Illinois there was a reported diarrhoea outbreak in inmates having contaminated milk with *V. fetus*. However, faecal culture examination was negative, whereas microscopic analysis of the stool

demonstrated *V.fetus* (Skirrow, 1977). This has been considered to be the first documented *Campylobacter* incidence in human history. In 1957, King observed similar characteristics as Vinzent described, but found out that this organism grew optimally at a higher temperature and hence she described it provisionally as a 'related *Vibrio'* (Butzler, 2004). In 1963, Sebald and Véron described a microaerophilic *Vibrio*. Later Sebald and Véron studied King's findings and renamed it *Campylobacter*, but they couldn't culture it, because they lacked a selective technique. In 1972, Butzler, a clinical microbiologist in Belguim, developed a selective culture technique (Altekruse et al., 1999, Skirrow, 1977, Butzler, 2004). Finally, in mid-1980, *Campylobacter jejuni* was identified and is now considered a major worldwide human pathogen (Butzler, 2004).

Escherich, King and Butzler have made contributions of finding this economically important bacterium, where Escherich is the first person who described it as a spiral shape. King believed the incidence of this bacterium was not as rare as reported, thus she was keen to find a method to culture the bacterium from the stool, but unfortunately this method was not developed in her time. Butzler developed a selective technique, because before that the culturing of *Campylobacter* filtered from faeces was masked by the coliforms. In this new method, the stool suspension was passed through a filter with a pore size of 0.65 µm, which allowed the passage of *Campylobacter* and retention of other bacteria on the filter, and then the filtrate was cultured on selective media. The other most important finding in *Campylobacter* era was the susceptibility of *C. jejuni* to erythromycin, which was used to demonstrate disappearance of infection in all treated patients (Butzler, 2004). In the 10 years from 1963 to 1972 there were fewer reports of *Campylobacter* incidence in comparison to the following decades; the reason could be explained that diagnosis was based on isolation from blood samples and also a selective method for *Campylobacter* isolation was lacking.

Arguably, veterinarians considered the *Vibrio* like organism (*Campylobacter*) as pathogenic to cows and sheep, given that infected animals aborted. Similarly, it was considered infective to humans where pregnant women contracting the bacterium also risked abortion. Nowadays *Campylobacter* cases in sheep and cows are still reported and yet *Campylobacter* is a burden to the economy and public health. Given that the incidence and impact of *C. jejuni* diarrhoea remains high then it is important to derive an understanding of how it colonises and causes disease in the host in order to reduce incidence and treat the infection.

1.2. Metabolism and physiology

C. jejuni lacks many pathways which other bacteria employ for nutrient metabolism such as glycolysis, Entner-Doudoroff and pentose phosphate pathways (Stahl et al., 2011). With the genomic sequences of many *C. jejuni* having been determined and many more likely in the future, the physiological and metabolic properties of the organism are beginning to be understood, however there remains the need to more fully investigate this area (Kelly, 2001). In particular, investigation is needed on how the bacteria thrive in the gut and acquire and metabolize vital nutrients because this may influence host colonization. Studies show that *C. jejuni* is metabolically flexible and complex, and as it efficiently uses citric acid cycle intermediates the organism can survive in different hosts and different environmental niches such as water (Stahl et al., 2012, Kelly, 2001). Primarily, *C. jejuni* grows in the guts of birds and human hosts under microaerobic conditions, hence for respiration *C. jejuni* utilises alternative electron acceptors such as fumarate and nitrate (Guccione et al., 2008). In addition to this, *C. jejuni* uses oxygen as the terminal electron acceptor (Sellars et al., 2002). It is possible *C. jejuni* switches between aerobic and anaerobic metabolic systems by regulating key enzymes involved in respiration whereas *E. coli* represses these enzymes (Mendz et al., 1997). It has been suggested that *C. jejuni* utilises only amino acids for carbon sources and

cannot import sugars such as glucose, galactose and lactose in order to thrive (Sellars et al., 2002, Stahl et al., 2012) . This has been related to the lack of proper sugar transporter uptake systems and in addition the lack of several important enzymes in the glycolysis pathway (Thompson and Gaynor, 2008). However, it was suggested that *C. jejuni* may utilise glycerol-3-phosphate at the end of the glycolytic pathway as there is a glycerol-3-phosphate transporter system (GlpT) in strain 81-176 (Stahl et al., 2012). Likewise, key enzymes were identified in the non-oxidative part of the pentose phosphate pathway, however, the possibility of *C. jejuni* using this pathway for carbon and energy sources has been excluded (Stahl et al., 2012). The mechanisms for transporting small molecules such as glycerol-3-phosphate and the role of the pentose phosphate pathway in *C. jejuni* still remain unclear (Stahl et al., 2012). Interestingly, in an earlier genomic study of *C. jejuni* other carbohydrate metabolic pathways were not annotated and it was suggested to be completely asaccharalytic (Parkhill et al., 2000), whilst recently a novel L-fucose pathway (Cj0486/FucP) has been identified, which *C. jejuni* uses as a substrate for growth, but the mechanism is not yet clear (Stahl et al., 2011). In addition to this, *C. jejuni* has been suggested to utilise the fermentation by products made by other bacteria for carbon and energy sources, molecules such as acetate and lactate, have been reported to be metabolised, however the mechanism still remains to be understood (Stahl et al., 2012, Weerakoon et al., 2009).

Pyruvate is the key precursor of metabolic pathway linking carbohydrates and amino acid metabolism for respiration and anabolic pathways. As a result of that certain amino acids readily enter the citric acid cycle for metabolism (Mendz et al., 1997). Thus, in the gut *C. jejuni* obtains serine, aspartate, asparagine, and glutamate, the utilisation preference being in this order. *C. jejuni* is also considered to metabolize proline, but only when other amino acids become depleted. Preferential utilization of these amino acids has been associated as being mostly found amino acids in chicken excreta (Stahl et al., 2012). In most conditions, serine

appears to be the favoured amino acid for growth, because *C. jejuni* uses serine dehydrogenase (SdaA) to convert serine to pyruvate and ammonia; also a *sdaA* mutant was deficient in colonisation of two week old chickens (Guccione et al., 2008, Stahl et al., 2012). Aspartate-glutamate aminotransferase (AspA) has been suggested to be necessary for *C. jejuni* to grow on the above mentioned amino acids (except serine) and in addition, by using mutant strains it has been shown to be essential for host colonization (Guccione et al., 2008). Both glutamate and aspartate are transported through the Peb1 uptake system. Subsequently, AspB and AspA carry out the transamination of glutamate to aspartate and aspartate into fumarate respectively (Stahl et al., 2012). It indicates that the biological of system of the *C. jejuni* is very complex and how it causes disease in the host still needs to investigate.

Iron acquisition plays an important role in the nutritional requirements of C. *jejuni* survival and growth in the host and hence this has been associated with infection (Galindo et al., 2001). Free iron availability is limited in the host because iron is sequestrated by iron specific proteins; hence *C. jejuni* has to overcome this condition to survive (Butcher and Stintzi, 2013). In iron depleted situations, *C. jejuni* has been reported to have a significant reduction in growth (Stahl et al., 2012). On the other hand, in environments with a high concentration of iron this poses risks to *C. jejuni* for survival and growth; this results from production of free radicals that could damage the cell. As a result, *C. jejuni* regulates and responds to these conditions (Butcher and Stintzi, 2013, Miller et al., 2008). Free iron in the host is not enough for *C. jejuni* to grow; therefore it scavenges iron from other iron complex systems such as haem-containing proteins, transferrin and lactoferrin and transports it into the cell. *C. jejuni* doesn't produce siderophores; however it hijacks siderophores, for example enterobactin, made by other bacteria. *C. jejuni* has been shown to express *chuABCD* and cfrA/*ceuBCDE,* for uptake and transport of haem/haemoglobin and ferric-enterobactin respectively, with the intention of growth and survival of iron restriction condition. Like *E. coli*, *C. jejuni* uses Fur

regulator for controlling interacelular ferrous ion concentration of the cell (van Vliet and Ketley, 2001, Stahl et al., 2012).

1.3. Genomics

Genomic based analyses have been carried out with the aim to have a better understanding of the pathogenicity of *C. jejuni* (Wu et al., 2013). *Campylobacter* species have been reported to have a small genome of approximately 1.6-1.7 Mbp of AT rich DNA; where GC content makes up 30% (Ketley, 1997) . The genomic sequence of NCTC 11168 confirmed *C. jejuni* to have a circular chromosome of 1,641,481 base pairs, which is expected to encode 1,654 proteins (Parkhill et al., 2000). In addition, no insertion sequences or phage-associated sequences were found in the genome of NCTC11168, however, there are short homo-polymeric repeat sequences in the genome and this has been revealed to be responsible for phase variation in *C. jejuni* (Parkhill et al., 2000, Fouts et al., 2005).

Relative to NCTC 11168, comparative genomic studies of different *C. jejuni* strains has showed a high degree of identity, however differences were identified in hypervariable regions, strain-specific regions and genomic islands (Wu et al., 2013). For instance the genome sequence of RM1221 has a conserved genome compared to NCTC 11168 except that there are four genomic islands referred to as *Campylobacter jejuni-integrated elements* (CJIE1) and *Campylobacter* Mu-like phage which encodes several proteins similar to Mu phage proteins (Parker et al., 2006). The strain specific genes were mostly involved in flagella, lipooligosaccharide (LOS) and capsular polysaccharide (CPS). These gene differences among *C. jejuni* strains may contribute to survival in host; nevertheless the survival mechanism still needs to be understood (Parker et al., 2006, Wu et al., 2013).

It has been hypothesised not all *C. jejuni* isolates are pathogenic to human. However differences in the gene content may not be the whole explanation. For instance, it was

reported that two genetically identical NCTC 11168 variants showed phenotypic difference in terms of colonization, translocation, invasion and motility. It might be difference in regulation of certain genes may contribute potential pathogenicity and adaptation of *C. jejuni* isolates. Also, may confer ability to survive in or colonise various environmental niches and hosts (Wu et al., 2013, Poly et al., 2005). Therefore the genome sequence of *C. jejuni* strain NCTC 11168 opened a new window to study proteins involved in outer membrane surface structures, glycosylation, as well as expression of contingency gene products e.g. glycosyl transferase and restriction enzymes (Fouts et al., 2005), however, in spite of that the pathophysiology of *Campylobacter* species still remains poorly understood (Fouts et al., 2005).

1.4. Pathogenicity and host infection

C. jejuni is a commensal of a wide range of animals and birds, for instance, the organism primarily asymptomatically colonizes the caeca and the intestine of chicken, because the microaerobic conditions and the 42 $^{\circ}$C host body temperature support the organism's continuous replication (Dasti et al., 2010, Ketley, 1997, Stef et al., 2013). In humans, symptoms of *C. jejuni* infections may vary from watery diarrhoea to dysentery and are accompanied occasionally with fever and often by abdominal pain (Poly and Guerry, 2008). *C. jejuni* infection may be transmitted via ingestion of undercooked poultry meat contaminated during slaughtering, drinking contaminated water or milk (Ketley, 1997). Most infections are self-limiting even without medication, however post-infection complications such as Guillain-Barré syndrome (GBS), which affects peripheral and facial nerves and results in paralysis, can lead to serious complications or death (Zilbauer et al., 2008). This complication has been linked with the expression of *C. jejuni* ganglioside like LOS that mimic human neuronal ganglioside; hence complement fixing antibodies against the outer

core of LOS can cross-react with host ganglioside in the peripheral nerves (Poly and Guerry, 2008, Nachamkin et al., 2002, Young et al., 2007). This nerve damaging syndrome results from an immunological response and is now clinically recognised for its importance (Winer, 2014).

Infective dose of *C. jejuni* has been estimated by using the observation that ingesting as little as 5-800 bacteria may manifest prodromal symptoms (Ketley, 1997). *C. jejuni* successfully colonise the mucus lining in the gut and finally adheres to epithelial cells; the colon is the target niche for colonisation. *C. jejuni* has been suggested to employ motility, chemotaxis and adhesins, but the relative significance of these to disease remains unclear (Poly and Guerry, 2008, Stef et al., 2013, Neal-McKinney and Konkel, 2012). Using an animal model, motility and chemotaxis were considered as important factors to successfully breach the mucus barrier and reach the colonization site (Poly and Guerry, 2008, Rubinchik et al., 2012). However, *C. jejuni* colonization mechanisms on epithelial cells remains hard to comprehend, as there is no type III secretion system similar to those found in other enteric pathogens which mediate epithelial cell adhesion/invasions. Studies suggest flagella mediate cell attachment and in addition the flagellar system seems to act as a type III secretion system and some proteins are secreted through it and are reported to affect invasion (Konkel et al., 2004). In any case, recent investigation has demonstrated a mechanism by which *C. jejuni* interacts with the host. Various structural proteins, glycans and glycoproteins have been suggested to contribute to host interaction; for instance, *Campylobacter* adhesion to fibronection (CadF) and fibronection-like protein (FlpA), *C. jejuni* lipoprotein A (JlpA), *Campylobacter* adhesion protein A (CapA), flagella (Rubinchik et al., 2012, Konkel et al., 2005, Flanagan et al., 2009). These components and their role in *C. jejuni* interaction with host cells will be discussed in later sections.

The colonization and invasion of *C. jejuni* in the host has been also related to the variability in length of homopolymeric G tract which may result from slipped-stand mispairing during cell replication. Expression of these genes is responsible for surface structure biosynthesis and flagellum modification is associated with phase variability of the organism (Parkhill et al., 2000). Hence, this is considered an important factor for host immune evasion, invasion of epithelial cells, virulence and chicken colonization. Furthermore, chemotaxis has been suggested undoubtedly to have a substantial role in both the commensal and pathogenic lifecycle of *C. jejuni* (Young et al., 2007).

1.4.1. Colonization

The mechanism by which *C. jejuni* colonizes the host is a multifactorial process which is poorly understood. However, *C. jejuni* encounters unfavourable in the host intestine which it must overcome to enable it to survive, grow and continue to colonize. Thus, *C. jejuni* has regulatory systems to enable it to respond to the hostile environment of the host; some of these have been studied and it was suggested that certain virulence factors are involved in host colonization (Hermans et al., 2011). For instance, morphological properties such as the spiral (corkscrew) shape and motility contribute to the ability of *C. jejuni* to penetrate the mucus layer covering the epithelial cell. In addition, the bacterium's darting movement, where straight swimming is followed by stops rather than tumbles, enables *C. jejuni* to break into the mucus barrier (Young et al., 2007). It has been demonstrated *in vitro*, that high viscosity and micro-aerobic conditions increases the motility to escape bile and immune response in the mucus; and in addition provides *C. jejuni* with the possibility to flourish for long time periods in the gut (Lee et al., 1986, Szymanski et al., 1995). Chemotaxis and motility have been considered to be primary virulence factors for *C. jejuni* to colonize the intestine, indeed chemotactic and motility mutant strains of *C. jejuni* are severely

compromised in colonization and pathogenicity (van Vliet and Ketley, 2001, Hermans et al., 2011). Likewise, sugar structures on the surface of the *C. jejuni* such as mannose/or N-acetylneuraminic acid have been suggested to establish binding on epithelial cells (Day et al., 2009). Similarly, the flagellum aids physical adherence (adhesin) to the epithelial cell; and results indicate that, flagella mutants have reduced adherence and invasion of epithelial cells (van Vliet and Ketley, 2001, Rubinchik et al., 2012). Nevertheless, it may be the reason that *C. jejuni* establishes colonization in the human intestine its ability to acquire essential nutrients for survival and growth is combined with the ability to avoid being washed away. Hence colonization contributes to bacterial pathogenesis in the host.

1.4.2. Virulence factors

The mechanism of *C. jejuni* pathogenicity is complex and multifactorial something which is yet to be understood. Regardless of that, potential virulence factors that are involved in the pathogenicity of *C. jejuni* have been reported, including adhesins attached to the host cell, motility (flagella), chemotaxis, and toxin production (van Vliet and Ketley, 2001, Konkel et al., 2005).

1.4.2.1. *Attachment*

Like other bacteria *C. jejuni* can synthesise surface macromolecules by which the organism can bind to a wide range of the host's intestinal epithelial surface. Surface exposed proteins, such as CadF, FlpA, CapA, and JlpA, have been identified to mediate *C. jejuni*-host cell interaction and have been suggested to be essential for attachment, colonization and disease progression (Day et al., 2012, Konkel et al., 2005, Konkel et al., 2010). In addition it is suggested that these surface proteins play a crucial role in *C. jejuni* virulence by binding to the extracellular matrix of the host cell (Konkel et al., 2010) and are also understood to be involved in the onset of autoimmune neuropathies (Day et al., 2012). The expression by C.

jejuni of proteins binding to specific host ligands promotes a physical interaction in order to prevent it's clearance from the intestine by flushing and peristalsis (Konkel et al., 2005). For instance CadF protein was suggested to assist *C. jejuni* binding to Fn (fibronectin) on the host epithelium. *cadF* mutants showed a 50% reduction in adhesion to human cells relative to the wild-type (Konkel et al., 2005, Rubinchik et al., 2012). Also, CapA is considered to be involved in *C. jejuni* attachment to host cells; it is defined as a contingency gene, where production of a functional protein depends on frameshifts within a homopolymeric tract found in the *capA* coding site (Konkel et al., 2005, Flanagan et al., 2009). Results have shown that *capA* mutants showed a reduction in attachment to human cells and in colonization of chickens (Konkel et al., 2005).

Some *C. jejuni* strains such as TGH9011 were reported to use JlpA to facilitate adherence to epithelial host cells; it has been confirmed as an adhesin, a *jlpA* mutant showed reduction in adherence to host cells (Backert and Hofreuter, 2013). In contrast, a *jlpA* mutant of strain F38011 didn't affect adherence to human cells or colonization of chicken (Backert and Hofreuter, 2013). It has been suggested that this is due to the cell type and strain and in addition to the fact that cells express a receptor for JlpA which may enable the strain to adhere specifically (Konkel et al., 2005, Flanagan et al., 2009). Expressing such surface proteins maybe important for *C. jejuni* host cell interaction, colonization and disease progression, because such interactions might prevent loss of the organism by flushing and peristalsis forces in the intestine.

The presence of sugar residues on the outer-membrane of *C. jejuni* such as in the LOS is regarded as an important virulence factor for adhesion and colonization on epithelial cells (Louwen et al., 2008). *C. jejuni* strains produce LOS with variable structures and thus such variation produces diverse antigenic epitopes on the surface of *C. jejuni* which may enable it to evade the host immune response (Muller et al., 2007, Parkhill et al., 2000). In addition, *C.*

jejuni strains are suggested to harbour genes involved in sialic acid biosynthesis and therefore produce sialylated LOS; these strains were found to bind epithelial cells better than non-sialylated LOS isolates (Louwen et al., 2008, Louwen et al., 2012). Therefore, it has been postulated that *C. jejuni* makes sialylated LOS for enhanced adherence and translocation across the epithelial cell layer (Javed et al., 2012). LOS mutant strains showed significant reduction in translocation relative to the wild-type or complemented mutants (Javed et al., 2012, Louwen et al., 2012, Louwen et al., 2008). Production of outer-membrane structures similar in structure to host molecules is an example of molecular mimicry and may be involved in avoidance of the host immune response.

1.4.2.2. *Toxin production*

Soon after the *C .jejuni* breaks through the mucus barrier and adheres to the epithelial cell surface of the host, *C. jejuni* was postulated to produce toxins that can lead to cell death. It was suggested that *C. jejuni* produces either enterotoxin or cytotoxin or both (van Vliet and Ketley, 2001). However, in the later studies, only cytolethal distending toxin (CDS) has been confirmed genetically in *C. jejuni* (Young et al., 2007). This toxin is produced by a number of Gram negative bacteria such as *E. coli* and *Salmonella*. CDT prevents the host cell entering the mitotic holding phase at G2/M and then increases cell apoptosis (Wassenaar, 1997, Dasti et al., 2010, Zilbauer et al., 2008). CDT was identified to comprise three subunits, CdtA, B and C, expressed by the three adjacent and overlapping *cdtABC* genes wherein only CdtB is the active subunit and has with homology DNaseI of eukaryotic cells. In order to be functionally active, CdtB must be delivered to the nuclear compartment. The CdtAC subunit's activity is unclear, however it was suggested to promote translocation into the nucleus (Zilbauer et al., 2008, Young et al., 2007). Nevertheless, CDT production is

something *C. jejuni* is considered to employ for colonization and in addition for immune evasion which seems to contribute pathogenicity.

1.4.2.3. *Environmental factors*

The hostile response for *C. jejuni* in the host is complex and the organism must be able to tolerate and respond to unfavourable conditions of the host intestine with extremes of pH and with limited nutrient (Jackson et al., 2009). In addition to that there are variable temperatures such as the avian gut at 42 °C, the human intestine at 37 °C, the temperatures encountered in faeces in the environment and 4 °C in food storage. Given that *C. jejuni* has established defence systems against oxidation, starvation, heat shock and osmotic pressures. It has been demonstrated that *C. jejuni* expresses a peroxidase dismutase (Jackson et al., 2009) protein under oxidative environment so that superoxide radicals can be removed by converting them into hydrogen peroxide and catalase (KatA) next converts this into water and oxygen. With these, *C. jejuni* survives the oxidative environment it is exposed to in the host. The *katA* mutants demonstrated significant reduction of survival and colonization in the host (van Vliet and Ketley, 2001, Jackson et al., 2009). Also, under nutrient starvation, pH, and temperature extremes, for instance, *C. jejuni* morphologically changes from a spiral form to coccoid in which it has been suggested to maintain a viable, non-culturable state (Jackson et al., 2009, Kumar-Phillips et al., 2013). Upon shifting temperature, for instance from optimum (42 °C) in the avian gut to human intestine (37 °C) or in food storage (4 °C), *C. jejuni* has been shown to synthesise a multipurpose heat-shock protein (HtrA), whose up-regulation means *C. jejuni* can degrade misfolded proteins and prevent from the aggregating and misfolding (Bui et al., 2012). Likewise, DnaJ chaperone protein plays an important role in thermo-tolerance in *C. jejuni* during chicken colonization and *dnaJ* is up-regulated in temperature adverse conditions. A *dnaJ* mutant was shown to be unable to colonize chickens (van Vliet and

Ketley, 2001, Brondsted et al., 2005, Poli et al., 2012, Garenaux et al., 2008, Bui et al., 2012). Taken together, *C. jejuni* up-regulates and down regulates necessary and unnecessary genes in order to survive extreme conditions such as in water and milk or on later ingestion into a potential host. Equally, in the extremes of the host's intestine, *C. jejuni* survives by employing most likely many regulatory systems that play an important role in survival and colonization in human and in chicken intestine and thus may contribute to persistence and pathogenicity.

1.5. Motility

In bacteria, motility can be characterized into flagellum-dependent and flagellum independent motility (Lux and Shi, 2004), wherein flagellum dependent bacteria swim in liquid and swim on environmental surfaces. Other bacteria which are flagellum-independent employ gliding or twitching motility while moving on these surfaces. This latter type has been suggested to utilize type-IV pili by which they bind to the surface then pull the cells forward (Wadhams and Armitage, 2004). Other bacteria use sliding (spreading) motility which can be observed in sheets of bacteria moving as one unit in different directions. Taken together, all of the above mentioned types of motility are used by bacterial surface colonization (Harshey, 2003). In *C. jejuni*, one study showed that motility is a prerequisite for colonization and is required for infection (Zilbauer et al., 2008), while others (Butler and Camilli, 2004) argue that motility might not be necessary for infection. However, motility and chemotaxis are believed to guide bacteria into their preferred colonization site (Butler and Camilli, 2004). The flagellar system is linked with chemotaxis so bacteria can navigate along certain chemical gradients and is correlated with the swimming and swarming modes of motility (Harshey, 2003). The movement of motile bacteria is also determined by the thickness and thinness of surface in regard to viscosity. In other words, in an aqueous environment motile bacteria

swims, whereas with a low fluidity surface, motile and swimming bacteria such as *Proteus mirabilis* become elongated, hyperflagellated and then move in a coordinated manner using a process known as swarming (Ottemann and Miller, 1997, Rashid and Kornberg, 2000).

Campylobacter motility is characterised by a rapid and darting movement which is facilitated by polar flagella. With this mode of movement *C. jejuni* penetrate the mucus layer coating epithelial cells (Baserisalehi and Bahador, 2011, Guerry, 2007). Although these events remain to be understood, motility has undoubtedly been shown to be important in disease initiation (Fahmy et al., 2012), as previous studies indicated that motility plays a pivotal role in intestinal colonization and invasion in epithelial cells (Poly and Guerry, 2008). Hence, together, motility and flagella of *C. jejuni* have been associated with the virulence factors the organism uses for adherence and colonization

1.5.1. Swimming

Swimming and swarming modes of movement are restricted to flagellated bacteria. Straight swimming is the result of the concerted action of a bundle of flagella in bacteria such as *E. coli*, which push the bacterium toward an attractant. Thus, in order to swim, the flagella are rotated in an anticlockwise direction. Unlike swarming, swimming is a mode of action of a motile individual bacterium (Harshey, 2003, Samatey et al., 2001) and is determined by when an organism is in an aqueous environment especially in a conditions where surface friction and viscosity is low (Rashid and Kornberg, 2000).

For example, *E. coli* and *Salmonella* have a swimming pattern of alternating run and tumble modes, where in the running mode the flagella is rotated counter-clockwise, and as result of that, flagella become bundled and the cell is able to propel itself forward. On the other hand, tumbling is a quick reversal of flagellar rotation to clockwise; this disaggregates flagella and generates forces that make a cell tumble and change orientation (Eisenbach *et al.* 2004). In

single polar flagellar cells such as *Vibrio*, the flagellum pushes forward or pulls backward in liquid media (Eisenbach *et al.* 2004).

1.5.2. Swarming

Swarming is defined as "an organised surface translocation which depends on extensive flagellation and cell-to-cell contact" (Burkart et al., 1998). For the single flagellated bacteria, lateral flagella are produced in addition to polar flagella on the surface media (Eisenbach *et al.* 2004). Swarming cells are morphologically hyper-flagellated and long because more flagella are needed for swarming cells, perhaps due to surface friction or higher viscosity caused by slime around the swarming cell (Burkart et al., 1998).

To compare the swarming to swimming, the rate in which organism colonize on surface via swarming is equal or often more than the rate at which a swimming cell of the same species could colonise in water filled spaces. For instance agar concentration determines the swarming behaviour of the cells, where higher an agar concentration results in an increased number of flagella than less concentrated agar media (Harshey, 2003). The optimum condition that bacteria can swarm in is considered to be in the range of 0.5%-0.7% agar concentration. However at concentrations above 1%, certain strains can swarm such as *Proteus*, *Vibrio*, *Rhodospirillum* and *Azospirillum* in 1.5%-2% concentrations. The most active swarming cells are found on the edges of the agar and the cells in the interior of the spreading colony are less active (Harshey, 2003). Studies show strains with swarming behaviour were more pathogenic and thus swarming may be related to pathogenesis (Burkart et al., 1998). Taken together, bacterial movement has an essential role of bacterial taxis, because the motor which rotates the flagella is directly linked to the bacterial signal transduction cascade, where chemotaxis receptors sense and transduce chemical gradients in the changing environment (Josenhans and Suerbaum, 2002).

Whether flagellated bacteria swim or swarm is determined by encountered environmental viscosity (Harshey, 2003). Thus, understanding bacterium movement in different environments may give insights of bacterial locomotion in the host (e.g. mucus or other niches). It also helps to understand the role chemotaxis plays in bacterial motility, wherein this signal transduction pathway regulates motility (flagella) and as result of that a bacterium is either biased toward attractant or escape from hostile environments. Therefore, a combination of motility and chemotaxis is believed to enable *C. jejuni* to establish itself in the intestine (Porter et al., 2008).

1.5.3. Flagella

Bacteria can possess a single (monotrichous) polar flagellum such as *C. jejuni* or multiple (peritrichous) flagella such as *V. cholerae* or *E. coli*. Under certain circumstances, some bacteria alternate between single and multiple flagella (Chen et al., 2011, Zhu et al., 2013). Some bacteria regulate the number of flagella, for instance, the polar flagellated *V. cholerae* freely swim in liquid with polar flagellum; however when they encounter a surface they develop peritrichous flagella which are referred to as 'lateral flagella', and supposedly alternating between polar and lateral flagella is a condition-dependent phenomenon. Lateral flagella are difficult to observe under the microscope (Zhu et al., 2013). *C. jejuni* is polar flagellated (Ketley, 1997) and has never been observed to express lateral flagella like *Vibrio.*

The basic structure of flagella, for instance in *E. coli*, consists of the basal body, hook and filament. The basic structure of flagella is conserved in bacteria (Eisenbach, 2001, Chen et al., 2011). In *E. coli* for instance the basal body consists of four rings (Figure 1.1). The M ring is made from FliF protein, whereas the C-ring is built from FliM, FliN and FliG. The P and L rings are comprised of FlgI and FlgH respectively (Eisenbach, 2001). The function of the P-L ring is to coat the rod from the outside so that proteins are secreted through it.

The flagellar motor consists of a rotor (MS and C rings) and serves as rotatory motor and a stator which is built from MotA and MotB proteins. The C-ring is flexible and carries forward the rotational force generated by the flagellar motor; in turn, the hook and filament which is structurally static acts as a helical propeller by rotating the flagellum. In addition to this, through the C-ring the necessary proteins for flagellar assembly are exported (Chen et al., 2011, Zhu et al., 2013). Flagellum spinning is regulated by the interaction between the rotor and the stator unit. The stator unit (MotA and a MotB) involves the interaction to the rotor unit. As mentioned above, the rotor unit is a flexible unit which consists of a C-ring, a MS ring and the rod which connected to the hook and filament. Structurally the stator proteins hold the rotor unit and prevent from rotation. The proton movement generates the torque of the flagellum. As proton follow through the motA/B channel, it binds to an aspartic residue of MotA/B proteins due to that conformational change of the MotA/B results to releases free the rotor unit and then flagella rotate (Morimoto and Minamino, 2014).

Many bacteria also use this hollow conduit to secrete proteins synthesised in the cytosol to the extracellular compartment (Neal-McKinney et al., 2010). Furthermore, the filament is built from FliC protein and is connected to the hook by a junction which is made from FlgK and FlgL proteins (Eisenbach, 2001).

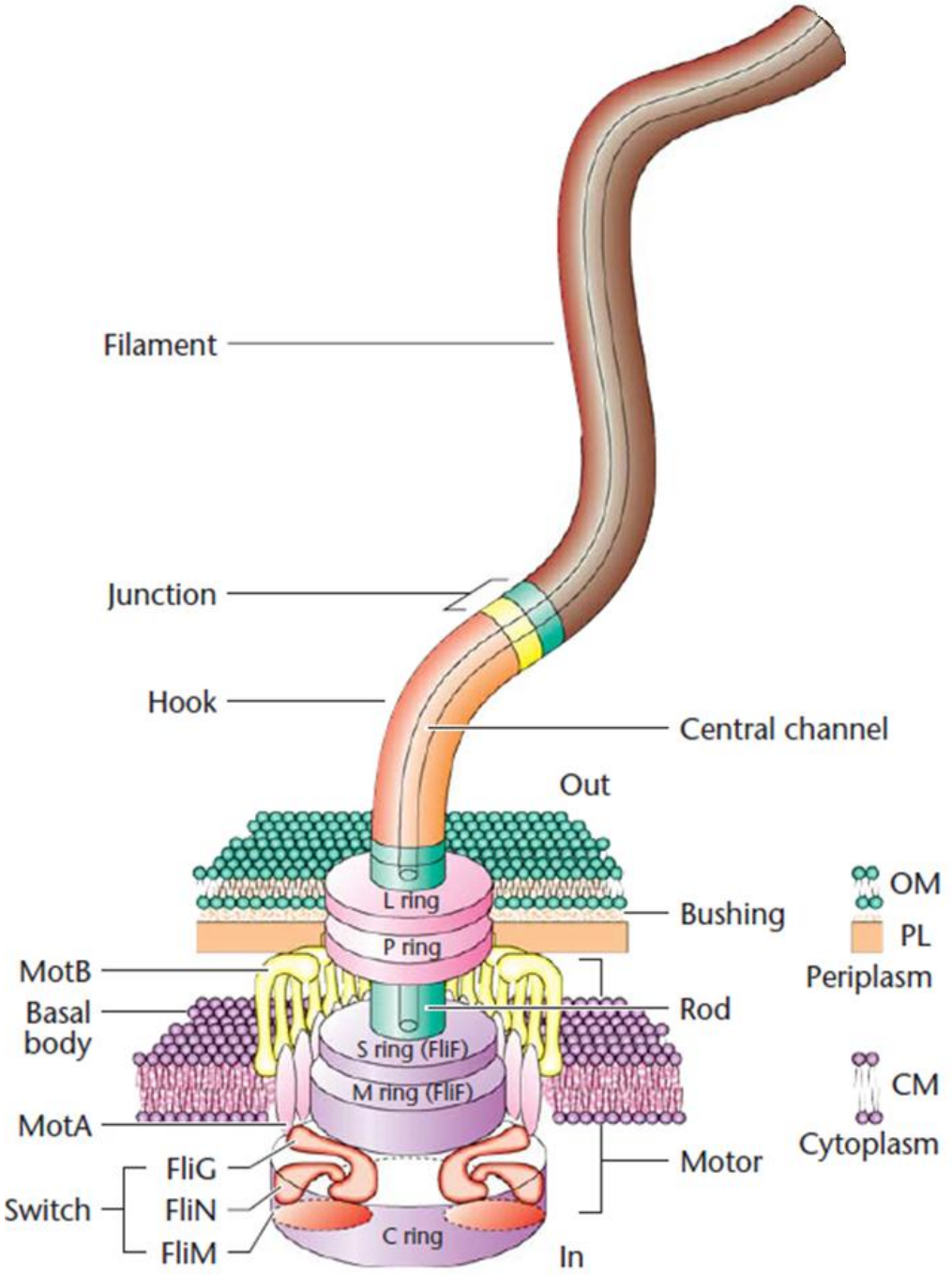

Figure 1.1. Schematic diagram of flagella structure of *E. coli*.

The **f**lagellum consists of basal body, hook and filament. The Basal body contains the C-ring (cytoplasm) with FliM and FliN proteins and is also called the switch. This is connected to the MS-ring (membrane and supramembrane respectively). P and L (peptidoglycan and lipopolysaccharide respectively) rings associate with the hook. PL (periplasm); OM (cell outermembrane). Proteins are secreted through the rod. The flagella motor consists of a motor which is made up of MS and C rings and a stator built from MotA and MotB. The hook is connected to the filament via a junction. This picture is taken from Eisenbach (2001)

In *Campylobacter*, the flagellum is reported to be involved not only in motility, which is required for colonization of mucus and invasion of epithelial cell, but also for secreting proteins that may modulate virulence, specifically invasion. The *C. jejuni* flagellar filament is comprised of the flagellin subunits, FlaA, the major subunit, and the minor subunit, FlaB, both of which are post-translationally modified by O-linked glycosylation (Harrington et al., 1997, Neal-McKinney et al., 2010, Guerry, 2007). Transcription of the two flagellins is regulated by two sigma factors, sigma^{28} (FlaA) and sigma^{54} (FlaB), but the biological basis of their differential regulation is unknown (van Putten et al., 2009). The importance of the glycosylation of flagellin has been shown as mutants demonstrated a non-motile phenotype (Guerry et al., 2006). May be the wider importance of glycosylation is not only related to bacterial motility but also glycosylation may affect the rate of flagellin protein export and changed glycosylation might result in antigenic diversity and the lack of evasion of host immune response.

A study suggested another role of the flagellum is to secrete *C. jejuni* invasion antigens (Cia), FsaA and FlaC virulence proteins in which *C. jejuni* establishes host attachment and colonization. It was also proposed that CDT is secreted through the T3SS-like flagellar apparatus (van Putten et al., 2009). As has been mentioned earlier, *C. jejuni* colonization and infection are multifactorial where, for instance, organelles like flagella function both for motility and as a secretion apparatus to transport crucial proteins or short chained molecules such as oligosaccharides for cell adherence or evasion; or there may be yet another role which has yet to be identified. Regardless of these, it seems that the flagellum of *C. jejuni* is very important for colonization and infection of the host. Clearly mutation of FlaA/or FlaB may effect colonization due to the lack of motility, but also subsequent disruption of T3SS may result that other proteins are not secreted and thus their role may be lost in colonization (Figure 1.2).

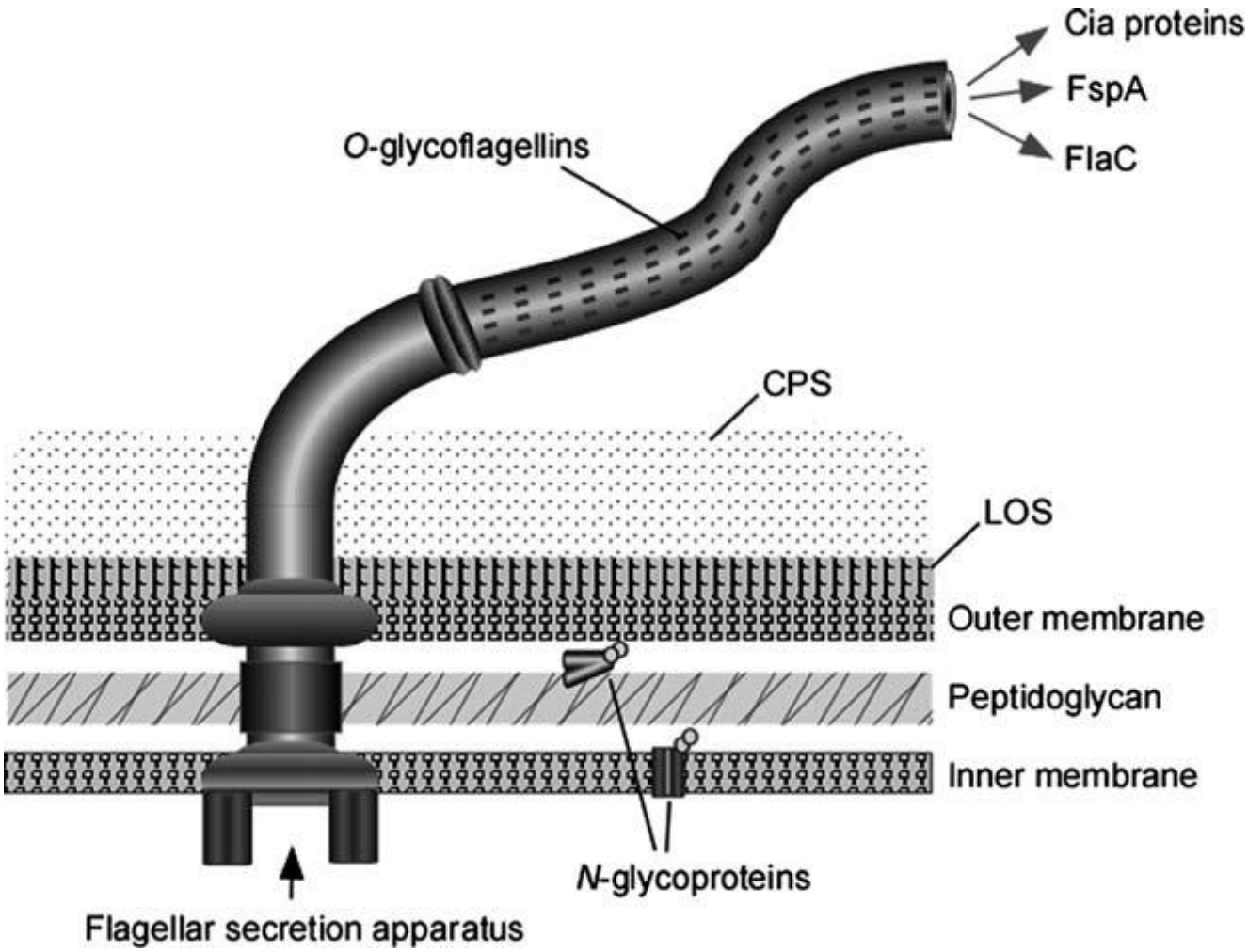

Figure 1.2. Schematic representation of secretion and glycosylation of *C. jejuni* flagellum.

Like *E. coli*, *C. jejuni* flagellum comprises basal body (MS and C-ring) attached with rod, PL ring, hook and filament. In addition, flagellin proteins (FlaA andFlaB) are O-glycosylated. The outer membrane is decorated with variable lipooligosaccharide (LOS) and polysaccharide capsule (CPS). Also, N-glycoproteins are found in the inner membrane and periplasm of the organism. In addition to flagellin proteins the flagellum also secretes FlaC, FspA and Cia proteins. This modified picture was taken from van Putten et al. (2009).

1.6. Chemotaxis

Chemotaxis is a mechanism by which bacteria rapidly and efficiently respond to changes in the chemical composition of the environment to either bias movement toward a beneficial chemical composition or escape unfavourable ones (Figure 1.4). Like motility, chemotaxis is essential for virulence in bacteria, for example, a chemotactic mutant of the medically important bacterium *Helicobacter pylori* was unable to colonize mucosa and was not able to cause gastric cancer (Porter et al., 2008).

In chemotactic bacteria environmental signals are detected in a form of ligand bound to a trans-membrane surface receptor protein and this signal is subsequently transferred to cytoplasmic components (Figure 1.3) such as histidine kinases and response regulators, which eventually modulate the direction of the flagellar motor accordingly (Bren and Eisenbach, 2000, Falke, 2002).

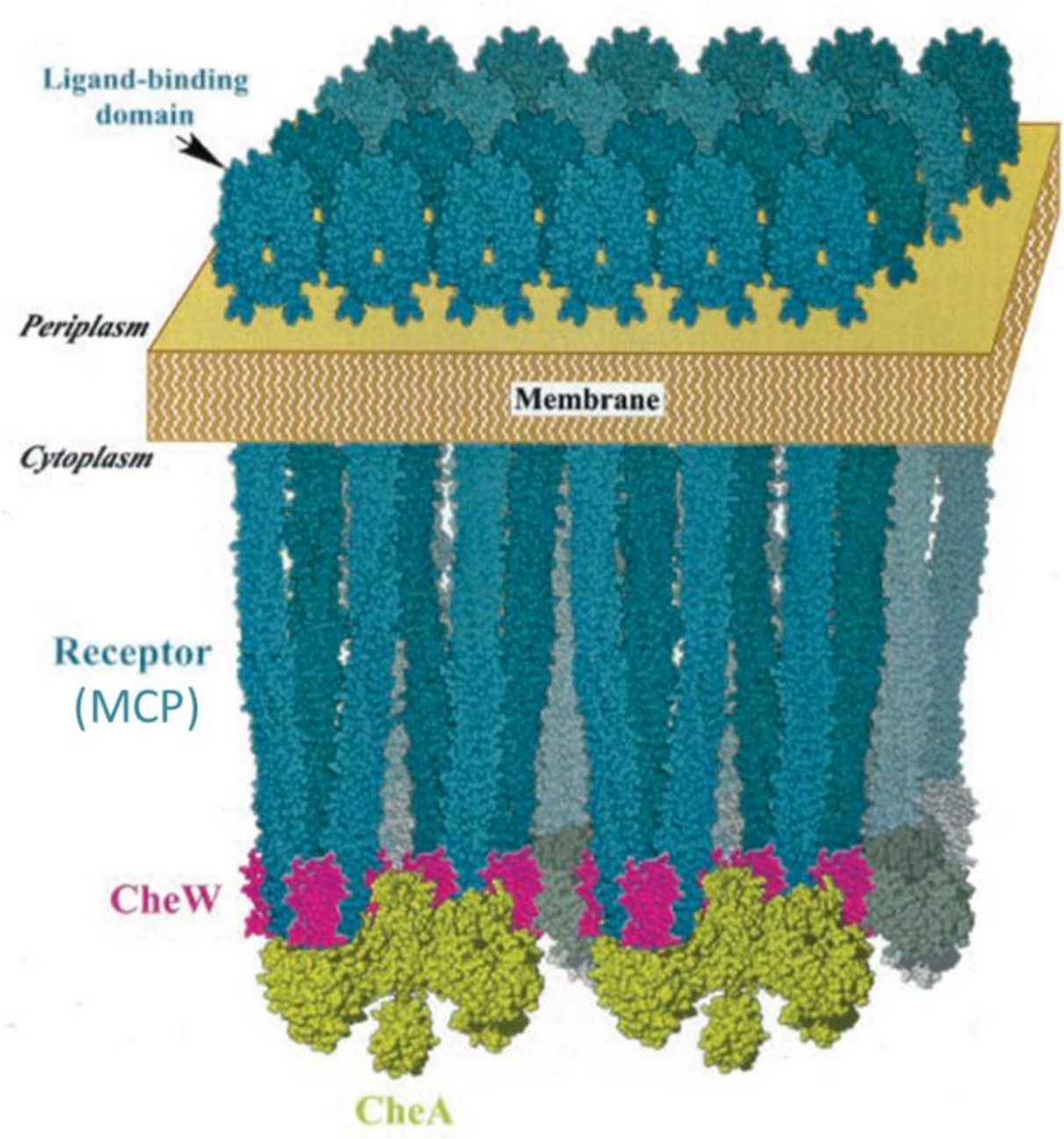

Figure 1.3. Chemotaxis sensory system depicting the location of signal cascade components in *E. coli*.
Signal is bound to receptors of the methyl accepting protein's (MCP) domain as a ligand. MCP is a transmembrane protein; the signalling parts extend to the periplasm and cytoplasm which interact with chemotactic components. This is modified picture taken from Levit et al. (2002).

1.6.1. Chemotactic walk

Depending on the number and location of flagella, bacteria show different patterns of motion. These motions include run and stop, run and reverse, and run and arc. Multi-flagellated bacteria such as *E. coli* and *Salmonella* use a run and tumble walk where, during running, flagella are packed together to efficiently propel swimming forward. Conversely as the helical rotation of flagella is changed the flagellar bundle fall apart and the cell tumbles (Vater et al., 2014). This is referred to as random walk bias as straight runs are interrupted by random changes of direction (Figure 1.4) this pattern is determined by the chemical gradient found in the surrounding environment. Therefore, chemotactic bacteria estimate changes of concentration over time for instance if concentration increases bacteria run up to the gradient, but if the chemo-attractant decreases then organism tumbles to reorient (Yi et al., 2007). With single flagellated bacteria, like *Pseudomonas aeruginosa,* they are unable to tumble, because tumbling is the result of unbundling flagella and they hence run during swimming and reverse flagellum rotation to change direction; this causes pulling forward and pushing backward movement. The frequency of switching between forward and back movement determine the organism's direction to move. Run and stop and arc motility are less well explained phenomena in bacteria (Vater et al., 2014). However, Eisenbach (2001) suggested the number of flagella and their location determines the pattern of motility, wherein polar flagellated bacteria (regardless of number of flagella) depending upon the rotation of flagella provide the organism with pull or push motility which results in movement either back or forth.

C. jejuni is characterized as polar flagellated which confers darting motility (Balaban and Hendrixson, 2011) to the bacterium which is possible depending on the flagellar rotation either to confer run and reverse bias, as in *P. aeruginosa,* or switching between run and stop motion as in *R. sphaeroides* for chemo-attractant or repellent conditions respectively

(Eisenbach, 2001). Thus, these patterns of motility that the organism establishes in a chemical environment, such as mucus in the intestine, may be important for pathogenic organisms during colonization and infection to escape away or move along a chemical gradient in the intestine.

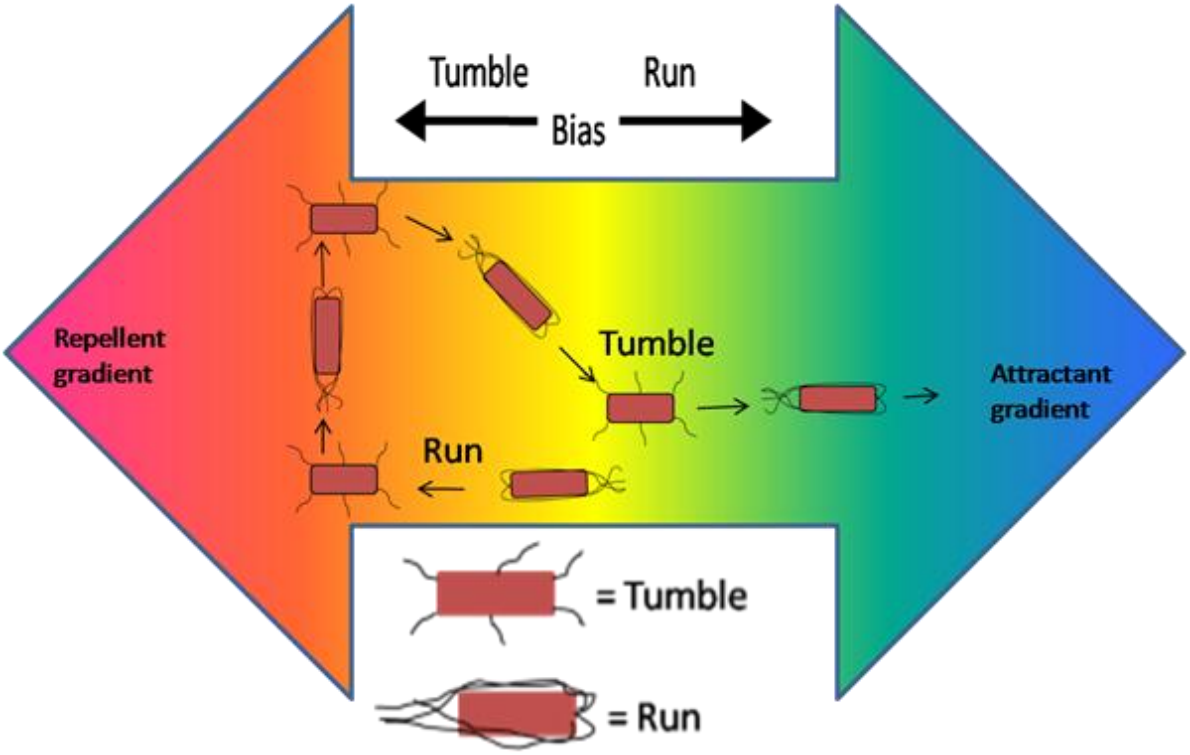

Figure 1.4. Random biased walk of *E. coli*.

When *E. coli* detects a low concentration of attractants or a high concentration of repellent, the flagella fly apart due to clockwise rotation and produce tumbling in order to change direction. Conversely, flagella are drawn together into a single bundle to propel forward for smooth swimming in clockwise rotation. The direction of the arrow indicates a decrease/increase in concentration. Red colour shows repellent. Blue colour shows attractant. This is a modified picture taken from Webre et al. (2003)

1.6.2. Two component systems

A two component system (TCS) describes a regulatory system found in bacteria, archaea and eukaryotic cells. They contain a sensing and response coupling mechanism in which the organism responds to changing chemical conditions in the surrounding environment. A typical TCS comprises a histidine kinase (HK) and a response regulator (RR). In eukaryotes, quite number of TCS has been identified, notably in *Saccharomyces cerevisiae* and *Candida albicans*, but not in animal cells (Stock et al., 2000). The bacterial two component system (BTCS) are mainly found associated with bacterial sensing and responses to environmental change (Capra and Laub, 2012) such as chemotaxis, osmoregulation, sporulation and differentiation.(Stock et al., 2000). The two central components of BTCS in chemotaxis signalling systems comprise CheA, the histidine kinase, and CheY, the RR (Kentner and Sourjik, 2006, MacKichan et al., 2004). By this central component the chemotactic bacteria can sense different environmental condition in order to survive and thrive in the best living conditions (MacKichan et al., 2004). The chemotactic bacteria using TCS, senses extracellular signals (ligands) by a transmembrane protein with a signal binding protein domain at the periplasm and a cytoplasmic domain which interacts with CheA protein (Figure 1.3). Consequently, CheA is autophosphorylated and rapidly transfers phosphate to CheY which in turn binds to the flagellar motor and promotes a change in bacterial swimming direction (Levit et al., 2002). In order to understand the structure and the function of BTCS in other bacteria, *E. coli* is used as a model (Kirby, 2009). Therefore, based on *E. coli* as a model system, the description of this and variant systems in other bacteria will be used to predict a model for *C. jejuni*.

1.6.2.1. *E. coli paradigm*

The control of the bacterial chemotaxis system is best understood in *E. coli* and *Salmonella*. These systems are considered paradigms for the bacterial chemosensory signal transduction pathway (Eisenbach, 1996). The chemotaxis proteins of the *E. coli* model consist of MCPs, CheA, CheW, CheY, CheB, CheR and CheZ proteins. Through these proteins the organism regulates its motility pattern in the environment wherein MCP receptor domains in the periplasm detects signals encountered in the surrounding environment. As the chemoreceptors bind ligand, the cyptoplasmic domain of the MCP forms a complex with CheA via the CheW protein. Subsequently, CheA uses ATP as a substrate to autophosphorylate at a histidine residue and then transfers this phosphate to CheY at an aspartate residue. In turn, the phosphorylated CheY-P binds to a motor switch FliM protein and this changes bacterial direction by rotating the flagella into clockwise (CW) rotation (Lux and Shi, 2004).

The CheB and CheR are adaptation proteins, where CheR attaches methyl groups onto the cytoplasmic part of the MCP and conversely CheB removes methyl from the cytoplasmic domain of the MCP. The CheZ protein is a phosphatase which removes phosphate from phosphorylated CheY-P (Szurmant and Ordal, 2004, Lux and Shi, 2004). *E. coli* employs these chemotaxis proteins to navigate chemical gradients in the host and therefore to establish host colonization. Other chemotactic bacteria employ similar strategies for host colonization and infection.

1.6.2.1.1. *E. coli* chemosensory receptors

There is a set of five chemosensory receptors which have been determined on the surface of *E. coli* and *Salmonella*, which are specific for different attractants and repellents, namely aspartate (Tar), serine (Tsr), ribose/galactose (Rg), redox potential (Aer), and dipeptides (Tap) (Bren and Eisenbach, 2000, Falke, 2002). Nevertheless, the levels of expression of receptors is different, for instance, the receptors for Tar and Tsr are expressed at high levels, whereas Tap, Trg and Aer are expressed in low levels. The chemoreceptors form dimers to bind a ligand, in turn, homodimers form trimers of dimers that interact with cytoplasmic components in order to transduce the signal further down (Hansen et al., 2008).

MCPs are transmembrane proteins which spatially and functionally contain periplasm (receptor), transmembrane and cytoplasmic domains (Lux and Shi, 2004). Thus, signal is transduced by the receptor from a periplasmic ligand binding domain which senses attractant/repellent from the environment. Subsequently, the signal is transferred to the cytoplasmic signalling domain and to the motor of the flagella (Figure 1.5). The periplasmic receptor domain is variable, while the cytoplasmic domain is highly conserved across species (Wang et al., 2012). This MCP receptor variability may be due to the diversity of attractants and repellents found in the environment (Baker et al., 2006). Amino acids bind directly to the MCP receptors, however, sugar and peptide binding to the receptors is facilitated by a periplasmic binding protein/substrate binding protein (Neumann et al., 2010). Hence any changes in the receptor ligand occupancy could trigger conformational changes in the signalling domain which in turn mediates phosphoryl influx to the CheA protein and then to other effector proteins of the cascade (Ames et al., 2002).

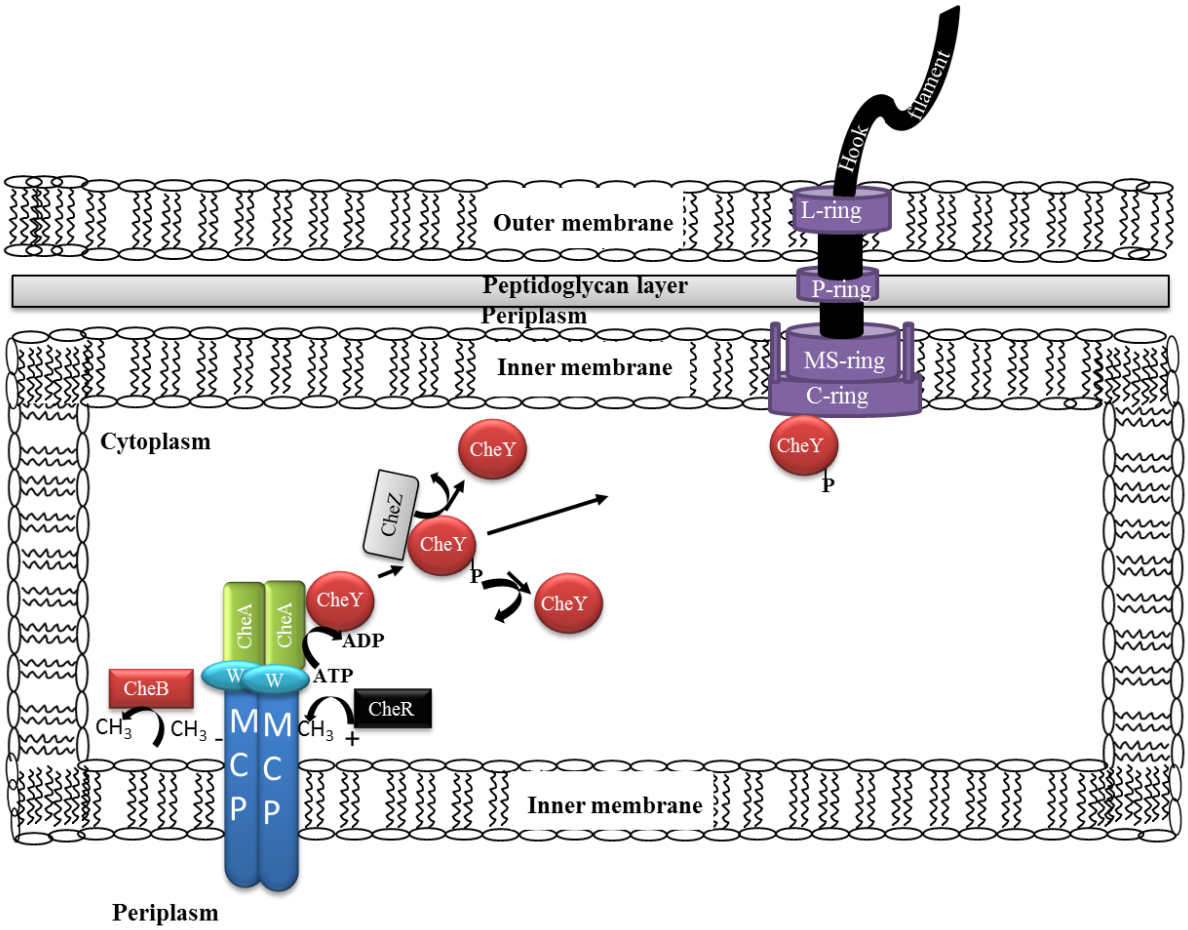

Figure 1.5. Schematic diagram of the *E. coli* chemotaxis signalling pathway.

In *E. coli*, ligands bound to receptors of MCPs activates CheA via CheW protein. In the absence of an attractant, at the periplasmic side of the MCP receptor ligand (repellent) binds then transfers signals to the cytoplasm that results in the formation of a ternary complex (MCP-CheW-CheA) and activates CheA. CheA autophosphorylates using ATP as substrate and subsequently transfers phosphate to CheY. Phosphorylated CheY binds the flagella motor at FliM and rotates the flagella clockwise (tumble) to reorient direction. CheY-P slowly autodephosphorylates, but CheZ (phosphatase) accelerates CheY-P dephosphorylation. CheB and CheR resets signalling sensitivity of the receptor. CheB removes methyl from MCP the rate of which depends on the level of CheB phosphorylation, whereas CheR adds methyl to the MCP.

1.6.2.1.2. Cytoplasmic components

In *E. coli* CheA is dimeric consisting of five domains: P1, histidine-containing phosphotransfer domain, P2, CheY and CheB binding domain, P3 dimerization domain, P4 catalytic and ATP binding domain, P5 regulatory domain. The histidine containing domain receives phosphate transferred from the ATP binding domain. CheA phosphate transfer is regulated by P5 which interacts with the chemoreceptor via CheW coupling protein. Hence this ternary (CheA, CheW and MCP) complex modulates CheA auto-phosphorylation (Wang et al., 2012).

In the presence of chemo-attractant this inhibits CheA activity which in turn significantly reduces CheY phosphorylation (Baker et al., 2006). Conversely, in the absence of chemo-repellent the cytoplasmic domain of the MCP interacts with CheA and results in auto-phosphorylation at the histidine residue (His-48), this enhances binding affinity between CheA and CheY. Soon after CheY is phosphorylated at the Asp-57 residue, there results a conformational change in CheY, which reduces binding affinity with CheA (Bren and Eisenbach, 2001, Korolik, 2008). Subsequently, CheY-P diffuses and has increased binding affinity with flagellar switch protein, FliM on the basal body (C-ring, Figure 1.1). It has been proposed that changing from a flagellar counter-clockwise rotation direction to a clockwise orientation is achieved when CheY-P occupies about 70% of the FliM protein (Bren and Eisenbach, 2001). This CheY-P-FliM complex induces multi flagellated *E. coli* to tumble, switching from one swimming direction to reorient to another direction (Bren and Eisenbach, 2001, Kirby, 2009). CheY is then dephosphorylated either spontaneously or this is accelerated by the CheZ protein. In fact, CheZ plays an essential role, not only for dephosphorylation and termination of counter-clockwise rotation, but also because it effectively accelerates signal deactivation and adaptation (Bren and Eisenbach, 2000, Lipkow, 2006).

In addition, CheA activity is indirectly regulated via CheR and CheB methylation (methyltransferase) and demethylation (methylesterase) respectively of the cytoplasmic domain of MCP. The methylation and demethylation takes place at the glutamic acid residue of MCP in the cytoplasmic domain (Porter et al., 2011) wherein CheR attaches a methyl group, which is sourced from S-adenosylmethionine, and conversely CheB removes the methyl group from the MCP (Meier et al., 2007). Increasing methylation on the MCP inhibits CheA autophosphorylation, whereas demethylation enhances the ability to increase CheA to phosphorylate CheY and CheB proteins (Baker et al., 2006). The reversible methylation and demethylation on MCPs, *E. coli* uses for adaptation; phosphorylation of CheB causes *E. coli* to return to the pre-stimulus environmental condition. Therefore, CheB and CheR proteins play an import role in the chemotaxis signalling pathway in *E. coli* (Clausznitzer et al., 2010, Yi et al., 2007) and without them the cell may regulate changing environmental signals.

In *E. coli*, there is production of two identical CheA proteins, $CheA_L$ (long) and $CheA_S$ (short) which contain 654 and 557 amino acids respectively. The two proteins are similar *per se*; however $CheA_L$ has 97 additional amino acids at its N -terminus (His-48), which includes the site of autophosphorylation. It has been demonstrated that mutation at the His-48 site of $CheA_L$ alters the chemotactic ability of the cell (Sanatinia et al., 1995). Expression of $CheA_S$ is restricted to enteric bacteria that express CheZ (Sourjik, 2004). The role of $CheA_S$ in chemotaxis is not entirely clear, however, it has been suggested that $CheA_S$ binds to and enhances activity of CheZ (Sourjik, 2004, McNamara and Wolfe, 1997) and in addition it possibly acts to modulate phosphoryalation of $CheA_L$ (Korolik *et al.* 2008).

1.6.2.2. *B. subtilis*

Bacillus subtilis has been demonstrated to employ a modified chemotaxis signalling system. Like *E. coli*, *B. subtilis* has been shown to utilize CheA, CheY, CheB, CheR, CheW proteins for chemotaxis signalling; however, extra chemotaxis proteins have been found such as CheV, CheD, CheC and the FliY protein. The *B. subtilis* system works with an opposite response mode to the *E. coli* signalling system, where the binding of attractant conversely activates autophosphorylation of CheA and subsequent transfer to CheY, resulting in the binding of CheY to the flagellar motor and rotation counter clockwise (Figure 1.6) (Garrity and Ordal, 1995, Porter et al., 2011). It has been revealed that the N-terminal of CheV is homologous to CheW, whereas the C-terminal is a RR domain. Mutation of either of the CheV or CheW showed partial chemotaxis deficiency on a swarming assay; however, the double mutant appeared to be severely chemotaxis deficient similar to the phenotype of a CheA mutant (Porter et al., 2011). Therefore, it has been concluded that CheV is required for adaptation and, in addition, that CheW and CheV link CheA to the MCP (Porter et al., 2011). Though CheV has been postulated to play an adaptation role, the CheR and CheB proteins still exist in *B. subtilis*. It is possible that CheV more efficiently and rapidly desensitises CheA activity by taking phosphate away since it is part of CheA-MCP complex and thus a better understanding of the biological function of CheV in *B. subtilis* may provide insight to predict its chemotactic role in other bacteria.

Investigation of CheC and CheD has indicated they function together, because without CheD the CheC protein appeared to be only a weak CheY-phosphatase (Porter et al., 2011). As a result of this it was suggested that CheD increases CheY-CheC interaction and phosphatase activity. Regardless of that, CheD has been suggested to regulate CheA activity by binding to chemoreceptors and increase CheA autophosphorylation. Likewise, the CheC/CheD complex was said to function as a feedback loop for CheY, where CheC presumably contests CheD

binding on chemoreceptors and this reduces the high level of CheY-P (Glekas et al., 2012). However, others propose that the main role of CheC is only to bind CheY rather than catalysing the removal of phosphate. In that sense, FliY has been suggested to play two roles, one of which is as a stronger phosphatase and the other is as an integral component of the flagellar C-ring (Glekas et al., 2012). It seems that CheD primarily binds to chemoreceptors in order to activate CheA, however, CheC presumably prevents this by binding to CheD so that the CheY level remains low and hence FliY may be the main phosphatase of CheY-P. The exact roles of these proteins remain unclear.

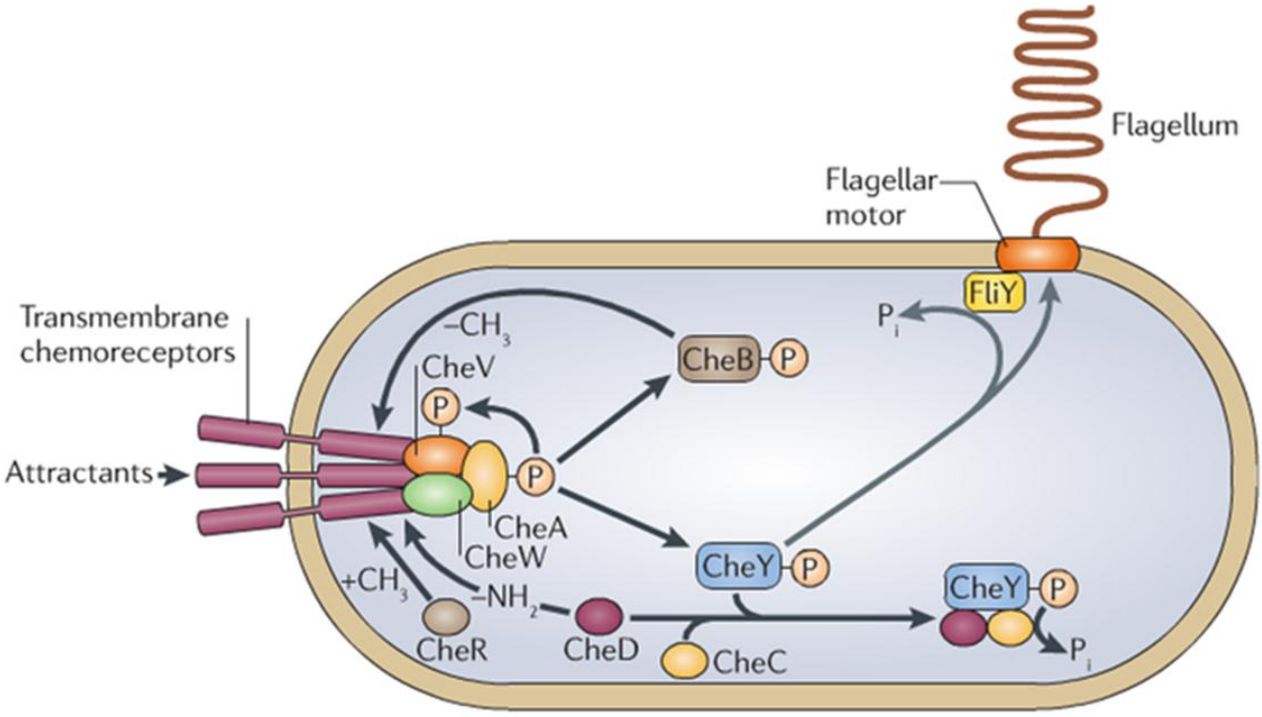

Figure 1.6. Schematic diagram of chemotaxis in *Bacillus subtilis*.

This is reversed signalling system of *E. coli*, as attractant binds on Chemoreceptors CheA is auto-phosphorylated, and then transfers phosphate to CheY, CheB and CheV RR. CheY-P binds of the flagellar motor and rotates flagella anticlockwise direction which makes the cell swim. FLiY removes phosphate from CheY.This picture is taken from Porter et al (2011).

1.6.2.3. *Rhodobacter sphaeroides*

Although *E. coli* is a paradigm it is simple system and many other bacteria have additional components such as *B. subtilis* or multiple sets of CheA-CheY and related proteins. The chemotactic system of *Rhodobacter sphaeroides* is more complex than the *E. coli* paradigm (Porter et al., 2008).

Unlike *E. coli*, *R. sphaeroides* employs four CheAs, six CheYs, four CheWs, two CheBs, three CheRs, one CheD and a CheBRA (a hybrid of CheB and CheR). No phosphatase homologues of CheZ, CheC, CheX and FLiY have been shown in Figure 1.7. MCPs of *R. sphaeroides* are clustered separately as cytoplasmic and transmembrane chemoreceptors that form separate signalling complexes. Though they form two distinct signalling clusters, these are however interconnected because deleting any protein in either cluster severely reduces the chemotaxis phenotype (Porter et al., 2008, Porter et al., 2011). It is possible that the signals from both clusters are somehow integrated thus producing a balanced chemotactic response (Porter et al., 2008).

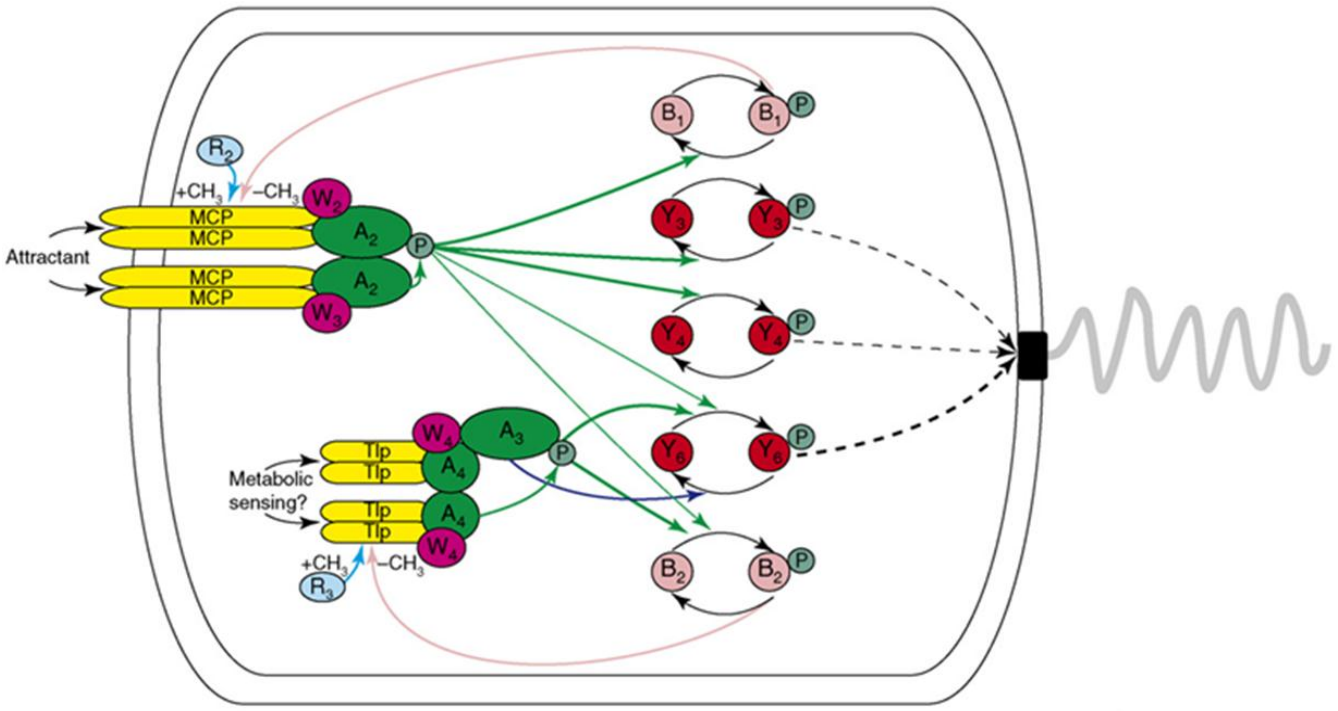

Figure 1.7. Schematic diagram representing the *Rhodobacter sphaeroides* chemotaxis pathway.
Diagram shows two transmembrane and cytoplasmic clusters (Tlp = transducer-like protein) employed for flagellum rotation. Attractants are understood to be sensed by MCPs; whereas metabolites are detected by Tlps. $CheY_6$ regulates flagella motor, but with support of $CheY_3$ and $CheY_4$. This picture is taken from Porter et al (2008).

R. sphaeroides has two identified flagella, the Fla1 and Fla2 flagellum, but under laboratory conditions the organism exclusively uses the Fla1 flagellum; however the reason for having both of these flagella still needs to be elucidated (Porter et al., 2011). Generally, The CheAs in *R. sphaeroides* phosphorylate CheYs and in turn phosphorylated CheYs bind to them to bind to Fla2/or Fla1 flagellum and change the rotational direction, but this is not yet clear. Nevertheless, it has been postulated that both flagella and all chemoreceptors are equally important and that deleting any signalling protein would abolish the chemotaxis signalling system. Hence, these chemoreceptors may produce a balanced response such that the organism navigates efficiently chemical gradient (Porter et al., 2011).

In *R. sphaeroides* $CheA_1$ and $CheA_2$ are homologue to CheA in *E. coli*, whereas $CheA_3$ and $CheA_4$ lack autophosphorylation domain. It has been shown that $CheA_2$ could phosphorylate

all RRs in the cell (Porter et al., 2008). Likewise, *in vitro* it has been shown that $CheY_6$ was phosphorylated by CheAs in both pathways. Conversely, CheAs in polar pathways can only phosphorylate $CheY_3$ and $CheY_4$. In addition, it has been shown that $CheY_6$ alone can only stop the flagellar motor, but to complete chemotaxis; it needs either $CheY_3$ or $CheY_4$. All CheYs was shown to bind to FliM, however chemotaxis effect is unknown (Porter et al., 2008). It is suggested CheYs compete to bind FliM so that to switch cell in swimming direction and therefore this might play an important role in integrating signals from both pathways(Porter et al., 2008).

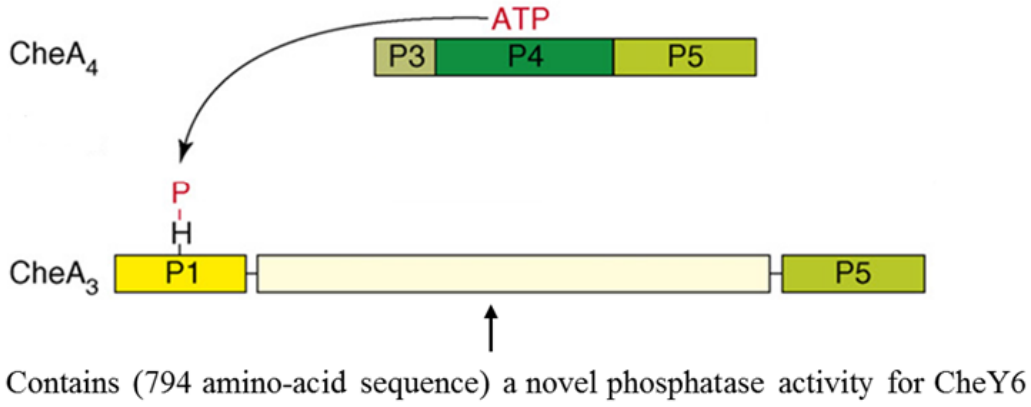

Figure 1.8. Diagram illustrating possible phosphatase site in CheA3 found in *R. sphaeroides*.
$CheA_4$ transfers phosphate to histidine residue at P1 in $CheA_3$. A novel phosphatase for $CheY_6$ with 794 amino acid sequence contains between P1 and P2 of $CheA_3$. This modified picture is taken from Porter et al. (2008).

Since *R. sphaeroides* has no annotated CheZ homologues, two suggestions to explain this have been postulated. First, the $CheY_6$ protein auto-dephosphorylates which removes phosphate itself in a manner faster relative to CheY in *E. coli*. The second notion is that these multiples (CheY1-5) *R. sphaeroides* uses as phosphate sink. $CheY_{1-5}$ working as phosphate sink was shown when complemented cheZ mutant of *E. coli*. Study also suggested that the 794 amino-acid sequence with phosphatase activity contained between two domains of $CheA_3$, the P1 and P5 (Figure 1.8), is likely to be a phosphatase for $CheY_6$ (Porter et al., 2011). This signalling system is the current model for *R. sphaerodies*, however, this needs

still to be further investigated. *Vibrio cholerae,* like *R. sphaerodies,* displays multiple chemotaxis systems compared to *E. coli* (Boin et al., 2004) and their functions are also as yet not elucidated; however, this will not be discussed here.

1.6.2.4. *Sinorhizobium meliloti*

The chemotaxis signalling system of *Sinorhizobium meliloti* deviates from the *E. coli* paradigm in regard to both flagellar rotation and signal transduction. It has been found that this bacterium possesses two RRs, CheY1 and CheY2 (Meier et al., 2007, Sourjik and Schmitt, 1998). Also, no CheZ orthologue for the two CheY RRs has been annotated. In addition to this, the flagellum is exclusively rotated in the clockwise direction. The CheY2 RR was shown to bind to FliM and reduces the speed of flagellar rotation instead of causing a switch in rotation direction, whereas $CheY_1$ was revealed (Schmitt, 2002) not to bind to the flagella (Figure 1.9). However, further studies (Meier et al., 2007) showed CheY1 acts as a phosphate sink which reversibly removes phosphate bound to CheY2 via CheA to CheY1. As CheA has a retro-phosphorylation property this enables it to remove phosphate from CheY2 and deactivates it. Subsequently CheA transfers the removed phosphate from CheY2 to CheY1 (Meier and Scharf, 2009, Meier et al., 2007, Porter et al., 2008).

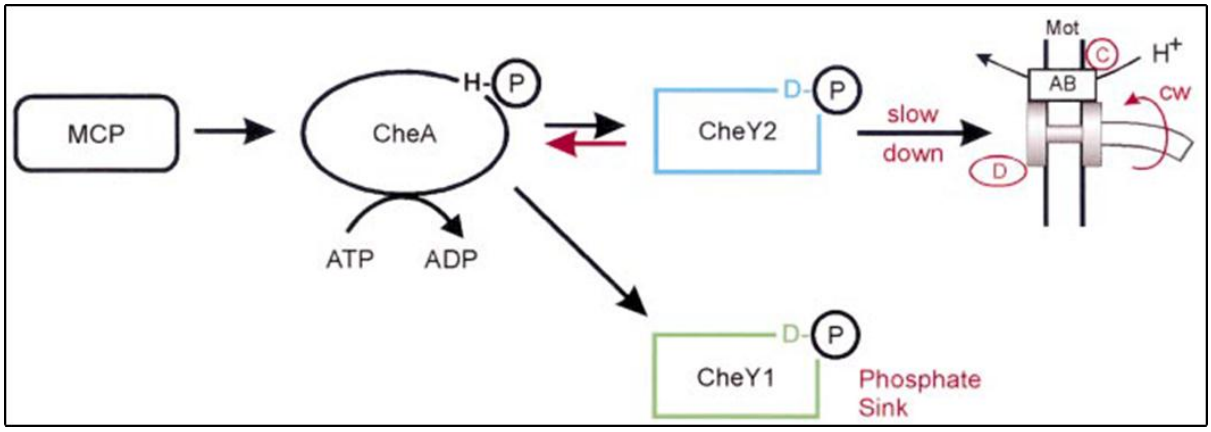

Figure 1.9. Schematic diagram illustrating chemotaxis signalling pathway of *Sinorhizobium meliloti*. Signalling cascade starts from MCP and then CheA is autophosphorylated at histidine site (H), after that phosphate (P) is transferred to $CheY_2$ at aspartate residue (D) and $CheY_2$-P binds to flagellar motor (mot). Then flagella rotation is slowed down. Flagellum rotates exclusively in a clockwise direction. CheY1 acts as a phosphate sink and removes $CheY_2$ via CheA. MotD-C (red) are motor proteins. This picture is take from Schmitt (2002).

1.6.2.5. *Helicobacter pylori*

Helicobacter pylori, which is a close relative to *C. jejuni*, is different from the chemotaxis signalling system in the *E. coli* paradigm (Figure 1.10). It has been shown that *H. pylori* possesses CheA, CheVs and ChePep with an additional CheY-like RR and Hp0170. In addition to this, CheB and CheR orthologues are absent in *H. pylori* (Jimenez-Pearson et al., 2005). Also, there are additional RR domains on CheA, CheV and ChePep, but yet these need to be understood, though CheV has been associated to the adaptation. CheZ phosphatase (Hp01070) was found serendipitously when mutating the other chemotaxis protein CheW (Howitt et al., 2011, Sweeney and Guillemin, 2011). Initially they found that the *cheW* mutant appeared to have a non-chemotactic phenotype; however, after an extended incubation time, the *cheW* mutant appeared to regain a chemotactic phenotype. Hence they suggested there might be a 'second-site repressor mutation'. Therefore DNA of the *cheW* mutant with the chemotactic phenotype was naturally transformed into wild-type *H. pylori* with the expectation that the chemotactic phenotype would be present in the recombinants;

however, all clones showed a non-chemotactic phenotype. As a result of a finding that did not support a suppressor mutation within the CheW, protein profiles of the two chemotactic and non-chemotactic *cheW* mutant variants were compared. Results showed that the *cheW* mutant with the non-chemotactic phenotype showed Hp0170 protein was present, whilst in the *cheW* mutant with the chemotactic phenotype this protein was missing. In addition, it was found that the *cheW* mutant with chemotactic phenotype had *hp0170* mutations (deletion/insertion). Double mutants (*cheW* and *hp0170*) showed a recovery of chemotactic phenotype on soft-agar but the extent was smaller to the previously observed phenotype. Therefore, it was concluded that the *cheW* mutant regaining its chemotactic phenotype was the result of an *hp0170* mutation (Terry et al., 2006, Howitt et al., 2011, Sweeney and Guillemin, 2011). Further investigation of Hp170 has shown that *H. pylori* encodes a distant homologue of the CheZ of *E. coli* (Lertsethtakarn and Ottemann, 2010).

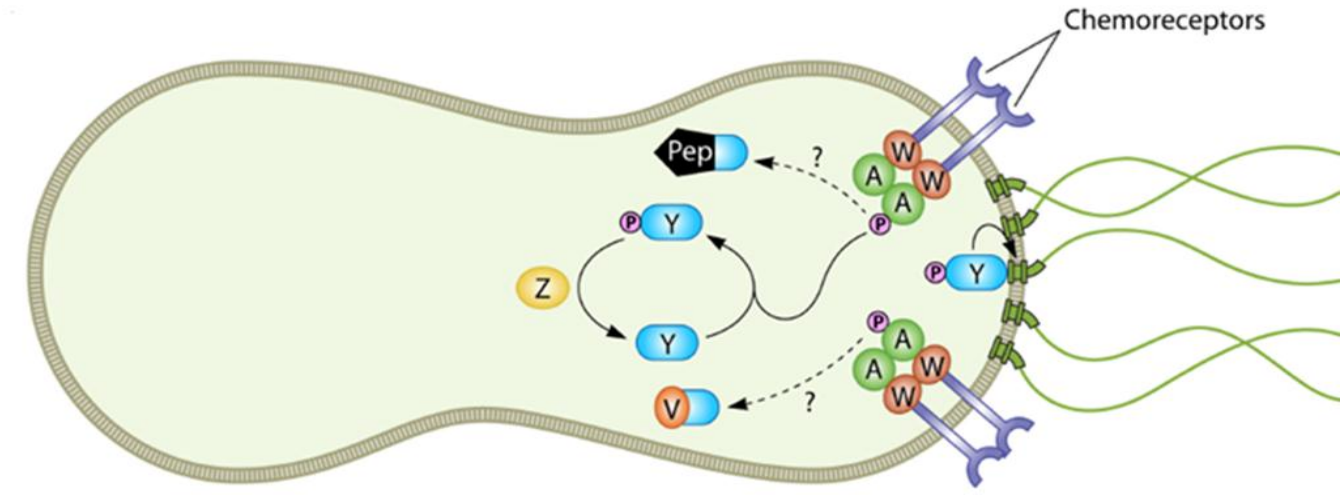

Figure 1.10. Diagram depicting chemotaxis signalling pathway of *H. pylori*.
In the absence of attractant from chemoreceptor, CheA is authophosphorylated via CheW (CheV). Then CheA phosphorylates CheY, in turn CheY-P binds to flagellar motor. CheA, CheV, and ChePep has additional RR domain. CheV is hybrid of CheW and RR. ChePep function is unknown. CheZ (Hp0170) is CheY phosphatase. This picture is taken from Sweeney et al. (2011).

1.6.2.6. *C. jejuni*

Motility and chemotaxis of strains of *C. jejuni* has been shown to play an essential role in colonization and infection in the host (Ketley, 1997). It is known that *C. jejuni* can actively swim and colonize the mucus lining of the epithelial cell layer. Hence, to break through the mucus barrier, *C. jejuni* employs the chemotaxis signalling pathway (Kanungpean et al., 2011b, Korolik, 2010a).

C. jejuni possesses unique chemotaxis pathway components. In the complete genome sequence *C. jejuni* NCTC11168 appears to employ the universal two- component regulatory system similar to other chemotactic bacteria (Korolik *et al.* 2008). The CheA, CheW, CheV, CheY, CheR and CheB homologues were annotated in *C. jejuni* and most likely form part of the chemotaxis pathway. The presence of these genes provides the basis to model the signal transduction pathways in *C. jejuni* (Parkhill et al., 2000).

According to the diversity of ligand binding transducer like protein (Tlp) receptors and differences of additional response regulator (RR) domains of chemotaxis signal transduction pathway in *C. jejuni* seems unique with several notable differences to that found in *H. pylori* (Marchant et al., 2002a). Therefore, the signal transduction pathway in *C. jejuni* lies somewhere in between the complexity of *R. sphaeroides* and the relative simplicity of *E. coli* (Korolik *et al.* 2008). Despite the uniqueness of several aspects of the system, *C. jejuni* expresses a conserved chemotaxis backbone comprising the receptor-CheW (CheV)-CheA-CheY, which is the centre of signalling system. Nonetheless, *C. jejuni* deviates from the *E. coli* paradigm by having additional RR domains on CheA and CheV. In addition, *C. jejuni* has ChePep, no homologue of CheZ was apparent (Parkhill et al., 2000, Marchant et al., 2002) and the RR domain is missing from the CheB protein relative to the *E. coli* model (Rahman et al., 2014, Howitt et al., 2011, Marchant et al., 2002a).

1.6.2.6.1. Chemoreceptors

The genome sequence of C. *jejuni* has identified that there are 10 chemoreceptors which have homology to methyl-accepting chemotaxis proteins in *E. coli*. These chemoreceptors were designated Transducer-Like proteins (Tlp) (Marchant et al., 2002a). Also, two aerotaxis homologues have been annotated which may transfer signals to the signal transduction pathway backbone via the CheA-CheW-CheY protein complex (Marchant et al., 2002a). Based on structural predictions the Tlps are grouped into A, B, C and AeR receptor groups (Rahman et al., 2014, Korolik, 2010a, Marchant et al., 2002a, Korolik, 2008). For instance, group A comprises Tlp1, 2,3,4,7 and 10, which have been suggested to be structurally equivalent to MCPs in *E. coli*; because they consist of a periplasmic domain, a transmembrane domain and a cytoplasmic domain. Group B is postulated to contain only Tlp9, while group C has been suggested to comprise Tlp5, 6 and 8 receptors. So far, Tlp 1 and 7 receptors have been successfully analysed and this suggested that each receptor binds a specific ligand (Rahman et al., 2014, Hartley-Tassell et al., 2010b).

1.6.2.6.2. Cytoplasmic components

To date the genomic sequence of *C. jejuni* NCTC 11168 has been shown to encode the chemotactic proteins CheA, CheY, CheV, CheB, CheW and CheR. It is worth mentioning in this context that the basic chemotaxis signalling backbone of *C. jejuni* is conserved; this comprises a chemoreceptor; a histidine kinase (CheA); coupling proteins (CheW/CheV) and a RR (CheY) (Parkhill et al., 2000, Rahman et al., 2014). However, CheA and CheV were identified to have an additional CheY-like RR. Like CheV in *B. subtilis*, the CheV in *C. jejuni* is a hybrid of CheW and CheY. Furthermore, CheB lacks a RR domain and hence its function in *C. jejuni* is as yet unclear (Parkhill et al., 2000). There is no chemotaxis CheZ orthologue identified in the *C. jejuni* genome and instead CheV was postulated by Korolik

(2010) to be a phosphate sink which would sequester phosphate from CheY (Korolik, 2010a, Parkhill et al., 2000).

The general organization of chemotaxis genes in *C. jejuni* was found to be similar to the chemotaxis genes of *H. pylori* except that the *cheR* and *cheB* genes are not present in the *H. pylori* genome. The chemotaxis genes were found to cluster in three locations with genes supposedly not related to chemotaxis and with which they may be co-transcribed and co-regulated, as they appear to be part of an operon. For instance *cheY* may be co-transcribed with its flanking genes which are presumably not related to chemotaxis (Figure 1.11). Likewise, *cheV*, *cheA* and *cheW* genes are likely to be co-transcribed with functionally unrelated genes. However, the *cheR* and *cheB* genes (Figure 1.11) seem not to be co-transcribed with unrelated genes (Marchant et al., 2002a).

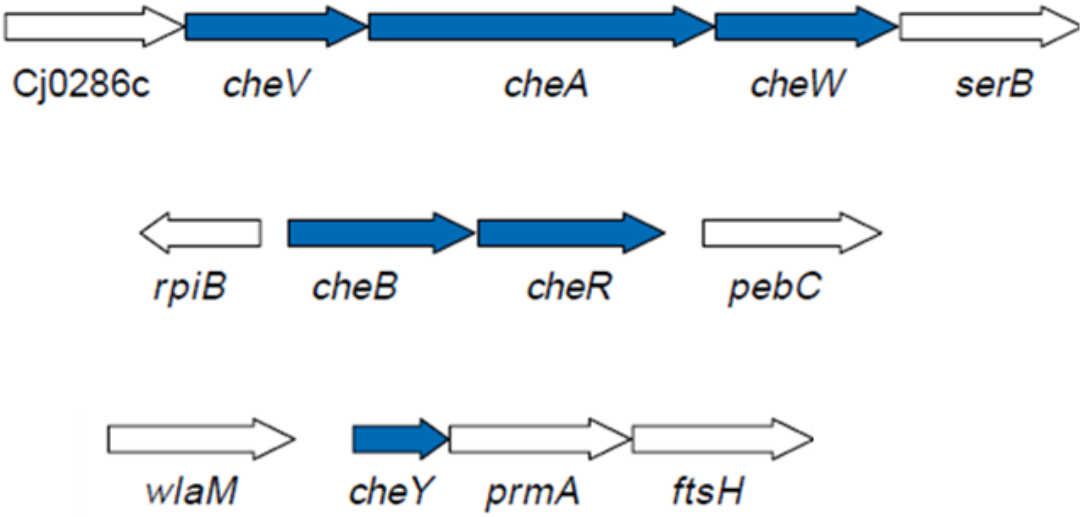

Figure 1.11. Diagram depicting chemotaxis genes organized in genome of *C. jejuni* NCTC 11168.
Chemotaxis genes are co-transcribed with non-chemotaxis genes in three different locations. Chemotaxis genes are designated by blue arrows. Chemotaxis genes of *cheV*, *cheA* and cheW are clustered with *cj0286c* (a hypothetical protein) and *serB* (putative phosphoserine phosphatase;tal transaldolase); *cheB* and *cheR* genes are clustered with non-chemotactic genes of *rpiB* (ribose 5-phosphate isomerase and pebC, (ABC-type amino-acid transporter ATP-binding protein); *cheY* gene is clustered with non-chemotaxis gene of *wlaM* (polysaccharide biosynthesis), *prmA* (a ribosomal protein L11 methyltransferaseand *ftsH* (a membrane bound zinc metallopeptidase). This picture was taken from Marchant et al. (2002).

1.6.2.6.2.1. *CheA*

In *B. subtilis* it has been shown that CheA phosphorylates CheV (Garrity and Ordal, 1995). *In silico*, the CheA of *C. jejuni* has been shown to contain a histidine kinase functional domain, which is 26% identical to the CheA in *E. coli*; the histidine phosphate transfer (P1), catalytic kinase (P4) and CheW–receptor binding (P5) domains were found to be conserved. In addition, the CheY and CheB binding domain (P2) and adjacent linkers (between P1, P2 and P3) were found not to be conserved in *C. jejuni* relative to the *E. coli* paradigm (Korolik, 2008, Wang et al., 2012). CheA short has not been identified in *C. jejuni*; however, a conserved methionine residue (Met-98) was found, which could be an alternative methylation

and transcription site of CheA short in *E. coli* (Szurmant and Ordal, 2004, Korolik, 2008). The role played by CheA's additional RR in chemotaxis signalling has not been elucidated, but this is not unique as other bacteria such as *H. pylori* and *Myxococcus xanthus* have been found to have similar RRs (Inclan et al., 2008, Lertsethtakarn and Ottemann, 2010).

Previous results (Bridle 2007) have indicated that a *cheA* mutant of *C. jejuni* demonstrates a reduced swarming phenotype relative to the wild-type. In addition to this, the bacterial two hybrid assay has also demonstrated that CheA interacts with CheY and CheV proteins, but that it didn't show binding affinity with the CheB protein (Bridle 2007). The protein-protein interaction seen is perhaps due to the process of phosphate transfer to the RR domain since CheV has additional RR; hence CheA interacted with CheV and not with CheB. In the *C. jejuni* chemotaxis system the CheA appears to be a functional homologue to CheA in *E. coli*.

1.6.2.6.2.2. *CheY*

The chemoreceptor-CheA—CheW/CheV–CheY-flagella motor group is believed to be the backbone of the *C. jejuni* signalling pathway. The amino acid sequence of CheY in *C. jejuni* has shown features of a RR in *E. coli* such as the phosphorylation and catalytic sites, which are usually conserved across CheYs. According to these characteristics, it has been suggested that phosphorylated CheY is the only RR in *C. jejuni* that binds to the flagellar motor, FliM (Korolik, 2008), because there were less sequence similarity between CheY the other RRs in the CheA and CheV. A CheY mutant showed a non-chemotatic phenotype, where cells show straight swimming under the microscope (Marchant et al., 2002a). Thus far, CheY interaction with FliM has not yet been investigated in *C. jejuni*, nevertheless all its characteristics indicate that CheY interacts with the flagellar motor.

1.6.2.6.2.3. *CheV and CheW*

In addition to a CheW homologous to that in *E. coli, C. jejuni* encodes a CheV protein, which has a CheW domain at the N-terminal and a CheY-like RR domain at the C-terminal (Korolik, 2010a, Rahman et al., 2014). The CheV protein is absent in *E. coli* paradigm, however the *C. jejuni* CheV is homologous to a CheV protein which was previously found in *B. subtilis* (Fredrick and Helmann, 1994). The CheV in *B. subtilis* has been postulated to play a role in adaptation by desensitising CheA kinase activity. *H. pylori* also encodes three CheV paralogues (Figure 1.12) and a CheW protein. It seems that CheVs and a CheW function differently because when the CheW mutant was complemented with CheVs, it has failed to repair it to generate a wild type phenotype of CheW (Pittman et al., 2001). Interestingly, the role of the CheVs in *H. pylori* are as yet not understood because the adaptation proteins CheB and CheR are both absent in *H. pylori* (Terry et al., 2006).

A recent study of CheV and CheW with Tlps using a protein-protein interaction assays suggested that Tlp1 preferentially binds to CheV and CheW; however CheV and CheW binding with other Tlps was shown to be variable (Rahman et al., 2014, Korolik, 2010a). Furthermore, a previous bacterial two hybrid assay as well as the recent one indicated CheV interacted with the CheA protein (Bridle 2007).

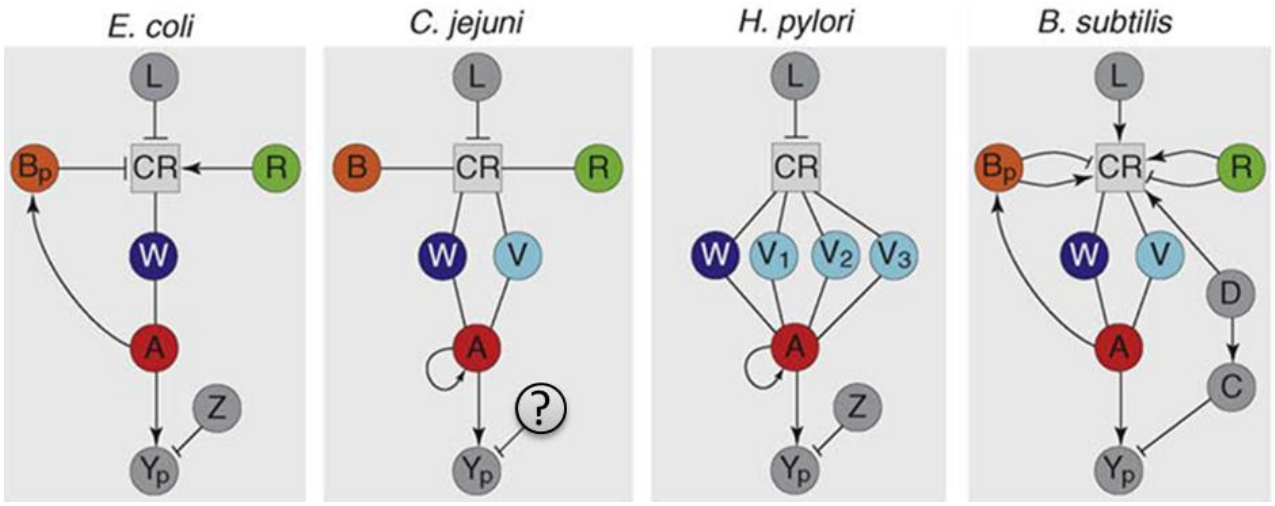

Figure 1.12. Schematic diagram illustrating variation in CheV/CheW and CheB/CheR proteins encoded in different chemotaxis bacteria.

Chemoreceptor (CR) detects signals in form of ligand (L), which ligand absence triggers signal cascade. In *B. subtilis* ligand presence trigger signal cascade. Arrows indicate activating, whereas blunt –ended lines shows inactivation of signals. Strait lines illustrate interaction proteins. B_p shows that CheB receives phosphate from CheA in *E. coli* and *B. subtilis* during adaptation; but *C. jejuni* and *H. pylori* CheA transfer phosphate to its fused RR. This is modified picture taken from Alexander et al. (2010).

1.6.2.6.2.4. *CheB and CheR*

CheB phosphorylation increases methylesterase activity by removing methyl groups from MCPs which in turn desensitises CheA so that the cell can reset to any increase or decrease in ligand concentration (Wadhams and Armitage, 2004). Nevertheless, CheB in *C. jejuni* is unique as it lacks a phosphate receiver domain but retains a methylesterase domain (Rahman et al., 2014, Kanungpean et al., 2011b, Marchant et al., 2002a). Arguably, it is not known whether CheA's additional RR compensates for the function of the CheB receiver domain or whether CheV plays that role. Interestingly *H. pylori*, which is closely related to *C. jejuni*, doesn't encode either a CheB or CheR (Figure 1.12); this raises the question of how adaptation is regulated there (Alexander et al., 2010).

Both recent and previous *in vivo* protein-protein interaction experiments have shown that CheB didn't interact with the cytoplasmic chemotactic proteins (Bridle 2007). Furthermore

results with CheB and CheR mutants have shown there is no motility defect on semisolid agar; this is presumably due to *C. jejuni* employing methylation independent adaptation via CheV protein as in *B. subtilis*. Interestingly, a *cheR* mutant was hyperadherent and hyperinvasive, while none of these phenotypes was observed in *cheB* mutant (Kanungpean et al., 2011b). In addition, a double mutant was unable to colonize chicken (Kanungpean et al., 2011b). Similar phenotypes has been also noticed in a *tlp1* mutant and this could be because *tlp1* is not methylated and hence *cheR* and *cheB* mutants demonstrate a similar phenotype to a *tlp1* mutant (Kanungpean et al., 2011b). It could be possible that CheB and CheR proteins are used for adaptation in the chemotaxis pathway of *C. jejuni* and hence are important for host cell colonization.

1.6.2.6.2.5. *ChePep*

ChePep is unique and conserved in the pathogenic epsiloproteobacteria such as *C. jejuni* and *H. pylori*. It is a novel protein that was first observed by chance in *H. pylori*. In addition, it has an N-terminal RR domain (Howitt et al., 2011).

Experimentally ChePep was localised to the poles of the cell and hence it was suggested it might regulate flagella via the chemotaxis signalling pathway (Howitt et al., 2011). ChePep mutant of *H. pylori* has a motile phenotype and a slightly decreased swarming ability, but they fail to colonize the epithelial surface of gastric glands in mice (Howitt et al., 2011). Furthermore, a ChePep mutant has shown a similar phenotype to a CheB mutant of *E. coli* and may possibly modulate CheY phosphorylation activity. Thus, it has been suggested that ChePep plays a role in adaptation in *H. pylori*. Interestingly, ChePep from *C. jejuni* has been shown to be able to complement a ChePep mutant in *H. pylori*; however as yet no experiment investigating ChePep in *C. jejuni* has been reported.

1.6.2.6.2.6. *Cj0700*

The central component of chemotaxis and motility in bacteria is CheA-CheY which regulates the direction of movement either toward an attractant or away from a repellent. However, the proteins that desensitise the signalling cascades are not universal across bacterial species; for instance, *E. coli* and *Salmonella* have CheZ, which is a CheY phosphatase (Lertsethtakarn and Ottemann, 2010, Rao et al., 2005) whereas others have evolved modified forms of CheZ for example *Bacillus subtilis* has been described to employ CheC and CheD in addition to the FliY protein (Pazy et al., 2010). Furthermore, *H. pylori,* which is closely related to *C. jejuni*, has been found to utilise Hp0170 which is a distant homologue of CheZ (Terry et al., 2006). *In C. jejuni*, a CheZ homologue has not been identified (Parkhill et al., 2000) and hence CheV was proposed as a phosphate sink that the organism could use for inactivating CheY-P (Korolik, 2008).

1.6.2.7. *Types of signal removal*

Chemotactic bacteria terminate their signalling cascades either by self-mediated phosphate removal from a RR, referred to as autodephosphorylation, or by a phosphatase or phosphate sinks. There may also be other ways chemotactic bacteria terminate the chemotatic signal, but thus far these three ways are the only ones known. Thus, these ways have been analysed and are well understood using *E. coli* as a model for understanding chemotaxis signalling systems in bacteria.

Broadly, the signal removal mechanisms target CheY-P using the conventional CheZ in *E. coli* and *Salmonella* and other CheZ distant homologues such as CheC/CheX/FliY as in *B. subtilis* and in *Thermotoga maritima* and the recently found Hp0170 in *H. pylori.* While structurally different from conventional CheZ, these proteins are functionally similar. Unlike phosphatases, other bacteria may encode additional RR in order to take phosphate from CheY

such as *S. meliloti* and *R. sphaeroides* (Szurmant and Ordal, 2004, Terry et al., 2006). Arguably, what has not yet been reported is if there are phosphatases specific only to CheY which bind to the motor switch or are general phosphatases to chemotaxis RRs such as CheA-RR and CheV-RR.

1.6.2.7.1. Self-mediated phosphate removal

The CheY RR is the backbone of the signal transduction pathway. Phosphorylated CheY diffuses through the cytoplasm to interact with the FliM protein of the flagella motor complex and to cause the cell to adopt CW direction (Falke et al., 1997). Alternatively, CheY has an autodephosphorylation role, where certain conserved residues have been described to mediate dephosphorylation (Zhu et al., 1996, Pazy et al., 2009); such properties are also suggested to be utilized by other CheY-like RR. It is believed that autodephosphorylation is the reversal of phosphorylation of CheY in which water is involved in hydrolysing the phosphoester bond (Zhao et al., 2002) However, this self-mediated autodephosphoryalation reaction is not fast enough to respond to changes in environmental conditions and is considered less effective by a factor of about 100 than the reaction enhanced by phosphatase (Silversmith, 2010) . Hence, cells need additional protein(s), which can quickly terminate the signalling cascade (Silversmith et al., 2001) and therefore the cells may employ either a phosphate sink or a phosphatase mechanism.

1.6.2.7.2. Phosphate sink

Several bacterial species that lack CheZ, or a CheZ homologue, have been found to have several CheY-like RR. These CheYs receive phosphate from CheA and consequently CheY-P binds to the flagellar motor to change flagellar rotation. Conversely, to remove phosphate

from CheY-P, phosphate is reversed to CheA and the phosphate is transferred to other CheY as in *S. meliloti* (Figure 1.9) (Wadhams and Armitage, 2004, Schmitt, 2002).

R. sphaeroides has been identified to express six CheY homologues (Figure 1.7), which all exhibit rapid phosphorylation rates; this has been suggested to compensate for CheZ. Further study has identified that only $CheY_6$ binds to the flagellar motor (Wadhams and Armitage, 2004, Porter et al., 2008). Since a redundant CheY was not identified in *C. jejuni*, it was proposed that the RR domains in CheA and CheV may act as a phosphate sink for reduction of CheY-P level (Korolik, 2008). However identification of the Hp0170 protein in *H. pylori* as a CheZ homologue has suggested a wider distribution of remote CheZ homologues in bacteria (Terry et al., 2006).

1.6.2.7.3. Phosphatase

Chemotactic cells regulate the concentration of phosphorylated CheY-P to respond to environmental changes. Some cells inactivate the signal by using phosphatase while others remove phosphate by means of a phosphate sink. However, most bacterial species do not possess this system therefore they have evolved a CheY phosphatase mechanism. Study shows that enteric bacteria, such as *E. coli*, encode a CheZ protein for CheY-P hydrolysis. In addition, another study has identified other distant homologues like Hp0170 found in *H. pylori*. Thus, this section mainly focuses on the phosphatases found so far in other bacteria, including *C. jejuni*, in comparison to the existing *E. coli* paradigm.

The CheZ protein has been described as the main chemotaxis phosphatase in *E. coli* which is the first recognized chemotaxis signalling system (Lertsethtakarn and Ottemann, 2010, Rao et al., 2005). It has been proposed that oligomerization enhances the catalytic activity of CheZ on CheY-P dephosphorylation. In an *in vitro* assay, the short form of CheA has been observed to bind selectively to CheZ and it has been suggested to enhance its

dephosphorylation activity. In addition, CheZ has been co-localized with polar receptors via $CheA_{short}$ (Sourjik, 2004, McNamara and Wolfe, 1997, Lipkow, 2006, Silversmith, 2010).

CheZ structural determination has revealed that the glutamine residue (Gln-147) contributes to CheY-P hydrolysis activity by putting water molecules at the active site of CheY (Szurmant and Ordal, 2004), whereas the aspartic acid residue (Asp-143) makes a salt bridge with amino acid residues in the active site of phosphorylated CheY-P. These amino acid residues are conserved (Zhao et al., 2002, Pazy et al., 2010). Mutation of the glutamine (Gln-147) residue has demonstrated a reduced activity of CheZ; nonetheless the binding affinity with CheY was only moderately effected. Mutation of CheY N59R, in the active site of CheY, where the (Gln-147) residue catalyses hydrolysis, resulted in high levels of phosphorylated CheY (Silversmith et al., 2003). Further work indicated that a *cheZ* mutant of *E. coli* regained chemotactic motility in a swarming assay when the mutation was complemented (Boesch et al., 2000). In addition, phosphorylation assays comparing the phosphatase activity of CheZ on CheY-P, has shown that a *cheZ* mutant of *E. coli* didn't remove phosphate from CheY-P in comparison to wild type (Boesch et al., 2000).

Structural resolution of CheZ has been achieved only when it was co-crystalized with CheY-BeF_3^--Mg^{2+}. However, the complete structure of CheZ was not obtained; it is suggested that this is because the amino acid residues co-crystalized with CheY were ordered, whilst the disordered CheZ failed to be crystalized (Zhao et al., 2002).

CheC/CheX and FliY are a family of RR phosphatases found in bacteria which do not encode CheZ protein (Pazy et al., 2010). In addition, *T. maritima* encodes another phosphatase, CheX. Though this phosphatase is not well understood studies have shown CheX dephosphorylates CheY-P, and in addition its secondary structure is similar to CheC except in certain regions (Park et al., 2004). Regardless of the structural differences between these

proteins they all employ the same strategy to remove phosphate from CheY-P (Silversmith, 2010).

CheC alone is a weak phosphatase of CheY-P, but when in conjunction with CheD this enhances the phosphatase activity on CheY-P (Silversmith, 2010). Also, it has been suggested that CheC plays a bi-functional role; one function is for adaptation and the other is for phosphatase activity on CheY-P. In *B. subtilis*, FliY is a hybrid of different domains, at the N-terminus is a motif from FliM for the CheY binding sequence and a CheC homologue domain, whereas at the C-terminus is a FliN domain homologous to *E. coli* (Figure 1.13) (Muff and Ordal, 2008, Park et al., 2004). Therefore, in *B. subtilis* FliY is suggested to be the main CheY-P phosphatase (Glekas et al., 2012, Muff and Ordal, 2008). Furthermore, CheC and FliY have two active sites, whilst CheX has only one site; it has been postulated that one site with a conserved glutamine is for binding to phosphorylated CheY-P whereas the other site with a conserved asparagine residue is for CheY-P hydrolysis (Muff and Ordal, 2008).

Experiments have shown that a CheC mutant has reduced phosphatase activity on CheY-P, despite the presence of CheD(Muff and Ordal, 2007). Also, a semisolid agar assay has indicated a reduction of the swarming diameter on the plate. Likewise, a CheX mutant has shown a similar effect in the swarming assay relative to the wild type. Protein-protein interaction experiments have indicated that, in the presence of CheD, CheC interacts with CheY (Muff and Ordal, 2007, Yuan et al., 2012).

Serendipitously the CheZ-like phosphatase protein Hp0170 was found in *H. pylori* during an investigation of a CheW mutant (refer to section 1.6.2.5). Further investigation has confirmed that Hp0170 is a distant homologue of CheZ in *E. coli*. Interestingly, the Hp0170 amino acid alignment with Cj0700 in *C. jejuni* revealed them to be about 50% identical (Terry et al., 2006). In addition, further study showed that amino acid residues corresponding to the active sites of CheZ in *E. coli* (D143 and Q147) are also conserved in Hp0170 (D189 and Q193).

These two conserved amino acid residues are postulated to exist in all CheZ orthologues (Lertsethtakarn and Ottemann, 2010). In an earlier study by Terry et al. (2006), the result of replacement of the aspartic acid at 189 by an asparagine (D198N) residue was loss of function of Hp0170; this was supported by a later phosphate release assay, where mutation at the same (D198N) site have shown a loss of function of Hp0170 protein. In addition the phosphate release assay also indicated that Hp0170 was able to remove phosphate from CheY in a similar manner as CheZ on CheY-P. Similarly, Hp0170 removed weakly phosphate from a truncated CheA-RR (response regulator) but not as efficiently as CheY-P. Conversely, Hp0170 was unable to remove phosphate from CheVs (Lertsethtakarn and Ottemann, 2010).

In *C. jejuni*, amino acids of putative Cj0700 were aligned with both CheZ in *E. coli* and Hp0170 in *H. pylori*. In addition to this, Cj0700 has shown conserved amino residues (D167 and Q171) corresponding to amino acid residues in the active site of the CheZ (D143 and Q147) and the Hp0170 (D189 and Q193) protein.

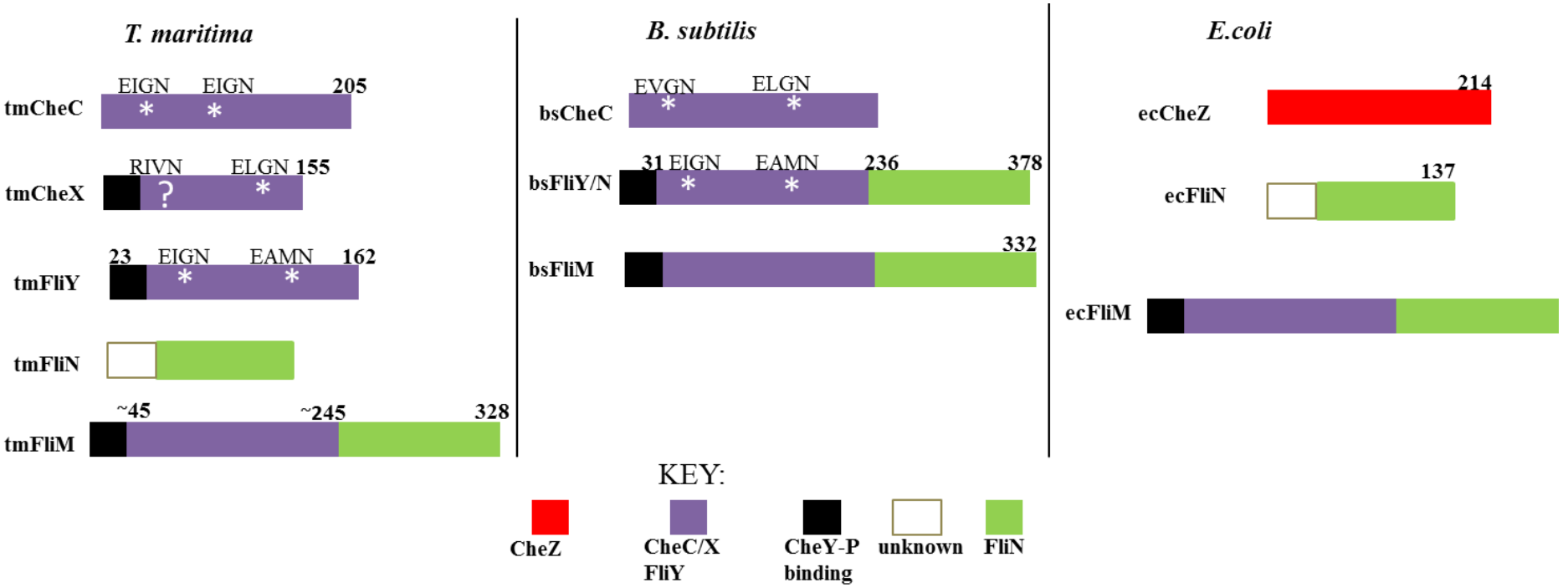

Figure 1.13. Diagram illustrating CheZ-like family phosphatases identified in two bacteria in comparison to CheZ in *E. coli*. Purple section illustrates CheC homologue. Green section stands for FliN homologue. Black box shows CheY-P binding region in FliY/N and FliM. White star shows conserved residues. This is a modified picture taken from Park et al. (2004).

1.7. Aims of the project

The chemotaxis signalling system of *C. jejuni* is known to be important for colonization and infection though the mechanism is not well understood. This is partly because *C. jejuni* chemotaxis is unique and as a result of that it has been difficult to establish a model based entirely on the existing chemotaxis signal paradigms. One may suppose that *C. jejuni* would be most loosely associated with *H. pylori*, but of course they reside in different niches. In addition to this, the study demonstrated the amino acid alignment of the Cj0700 to Hp0170, which is a remote homologue of CheZ in *E. coli*, to be about 50% identical (Terry et al., 2006). The preliminary study (Bridle 2007) of Cj0700 interacting with RR domains has speculated that Cj0700 may be involved in CheY-P dephosphorylation. Thus, this finding has prompted us to hypothesize that Cj0700 protein plays an important part in the chemotaxis signalling pathway in *C. jejuni* by acting as a phosphatase which promotes removal of phosphate from CheY. Also we hypothesized that Cj0700 may possibly remove phosphate from additional RR domains in CheA and CheV. In order to test this supposition, a *cj0700* mutant will be created and tested to see if the mutant will affect chemotaxis. But the genomic organisation of Cj0700 may mean that mutation may be polar (Figure 1.14). It is expected that a *cj0700* mutant will show reduced chemotactic motility and that complementation of the *cj0700* mutant will show a regain of wild-type motility phenotype as seen using soft-agar plates (swarming assay).

If Cj0700 has phosphatase activity it would be expected that Cj0700 should promote rapid dephosphorylation of CheY and possibly other RRs. In order to dephosphorylate specific chemotaxis proteins, Cj0700 would be expected to interact with the right proteins and therefore, it would be predicted that Cj0700 interacts with CheY and perhaps the CheA-RR and CheV proteins. Cj0700 interactions with RRs will be confirmed using an *in vitro* pull-down assay and an *in vivo* BTH assay. Cj0700 has a shape similar to distant homologues. In

this research is to study structure of Cj0700 protein and if Cj0700 stimulates dephosphorylation of CheY in which mechanism phosphate is removed from CheY because crystalizing Cj0700 will give better understanding of which amino acid residues interact with CheY.

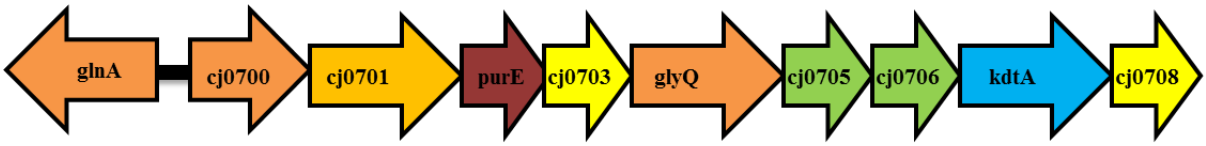

Figure 1.14. Genomic organization of *cj0700.*

glnA (glutamine synthetase), *cj0701* (putative protease), *purE* (phosphoribosylaminoimidazole carboxylase catalytic subunit), *cj0703* (hypothetical protein), *glyQ* (glycyl-tRNA synthetase subunit alpha), *cj0705* (hypothetical protein), *cj0706* (hypothetical protein), *kdtA* (3—deoxy-D-manno-octulosonic-acid transferase), *cj0708* (putative ribosomal pseudouridine synthase). Source was drawn from http://xbase.bham.ac.uk/campydb/.

Chapter 2 : Materials and Methods

2. Bacterial culture and storage

Campylobacter jejuni NCTC11168, NCTC11828 (81116) and 81-176 strains (Table 1) in this study were grown on MHA (Mueller-Hinton Agar, Oxoid , Basingstoke, UK) supplemented with vancomycin (10 µg/ml) and trimethoprim (5 µg/ml) as standard antibiotics to avoid contamination. Additional antibiotic supplementation as required for mutant selection included chloramphenicol (20 µg /ml), erythromycin (5 µg /ml) and kanamycin (50 µg /ml).
C. jejuni liquid cell cultures were grown for a 2-5 days in micro-aerobic (80% Nitrogen, 10% CO_2 and 5% O_2) conditions at 42 ^oC in a VAIN cabinet (Variable Atmosphere Incubator; Don Whitley Scientific Ltd, Shipley, UK). In addition, cells were grown in liquid MH broth supplemented with vancomycin (10µg/ml) and trimethoprim (5µg/ml) with shaking at 250 rpm. Cell density was measured at A_{600} (Ultaspec^{TM} 10 Cell Density Meter, Amersham Bioscience, UK) unless otherwise specified.

E. coli cells (Table 2) were normally grown on LA (Luria-Bertani Agar), MacConkey agar plates or in liquid media (LB; Luria-Bertani Broth) supplemented with the appropriate antibiotics required for selection (Table 10). *E. coli* cells carrying recombinant plasmids were selected with suitable antibiotics on the growth media, depending on the selection required, for instance *E. coli* XL-1blue strains carrying cj0700 plasmids were grown on media supplemented with ampicillin (100 µg /ml) and tetracycline (10 µg /ml) . Plasmids constructed and used during this study are presented in tables 3, 4, 5 and 6.

For long term storage at -80 ^oC bacterial strains were stored in MHB containing 25% (v/v) glycerol. To prepare the glycerol stock, *C. jejuni* was grown on MHA plates supplemented with vancomycin and trimethoprim and then incubated at 42 ^oC for 1-3 days in the VAIN. *E. coli* cells were grown either on LA plates or in 5 ml of LB overnight at 37 ^oC with shaking at

250 rpm. For small volume preparations cell growth was re-suspended in 2 ml of MHB or LB for *C. jejuni* and *E. coli*, respectively, and the cell suspension from plates was transferred to 1.5 ml micro-centrifuge tubes. Afterwards, cells were pelleted at 1100 xg in an Eppendorf MiniSpin Plus centrifuge for 5 minutes at room temperature. For bigger volumes, cell growth from plates was re-suspended in 10 ml MHB or LB for *C. jejuni* and *E. coli*, respectively, and then scrapped cells were transferred into a 15 ml Falcon tube and centrifuged at 3200 xg (Eppendorf centrifuge 5810R) for 20 minutes at room temperature. Cells were re-suspended with 1.5 ml MHB or LB for *C. jejuni* and *E. coli* respectively. Next aliquots of 750 µl of the cell suspension was transferred into cryo-tubes, to which equal volumes of 50% (v/v) glycerol was added, snap frozen on dry –ice and stored at -80 ^{o}C.

To subculture glycerol stocks, stored vials were put on dry-ice and then cells were plated on suitable plates by scraping off cells with stick end of sterilised swab before being spread on to the solid media, and then incubated under suitable growth conditions with appropriate antibiotics.

2.1. Bacterial strains and Plasmids used in this study

Bacterial strains and plasmids used in this study are shown in tables 1, 2, 3, 4, 5 and 6.

Table 1. *Campylobacter jejuni* and mutant strains used or created in this study.

Name	**Description**	**Source**
Campylobacter jejuni NCTC 11168	Wild-type	National Collection of Type Culture, Colindale, London, UK
C. jejuni NCTC 11168 Motile variant	Wild-type motile variant made from *Campylobacter jejuni* wild type 11168 NCTC strain	Laboratory stock
C. jejuni BAJ1CJ700	NCTC 11168 Δ*cj0700:cat* (Cm^{r})	This study
C. jejuni 81116 (NCTC11828)	Wild type motile from isolated *C.jejuni*	Manning *et al*., 2001
C. jejuni NCTC 81176	Clinical isolates	Korlath *et al*.,

Motile		1985
C.jejuni 81116 BAJ4CJ700	NCTC11828 Δ*cj0700:cat* (Cm^r)	This study
C. jejuni 81-176 Motile BAJ5CJ700	81-176 Δ*cj0700:cat* (Cm^r)	This study
C. jejuni 81-176 Motile BAJ6CJ700	81-176 Δ*cj0700::cat* (Cm^R):: *cj0046::cj0700* (km^R)	This study
C.jejuni NCTC11828 Motile BAJ7CJ700	NCTC11828 Δ*cj0700::cat* (Cm^R):: *cj0046::cj0700* (km^R)	This study
C.jejuni NCTC 11168 motile merodiploid BAJ8CJ700	NCTC 11168 *cj0700::cj0046* (km^R)	This study
C.jejuni NCTC 81116 motile merodiploid BAJ9CJ700	NCTC11828 *cj0700::cj0046* (km^R)	This study
C.jejuni 81-176 motile merodiploid BAJ10CJ700	NCTC 81-176 *cj0700::cj0046* (km^R)	This study
C.jejuni BAJ2CJ700	NCTC 11168 *cj0046::cj0700* (km^R)	This study
C.jejuni BAJ3CJ700	NCTC 11168 Δ*cj0700::cat* (Cm^R):: *cj0046::cj0700* (km^R)	This study

Table 2. *E. coli* strains used in this study.

Name	**Description**	**Source**
Escherichia coli XL-1blue	*recA1 endA1 gyrA96 thi-1 hsdR17 supE44 relA1 lac* [F´ *proAB lacI*q*Z*Δ*M15* Tn*10* tet^r]	Stratagene, USA
E.coli BL21	*F-, ompT, hsdS (rB-, mB-), gal, dcm*	New England Biolabs (NEB, Hitchin, UK).
E.coli DH5αE	F-Φ80*lac*ZΔM15 Δ(*lac*ZYA-*arg*F) U169 *deo*R *rec*A1 *end*A1 *hsd*R17 (rK–, mK+) *gal-pho*A *sup*E44 λ- *thi*-1 *gyr*A96 *rel*A1	Invitrogen (Paisley, UK).
E. coli Rosetta	Lactose permease (*lacY*) mutant, deficient in *lon* and *ompT* proteases; contains plasmid encoding *argU, argW, glyT, IleX, leuW, metT, proL, thrT, thrU,* and *tyrU*	Novagen
E.coli BTH101	*F- cya-99 araD139 galE15 galK16 rpsL1 (Strr) hsdR2 mcrA1 mcrB1*	Euromedex, UK

Table 3. Vectors used in this study.

Plasmid	Description	Antibiotic resistance	Source
pTrcHisB	N' terminal polyhistidine tag vector used for protein expression	Amp^R	Invitrogen (Paisley, UK)
pKmetK	Vector contains *metK* promoter and used for *Campylobacter* sp.complementation	Km^R	R. Haigh
pGex-4T-1	N' terminal glutathione tag vector used for protein expression	Amp^R	GE Healthcare (Chalfont St. Giles, UK)
pAV110	Contains promoter-less resistance cassette	Cm^R	A. van Vliet
pLEICS03	N' terminal polyhistidine tag vector used for protein expression	Km^R	(PROTEX, University of Leicester)
pUC19	Cloning vector with high copy number	Amp^R	New England Biolabs Ltd, Hitchin, UK
pKT25	Encode the T25 domain of the adenylate cyclase. Target allele cloned in C-terminus of the vector used for bacterial two hybrid system	Km^R	Euromedex, UK
pUT18	Encode the T18 domain of the adenylate cyclase. Target allele cloned in C-terminus of the vector used for bacterial two hybrid system	Amp^R	Euromedex, UK
pUT18C-zip	Zip sequence into C-terminal of p18 plasmid multi-cloning site	Amp^R	Euromedex, UK
pKT25-zip	Zip sequence into C-terminal of pT25 plasmid multi-cloning site	Km^R	Euromedex, UK

Table 4. Plasmids constructed for mutagenesis and complementation.

Plasmid	Description	Insert size in bp	Antibiotic resistance	Source
pAJ1	Contains promoter-less kanamycin cassette cloned into pUC19	795	Km^R, Amp^R	This study
pAJ2	Contains promoter-less and terminator-less erythromycin resistance cassette cloned into pUC19	735	Erm^R, Amp^R	This study
pAJ3	Contains promoter-less erythromycin resistance cassette cloned into pUC19	1100	Erm^R, Amp^R	This study
pAJ4	Contains *cj0700* with 600 bp	1896	Amp^R	This study

	flanking sites either sides cloned into pUC19			
pAJ5	Contains promoterless chloramphenicol resistance cassette cloned into *cj0700* in pAJ4 plasmid	2084	Cm^R	This study
pAJ6	Contains *cj0700* cloned into pKmetK vector	896	Km^R	This study
pAJ7	Contains cj0700D167N cloned into pKmetK vector	893	Km^R	This study

Table 5. Plasmid constructed for protein expression.

Plasmid	**Description**	**Insert Size in bp**	**Antibiotic resistance**	**Source**
pAJ8	*cj0700* gene cloned into C-terminal of pLEICS03 plasmid multi-cloning site	696	Km^R	(PROTEX, University of Leicester)
pAJ9	Flag tag sequence cloned into pTrcHisB vector multi-cloning site	24	Amp^R	This study
pAJ10	Flag-*cheV* recombinant cloned into pTrcHisB vector multi-cloning site	968	Amp^R	This study
pAJ11	flag-cheA (Δ histidine kinase) recombinant cloned into pTrcHisB vector multi-cloning site	1972	Amp^R	This study
pEKG1	Expression plasmid. *cj0700* cloned into the pGex-4T-1 multiple cloning site	696	Amp^R	E. Karunakaran
pPA016	*cheV* cloned into the pTrcHisB multiple cloning site	968	Amp^R	P. Ainsworh
pPA017	*cheA* cloned into the pTrcHisB multiple cloning site	2323	Amp^R	P. Ainsworh
pPA019	c*heB* cloned into the pTrcHisB multiple cloning site	479	Amp^R	P. Ainsworh
pPA021	*cheY* cloned into the pTrcHisB multiple cloning site	430	Amp^R	P. Ainsworh
pPA025	c*heA* response regulator domain (including CheW domain) cloned into the pTrcHisB multiple cloning site	1972	Amp^R	P. Ainsworh
pPA035	c*heV* cloned into the pGex-4T-1 multiple cloning sites	968	Amp^R	P. Ainsworh
pPA024	*cheA* histidine kinase domain (ΔRR	1906	Amp^R	P.

	and ΔCheW domain) cloned into the pTrcHisB multiple cloning site			Ainsworh
pPA037	c*heY* cloned into the pGex-4T-1 multiple cloning site	430	Amp^R	(Bridle 2007)
pRR53	*racS* cloned into the pTrcHisB vector	1236	Amp^R	R. Ran
pRR46	*racR* cloned into the pTrcHisB vector	573	Amp^R	R.Ran

Table 6. Plasmids constructed for bacteria two hybrid assays.

Plasmid	**Description**	**Size in bp**	**Antibiotic resistance**	**Source**
pKT25-CheY	*cheY* construct into C-terminal of pKT25 plasmid multi-cloning site.	417	Amp^R	(Bridle 2007)
pKT25-CheV	*cheV* construct into C-terminal of pKT25 plasmid multi-cloning site	968	Km^R	(Bridle 2007)
pKT25-CheB	*cheB* construct into C-terminal of pKT25 plasmid multi-cloning site	575	Km^R	(Bridle 2007)
pKT25-CheA	*cheA* (response regulator domain) construct into C-terminal of pKT25 plasmid multi-cloning site	1972	Km^R	(Bridle 2007)
pUT18-Cj0700	*cj0700* gene into C-terminal of pUT18 plasmid multi-cloning site	722	Amp^R	(Bridle 2007)

2.2. Chromosomal DNA Extraction

Chromosomal DNA of *C. jejuni* was prepared by the modified method of Chen and Kuo (1993). *C. jejuni*, grown to confluence on MHA for 2-4 days, was scraped off into 2 ml or 10 ml of MHB. The cell suspension was transferred into a micro-centrifuge tube and centrifuged at 11300 xg for 3 min, or for larger volumes, centrifuged at 3500 xg for 15 min. Pelleted cells were re-suspended in 600 µl of buffer 1 (40 mM Tris-acetate pH 7.8, 20 mM sodium acetate, 1mM EDTA, 1% SDS). Next, 200 µl of 25 mM NaCl was added to the lysate and mixed by shaking. Proteins and cell debris were pelleted by centrifugation at 11300 xg for 15 min. The supernatant was transferred into a micro-centrifuge tube and 600 µl of

chloroform/iso-amyl alcohol (24:1, v/v) was added and mixed by inverting the tube approximately 100 times. The upper layer was transferred into a new micro-centrifuge tube. This was repeated twice. The separated top layer was added to an equal volume of 100% ethanol and mixed by inversion before centrifugation at 11300 xg for 5 min. Finally, the supernatant was mixed with 800 µl of 70 % ethanol and centrifuged at 11300 xg for 2 min. The dried pellet was re-suspended in H_2O.

2.3. Plasmid DNA Extraction

For plasmid extraction, *E. coli* was grown in LB overnight at 37 ^{o}C with suitable antibiotic supplementation. Then the cell suspension was used to extract plasmid DNA with small size plasmid/DNA preparation kit (Omega, Bio-Tek. Inc, USA) according to the manufacturer's instructions. The concentration of extracted plasmid DNA was quantified either by comparison to a DNA standard following agarose gel electrophoresis or by Nano Drop 2000C (Thermo Scientific, UK). Purified plasmids were stored at -20 ^{o}C for future use.

2.4. Molecular biology methods

2.4.1. PCR

PCR for cloning (Sambrook, 2001) genes from *C. jejuni* and *E. coli* strains used high fidelity Phusion DNA polymerase (New England, Biolabs, UK) according to the instructions provided by manufacturer in order to reduce the incorporation error rate. However, with PCR for testing primer specificity and screening for recombinant clones, Taq DNA polymerase (New England, Biolabs® inc., UK) was used.

Normally, 10 µl and 50 µl reaction volumes were used with a concentration of 1x reaction buffer comprising 1.5 mM $MgCl_2$; 10 pmol dNTP; 10 pmol primers; 1-30 ng chromosomal DNA template (1-30 ng chromosomal DNA or 1-20 ng plasmid DNA). For every PCR

reaction and dilutions as well, autoclaved ddH_2O was utilised. DNA amplification was carried out in a thermal cycler (Eppendorf, Scientific Support Inc., UK) using the cycle programs shown in table 7. The extension time and annealing temperature was varied according to the primers used (Table 8).

2.4.1.1. Colony PCR

Colony PCR was used to verify the presence of a correct recombinant plasmid directly from transformants isolated on selective agar. Colonies were picked by toothpick and re-suspended in 100 µl of distilled water in a 500 µl PCR micro-centrifuge tube. The same toothpick was used to streak the individual clones onto on selective agar and the plate was incubated at 37 ^{o}C to provide a stock of each clone. The cell suspension was heated at 98 ^{o}C for 5 minutes then cells were centrifuged at 1100 xg for 3 min. Finally the PCR reaction was performed according to the conditions described above and shown in table 7.

Table 7. PCR conditions.

Step	Temperature ^{o}C	Time
1	98 ^{o}C	1 min.
2	98 ^{o}C	30 sec.
3	5-10 ^{o}C below melting temperature of primers	15 sec.
4	72 ^{o}C	1 Kb/ 1 min.
5	Repeat step 2 to step 4 for 29 times	
6	72 ^{o}C	5 min.
7	end	

2.4.1.2. PCR primers

The oligonucleotide primers for this study were designed using Clone Manager (version 8, Scientific and Educational Software, 2006) software and synthesised by Sigma-Aldrich (UK). In addition, necessary primers also incorporated restriction sites at the 5' end to facilitate subsequent cloning of amplified fragments. Template of sequences of *cj0700* and other genes in *C. jejuni* for primer use in primer design were acquired from the CampyDB data base (http://campy.bham.ac.uk). All primers sets used in this study are listed in table 8.

Table 8. List of primers used in this study. Restriction enzyme sites are underlined.

Primer name	**Sequence (5' -> 3')** **Restriction sites are underlined**	**RE**
Cj0700 cloning primers		
cj0700-F	CCCGGATCCGCGGCCGCCAGTATCAGCTATGC CACTATT	*Bam*HI, *Not*I
Cj0700-R	CCCGGATCCGCGGCCGCGCACAAGATCCACGA TTG C	*Bam*HI, *Not*I
GlnAF	CCCGAA CAT TGT CAG CTG CT	N/A
Cj0701R	CCCGGA CGC GAA ACA AGA TA	N/A
Complementation primers		
Ccj0700F2	GGGAGATCTCATGGTTTTTACTCCTTTATGT	BglII
CCj0700_F	CCCCCATGGTTTTTACTCCTTTATGTAATTAA	*Nco*I
CCj0700_R	CCCCCATGGTCATTTTTGCCCTAAAC	*Nco*I
Cj0046 F	CTCTCTCCGCTAGAAATTAAATCC	N/A
KmF	GGGAGATCTAAATTAAAAAGCTAGGCCG	BglII
Cj0700 inverse PCR primers		
cj0700-invr-2	CCCAGATCT GCT TTA AGC CGT TAT ATG AGT	*Bgl*II
cj0700-invr-2	CCCAGATCT GCT TTA AGC CGT TAT ATG AGT	*Bgl*II
Chloramphenicol resistance cassette primers		
CATinvF	GGAATGTCCGCAAAGCCTAATCC	N/A
CATinvR	GCGGTCCTGAACTCTTCATGTC	N/A
Kanamycin resistance cassette primers		
BNKanFpt	TTTGGATCCGCGGCCGCAGAGGAAGGAAATA ATAAATGGC	*Bam*HI, *NotI*
BNKanRpt	TTTGGATCCGCGGCCGCTAGGTACTAAAACAA TTCATCCAG	*Bam*HI, *Not*I
BNErmFpt2	TTTGGATCCGCGGCCGCTAAAGAGGGTTATAA TGAACGAG	*Bam*HI, *Not*I
BNErmFpt1	TTTGGATCCGCGGCCGCCATGCAAGCTAGCTT TGGC	*Bam*HI, *Not*I

BNErmRpt	TTTGGATCCGCGGCCGCCTTACTTATTAAATA ATTTATAGCTATTG	*Bam*HI, *NotI*
M13 primers		
pUCF	GCCAGGGTTTTCCCAGTCACGA	N/A
pUCR	GAGCGGATAACAATTTCACACAGG	N/A
Site direct mutagenesis primers		
single cj0700 mutagenesis R	TTGACGATGTATATTTTGATACTG	N/A
single cj0700 mutagenesis F	ATGCAGTATCAAAATATACATCGTCAA	N/A
double cj0700_F mutagenesis	GATGCAATGCAGTATCAAAATATACATCGTCG TAAAATCGAACGTGTTATTAATGTAATG	N/A
double cj0700_R mutagenesis	CATTACATTAATAACACGTTCGATTTTACGAC GATGTATATTTTGATACTGCATTGCATCC	N/A
Cj0700 expression primers		
HisF_700	CGGGATCCGACTCAAGAAGAGCTTGATG	*Bam*HI
HisR_700	GGAATTCTCATTTTTGCCCTAAACTTG	*Eco*RI
Cj0700_HisF	CCCGGATCCATGACTCAAGAAGAGC	*Bam*HI
Cj0700_HisR	CCCGAATTCTCATTTTTGCCCTAAACTTG	*Eco*RI
Cj0700_GSTF	CCCGAATTCATGACTCAAGAAGAGCTTG	*Eco*RI
Cj0700_GSTR	CCCGTCGACTCATTTTTGCCCTAAACTTG	*Sal*I
Other primers		
CheV_flag_ R_NotI	GCGGCCGCAGAACCCCCCATGGTTTATTCCTC	*Not*I
CheV_flag_ F_NotI	GCGGCCGCGATTACAAGGATGACGATGACAA GGGTATGGCTAGCATGAC	*Not*I
CheA_RR_flag_ F_NotI	GCGGCCGCGATTACAAGGATGACGATGACAA GGGTATGGCTAGCATGACTG	*Not*I
CheA_RR_flag_R _NotI	GCGGCCGCAGAACCCCCCATGGTTTA	*Not*I
pTrcFlag_F_NotI	GCGGCCGCGATTACAAGGATGACGATGACAA GGGTATGGCTAGCATGACTG	*Not*I
pTrcFlag_R_NotI	GCGGCCGCAGAACCCCCCATGGTTTATT	*Not*I
CheZ-R reverse	CATGCCATGGTCGTCAGCAGGTTTGATTG	*Nco*I
cheZ-F inverse	CATGCCATGGAGGTGGACGATTTGTTGGATAG	*Nco*I
Hp0170_F	CATGCCATGGCTAAAATGACAGCCGATAAA	*Nco*I
hp0170_R	CATGCCATGGCCATTGATCGTGGCATAGAC	*Nco*I

2.4.2. Sequencing

Sequencing of DNA templates was carried out using the Big Dye 3.1 terminator kit obtained from Protein and Nucleic Acid Chemistry Laboratory (PNACL; University of Leicester). The standard sequencing reaction mixture of 10 µl total volume was made up from DNA template (≥ 100 ng); plasmid (≥ 20 ng) ; primer and Big Dye 3.1 (1/8 dilution of 5x sequencing buffer and H_2O). Table 9 details the thermal cycling conditions used for sequencing reactions. Afterwards, the sequencing reaction product was mixed with 2 µl of 2.2% SDS, heated at 98 ^{o}C for 5 minutes and purified using by Cycle Pure Kit according to manufacturer's instructions to get rid of excess terminator. Finally, the sequencing reaction was sent to PNACL.

Table 9. Standardised sequencing PCR condition.

Step	**Temperature ^{O}C**	**Time**
1	95 ^{o}C	5 min.
2	96 ^{o}C	10 sec.
3	50 ^{o}C	10 sec.
4	60 ^{o}C	4 min.
5	Repeat step 2 to step 4 for 29 times	
6	60	5 min.
7	end	

2.4.3. Enzymatic modification of DNA

All restriction enzymes and buffers were acquired from NEB (New England Biolabs Ltd, Hitchin, UK) and used in accordance with manufacturer's instructions. Generally, a restriction mixture of 50 µl reaction volume was used and incubated at 37 ^{o}C in a water bath for 3 hours.

Restricted PCR products and plasmids were treated with Shrimp Alkaline Phosphatase (SAP, Roche Diagnostics, Germany) to remove 5' phosphate with the purpose of reducing self-ligation of DNA templates. Dephosphorylation reactions were carried out in a 50 µl total volume and incubated for 1 hour at 37 ^{o}C in accordance to manufacture's guidelines.

Ligation reactions were carried out using a molecular ratio of 3:1 of insert to vector. Ligation reactions consisted of 10X buffer (NEB), T4 DNA ligase 5-10 units for 1 µg of DNA, 10 mM ATP, sterile H_2O and DNA template in a total of 10 µl. Reactions were incubated overnight at RT and then ethanol precipitation was used to prepare the ligation products for transformation.

2.4.4. DNA purification

Ethanol precipitation of DNA was used to desalt, concentrate or change buffering conditions of purified DNA fragments. Briefly, DNA was precipitated by adding 1/10th to reaction volume of 3 M sodium acetate, 2.5 volumes of ice-cold 100% ethanol and 10 mM of tRNA. Following 5 min incubation on ice, precipitated nucleic acid was pelleted at 11300 xg for 10 minutes. Finally, the DNA pellet was washed in 70% (v/v) ethanol (800 µl), re-centrifuged at 11300 xg for 2 min, the ethanol was aspirated and the pellet was dried. DNA was re-suspended with sterile dH_2O and stored at -20 ^{o}C until used.

Amplified DNA products derived from PCR were purified from primers, primer dimers, salts and enzymes using the E.Z.N.A. Cycle Pure kit (Omega, Bio-Tek. Inc, USA). DNA was re-suspended with sterile dH_2O and stored at -20 ^oC until used.

The Zymoclean Gel DNA recovery Kit was used to purify PCR products/plasmids excised following agarose gel separation. DNA fragments, visualised under UV light following EtBr staining, were excised using a sterile razor blades or scalpel. The sliced gel was transferred into a 1.5 ml micro-centrifuge tube, weighed and 3 gel volumes (1g ~ 1 µl) of agarose dissolving buffer (ADB) was added. Gel and buffer mixture were incubated at 55 ^oC in a water bath until the gel-slice was completely dissolved. After that, the dissolved mixture was transferred into a Zymo-spin column, before centrifugation at 11300 xg for 1 min and subsequently washed with DNA wash buffer and centrifugation at 11300 xg for 1 min. Finally, DNA was eluted in ddH_2O and stored at -20 ^oC for later usage.

2.5. Transformation

2.5.1. Preparation of competent cells

Competent host cells of *E. coli* were prepared for either transformation by heat shock ($CaCl_2$) or electroporation technique. *C. jejuni* was transformed by electroporation or taking advantage of its natural competence, by natural transformation.

2.5.1.1. Electroporation technique

Prior to transformation by electroporation, plasmids or ligation reactions were prepared by removal of excess salts as described in section 2.4.4, with the purpose that competent cells could easily take up DNA by electrical pulse under low ionic conditions.

2.5.1.1.1. Campylobacter jejuni

C. jejuni cells were grown on Mueller-Hinton plates added with vancomycin and trimethoprim (MHA-VT) and were grown for 32 hours at 42 ^{o}C micro-aerobically in VAIN. The cells from each plate was scrapped off into 2 ml of MH broth and transferred into a 1.5 ml micro-centrifuge tube and pelleted at 1100 xg in an Eppendorf MiniSpin Plus centrifuge for 5 minutes at RT. Next, the supernatant was discarded and the pellet was re-suspended in filter sterilised ice-cold washing buffer (272 mM sucrose, 15% (v/v) Glycerol, sterilised using a 0.2 µm Acrodisc PALL Life Sciences, Portsmouth UK). Centrifugation of the cell suspension was repeated three times each time adding 1 ml of ice-cold wash buffer. Finally, the pellet was re-suspended in 200 µl ice-cold washing buffer, snap frozen on dry ice and stored at -80 ^{o}C. Before transformation, cuvettes, DNA and *C. jejuni* competent cell were kept on ice. Then, 5 µl (1-5 ng) of DNA was transferred to pre-chilled cuvette and 50 µl of competent cell added and both were mixed together. The cell suspension-DNA mix was pulsed once using GenePulser electroporator (Bio-Rad) set as 2.5 KV, 200 Ω and 25 µF. The optimum time constant (resistance-capacitance time constant) was 4.6 (ms) units. Finally cells were flushed from the cuvette with 1000 µl of MHB, spread on non-selective MHA plates and incubated overnight at 42 ^{o}C micro-aerobically in the VAIN to allow for expression of antibiotic resistance genes. Following overnight growth, cells were harvested from the non-selective plates with 1 ml of MHB and spread (1/10 and 9/10 dilutions) on MHA plates containing appropriate selection and incubated in the VAIN at 42 ^{o}C for 3-5 days.

2.5.1.1.2. E. coli

E. coli was grown on LA plates overnight at 37 ^{o}C. The cultured cells were removed into 2 ml Luria broth or 1 ml O/N grown cells were diluted into 10 ml LB and further grown with shaking till cells reached an OD of 0.5 at 600 nm. Cells were transferred to a 1.5 ml micro-centrifuge tube and pelleted as described in section 2.5.1.1.1. The cell pellet was re-suspended in filter sterilised ice cold *E. coli* electroporation buffer (1mM MOPS, 20 % (v/v) glycerol). Washing steps were repeated twice followed by resuspension in 200 µl of buffer. Finally competent cells were snap frozen on dry ice and stored at -80 ^{o}C.

E. coli competent cells, cuvettes and DNA were kept on ice. A 5 µl volume (1-5 ng) of plasmid DNA or ligation mix was transferred to the pre-chilled cuvette, mixed carefully with 50 µl *E. coli* competent cells and then electroporated as above with settings of 2.5 KV, 1000 Ω and 25 µF.

Cells were pulsed once and the resultant time constant was normally 22.6 ms. If constant times were less than 18, it was considered poor transformation; extra washing with ice-cold solution stopped this phenomenon. Immediately following electroporation, cells were flushed with 1 ml of SOC (Table 14), and incubated at 37 ^{o}C for an hour. Then transformed cells were spread on (1/10 and 9/10 dilution) LA selective plates and incubated aerobically O/N at 37 ^{o}C.

2.5.1.2. Preparation of heat shock competent cells

Chemically competent cells for $CaCl_2$ transformation were prepared from *E. coli* strains: DH5αE, BL21, XL-1blue and Rosetta. Briefly, 50 µl of $CaCl_2$ as heat shock method competent cells and 5 µl of plasmid DNA (1-5 ng) were mixed in a 1.5 ml micro-centrifuge tube and kept on ice for 25 minutes. The mixture was transferred into a water bath and incubated for 5 minutes at 37 ^{o}C before being placed on ice for 5 minutes. After that, the cell

mixture was flushed with 950 µl of LB and incubated at 37 ^{o}C for an hour. Transformed cells were spread on to (1/10 and 9/10 dilution) LA plates and incubated overnight at 37 ^{o}C with appropriate selection.

2.5.1.3. Natural transformation

C. jejuni is a naturally competent species, such that it uptakes DNA from its surroundings through cell surface binding and transfers the DNA into the cytoplasm. One strand is degraded whilst the complementary strand recombines into the chromosome of *C. jejuni* through homologous recombination (Fitzgerald *et al*., 2005, Wang *et al*., 1990).

2.5.1.3.1. Campylobacter jejuni

C. jejuni cells were grown on MHA at 42 ^{o}C for 12-32 hours then harvested with 2 ml MH broth and the cell density adjusted to 0.5 OD (600 nm) using a spectrophotometer. Subsequently, 500 µl of this cell suspension was transferred to a 15 ml sterile a Falcon tube containing 1 ml MHA. Initially, the cell suspension was incubated at 42 ^{o}C in the VAIN for 3 hours before 5 µl (1-5 ng) of DNA was added and the mix incubated statically O/N at 42 ^{o}C. The cell suspension was carefully removed from the surface of the MHA, and dilutions spread (1/10 and 9/10) onto MHA selective plates. Alternatively, 100 µl of adjusted cell suspension (0.5 OD_{600}) and 5 µl (1-5 ng) of DNA were spread on to non-selective MHA and incubated overnight at 42 ^{o}C in the VAIN. Then transformants were harvested and dilutions spread (1/10 and 9/10 dilution) onto MHA plates containing appropriate selection. Plates were incubated at 42 ^{o}C in the VAIN for 3-5 days.

2.6. Screening recombinants

2.6.1. Antibiotic resistance selection and white/Blue screening for recombinants

The presence of *cj0700* recombinant (pUC19::cj0700) in the *E. coli* strains was screened detecting white colour. Intact *lacZ* gene expresses β-galactosidase enzyme and can be detected using X-gal which shows blue clones on the plates. Nevertheless, the presence of white clones indicates recombination was successful, as an insertion interrupts expression of *lacZ* reporter gene. The Blue/white screening method, LA plates were supplemented with IPTG (40µg/ml) and X-gal (30µg/ml), and then cells were incubated overnight at 37 ^{o}C. Hence, white *E. coli* colonies carrying possible recombinant plasmid were selected and screened as mentioned in section 2.4.1. 1.

For the maintenance of plasmid presence and selection of transformants and chromosomal insertion mutants, solid and liquid media were supplemented with appropriate antibiotics to select for the presence of antibiotic resistance genes. In this study, antibiotics used for selection of *E. coli* and *C. jejuni* strains are presented in table 10.

Table 10. Antibiotics used for selection of strains and plasmids.

Name	Stock Concentration	Diluted with	Final Concentration
Trimethoprim	5 mg/ml	50% EtOH	5 μg/ml
Vancomycin	10 mg/ml	ddH_2O	10 μg/ml
Chloramphenicol	20 mg/ml	50% EtOH	20 μg/ml
Kanamycin	50 mg/ml	ddH_2O	50 μg/ml
Ampicillin	100 mg/ml	ddH_2O	100 μg/ml
Erythromycin	5 mg/ml	50% EtOH	5 μg/ml
Tetracycline	10 mg/ml	50% EtOH	10 g/ml

2.7. Preparation of *C. jejuni* motile variants

Wild-type motile variant of *C. jejuni* NCTC 11168 employed in this study was originally isolated by Bridle (2007). All mutations constructed in *C. jejuni* were produced in wild-type NCTC11168, verified, and then transferred by natural transformation into a motile variant of NCTC11168 for phenotype testing. Motile variants were also used for mutants in NCTC11828 and 81-176.

2.8. Chemotaxis and motility assay

2.8.1. Motility test

In order to determine motility visually, bacteria cells were assessed microscopically. *C. jejuni* strains were grown on MHA plates O/N at 42 ^{o}C under microaerobic conditions. Then cells were harvested with 0.5 ml MH broth, 20 μl of cell suspension spotted at the centre of a glass-slide and covered with a cover-slip. Motility of the cells was examined by phase contrast microscopy, where motile *C. jejuni* were characterised by darting quickly in the field and changing direction.

2.8.2. Swarming assay

Swarming assay was established on a modification of the method of Wolfe et al. (1989), where *C. jejuni* was grown O/N at 42 ^{o}C in 5 ml MH broth and supplemented with vancomycin and trimethoprim. A 20 µl of overnight cell suspension (1.0 OD_{600}) was spotted at the centre of a semisolid MHA (0.4 % agar) plate and incubated at 42 ^{o}C micro-aerobically in the VAIN for 3-5 days. Plates were viewed under indirect light (Syngene Gene, Cambridge, UK) in the dark room and photographed.

2.8.3. Growth assay

C. jejuni NCTC 11168 strains were inoculated into 7 ml of MHB supplemented with vancomycin and trimethoprim and then grown overnight at 42 ^{o}C in the VAIN. Afterwards, 0.05 OD_{600} of cells from overnight culture was inoculated into 5 ml MH broth supplemented with vancomycin and trimethoprim and further incubated at 42 ^{o}C with shaking under microaerobic conditions. Growth of *C. jejuni* NCTC11168 cells was measured every 12 hours up to 72 hours. Alternatively, *C. jejuni* strains were grown overnight at 42 ^{o}C in the VAIN on MHA plates supplemented with vancomycin and trimethoprim. Then, cells were further inoculated into 5 ml MHB and incubated overnight at 42 ^{o}C with shaking under micro-aerobic conditions. After that, 0.05 OD_{600} of cells from the overnight culture was inoculated into 1 ml MHB and subsequently 200 µl pipetted into 96 microtiter plates, sealed with gas permeable film and incubated overnight at 42 ^{o}C with shaking under micro-aerobic conditions for 24 hours. Cell growth was measured every 3 hours post inoculation.

2.8.4. Phosphate release assay

2.8.4.1. CheY dephosphorylation assay

The purity of proteins for this assay was confirmed utilising sodium dodecyl sulphate polyacrylamide gel electrophoresis (SDS-PAGE) and Western blot analysis to avoid any artefacts produced by contamination of other proteins. The CheY phosphorylation/de-phosphorylation assay was carried out *in vitro* using γ^{32}-P (3000 Ci/mmol and 10µCi/µl) ATP. Hence, 120 µl of ice-cold reaction buffer (50 mM Tris-HCl (7.5), 50 mM KCl, and 20 mM $MgCl_2$) was added 20 µCi of the (γ^{32}-P) ATP was diluted with 10 mM ATP and 5 µM CheA-HK. This reaction mixture was incubated for 10 minutes at 30 ^{o}C. Then, 10 µl of this mixture, containing CheA-HK exposed to γ^{32}-ATP, was transferred into a 0.5 ml microcentrifuge tube containing an equal volume of 2xSDS sample loading buffer for inactivation. This sample formed the pre-CheY interaction control. Next, 50 µl of the reaction mixture was transferred into one 0.5 ml microcentrifuge tube containing 15 µM CheY and another 50 µl of reaction mixture was placed into a 0.5 ml tube containing 15 µM CheY and 15 µM Cj0700. Pi transfer from CheA-HK to CheY and release rate from CheY-P was monitored at 0, 30, 60 and 90 seconds by the removal of 10 µl of reaction mixture at each time point, inactivating the reaction with an equal volume of 2xSDS sample loading buffer and placement on ice. For each time point, 15 µl of reaction mixture in sample loading buffer was run on a 15% SDS-PAGE. The gels were dried with a heat vacuum drier for 2 hours then transferred to a phosphor screens overnight at RT to visualise radiolabelled proteins. Finally, γ^{32}-P signal intensity was analysed in a Typhoon 9400 Variable Mode Imager (Amersham Biosciences).

2.8.4.2. CheA-RR dephosphorylation assay

This assay was designed to examine the *in vitro* effect of putative phosphatase Cj0700 against CheA-RR-Pi phosphorylated by CheA-HK. The assay was carried out as described in section 2.8.4.1 above with the exception of the CheA-RR concentration, reaction temperature and sampling time points being modified. Briefly, radioactive (γ^{32}-P) ATP was mixed with 5 µM CheA-HK in 70 µl of reaction buffer and incubated at 30 ^{o}C for 10 minutes. As a control, 10 µl of this reaction was transferred into a 0.5 ml microcentrifuge tube containing 2xSDS sample loading buffer. Next, 25 µl of the reaction mixture was aliquoted into one 0.5 ml microcentrifuge tube containing 5 µM CheA-RR and another 25 µl of reaction mixture was placed into a separate 0.5 ml tube containing 5 µM CheA-RR and 15 µM Cj0700. The concentrations of CheA-RR in both mixtures were kept equal by adjustment with storage buffer.

The assay was carried out at 30^{o}C in a heat block and samples were taken at 5, 10, 20 and 30 min time points. At each time point 10 µl of reaction mixture was inactivated with an equal volume of 2xSDS sample loading buffer on ice. Next, 15 µl reaction samples were run on 10% SDS-PAGE, and prepared for imaging by Typhoon densitometry (Amersham Biosciences) as before.

2.8.4.3. CheV dephosphorylation assay

To examine the dephosphorylation of phosphorylated CheV-P by Cj0700, the assay was carried out as above with following modifications. 10 µM CheV was mixed with 5 µM CheA-HK and with 15 µM Cj0700. Samples were taken at 0, 30, 60 and 90 seconds time points and γ^{32}-P signal intensity of the samples was analysed as before.

2.8.4.4. RacR dephosphorylation assay

The aim of this *in vitro* assay was to examine whether putative Cj0700 phosphatase could dephosphorylate an unrelated two component regulatory system, RacRS. Similar to the CheA-based assays (Section 2.8.4.1), 10 µM RacS-HK was exposed to 5 uCi (γ^{32}-P) ATP in a 60 µl reaction buffer for 10 minutes. After that, 25 µl of RacS-HK reaction was put in to a 0.5 ml microcentrifuge tube and then mixed with 20 µM RacR. Likewise, 25 µl of RacS-HK reaction was put in another 0.5 ml tube, which was then mixed with 20 µM RacR and 15 µM Cj0700. The assay was carried out at 30 ^{o}C in a heat block with samples taken at 5, 10, 20 and 30 minutes time points. At each time point 10 µl of reaction mixture was inactivated in 2xSDS sample loading buffer on ice. Then, 15 µl was run on 10% SDS-PAGE and the gels were then dried with a heat vacuum drier for 2 hours. Gels were transferred into a phosphor screen overnight at room temperature. Finally, γ^{32}-P signal intensity was analysed in a Typhoon 9400 Variable Mode Imager (Amersham Biosciences).

2.9. Expression and Purification of proteins tagged proteins

Proteins wee expressed for purification using IPTG induction of recombinant plasmids in *E. coli* BL21 or Rosetta followed by His-tagged and GST-tagged chromatography.

Details of each protein purification scheme will be discussed in detail in the next sections.

2.9.1. Histidine tagged proteins

Proteins under study were cloned so as to construct a 6xhistidue residues fusion at the C-terminus. The His tagged proteins were purified through affinity Hi trap FF columns packed with Sepharose and pre-charged Ni^{2+} resins (GE Healthcare Life sciences). The purity of these fusion proteins was normally evaluated using SDS-polyacrylamide electrophoresis gel analysis. Further details of expression and purification methods of his tagged fusion proteins

are described in next sections. Normally 1000 ml cell cuture produced about 2 mg of His fused protein.

2.9.1.1. His-tagged Cj0700

The open reading frame (ORF) of *cj0700* was fused at the C-terminal to 6xhistidine residues in pLEICS03 (PROTEX, University of Leicester). The *pLeics03*::*cj0700* construct (pAJ8) was transformed into *E. coli* BL21 (section 2.5). In addition, construct of cj0700 (D167N) mutant was cloned into His tagged pLEICS03 plasmid. It was achieved by removing the aspartic acid coding sequence and replaced asparagine coding sequence sequence by site directed mutagenesis. An inverse PCR product was made using inversely overlapping primers (Table 8) each with an asparagine coding sequence attached at the 5' end, using pAJ8 plasmid as a template. The His-tagged pAJ8 plasmid was amplified leaving out the aspartic acid coding sequence and inserting the asparagine coding sequence creating a *cj0700* (D167N) mutant plasmid. The resultant plasmid was sequenced and named pAJ7, then transformed into *E. coli* strain BL21 for later expression work.

The pAJ and pAJ8 plasmids in *E. coli* BL21 cells were inoculated into 5 ml of Luria broth supplemented with kanamycin in a 15 ml test tube and incubated overnight at 37 ^{o}C with shaking at 250 rpm. Overnight cell cultures were diluted 1/100 with LB without antibiotics and grown until cell density reached 0.5 OD_{600}. Afterwards, 1.0 mM IPTG was added to the cell suspension so as to induce Cj0700 protein expression and incubated at 30 ^{o}C for 3 hours with shaking. Cells were centrifuged at 3200 xg at 4 ^{o}C for 20 minutes. The cell pellet was stored at 4 ^{o}C or at -80 ^{o}C depending on the required storage period. Cell pellets were re-suspended with binding buffer (Table 13) containing protease inhibitor (Roche); 1 tablet for each 10 ml cell suspension and 0.35 mg/ml lysozyme enzyme (Sigma, UK) were added before incubating at room temperature for 1 hour with rocking. The cells were physically

lysed by using a Bioruptor sonicator (Diagenode, Belgium). During sonication, the cell suspension was lysed in ice cooled conditions with 30 seconds on/off for 5 minutes, and subsequently cell lysates were centrifuged at 3200 xg for 20 minutes at 4 ^{o}C.

The protein purification stage was carried out at 4 ^{o}C and supernatants of cell lysates were run through pre-equilibrated HisTrap FF columns with Ni^{2+} Sepharose packed (GE Healthcare Life sciences) resins which have affinity for His-tagged fusion protein. Briefly, each column was washed through with 25 ml of ddH_2O to remove residual alcohol and then equilibrated with 25 ml binding buffer at 4 ^{o}C. Cj0700 fusion protein was run through the column which was then washed three times with 25 ml binding buffer before it was eluted with 15 ml elution buffer (Table 13). Eluates were stored at 4 ^{o}C, before processing by centrifugation at 3200 xg for an hour at 4 ^{o}C using an Amicon Ultra-15 Centrifugal Units column (Millipore, UK). Purity of Cj0700 protein was determined using a SDS-PAGE. Purified proteins were removed from elution buffer and replaced in storage buffer using the Amicon Ultra-15 Centrifugal Units column (Millipore, UK). Finally, Cj0700 fusion protein was concentrated using Amicon Centrifugal Units columns (Millipore, UK) and the yield using calculated by Bradford assay standard curve (BioRad).

Plasmids pPA024, pPA016, pPA021, pPA025, pRR53 and pRR46 expressing CheA-HK, CheY, CheA-RR and CheV, RacS and RacR His-fusions (Table 5) were transferred into *E. coli* Rosetta cells. Each His-fused protein was expressed and purified using the same method as described for pAJ and pAJ8 plasmids with following modifications. Plasmids pPA016, pPA021, pPA025 and pRR46 were expressed at 37 ^{o}C.

2.9.2. GST tagged proteins

Coding sequence of each protein to be fused to GST was cloned so as to construct a C-terminus Glutathione S-transferase residue fusion. The GST tagged proteins were purified through affinity Hi trap FF columns packed with Sepharose and glutathione (GE Healthcare Life sciences). The GST fusion proteins were contained 26 kDa size GST protein. Purity of these proteins is evaluated as above (Section, 2.9.1). Generally 1000 ml of cell culture produced 3-4 mg of GST tagged fused protein.

2.9.2.1. GST-tagged Cj0700

In order to form a C-terminus fusion of GST to Cj0700, the coding sequence of Cj0700 was cloned into pGEX-4T-1 GST tagged expression vector. The pEKG1 (pGEX-4T-1: cj0700) plasmid in *E. coli* BL21 cells were expressed as above described (2.10.1.1).

For expressed GST fused to Cj0700 protein purification, a 1 ml GST Trap FF (GE Healthcare Life sciences) column was washed through with 5 ml ddH_2O and then 5 ml of PBS binding buffer (Table 13**)** to pre-equilibrate. Next, the supernatant of cell lysis was run through the column and this was washed three times with PBS before the Cj0700 protein was eluted with 10 mM reduced glutathione in PBS. Purified eluates were washed in 5 ml to remove elution buffer and replace with storage buffer using the Amicon Ultra-15 Centrifugal Units column (Millipore, UK). Finally, GST-Cj0700 fusion protein was concentrated using Amicon Centrifugal Units column (Millipore, UK) and the yield calculated using a Bradford assay standard curve (BioRad).

Plasmids pPA037, pPA025 and pPA035 expressing CheY, CHeA-RR and CheV GST-fusions respectively were transformed into *E. coli* Rosetta and each GST-fusion protein expressed and purified as described for pEKG1 plasmid.

2.9.3. Flag tagged proteins

Flag-tagged proteins produced from *E. coli* BL21 (pTrcFlag:*cheV*) and (pTrcFlag:*cheA*) were expressed and purified as follows.

2.9.3.1. Flag tagged plasmid

The plasmids carrying flag tag gene fusions were created by an inverse PCR mutagenesis scheme using a plasmid containing the target gene derived from a pTrcHisB vector (Table 3). Primers were designed to anneal either side of the His tag sequence with the 5' ends proximal to the target coding sequence to create a PCR product without the His tag. Then the PCR product was digested with *Not*I restriction enzyme, ligated and transformed into *E. coli* BL21. For expression, cultured cells were exposed to 1 mM IPTG growth media as described previously for expression of other fusion proteins used in this study. Cells were lysed using TBS buffer (Table 13).

Expressed Flag tag fused protein purification involved the use of anti-Flag M2 magnetic beads (Sigma-Aldrich, UK). 200 µl magnetic beads were put into 1.5 ml microcentrifuge tubes, and then the beads were washed and equilibrated with 1 ml ice-cold TBS buffer four times. Finally, Flag-fused proteins were eluted with elution buffer (0.1 M Glycine-HCl; table 13).

2.10. Pull-down

GST, GST-CheY, GST-CheA-RR and GST-CheV fusion proteins were immobilised on beads of glutathione Sepharose 4B resin as the bait protein then His-Cj0700 tagged protein was added and protein-protein interactions determined by pull-down assay. Alternatively, tagged GST-Cj0700 was immobilised on glutathione beads and tagged His-CheY, His-CheA-RR and His-CheV proteins were used to investigate interactions. Finally, Flag tagged CheV and CheA-RR proteins were immobilised on anti-Flag magnetic beads ((Sigma-Aldrich, UK), and then His-Cj0700 was used and any protein-protein interactions characterised.

Pulled down proteins were eluted from beads with 1x SDS sample loading buffer and visualised using 10-15% SDS-PAGE followed by coomassie blue staining. In addition, proteins were visualised by western blotting, where the sample proteins were transferred to a PVDF membrane and proteins probed with primary (anti-His) and secondary (anti-anti-His horseradish peroxidase complex) conjugate antibodies at 1:20000 and 1:40000 dilutions respectively. Finally, proteins were detected by enhanced chemilunescence reaction using HRP conjugate.

2.10.1. Cj0700 pull down to response regulator fusion proteins

The interaction assay between His-Cj0700 and GST-CheY, GST-CheA-RR protein was carried out. His-CheV and His-CheA-RR proteins were combined with tagged GST-Cj0700 fusion protein. To immobilise GST tagged proteins, 10 µl glutathione beads were transferred into a 1.5 ml microcentrifuge tube and kept on ice. According to manufacturer's instructions, beads were washed four times with 100 µl TGEM (0.1 M NaCl) buffer. After the last wash beads were re-suspended in 30 µl of the same buffer and 20 µl of 1% BSA added before transfer to ice. GST-CheY and GST-Cj0700 proteins were diluted with TGEM (0.1) buffer.

Subsequently 40 µl of 0.5 µg of each protein was added into the glutathione resin bead mix and incubated at 4 ^{o}C for an hour with slow shaking to mix. The mixture was washed twice with 100 µl ice-cold TGEM (1 M NaCl) buffer followed by two washes with 100 µl ice-cold TGEM (0.1 M NaCl) buffer. Then, after the last wash 20 µl of ice-cold TGMC (0.1 M NaCl) was added to retain hydration of the beads. His-Cj0700, His-CheA, His-CheA-RR and His-CheV tagged proteins were diluted with ice-cold TGMC (0.1) buffer. A 30 of µl volume containing 0.5 µg His-Cj0700 fusion protein was put into each tube of GST-CheY and GST-CheA-RR and to a control tube of GST protein. Alternatively, an equal volume of His-CheV and His-CheA-RR were put into each tube of the GST-Cj0700 and to the control tube of GST protein. In addition 10 µl of 30 mM acetyl phosphate and 20 µl 1% BSA was added into each mixture then incubated at 4 ^{o}C with slow shaking for 5-10 minutes. Finally, the mixture was washed four times with 100 µl ice-cold TGEM (0.1). Beads were re-suspended with 10 µl 2x SDS sample buffer to inactivate the reaction. Putative interaction between prey of Cj0700, CheY, CheA, CheA-RR and CheV with bait of CheY and Cj0700 proteins was visualised by SDS-PAGE and western blot.

In the Flag tagged protein-protein interaction assay, 20 µl of beads were put into one 1.5 ml microcentrifuge tube as a negative control and 20 µl of beads into another sample tube for two fusion proteins (Flag-CheV/His-Cj0700 or Flag-CheA-RR/His-Cj0700) expected to interact each other. Next, the beads were washed with 200 µl of ice cold TBS four times using the MagneSphere® Technology Magnetic Separation Stand (PROMEGA UK) to separate the wash supernatant. The 20 µl of TBS was used to re-suspend the beads to maintain the hydration of beads. Subsequently, 1% BSA and 0.5 µg of purified flag proteins was put into control and sample interaction tube and both kept for 30 minutes at 4 ^{o}C with rocking. The protein-bead mixture was washed with 200 µl ice-cold TBS buffer four times and then 0.5 µg of His-Cj070 fusion protein was added to both tubes, whereas 30 mM acetyl

phosphate and 10 mM $MgCl_2$ was added into the sample reaction tube. Immediately, the reaction was washed with 200 µl ice-cold TBS buffer four times and eluted with 20 µl of 2xSDS sample loading. Fusion proteins were visualised by SDS-PAGE and Western blotting.

2.11. SDS- Polyacrylamide gel and sample preparation

Expressed proteins were visualized on SDS-PAGE. Generally, purified proteins and expressed cell pellets were mixed 2x in an equal volume of SDS sample loading buffer (table 13) at equal volume. Subsequently, samples were boiled at 98 ^{o}C for 5 minutes then centrifuged at 1100 xg for 3 minutes. Finally, samples were loaded into 10-15% SDS-PAGE (Table 11, Table 12) and were electrophoresed constantly at a current of 80 volts.

For SDS-PAGE preparation, gels were to cast using the Clarit-E Mini Vertical System (Alpha Laboratories Ltd), which produces mini gels with a dimension of 7.5 x 8cm. Briefly, the casting unit was assembled then a separating gel which comprised of a mixture of buffer A, 30% (v/v) acrylamide, 1% (w/v) Ammonium persulphate (APS) and Tetramethylethylenediamine (TEMED), was loaded at the bottom of the casting unit. Once the bottom separating gel had solidified, a stacking gel which comprised buffer B, 30% (v/v) acrylamide, 1% APS and TEMED, was loaded on top of the separating gel and the comb was instantly inserted into the gel. Soon after the gel had solidified, the gel casting unit was transferred into the electrophoresis tank which was filled with 1x SDS-PAGE running buffer (Table 13), and the comb was removed. Then protein samples, mixed with 2x an equal volume of SDS sample loading buffer, were loaded onto the gel with pre-stained protein markers and were run constantly at voltage of 80.

Table 11. Preparation of 10% SDS-PAGE.

Component	Stacking (5%) gel	Separating (10%) gel
Buffer B	1 ml	-
Buffer A		2.7 ml
30 % acrylamidine	330 µl	1.83 ml
H_2O	616 µl	765 µl
1% APS	50 µl	190 µl
TEMED	4 µl	15 µl

Table 12. Preparation of 15 % SDS-PAGE.

Component	Stacking (5%) gel	Separating 15% gel
Buffer B	1 ml	-
Buffer A	-	2.7 ml
30 % acrylamidine	330 µl	2.75 ml
H2O	616 µl	50 µl
1% APS	50 µl	190 µl
TEMED	4 µl	15 l

2.11.1. Preparation of western blot

GST and His tagged proteins separated in SDS-PAGE were transferred onto a PVDF membrane. Prior to use, the membrane was activated by soaking with either IMS or 100% methanol for five minutes with shaking and rinsed out with dH_2O. After that, the PVDF membrane was placed on the surface of the assembled blotting unit which was soaked with

transfer buffer. The blot unit comprised the red plastic cassette, sponge (OmniPAGE mini, Geneflow, UK) and 3MM filter paper (Whatman 3 MM chromatography paper). The protein gel was loaded onto the surface of the black cassette with sponge and 3MM filter paper. These cassettes were tightened together and transferred to tank the (OmniPAGE mini, Geneflow, UK) filled with transferring buffer in accordance of manufacturer's instructions. Protein samples were run at 100 mA for 1 hour.

2.11.2. Buffers, reagents and solutions

The buffers (Table 13), solutions, reagent and media (Table 14) used in this study are presented below.

Table 13. Buffers used protein purification and analysis in this study.

Buffer	Contents
Buffer A (for separating gel). pH 8.8	375 mM Tris-HCl , 0.1% (w/v) SDS
Buffer B (for separating gel). pH 6.8	250 mM Tris-HCl, 0.1 % (w/v) SDS
Western blotting transfer buffer. pH 6.8	20 mM Tris, 152 mM glycine, 0.037 % (w/v) SDS and 20% (v/v) methanol
Phosphate buffered saline (PBS) for western blot washing buffer. pH 7.3	10 tablet of PBS (ICN Biomedicals) was dissolved in 1L of dH2O
SDS-PAGE running buffer. pH, 8.3	25 mM Tris-HCl, 192 mM Glycine, 1% (w/v) SDS
SDS-PAGE sample loading buffer. pH 6.8	50 mM Tris-HCl 100 mM DTT, 10% (v/v) Glycerol, 5% (w/v) BPB, 10% (v/v) Glycerol
Phosphate Buffered Saline (PBS).pH, 7.3 Binding buffer for GST tagged	10 mM NaH2PO4, 1.8 mM KH2PO4, 2.7 mM KCl, 140 mM NaCl, 5 mM DTT
Elution buffer for GST tagged proteins. pH, 8.0	50 mM Tris (pH, 7.6), 10 mM reduced glutathione, 5 mM DTT
Binding buffer for His tagged proteins. pH, 7.6	50 mM Tris-HCl, 0.5 NaCl, 20 mM imidazole.
Elution buffer for His tagged proteins. pH 7.6	100 mM Tris-HCl, 0.5 NaCl, 200 mM imidazole
Protein storage buffer. pH, 7.6	50 mM Tris-HCl, 200 mM KCl, 10 mM $MgCl_2$, 10% (v/v) Glycerol and 0.1 mM EDTA
Tris-Buffered Saline (TBS) for Flag tagged proteins. pH, 7.4	50 mM Tris HCl, 150 mM NaCl
Flag tag elution buffer. pH,3.0	0.1 M Glycine-HCl
TGEM(0.1): (0.1 refers to the NaCl	20mM Tris-HCl (pH 7.9), 20% (v/v)

concentration) for protein pull down reaction	glycerol, 1 mM EDTA, 5 mM $MgCl_2$, 0.1% (v/v)NP-40, 1 mM DTT, 0.1 M NaCl
TGEM (1.0): (1.0 refers to the NaCl concentration) for protein pull down reaction	20 mM Tris-HCl (pH 7.9), 20% glycerol, 1 mM EDTA, 5 mM $MgCl_2$, 0.1% (v/v)NP-40, 1 mM DTT, 1 M NaCl
TGMC (0.1): (0.1 refers to the NaCl concentration)	20 mM Tris-HCl (pH 7.9), 20% (v/v) glycerol, 5 mM $MgCl_2$, 5 mM $CaCl_2$, 0.1 %(v/v) NP-40, 1 mM DTT, 0.1 M NaCl

Table 14. Solutions and reagents used for this study.

Reagent	**Contents**
Chloroform:Iso-amyl alcohol (24:1)	240 ml chloroform (Fisher Scientific) and 10 ml Iso-amyl alcohol (Fisher Scientific)
EDTA-HCl, pH 8.0	500 mM
Sodium dodecyl sulphate	2% or 10% (w/v) SDS (Fisher Scientific)
Sodium acetate, pH 5.2	3 M Sodium acetate
X-Gal (5-bromo-4-chloro-3-indolyl-β-D-galactopyranoside)	X-gal 40 μg/ml
IPTG(Isopropyl-β-D-thiogalactopyranoside	1 M IPTG prepared into dH_2O
Media	**Contents**
SOC medium	SOB medium 2% (w/v) Bacto-tryptone, 5% (w/v) Bacto-yeast extract, 10 mM NaCl, 2.5 mM KCl, 10 mM MgSO4 and 20 mM glucose
Mueller-Hinton(MHA-VT) Medium added trimethoprim and vancomycin (*Campylobacter* selective)	15.2 g Mueller Hinton Agar (Oxoid, Basingstoke, UK), dissolved with 400 ml dH2O. For Mueller Hinton Broth, 8.4 g powder(Oxoid, Basingstoke, UK) was mixed with 400 ml dH_2O
Luria-Bertani (LB) medium. pH 7.0	Luria Broth (LB) contain: 0.4% (w/v) bactor-tryptone, 0.2% (w/v) bacto-yeast extract and 0.4% NaCl mixed with 400 ml dH_2O. Luria agar (LA) added 1.5 % agar (Bioagar,Biogene Ltd, UK) and autoclaved 121°C for 15 minutes
Solution	**Contents**
Wash solution	272 sucrose, 15% (v/v) Glycerol

2.12. Bacteria two hybrid system

For the experiments described here, pKT25-cheY, pKT25-cheA, pKT25-cheV, pKT25- cheB and pUT18-cj0700 plasmids in *E. coli* JM109 cells were grown on LA overnight at 37 ^{o}C with appropriate selection. Plasmids were extracted and purified as described above (section, 2.4 and 2.4.4). Purified plasmids were verified by PCR before transformation into *E. coli* strain BTH101. After that, plasmids were co-transformed into competent cells of *E. coli* strain BTH101 by heat shock and grown on LA overnight at 37 ^{o}C with appropriate selection to produce single colonies. Correct transformants were verified by colony PCR using insert specific primers as described above (Table 8, section 2.4.1.2).

For the *in vivo* protein-protein interaction assay, the co-transformed plasmid of pKT25-cheY/pUT18-cj0700, pKT25-cheA/pUT18-cj0700, pKT25-cheV/pUT18-cj0700 and pKT25-cheB/ pUT18-cj0700 in *E. coli* strain BTH101 strains were grown on MacConkey (Sigma) agar plate supplemented with filter sterilised 1% (w/v) glucose free maltose at 30 ^{o}C for 3 days. When two fusion proteins interact transformant cells produce a red colour on MacConkey plates, whereas where there is no interaction the agar turns yellow. Negative and positive controls were included in the assay to compare interactions of the proteins, where each plate was divided in three sections into which negative, positive and each of cheY/pUT18-cj0700, pKT25-cheA/pUT18-cj0700, pKT25-cheV/pUT18-cj0700 and/or pKT25-cheB/ pUT18-cj0700 cotransformats were plated. Colour change was evaluated and interpreted as no interaction, weak interaction and strong interaction.

2.13. Cj0700 crystallization

Preliminary crystallization trials of Cj0700 protein were undertaken by sparse matrix JCSG, Cryo I&II (Emerald Biosystems) and Proplex screens (Molecular Dimensions) with the aim of getting the protein aggregated. In total, 14 mg of purified Cj0700 was used in the crystallization screening, where 100 nl of the protein (14 mg) and precipitant mixture was dispersed into each well of a MRC 96 well plate. Protein and buffer mixing and dispensing was carried out by Cartesian dispensing robot (Genomic Solutions, Harvard Bioscience). In addition, the sitting drop diffusion method was performed for Cj0700 protein crystallisation. Replicates of the samples were carried out in order to screen the best temperature that would crystalize the protein. Sample plates were sealed with adhesive film to avoid dehydration and incubated at 4 ^{o}C, room temperature or 16 ^{o}C for three weeks. Crystal formation was monitored using a LEICA microscope (Spectrographic limited, UK). This crystallisation experiment was done in collaboration with Professor Peter Moody's research group in Department of Biochemistry, University of Leicester.

2.13.1.Nuclear Magnetic Resonance (NMR)

Cj0700 protein was expressed and purified as described above (section 2.9). Purified cj0700 protein was diluted with phosphate buffer containing 10 mM NaH_2PO_4, 1.8 mM KH_2PO_4, 2.7 mM KCl, and 100 mM NaCl (pH7.3). Folding conformation of Cj0700 was examined at 1D ^{1}H NMR spectrum using total volume of 350 µl Cj0700 with a 100 µM concentration in phosphate buffer. NMR spectra of Cj0700 were collected by a Bruker Avance II 800 MHz spectrometer operating at 25 ^{o}C. The Cj0700 spectrum was plotted as a resonance signal intensity against chemical shift in parts per million (ppm). To conduct this NMR experiment was done collaboration with Professor Peter Moody's research group in Department of Biochemistry, University of Leicester.

2.13.2. Circular Dichroism (CD)

For CD spectrum assessment, a final concentration of 20 µM Cj0700 protein was used, diluting with 20 mM Tris-buffer (pH of 7.6). All CD experiment was carried out at room temperature using a wave length range between 185 and 260 nm with a 0.1 cm path length. In addition, each spectrum recorded were the average of 10 accumulations at scan speed of 20 nm^{-1} min, with bandwidth 1 nm at 0.5 nm stepwise and a 3 second time constant. Furthermore, the effect of temperature on Cj0700 was also examined by gradually increasing by 1 ^{o}C over the range of 20 to 80 ^{o}C. To conduct this CD experiment, it was collaborated with Dr. Renshaw in Department of Biochemistry, University of Leicester.

2.13.2.1. Chemical denaturation

In this experiment of fluorescence spectroscopy was used to examine the tertiary structure of Cj0700 protein. Cj0700 was titrated against guanidine-HCl, where each time a 0.5M concentration was gradually increased up to a 6 M of guanidine-hydrochloride. The intrinsic fluorescence emitted by tryptophan exposed into aqueous solution was monitored by Perkin Elmer Life Sciences LS50B luminescence spectrometer at 1 cm quartz cell at room temperature. 20 µM concentration of Cj0700 in 20 mM Tris buffer (pH 7.6) was used in this assay. As a control an equal concentration of Cj0700 without guanidine hydrochloride was included in the assay. The Cj0700 was excited at 280 nm and emitted fluorescence was monitored from 300 to 450 nm. The final spectra was recorded the average of 10 accumulations with scan rate of 150 nm per minute. To conduct the tertiary structure of Cj0700 protein experiment was done in collaboration with Dr. Renshaw in Department of Biochemistry, University of Leicester

Chapter 3 : Mutagenesis, complement, swarming and growth assay of cj0700

3. Introduction

With the aim of determining the role of Cj0700 in chemotaxis, the first objective was to construct an isogenic *cj0700* mutant in NCTC 11168 and the next objective was to test the chemotactic phenotype of this *cj0700* mutant. In addition, in order to verify, by genetic complementation, any observed alteration in phenotype, the *cj0700* wild-type allele was re-introduced into the *cj0700* mutant.

3.1. Cloning *cj0700* into *pUC19*

In order to create a *cj0700* mutant, the entire cj0700 coding sequence of 696 bp along with 600 bp of flanking sequence was amplified using *C. jejuni* chromosomal DNA as template. The addition of the flanking sequences was to enable allelic exchange between the mutant allele in the introduced recombinant plasmid and the chromosomal wild type allele in *C. jejuni*. Primers Cj0700F and Cj0700R (Table 8), incorporating 5' *Bam*HI restriction sites, were used to amplify a fragment with a predicted size of 1896 bp (Figure 3.1). The amplified PCR product was purified (Chapter 2; section 2.4.4), digested with *Bam*HI and cloned into the *Bam*HI site in the poly linker of pUC19.

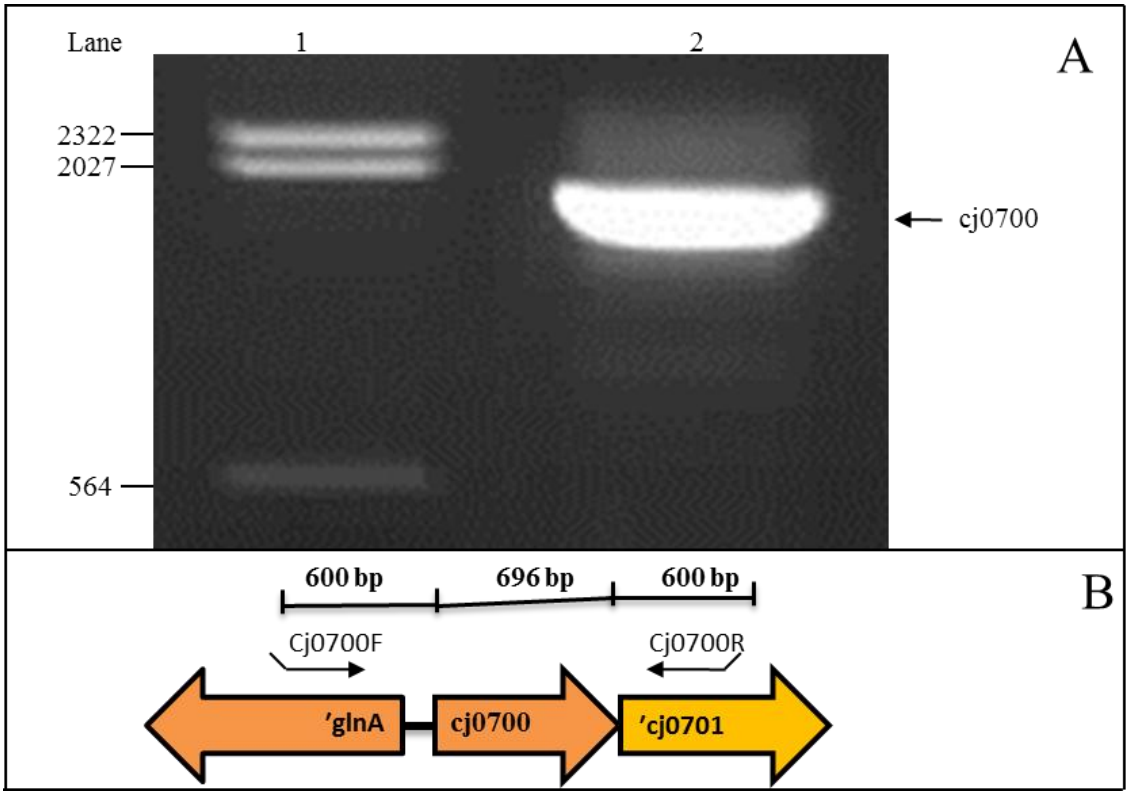

Figure 3.1. PCR amplification of *cj0700* from *C. jejuni* NCTC 11168.

Panel A: Agarose gel electrophoresis of amplification of fragment containing the *cj0700* gene. The entire gene of *cj0700* along with 600 bp of flanking sequence was amplified using primers (Cj0700R and Cj0700F) containing 5' *Bam*HI restriction sites. Lane 1= λ *Hin*d III DNA marker, lane 2 PCR product of *cj0700* amplification with predicted size of 1896 bp. 1% TAE agarose gel with molecular marker sizes shown on left. Planel B: diagram representation of PCR amplification of cj0700. Open arrows show coding sequence orientation and solid arrows indicate primer position of primer annealing.

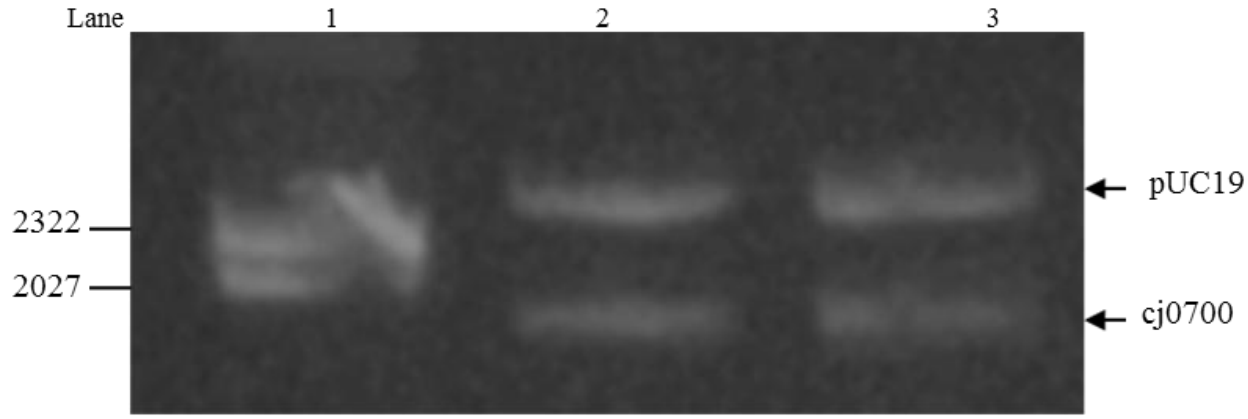

Figure 3.2. Verification of pAJ4 by restriction digestion.

Cj0700 presence in the pAJ4 recombinant plasmid.Two putative recombinant clones of the amplified cj0700 fragment (1896 bp) cloned into pUC19 (2686 bp) were restricted with *Bam*HI. Lanes: 1= λ *Hin*d III DNA marker, 2 and 3= pAJ4. 1% TAE agarose gel with molecular marker sizes shown on left and fragment identity on right.

The restricted PCR products of *cj0700* and pUC19 plasmid were ligated (Chapter 2, section 2.4.3) and transformed by electroporation (Chapter 2, section 2.5.1.1.2) into *E. coli* XL-1blue and recombinants screened for disruption of the plasmid-encoded *lacZ* gene (Chapter 2; section 2.6.1). Recombinant clones with an insertion of the *cj0700* fragment were identified by colony PCR with primers Cj0700F and Cj0700R and verified by digestion with *Bam*HI (Figure 3.2) by the presence of an 1896 bp fragment with the 2686 bp pUC19 fragment. The clone was further verified using M13 primers to sequence the DNA flanking the *cj0700* CDS to ensure subsequent homologous recombination of error-free DNA. The resultant plasmid was named pAJ4 (Figure 3.3) and this was used as the template for constructing the *cj0700* mutant plasmid.

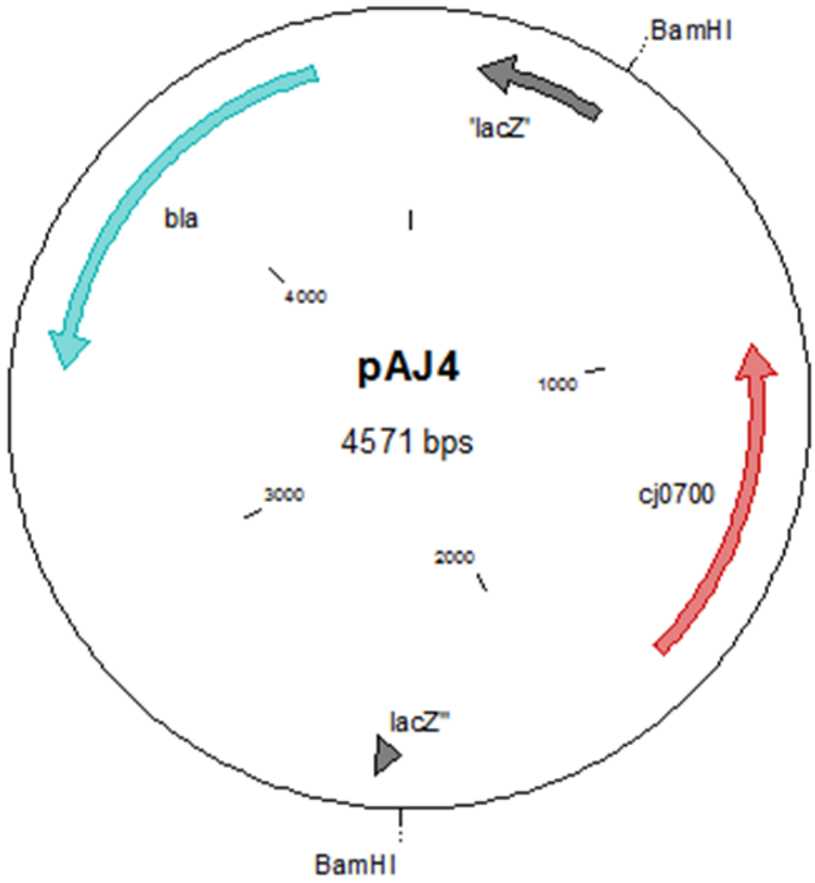

Figure 3.3. Plasmid map of *cj0700*- containing amplified fragment cloned into pUC19 vector.
The *cj0700* gene along with 600 bp of flanking sequence was cloned into *pUC19* vector into the *Bam*HI site consequently interrupting the l*acZ* gene. *bla* gene is ampicillin resistance. Only the *Bam*HI restriction site used for cloning has been indicated. Plasmid construct was designated pAJ4.

3.2. Mutagenesis of *cj0700*

The strategy for mutagenesis in campylobacters usually involves insertional inactivation, sometimes combined with a deletion of target gene coding sequence, by the incorporation of an antibiotic resistance cassette (Karlyshev and Wren, 2005). Therefore, it is important to consider the possible polar effects of such a mutation approach on genes flanking *cj0700* (Figure 3.4). It is possible that *cj0700-cj0708* are co-transcribed and *cj0700* and *cj0701* overlap each other by 3 bp and thus the *cj0701* Shine-Dalgardo is likely to be internal to the

cj0700 ORF. Indeed, initial attempts to construct a cj0700 mutant by other members of the laboratory (Karunakan, MSc dissertation, 2007 and Muthukumumaran MSc dissertation, 2008) had not proved successful; therefore, more careful consideration of the possibility of polar effects was made in the design of a modified mutagenesis strategy.

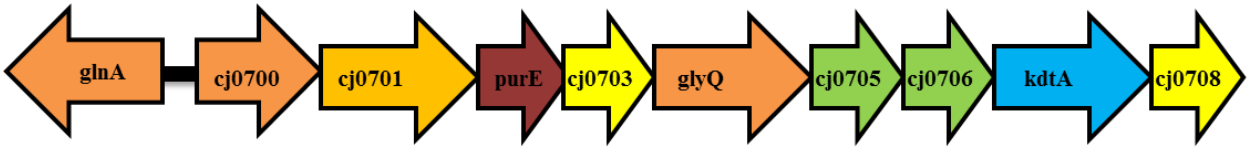

Figure 3.4. Diagram of *Cj0700* gene organized in genomic DNA of *C. jejuni*.

glnA (glutamine synthetase), cj0701 (putative protease), *purE* (phosphoribosylaminoimidazole carboxylase catalytic subunit), *cj0703* (hypothetical protein), *glyQ* (glycyl-tRNA synthetase subunit alpha), *cj0705* (hypothetical protein), *cj0706* (hypothetical protein), *kdtA* (3—deoxy-D-manno-octulosonic-acid transferase), *cj0708* (putative ribosomal pseudouridine synthase). Source was drawn from http://xbase.bham.ac.uk/campydb/.

To mutate *cj0700*, inverse PCR was used to enable deletion of a large part of the coding sequence of *cj0700* and a promoter-less and terminator-less *cat* (chloramphenicol acetyl-transferase) cassette was inserted by ligation. Hence, inverse primers (Cj0700-invf-1 and Cj0700-invr-2; table 8) with a 5' *Bgl*II restriction site were used to create the *cj0700* mutant. Amplification of pAJ4 template with the inverse PCR primers was carried out to produce a 4036 bp fragment. The produced PCR fragment consisted of 600 bp each of 5' and 3' sequence flanking the *cj0700* coding sequence with 150 bp of the 3' end of *cj0700* also left in the amplified fragment along with the remaining pUC19 sequences (Figure 3.6). The inverse PCR product was digested with *Bgl*II, and a 730 bp chloramphenicol resistance cassette digested with *Bam*HI was ligated with it forming a 4770 bp plasmid (Figure 3.5). The coding sequence for *cat*, which was not associated with a promoter or transcriptional terminator, was excised from pAV110 with *Bam*HI. The main purpose of using a promoter-less and

terminator-less *cat* resistance cassette was to reduce possible polar effects in the *cj0700* mutant.

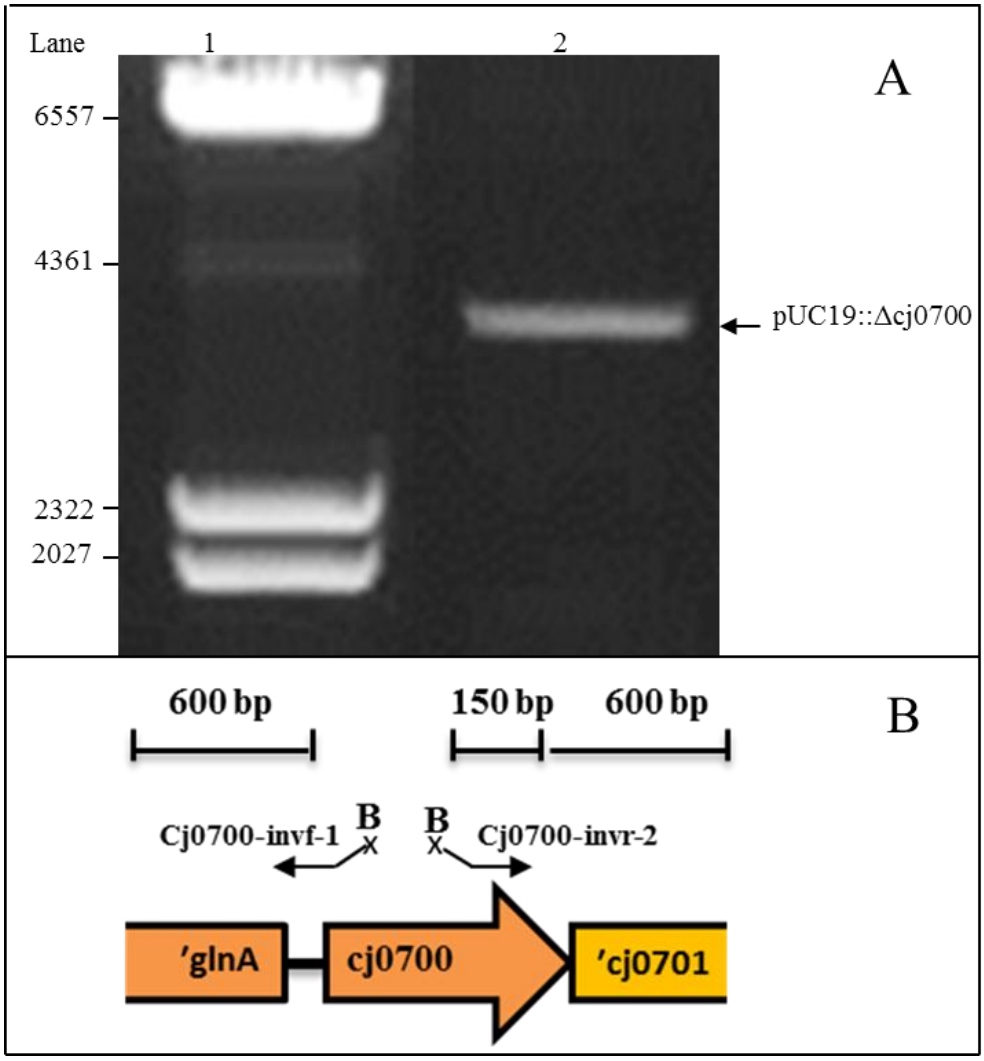

Figure 3.5. Mutation of cj0700: Inverse PCR product from pAJ4.

Panel A: The PCR product was inversely amplified using primers Cj0700-invF-1 and Cj0700-invR-2 that anneal to *cj0700* in plasmid pAJ4 to produce a 4036 bp amplicon. Lane: 1= λ *Hin*d III DNA marker, 2 = Inverse PCR product from pAJ4. 1% TAE agarose gel. At left shows sizes of DNA ladder in bp. Panel B shows the approximate position of inverse PCR primer annealing.

Following insertion of the *cat* cassette into the *cj0700* locus, the expression of *cat* was expected to be driven from the *cj0700* promoter, both in *E. coli* and when the mutant allele was inserted into the *C. jejuni* chromosome (Figure 3.9). The resultant ligation was

electroporated into *E. coli* and recombinants selected on LA media supplemented with chloramphenicol (50µg/ml).

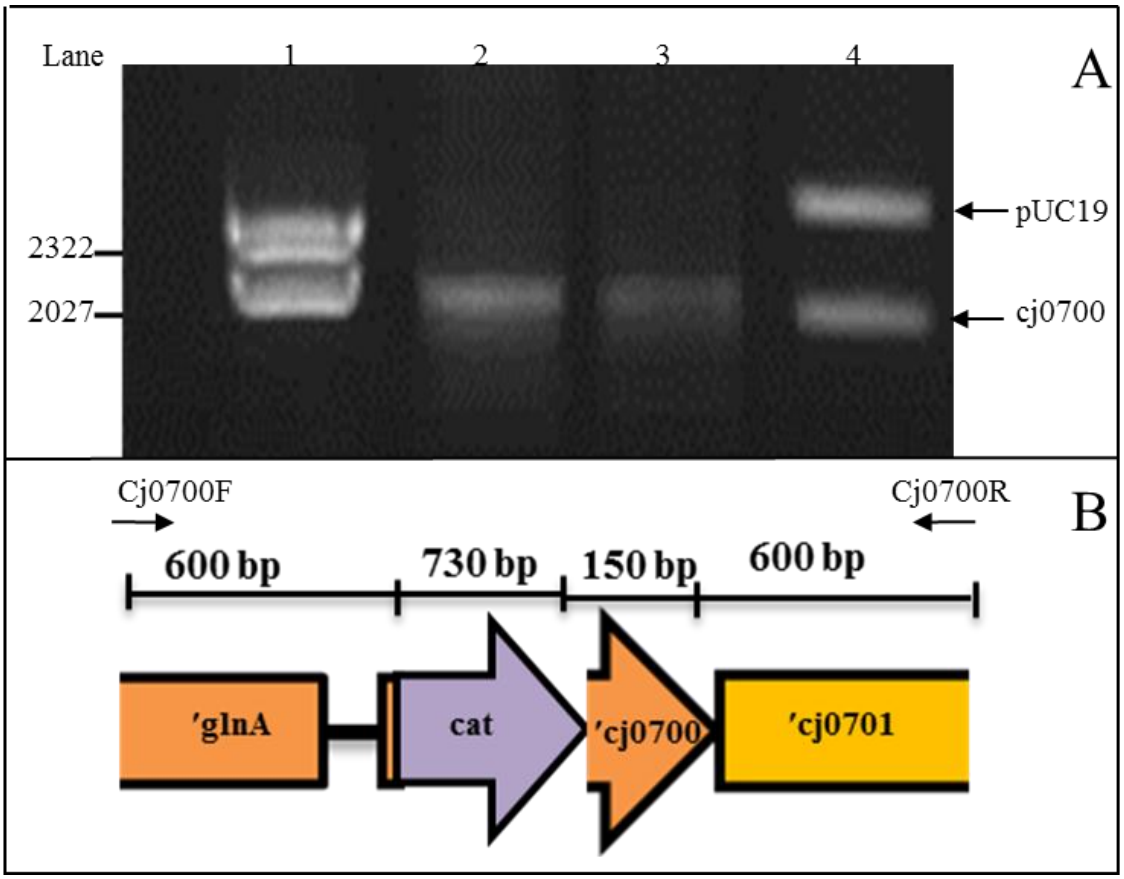

Figure 3.6. Verification of insert in PAJ5 PCR and restriction digestion.

Two potential transformant clones derived from the inverse PCR mutagenesis of pAJ4 were amplified using Cj0700F and Cj0700R primers. Purified plasmid DNA of clone 1 was restricted using *Bam*HI. The predicted size of the Δ*Cj0700::cat* fragment is 2084 bp. Panel A. Lanes: 1, λ *Hin*d III DNA marker, 2 and 3, PCR products of clone 1 and 2. Lane 4, clone 1 plasmid digested with *Bam*HI.. 1% TAE agarose gel. At left shows size of DNA ladder. Panel B. Annealing position of primers Cj0700F and Cj0700R used to determine the size of the Δ*Cj0700::cat* insert in clone 1 and 2.

The predicted size of the construct was 4770 bp, consisting of the insert (*cat* and Δ*cj0700*) fragment and pUC19 plasmid backbone. Screening for the presence of the insert (Δ*cj0700*::*cat*) in putative recombinant plasmid clones from transformant cells was carried out by colony PCR (Chapter 2; section 2.4.1.1), using M13 primers (Table 8). In addition, purified plasmid from potential clones was digested with *Bam*HI to confirm the altered size

of the insert. When digested, there were two fragments with sizes of 2084 and 2686 bp for the insert (Δ*cj*0700::*cat*) and pUC19, respectively. Also, amplification using Cj0700F and Cj0700R primers indicated a PCR product of 2084 bp (Figure 3.6). Finally, the insert of a plasmid recombinant clone was sequenced using M13 forward and reverse primers to verify that there were no sequence errors. It was essential that there are no errors in the flanking *glnA* and *cj0701* sequences which may have been recombined into any future *C. jejuni* mutant. The construct containing Δ*cj0700::cat* was designated pAJ5 (Clones 1; Figure 3.7).

The pAJ5 plasmid was electeroporated into *C. jejuni* NCTC 11168 competent cells to enable the mutated Δ*cj0700::cat* recombinant allele to replace the wild-type allele of *cj0700*. Transformant cells were selected on MHA media supplemented with chloramphenicol (35μg/ml). Since expression of the *cat* gene is driven from the promoter of *cj0700*, a lower chloramphenicol concentration (35μg/ml) was used for the first selection with subsequent re-plating at normal concentrations (50μg/ml). Furthermore, the pAJ5 plasmid was used to mutate *cj0700* not only in NCTC11168, but also strains 81116 and 81-176 (Chapter 2, table 1 and section 2.1). Mutation of these strains was carried out by Sherline Benedict (post-graduate diploma student) under my direct supervision. In addition, primers designed for *cj0700* cloning from NCTC11168 were also used for *cj0700* cloning from 81116 and 81-176 strains since *cj0700* gene with flanking sequences were shown to be similar a cross the three strains. Their alignment has shown to share 99% similarity, where some places indicated base pair differences at the upstream of CDS of Cj0700 (Figure 3.8).

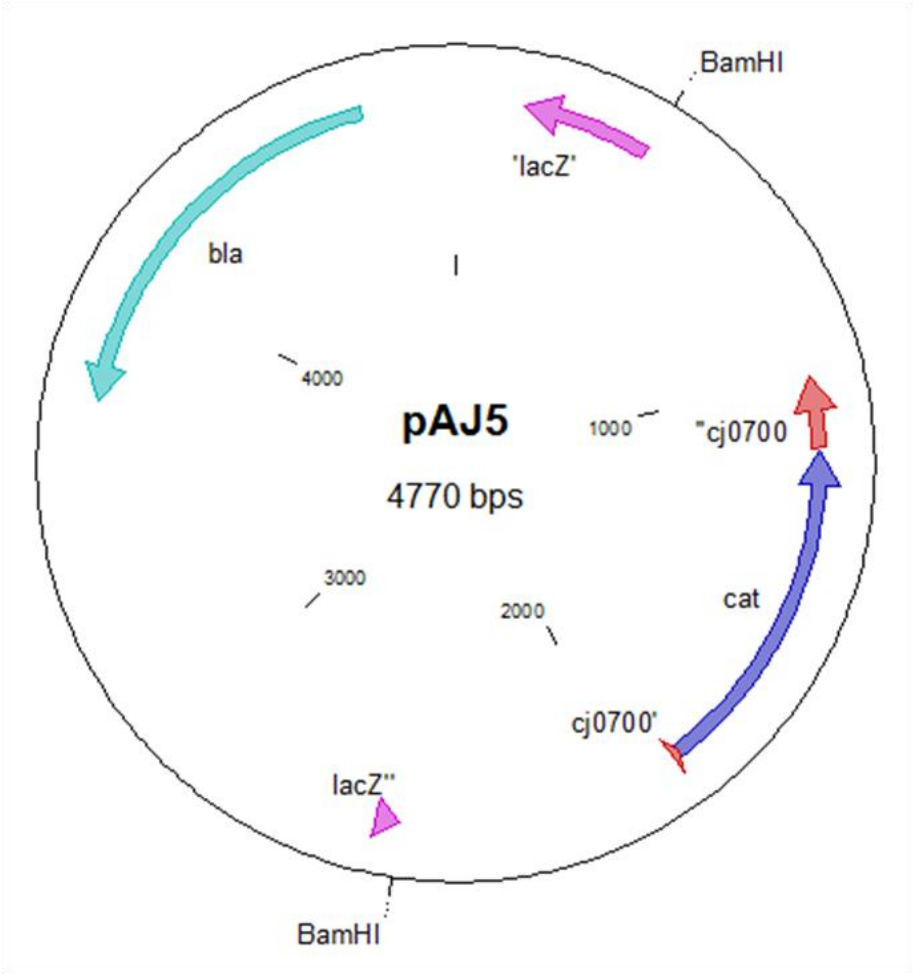

Figure 3.7. Plasmid map of pAJ5 containing Δ*cj0700::cat.*

The *cj0700* gene in pAJ4 was insertionally inactivated by using a chloramphenicol resistance cassette (chloramphenicol acetyl-transferase, *cat*). The cassette is positioned 18 bp 3' to the start codon and after deletion of *cj0700* coding sequence, approximately 150 bp 5' to the stop codon remains. In constructing Δ*cj0700::cat* the cat cassette, restricted with *Bam*HI was cloned into *Bgl*II sites generated by inverse PCR. Only *Bam*HI sites used initial cloning of the *cj0700* fragment into pAJ4 are indicated.

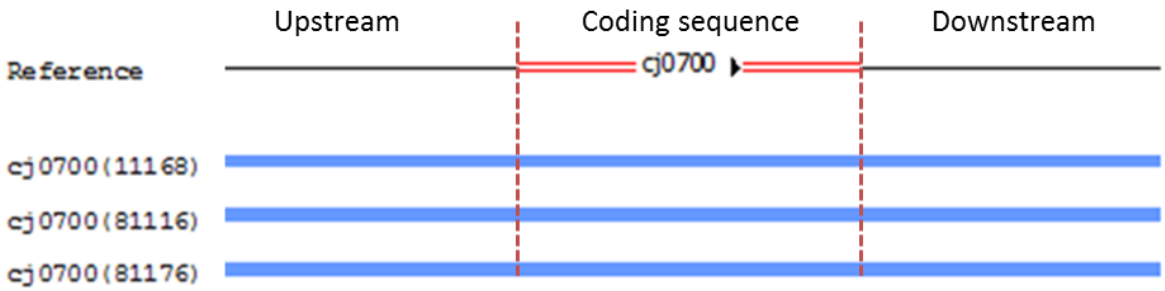

Figure 3.8. Alignment diagram illustrating a *cj0700* locus similarity cross three *C. jejuni* strains. DNA sequence of *cj0700* gene with flanking 600 bp of NCTC11168 (reference) aligned with 81116 and 81-176 strains. Blue lines indicate significant similarity of *cj0700* in the three strains. Red lines show coding part of *cj0700* locus. ►= *cj0700* orientation in the chromosome. Black lines at either side of *cj0700* gene (red lines) represent 600 bp flanking sequences at upstream and downstream of cj0700 genes. Vertical red dots = separation of coding sequence of *cj0700* gene and flanking sequence. Aligment the DNA sequence was used CloneManager software.

The pUC19 ColE1replicon cannot be maintained in *C. jejuni* and therefore if pAJ5 transformants are selected on chloramphenicol, resistance should be the result of a cross-over event. In *C. jejuni*, the expected plasmid integrant resulting from a single cross-over when using pUC19-derived plasmids is not thought to be stable. Therefore, recombinants isolated from transformation of NCTC 11168 with pUC19 derivatives have undergone the equivalent of a double cross-over. Colonies from potential recombinants were screened by using *cat* cassette-specific primers to confirm the presence and orientation of the *cat* cassette in the *cj0700* chromosomal locus. In addition, primers specific (Table 8) for *glnA* and *cj0701* sequences which are upstream and downstream respectively of *cj0700* were used to confirm the predicted allelic exchange event (Δ*cj0700::cat*). Moreover, primers specific (Table 8) for *cj0700* were used to confirm the presence and orientation of the Δ*cj0700::cat* insert (Figure 3.9). Hence, glnAF and Cj0701R produced PCR fragment with predicted size 2575 bp (Figure 3.9, lane 2); these primers amplify from outside the predicted allelic exchange site in the chromosome. In addition, glnAF/cj0700R produced PCR fragment with predicted size 2253 bp (Figure 3.9, lane 3). Equally, Cj0700F/Cj0700R primers produced PCR fragment of

insert (Δ*cj0700::cat*) with predicted size 2084 bp (Figure 3.9, lane 4). Similarly, *cat* cassette orientation was confirmed using Cj0700F/CatinVF (Figure 3.9, lane 5), CatinvR/Cj0700R (Figure 3.9, lane 6), glnAF/CatinvF (Figure 3.9, lane 7) and CatinvR/Cj0701 (Figure 3.9, lane 8) primers. Furthermore, as a control, Cj0700F/Cj0700R primers were used to amplify from wild-type chromosomal DNA of *C. jejuni*, producing PCR fragment with predicted size 1896 bp (Figure 3.9, lane 9). These primers confirmed the predicted size of the PCR fragments, location and orientation of the insert (Δ*cj0700::cat*) in the chromosomal DNA of *cj0700* mutant strain were correct. Also, sequences of the insert were confirmed using Cj0700F/Cj0700R primers. Finally, the verified mutant of *cj0700* in *C. jejuni* was designated BAJ3CJ700 strain.

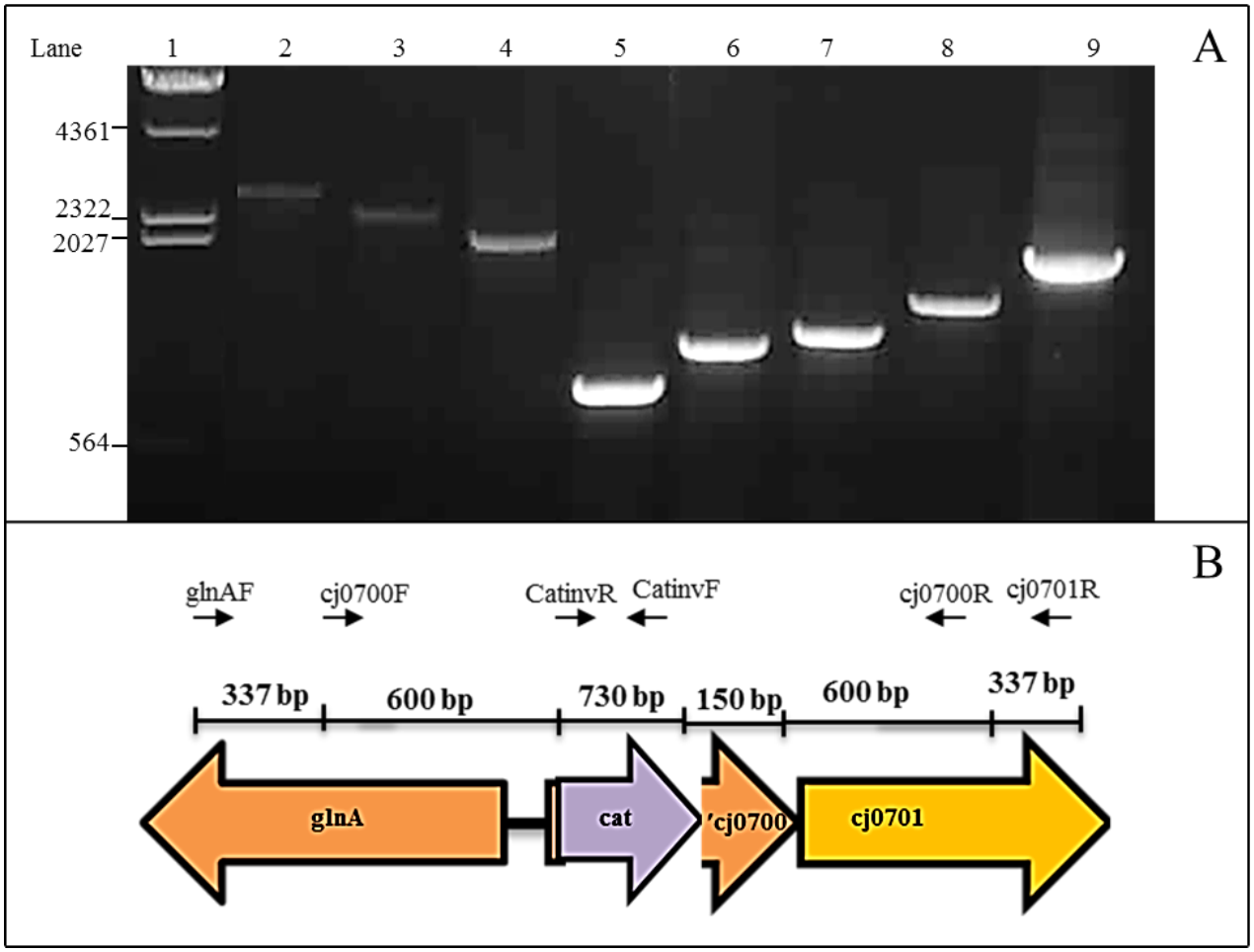

Figure 3.9. Verification of mutation of *cj0700* in strain BAJ1CJ700.

Panel A. PCR of NCTC11168 pAJ5 transformants to verify allelic exchange resulting in the insertion of the *cat* cassette into a deletion in the *cj*0700 chromosomal locus. Lanes 1 to 7 contain PCR products derived from one clone using primer pairs with annealing positions shown in panel B. Lane 9 contains PCR amplicon derived from wild type NCTC11168. Lane 1= λ Hind III DNA marker. Lane 2= GlnAF/cj0701R (predicted size 2575 bp). Lane 3= glnAF/cj0700R (predicted size 2253 bp). Lane 4 = Cj0700F/Cj0700R (predicted size 2084). Lane 5= Cj0700F/catinvF (predicted 848bp). Lane 6= CatinvR/cj0700R (predicted size 1079 bp). Lane 7= GlnAF/CatinvF (predicted size 1187 bp). Lane 8= CatinvR/Cj0701 (predicted size 1267 bp). Lane 9 = cj0700F/Cj0700R (WT as a control, predicted size 1896 bp) . 1% TAE agarose gel. Panel B. The lower picture shows the primer annealing positions corresponding to panel A. The colouration of the arrows indicates corresponding forward and reverse primer pairs shown in panel A.

3.3. Complement of *cj0700* mutant

While mutagenesis techniques have become routinely successful in *C. jejuni*, putting a copy of an exogenous allele *in trans* and ensuring expression of it still remains difficult. In addition to that, the use of a shuttle vector for complementation as in *E. coli* is not possible as the recombinant plasmid is unlikely to be maintained in *Campylobacter* (Karlyshev and Wren, 2005).

In this project, pKmetK vector was employed for complementation by chromosomal insertion in *Campylobacter* sp. In this approach the complementing allele is targeted to the *cj0046* pseudogene (NCTC11168) and others in the group have used pKmetK vector successfully for complementation of several mutants in iron metabolism (Haigh, personal communication). Hence pKmetK::*cj0700* was constructed whereby *cj0700* was placed under the control of the *metK* promoter using the pKmetK plasmid (Haigh, personal communication). Therefore the complementation of the BAJ1CJ700 strain (*cj0700* mutant) can confirm the role of the *cj0700* mutation in any observed phenotype. Also, pKmetK::*cj0700* recombinant can be used for the construction of a strain merodiploid for *cj0700* (Chapter 2; table 1).

To create the pKmetk::*cj0700* recombinant plasmid, a 900 bp fragment (Figure 3.10) containing both the *cj0700* gene and 200 bp of upstream sequence was amplified by PCR from NCTC 11168 genomic DNA with CCj0700_F and CCj0700_R primers , each having a *Nco*I site at the 5' end (Table 8). The purified PCR fragment was digested with *Nco*I and cloned into *Esp*3I-digested pKmetK to create pKmetk::*cj0700*. Each of these restriction enzymes creates compatible 5'overhangs when cleaved. Also the *Esp*3I site is maintained in the recombinant because the enzyme cuts 5' of its recognition site. Furthermore, incorporation of the upstream region likely to contain the *cj0700* promoter ensured expression of the gene from both its own promoter and the constitutive low level promoter, p*metK*.

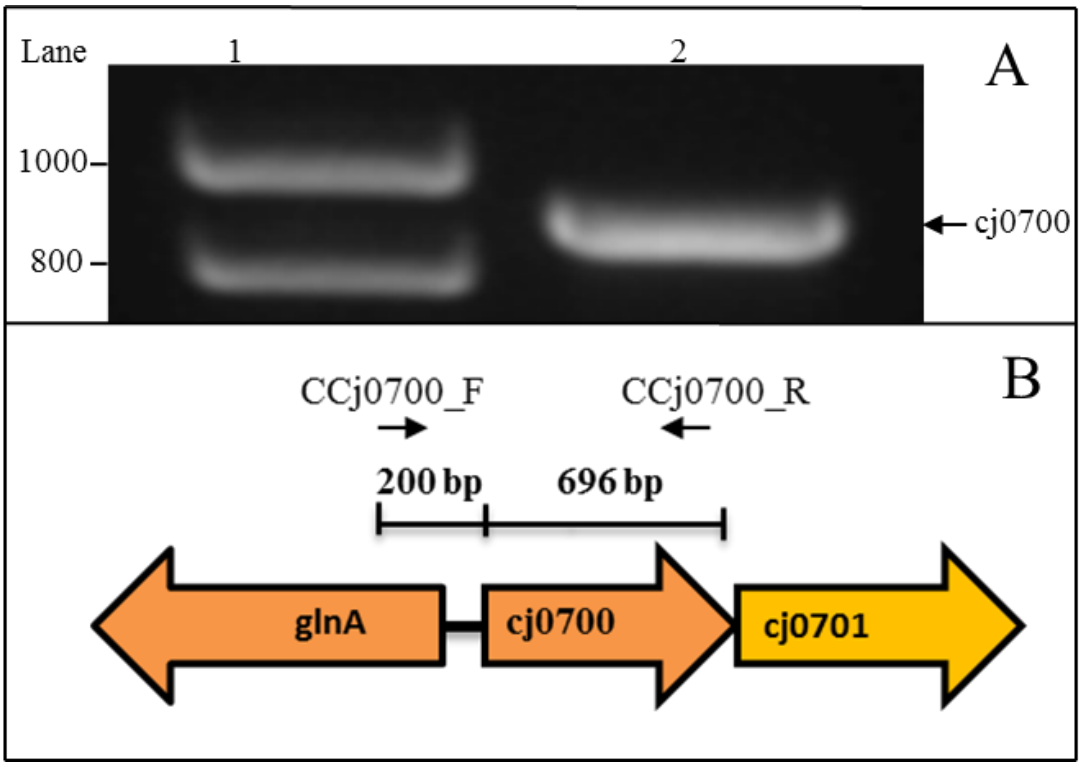

Figure 3.10. The *cj0700* PCR product used for the construction of pKmetK::*cj0700*.
Planel A. Lane 1 indicates Hyper-ladder I marker with relevant sizes, in bp, shown on the left. Lane 2 is the Cj0700 PCR product amplified using CCj0700-F and CCj0700R primers from 11168 *C. jejuni* genomic DNA. 1% TAE agarose gel. Panel B (Bottom) illustrates primer binding sites for *glnA* and *cj0700* (small arrows) in NCTC11168.

The pKmetK::cj0700 construct was electroporated into *E. coli* DH5αE competent cells and kanamycin was used to select transformants. Four clones were picked randomly and tested using colony PCR with primers Ccj0700F and Ccj0700R to identify the presence of a 900 bp amplicon consisting of *cj0700* and flanking sequence (Figure 3.11). Similarly, in order to verify location and determine orientation of the insert (*cj0046*::*cj0700*), primers Ccj0700F and Cj0046F were used with extracted plasmids as template. A 1000 bp fragment containing the *cj0700* gene with 200 bp of upstream sequence and 100 bp of *cj0046* downstream was observed, confirming the correct orientation of *cj0700* within the pKmetK vector with respect to the *metK* promoter (Figure 3.12). Subsequently, recombinant plasmids were sequenced to

confirm that there were no sequence errors created by PCR within the *cj0700* coding sequence and promoter. Once pKmetK::*cj*0700 recombinant plasmid was confirmed, it was designated pAJ6 (Figure 3.13).

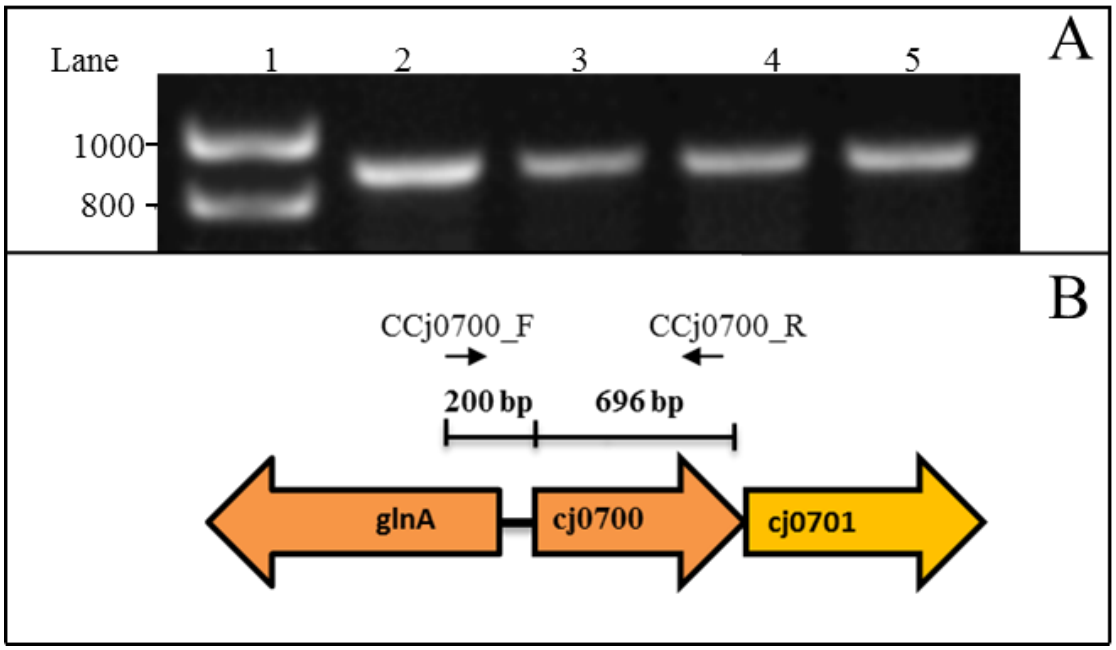

Figure 3.11. Verification of presence of *cj0700* in pAJ6.

Four transformant clones resulting from the insertion of cj0700 amplified from NCTC11168 using primers CCj0700F and CCj0700R into pKmetK were screened by PCR using primers Cj0700F and Cj0700R. A fragment size of 900 bp was predicted. Panel A. Lane 1 is the Hyper- ladder I marker with fragment sizes shown in bp on the left. Lane 2, 3, 4 and 5 contain individual putative clone plasmid DNA amplified with primers Cj0700F and Cj0700R. Panel B illustrates the location of primer annealing of glnA and cj0700 in NCTC11168. 1% TAE agarose gel.

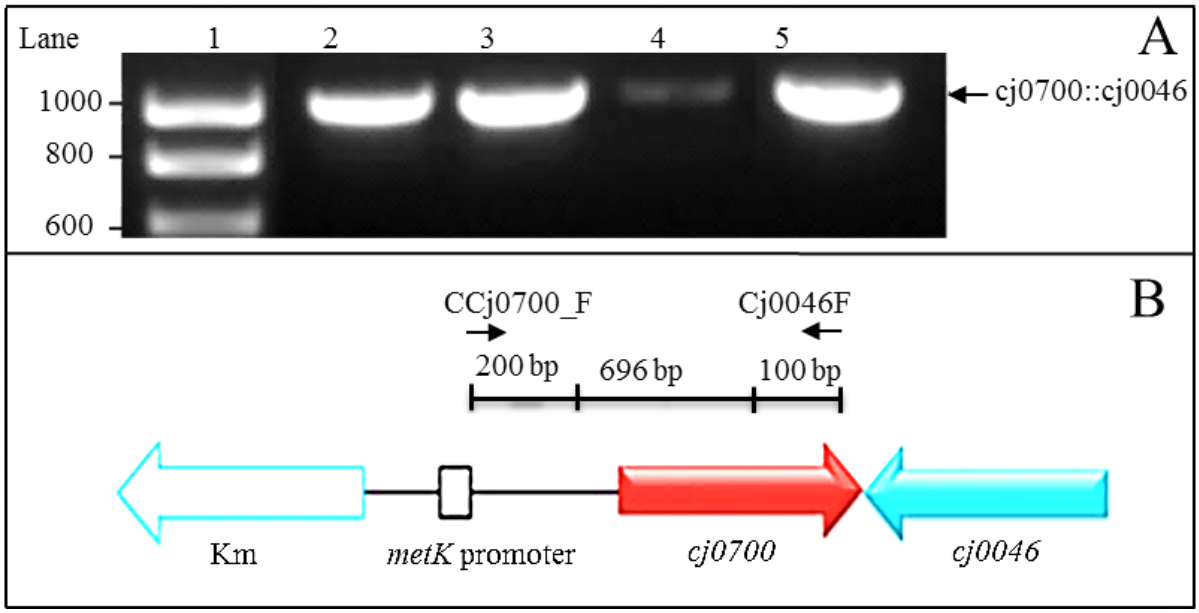

Figure 3.12. Verification of location and orientation of *cj0700* in pAJ6.

Four transformant clones resulting from the insertion of *cj0700* amplified from NCTC11168 using primers CCj0700F and CCj0700R into pKmetK were screened by PCR using primers Cj0700F and Cj0046F. Three clones were found to contain the insert in the required orientation. Panel A. Lane 1 is the Hyper- ladder I marker with fragment sizes shown in bp on the left. Lane 2, 3, 4 and 5 contain individual putative clone plasmid DNA amplified with primers Cj0700F and Cj0046F. Panel B illustrates the location of primer annealing of Cj0700F in the insert and Cj0046F in pAJ6. 1% TAE agarose gel.

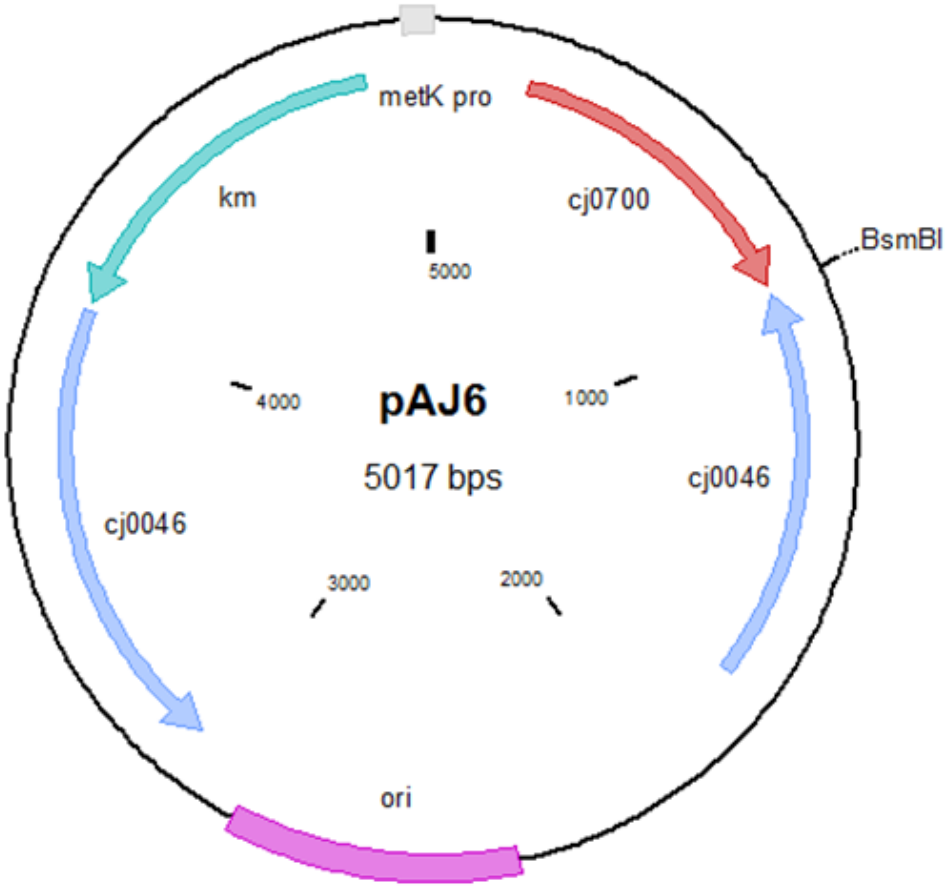

Figure 3.13. Map of pAJ6 containing the *cj0700* gene inserted into the *cj0046* pseudogene site of pKmetk. The position of the metK promoter is shown as a grey box and the *Bsm*BI (*Esp*3I) site where the NcoI restricted *cj0700* (red arrow) amplicon was inserted into pKmetK is indicated. The kanamycin resistance gene is indicated by a green arrow and the *cj0046* flanking sequences to enable targeting of the insertion into the chromosomal *cj0046* pseudogene are shown in blue (arrow).

The pAJ6 plasmid was electroporated into NCTC11168 BAJ1CJ700 (Δ*cj0700::cat*), 81116 BAJ4CJ700 (Δ*cj0700::cat*) and (Δ*cj0700::cat*) 81-176 BAJ5CJ700. Hence pAJ6 transformants were selected on MHA-VT plates (Chapter 2; table 14) supplemented with kanamycin to select for allelic exchange of the kanR-*pmetK-cj0700* fragment into the *cj0046* locus. Subsequently, resistant colonies to kanamycin were further sub-cultured on plates supplemented with chloramphenicol for Δ*cj0700::cat* mutation confirmation. Kanamycin and chloramphenicol resistant colonies were screened using Cj0700F and CATinvF primers for Δ*cj0700::cat* verification and CCj0700F/Cj0046F and CCj0700F/CCj0700R primer pairs

were used to verify the *cj0046::cj0700* mutation. The expected PCR product size from CCj0700F/Cj0046F was predicted to be 1000 bp, whereas in the wild-type the fragment was not present; recombinants producing the correct size were observed (Figure 3.14). The CCj0700F/CCj0700R primers were observed to produce the expected 900 bp fragment in both the recombinants and wild type verifying the presence of the wild type *cj0700* allele (Figure 3.14). Finally, the presence of the chloramphenicol resistance cassette in the original Δ*cj0700::cat* mutation of the transformed cells was confirmed using CATinvR and CCj0700R. A 450 bp fragment containing part of the *cat* cassette and part of *cj0700* was observed as expected in the recombinant clones, but not in NCTC11168 (Figure 3.15).

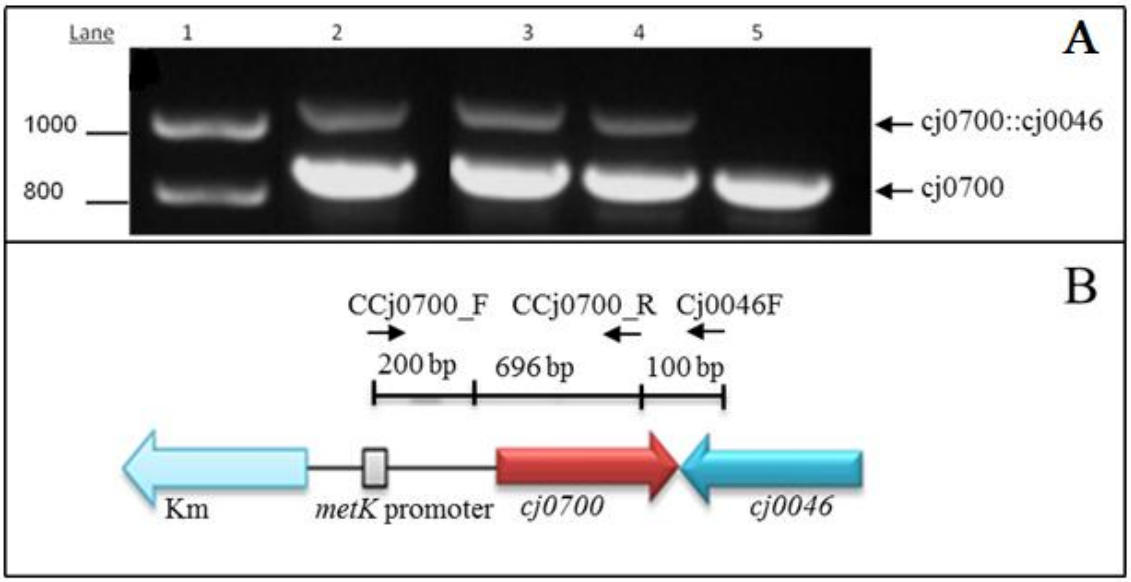

Figure 3.14. Confirmation of the location and orientation of the cj0700::0046 insertion in BAJ2CJ700. Primers CCj0700F/CCj0700R and Ccj0700F/Cj0046F were used in a multiplex PCR to confirm the presence and determine the orientation of the KmR-p*metK*::*cj0700* cassette inserted into the *cj0046* pseudogene in strain 11168 BAJ2CJ700 for Δ*cj0700::cat*, respectively. Panel A shows the products of the multiplex PCR analysis (primer pairs Cj0700F/Cj0700R and Ccj0700F/Cj0046F) of 3 potential recombinant clones and NCTC11168 as a control. Primers CCj0700F/CCj0700R were predicted to give a fragment size of 900 bp and Ccj0700F/Cj0046F a fragment size of 1000 bp. Panel A. Lane: 1 = Hyper-ladder I marker with fragment sizes in bp shown on left. Lane 2-4 potential individual recombinant strains, Lane 5 = NCTC11168 negative control. Panel B. Bottom diagram shows the annealing position of primer pairs Cj0700F/Cj0700R and Ccj0700F/Cj0046F (small arrows) in the predicted recombinant cj0046 locus in BAJ2CJ700 strain.

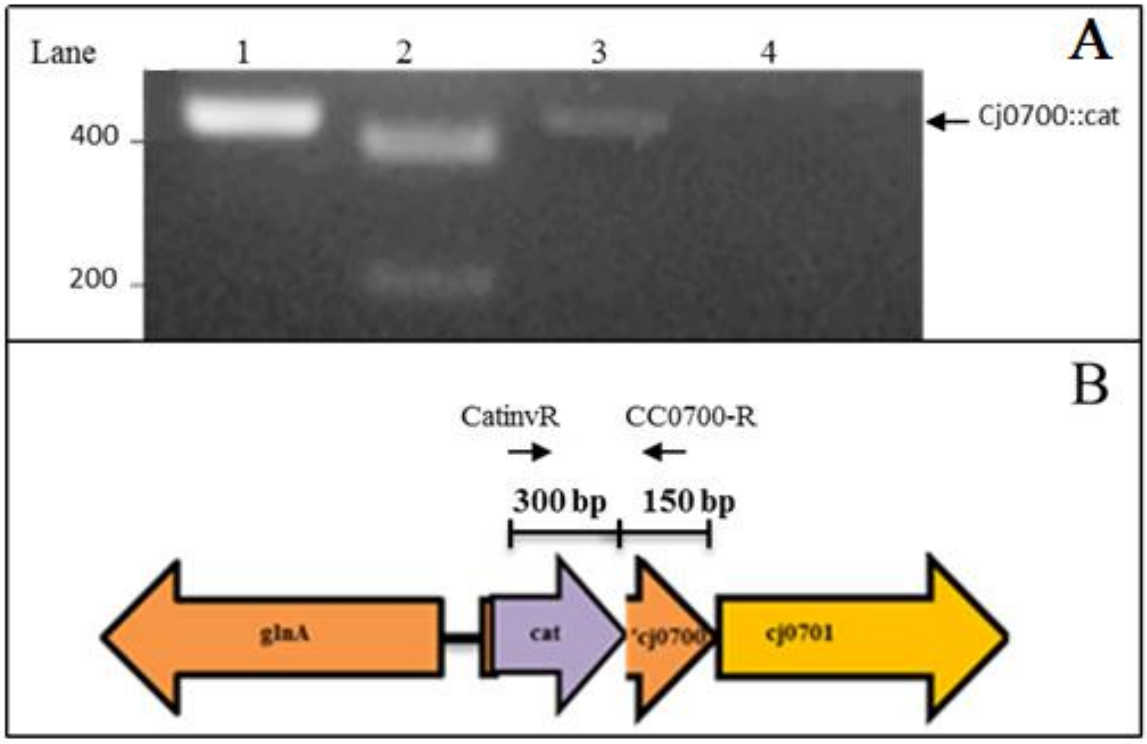

Figure 3.15. Verification of the presence of a mutant cj0700 allele in complement strain BAJ2CJ700. Potential complementing *cj0046::cj0700* recombinant strains were tested to verify the presence of the mutated *cj0700* locus using the CATinvR/Cj0700R primers specific to the *cj0700* gene and inserted *cat* selective marker. A fragment size of 450 bp was expected. Panel A Lanes: 1&3 = putative *cj0046::cj0700* recombinants amplified with CATinvR/Cj0700R primers, Lane 4: = NCTC11168 amplified with CATinvR/Cj0700R primers, Lane 2: = Hyper-ladder I marker with fragment sizes shown in bp on the left. Panel B diagram showing primer binding site in the mutated cj0700 locus of 11168 strain (cj0700::cat) BAJ2CJ700.

3.3.1. Screening motility of *cj0700* mutant and complement

Merodipolids of *cj0700* constructed into BAJ8CJ700 (11168), BAJ9CJ700 (81116) and BAJ10CJ700 (81-176) and in addition *cj0700* mutants of NCTC 11168 BAJ1CJ700, BAJ4CJ700 (81116) and BAJ5CJ700 (81-176) strains were reintroduced naturally into wild-type motile background of *C. jejuni*. The aim was to avoid selecting a non-motile variant due to the electroporation. Hence, after cells were retransformed naturally into a motile background then motility was screened, where 20 µl cell suspensions were spotted at the

centre of the glass-slide and overlaid with a cover-slip and examined phase contrast microscope (Chapter 2; section 2.8.1). Cells of *cj0700* mutants, wild-type, merodiploids and complements of *cj0700* mutants have shown darting quickly in the field and changing direction (data not shown).

3.4. Effect of the mutation of *cj0700* in *C. jejuni*

Main objective of the experiment was to test the chemotaxis features of *cj0700* mutants and complements of *C. jejuni*. Prior to that, cells were confirmed to be motile (Chapter 2, section 2.8.1), and therefore possessing functional flagella, to enable the assessment of chemotaxis signal transduction pathway to be undertaken.

Chemotactic phenotypes of *C. jejuni* strains were examined using a semisolid agar-based technique which is widely used as a method to determine chemotactic motility (Lertpiriyapong et al., 2012). The Swarm Assay measures the swarming motility of bacterial cells in the semisolid agar media (Niu et al., 2005). A modified variant of this swarm assay, based on that developed by Wolfe *et al*. (1989) was used in order to examine *C. jejuni* strains. Briefly, strains to be tested are spotted on the centre of semisolid MHA plates and incubated for 3-5 days in microaerobic (10% O_2 and 7 % CO_2 and 83% N_2) conditions and the extent of motility and growth to the outer parts of the plate observed.

3.4.1. Chemotaxis phenotype of *cj0700* mutation in strain NCTC11168

In this chemotaxis experiment, the chemotactic phenotype of strain BAJ1CJ700 of *cj0700* mutant in NCTC11168 was compared to both the wild type NCTC11168 strain and a *cheY* mutant constructed in the same background. A cell suspension was spotted in the centre of the semisolid agar plate, whereby chemotactic cells swarm from centre and spread to the

edges of the plates in contrast to cells with a defect in chemotaxis which show reduced swarming towards the plate edge.

The comparison indicated that, when comparing the *cj0700* mutant to the wild-type, the mutant showed markedly less movement from the centre of the plate, whilst wild-type spread and demonstrated a characteristic ring pattern. Conversely, the *cj0700* mutant swarmed better than a *cheY* mutant strain (Figure 3.16). This chemotaxis result demonstrates that the *cj0700* gene may have a role in *C. jejuni* chemotaxis.

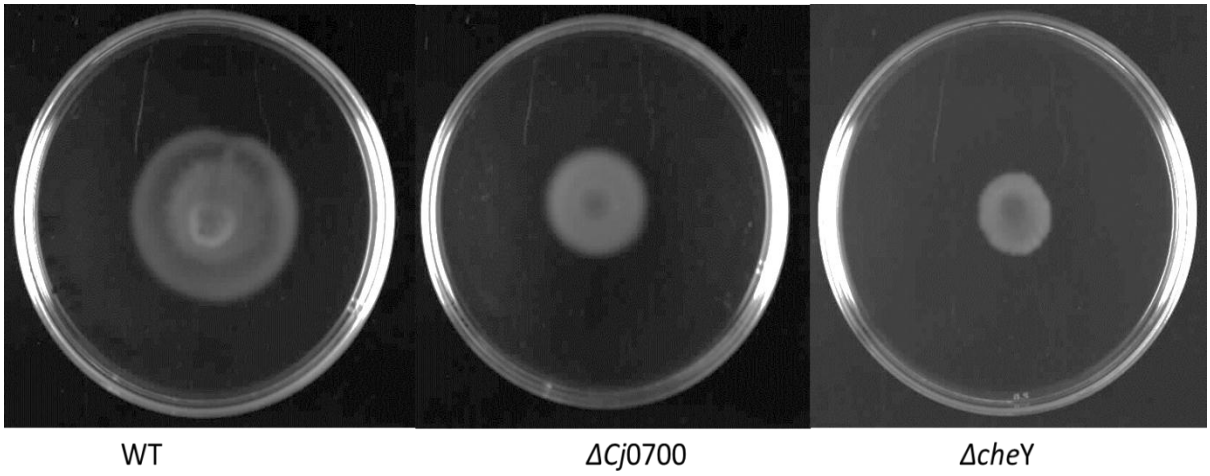

Figure 3.16. Assessment of chemotaxis phenotype of the *cj0700* mutant in a NCTC11168 background. Wild type NCTC11168 cells were compared to the *cj0700* mutant NCTC11168 BAJ1CJ700 of cj0700 mutant strain and a *cheY* mutant. Cells were inoculated into the centre of a 0.3% (w/v) MHA plate and grown for 72 hours at 42 ^{o}C in a microaerobic atmosphere.

3.4.2. Verification of the chemotaxis defect of BAJ1CJ700 strain by complementation

The *cj0700* mutation in BAJ1CJ700 resulted in a defect in chemotaxis when compared to the wild type and a *cheY* mutant. In order to determine that the observed phenotype in BAJ1CJ700 was due to the mutation in *cj0700*, then the strain of BAJ3CJ700 in NCTC11168 was tested in the swarm assay.

Complemention of the *cj*0700 mutant was carried out using the swarm assay. Cells used for this test where the wild-type, mutant and complemented mutant were made from overnight

culture and also, incubation conditions were set at microaerophilic atmosphere. Plates were inspected every 24 hours up to 72 hours. The *cj0700* mutant strain, BAJ1CJ700 again showed a defect in the swarming phenotype when compared to wild type. In contrast, the complemented strain, BAJ3CJ700 in NCTC11168 when compared to the mutant and wild-type, showed a greater degree of swarming out to the edge of the plate where nutrient levels increase (Figure 3.17). Although re-insertion of *cj0700* restored the ability of the cj0700 mutant to swarm, this restoration was only partial as the degree of swarming was not identical to wild-type. Nevertheless, this comparison indicates that the *cj0700* mutant has been successfully restored, albeit partially, back to the wild phenotype by putting a *cj0700* allele in the *cj0046* pseudogene of NCTC11168. This supports a role for *cj0700* in *C. jejuni* chemotaxis.

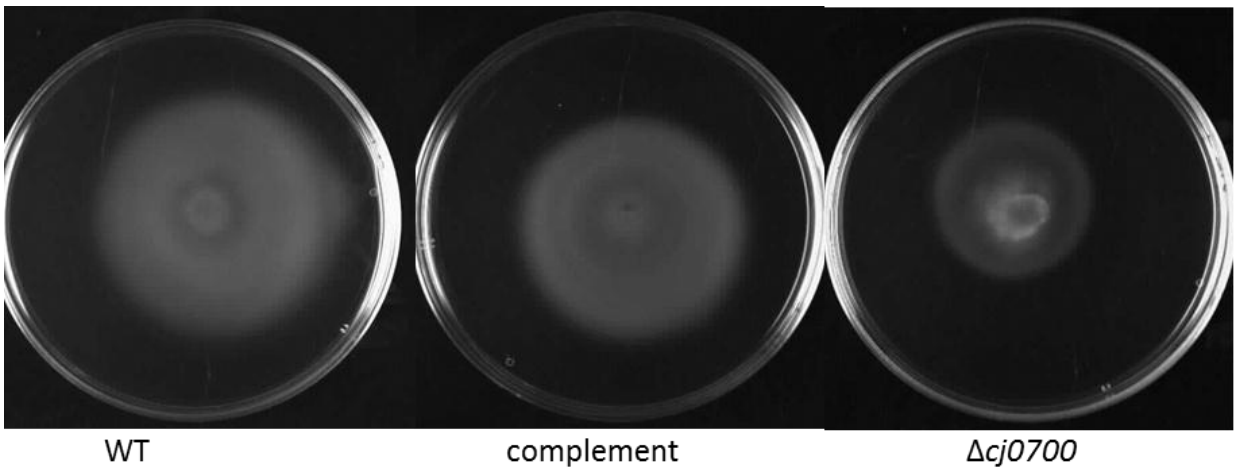

Figure 3.17. Assessment of chemotaxis phenotype of the complemented cj0700 mutant in a NCTC11168 background. Wild type NCTC11168 cells were compared to the *cj0700* mutant (BAJ1J700) and complement with the cj0700 gene replaced into cj0046 (BAJ3CJ700). Cells were inoculated into the centre of a 0.3% (w/v) MHA plate and grown for 72 hours at 42 ^{o}C in a microaerobic atmosphere.

3.4.3. Determination of the role of *cj0700* in other *C. jejuni* strains

Mutation and subsequent complementation of *cj0700* in NCTC11168 showed a role for this *cj0700* gene in chemotaxis when the strains were tested in a swarm assay. Given this observation it was decided to determine whether *cj0700* is conserved across *C. jejuni* strains, notably 81116 and 81-176, and if mutation of the gene in these strains resulted in a similar swarming phenotype.

In *C. jejuni* 81116 the cj0700 homologue is annotated as C8J_0667 and in strain 81-176 it is annotated as cjj81176_0723. The size and sequence of the gene in both strains is similar to that found in NCTC11168 (alignment diagram, Figure 3.8). Given the sequence conservation, the purpose of this chemotaxis experiment was to investigate whether these sequence homologues are functionally conserved.

Mutant, complement and wild type strains of overnight cell cultures of both strain backgrounds were stabbed at the centre of 0.3% semisolid Mueller Hinton plates. Cells were incubated at 42 ^{o}C for 72 hours in micro-aerobic (10% O_2 and 7 % CO_2 and 83% N_2) conditions. For strain 81116 the *cj0700* mutant had decreased migration to the edge of the plates compared to wild type (Figure 3.18). Complementation of the mutation in 81116 showed that the wild type phenotype could be almost completely restored by the NCTC11168-derived *cj0700* allele (Figure 3.18). For strain 81-176 a similar situation to that found with 81116 was observed (Figure 3.19). Mutation of *cj0700* reduced swarming and complementation with the NCTC11168-derived *cj0700* allele again largely restored the wild type swarming behaviour. The assessment of the phenotype of a *cj0700* mutation constructed in two additional strains supports the role of *cj0700* in chemotaxis across *C. jejuni*.

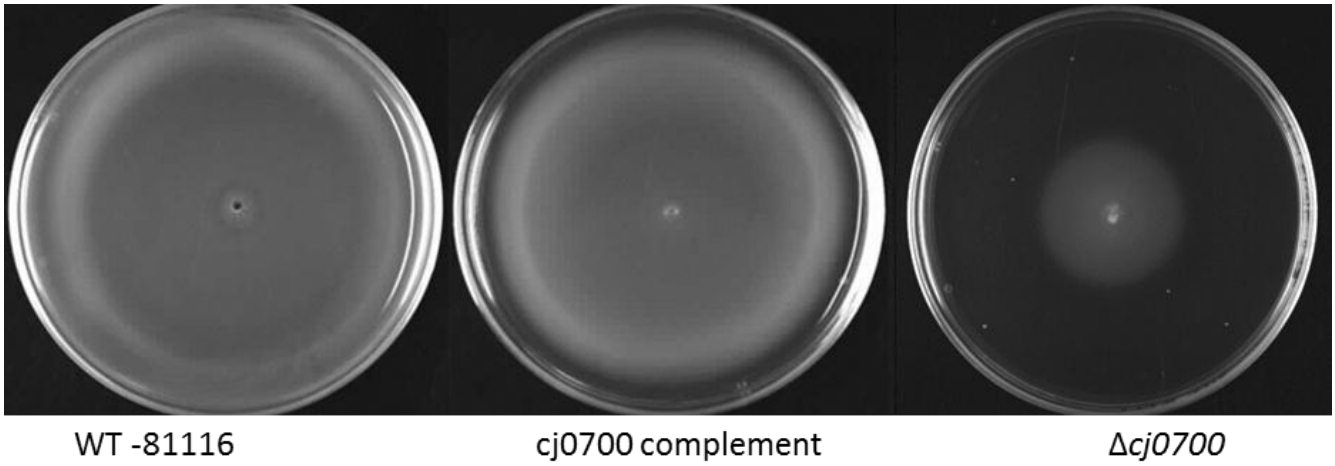

Figure 3.18. The role of Cj0700 in 81116 as assessed by swarming assay.

The chemotactic phenotype of the *cj0700* mutant (BAJ4CJ700) and complement (BAJ7CJ700) compared to wild type on 0.3% (w/v) semisolid MHA plate. Cells were grown for 72 hours on 0.3% (w/v) MHA at 42 ^{o}C under micro-aerobic conditions.

Figure 3.19.The role of Cj0700 in 81-176 as assessed by swarming assay.

The chemotactic phenotype of the *cj0700* mutant (BAJ5CJ700) and complement (BAJ6CJ700) compared to wild type on 0.3% semisolid MHA plate. Cells were grown for 72 hours on 0.3% MHA at 42 ^{o}C under micro-aerobic conditions.

3.5. Growth assay

The growth assay was carried out to examine whether the reduced swarming phenotype of the mutant seen in the swarming assay is related to a true chemotaxis deficiency rather than slow growth rate of the mutant relative to the wild-type and complement.

3.5.1. Growth assay of Δ*cj*0700 in *C. jejuni* strains

Following the construction of the Δ*cj0700* mutant of NCTC11168 (BAJ1CJ700) the pattern and rate of growth was compared to the cognate wild-type and a *cheY* mutant. The assay was carried out using 5 ml microcentrifuge tubes with the bacterial strains grown in 5 ml MHB under micro-aerobic conditions with shaking for 72 hrs (Chapter 2; section 2.8.3.). The growth assay (Figure 3.20) showed that BAJ1CJ700 and the *cheY* mutant grew at similar rate to the wild-type indicating that the apparent differences in swarming seen between the chemotactic mutant and the wild type is not simply due to a difference in growth rate. The growth of the Δ*cj0700* mutants and their complements in 81116 and 81-176 was also assessed (Figure 3.21 and Figure 3.22 respectively). The growth of these strains was assessed using a different format (Chapter 2; section 2.8.3.), whereby the assay was carried out for 24 hours in 96 micro-plates at 42 ^{o}C under micro-aerobic conditions. Although there are some minor differences between the strains, the data for the two additional strains support the conclusion that the phenotype seen in the swarming assay is not due to growth rate differences.

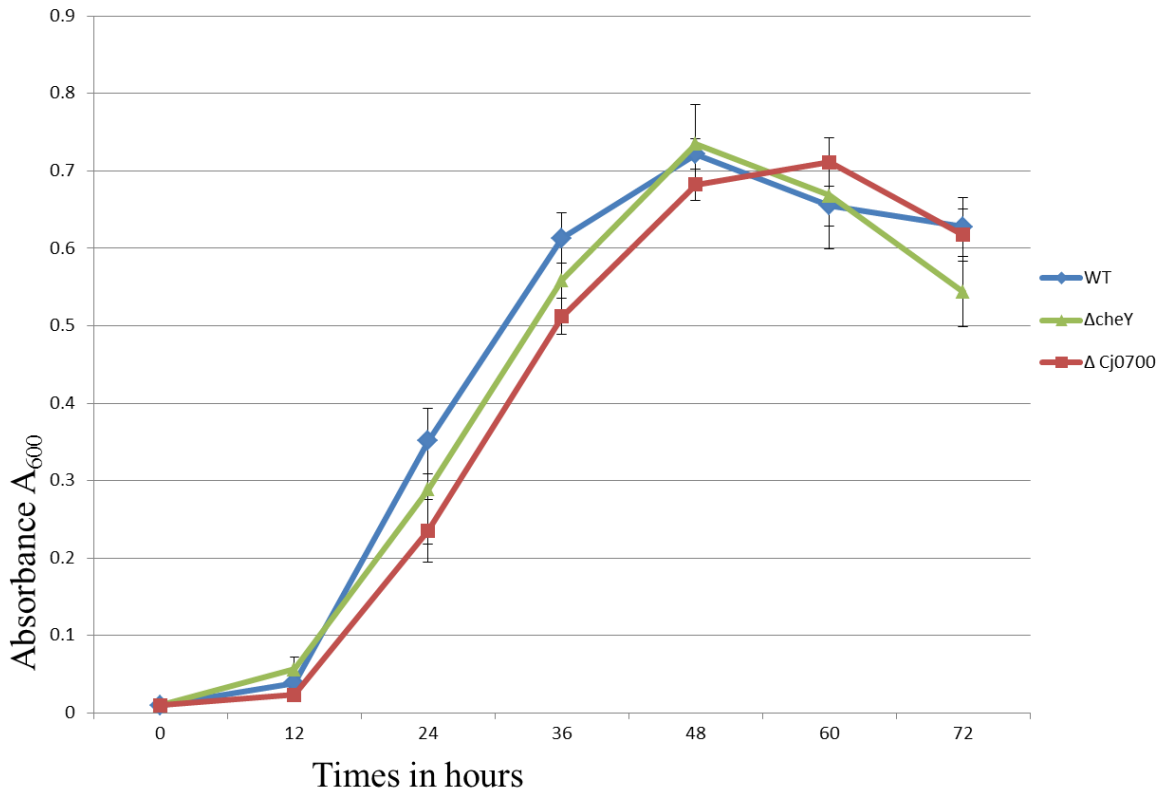

Figure 3.20. Growth of BAJ1J700, Δ*cheY* and NCTC11168 cells.

Strains were grown under micro-aerobic conditions at 42 ^{o}C for 72 hours. Cell innocula were adjusted to 0.05 OD at A_{600} in 5 ml MH broth and samples were taken every 12 hours. Total cell count was measured at A_{600}. Error bars show the standard error of the mean of data from six samples at each time point. Δcj0700 = cj0700 mutant (red line and ■), WT = wild-type (blue line and◆) and ΔcheY = cheY mutant (green line and ▲).

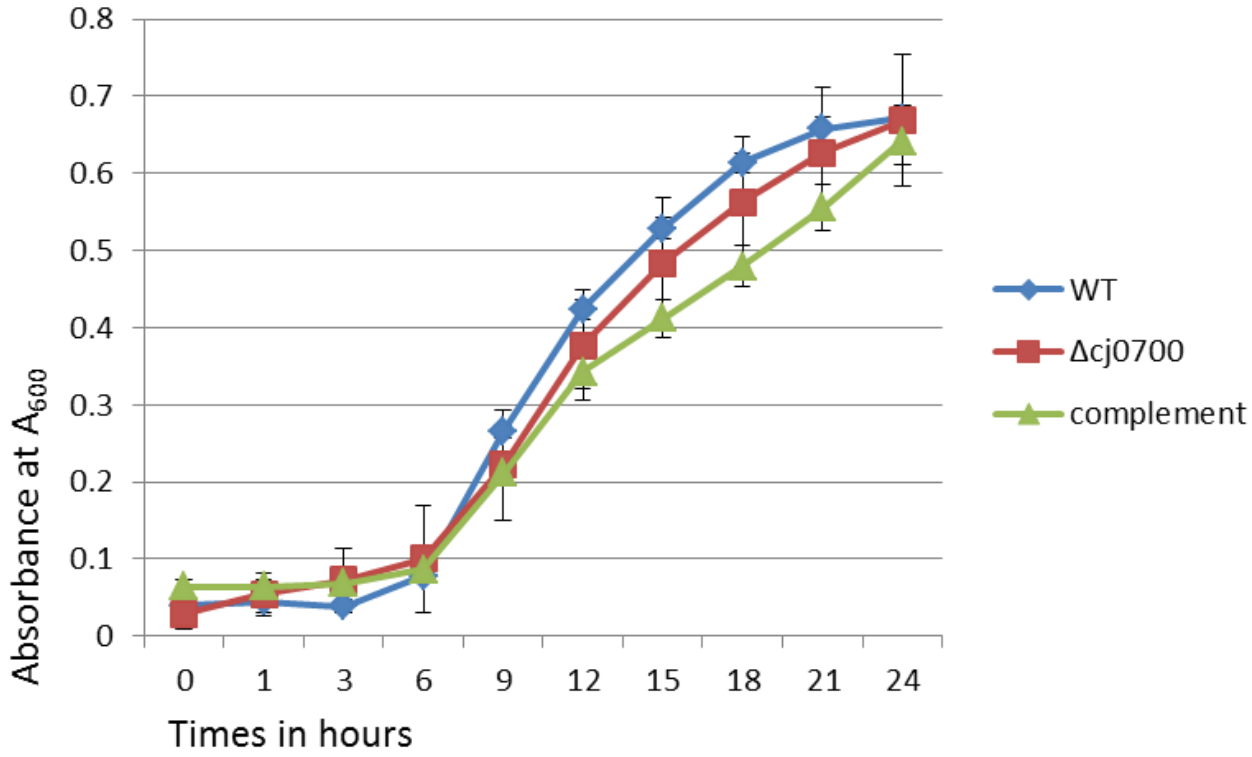

Figure 3.21. Growth of BAJ4CJ700, BAJ7CJ700 and 81116 cells.

Strains were grown under micro-aerobic conditions at 42 ^{o}C for 24 hours. Cell innocula were adjusted to 0.05 OD at A_{600} in 200µl MH broth in a 96 well format and samples were taken at 1 hour post inoculation and then every 3 hours post inoculation. Total cell count was measured at A600. Error bars show the standard error of the mean of data from six samples at each time point. Δcj0700 = cj0700 mutant (red line and ■), WT = wild-type (blue line and◆) and complement = Δcj0700 complement (green line and ▲).

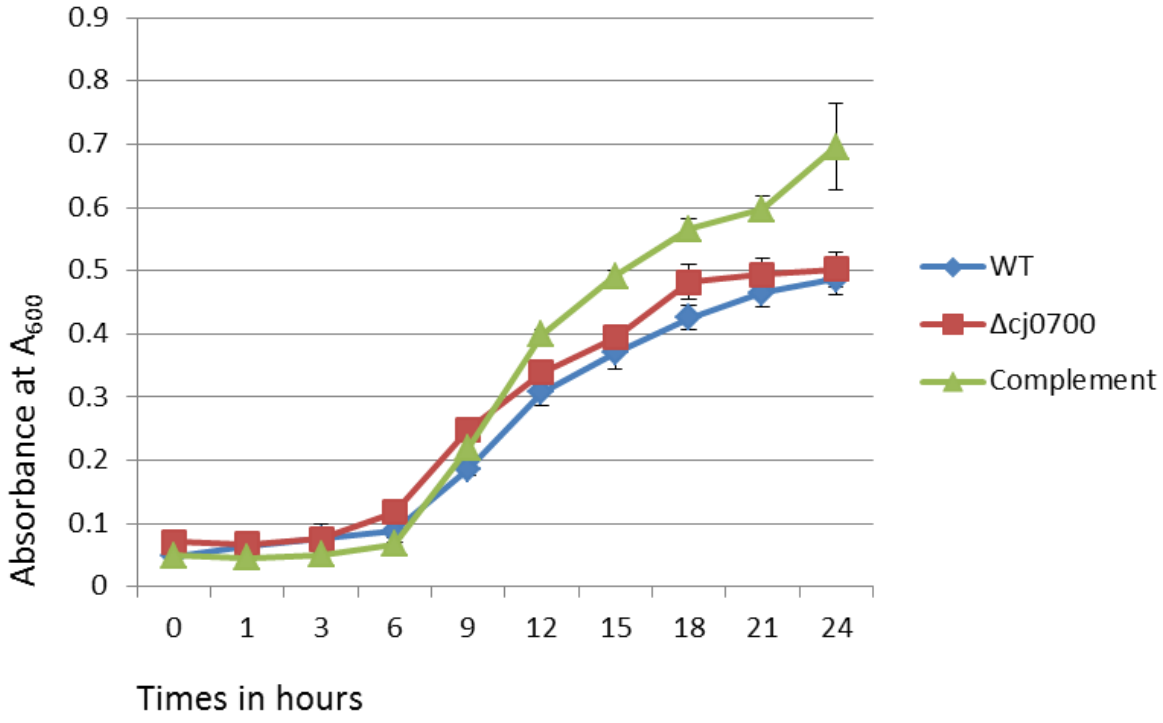

Figure 3.22. Growth of BAJ5CJ700, BAJ6CJ700 and 81-176 cells.

Strains were grown under micro-aerobic conditions at 42 ^{o}C for 24 hours. Cell innocula were adjusted to 0.05 OD at A_{600} in 200 µl MH broth in a 96 well format and samples were taken at 1 hr post inoculation and then every 3 hours post inoculation. Total cell count was measured at A600. Error bars show the standard error of the mean of data from six samples at each time point. Δcj0700 = cj0700 mutant (red line and ■), WT = wild-type (blue line and◆) and complement = Δcj0700 complement (green line and ▲).

3.6. Discussion

In this discussion, focus will be placed on cloning strategies used for cloning and mutagenesis of *cj0700*. Furthermore, testing chemotactic ability of *cj0700* will also be discussed.

3.6.1. Cloning and mutagenesis of *cj0700*

In order to clone the gene, *cj0700* was amplified from chromosomal DNA of NCTC 11168, 81116 and 81176. At the beginning Taq polymerase was used to screen that primers would not mismatch but would bind specifically on the target DNA. During primer design, the AT rich nature of *C. jejuni* chromosomal DNA was taken into consideration. Hence, primer sequences were lengthened /shortened until at least good primer annealing was achieved. Most designed primers were successful; however, in certain conditions where DNA was not amplified, the annealing temperature was changed. Most of the time, annealing temperature ranging from 50 ^{o}C to 70 ^{o}C was used. For cloning, cj0700 was amplified using Phusion polymerase, which has a low level of error according to the manufacturer's recommendations. In addition, when *cj0700* was cloned into pUC19, and confirmed with PCR, subsequently inserts were sequenced to ensure subsequent error-free homologous recombination; hence those with errors were discarded.

Mutating *cj0700* was carried out by inverse PCR and cloned in chloramphenicol antibiotic cassette to enable deletion of a large part of the coding sequence of *cj0700*. In this case, it was most tricky step, the reason being that, it was carefully designed mutating strategy of *cj0700*. Because, this step, two attempts has been earlier carried out by MSc student in their project, both were unsuccessful. As a result, it was considered (i) *cj0700* mutation would not have effect on the downstream genes, because it is possible to co-transcribe *cj0700* with 8 downstream genes. (ii) *cj0700* and *cj0701* overlap three base pairs, hence it was decided to

leave 150 bp of the 3' end of *cj0700* CDSs, in case second promoter of downstream gene(s) and Shine-Dalgarno of *cj0701* may be buried within *cj0700*. (iii) To reduce possible polar effects in the *cj0700* mutant, a promoter-less and terminator-less *cat* resistance cassette insertion was established. In addition, another *cj0700* mutagenesis strategy was designed, in case the first strategy was found to to fail, for instance, the *glnA* (glutamine synthetase) gene (Figure 3.4) is upstream of *cj0700*, which transcribes in the opposite direction. The *glnA* gene in bacteria is able to assimilate ammonia by converting glutamate into glutamine and this has been confirmed in *H. pylori* (Marais et al., 1999). Hence, the plan was to put an antibiotic resistance cassette in the *glnA* gene and, with appropriate use of flanking sequences, and then mutate the *cj0700* gene.

Cloning and mutagenesis of *cj0700* in the pUC19 plasmid did not encounter any difficulties, except that transforming the suicide pAJ5 into NCTC11168 competent cell. It was attempted two times, both were unsuccessful; however, the reason may have related to the chloramphenicol concentration being too high for the *cj0700* mutant cell. Since expression of the *cat* gene is driven from the promoter of *cj0700*, a lower chloramphenicol concentration (35μg/ml) was used for the first selection with subsequent re-plating at normal concentrations (50μg/ml). This has produced successful *cj0700* mutant in NCTC11168.

Creating a *cj0700* mutant in NCTC11168 was a great achievement; however, one very important point that had to be taken into consideration was that the chemotaxis phenotype was not due to the phase variation. Phase variation is presumably the result of selective pressure during transformation (electroporation) and as a result a non-motile variant may be created. Hence to avoid that, the *cj0700* mutant was reintroduced into a motile NCTC 11168 background using natural transformation. The genome sequence of NCTC 11168 has been shown to contain homopolymeric G/C tracts, which are presumably variable due to slipped stand mismatching during DNA replication. In addition, genes containing homopolymeric

tracts have been identified to involve flagellin modification and LOS biosynthesis (Parkhill et al., 2000, Linton et al., 2000, Bayliss et al., 2012). Hence, it is important to make sure that motility of the cell, especially flagellum was not affected by this selective pressure, which would otherwise have given a false result in chemotaxis investigation. In addition, cell motility and morphology was examined by microscopy, which indicated that the mutants were normal relative to the wild type in phenotype. Hence, motility of mutant and complement assured that chemotaxis phenotypes were genuine.

Complementing *cj0700* mutant strains was first carried out by the student Sherline Benedict under my supervision, where BAJ1CJ700 in NCTC 11168 was directly transformed into 81116 and 81-176 creating *cj0700* mutants. However, Δ*cj0700* mutants of strains had shown aggregation on semisolid plates. It could have been the result of creating new strains derived from both genetic backgrounds. Therefore, this mutagenesis strategy was abandoned and pAJ5 was used to make mutants directly in competent cells of 81116 and 81-176. Confirmation of allelic exchange event in the *cj0700* locus in both strains used primers designed (Cj0700F/Cj0700R) for NCTC 11168; because the *cj0700* locus and flanking DNA were 99% similar to NCTC11168. As a result mutating *cj0700* in 81116 and 81176 strains has proved to be successful.

3.6.2. Chemotactic phenotype of *cj0700* mutants

In order to investigate the chemotactic phenotype of the *cj0700* mutant, there are three techniques that have been employed so far for chemotaxis evaluation namely, Capillary assay, Hard- agar plug (HAP) assay and swarming assay. Unlike, swarming assay, the capillary and HAP assay has known drawbacks that made them unreliable for chemotaxis assessment of the *cj0700* mutant. Therefore in this chemotaxis study was decided to employ swarming assay technique for chemotaxis investigation in *cj0700* mutants.

The capillary technique has been used to assess chemotactic phenotypes exhibited by strains of *Campylobacter* (Hartley-Tassell et al., 2010b, Baserisalehi and Bahador, 2011), however, previous results in *C. jejuni* has shown inconsistent results and has failed to produce reproducible results (Sandhu, PhD thesis 2011). Hence, this capillary technique has not been used to investigate *cj0700* mutants. Likewise, HAP assay has shown false results for examining non-chemotactic phenotypes, where assays indicated the non-chemotactic phenotype appeared to be chemotactic phenotype. As a result, assay reliability for chemotaxis investigation has been speculated (Kanungpean et al., 2011a). Recently a modified HAP assay has been developed in the Department of Genetics, University of Leicester (Elgamoudi, 2013). The modified HAP assay is supplemented with the cellular redox indicator Triphenyl Tetrazolium Chloride (TTC) so that as cells spread out the colour change can be more easily detected around the edges of the plate. However, false results may still be possible therefore further optimization is required. Elgamoudi has also developed a chemotaxis assay where the chemotactic bacteria are monitored using chemotaxis slides; these slides have two reservoirs connected by a channel. A 1% agarose gel is cast in the channel between the two reservoirs. In one reservoir is placed a known concentration of the motile bacteria of to be examined whereas in the other reservoir is pipetted a chemoattractant. After a defined incubation period the number of cells which have crossed from the channel is counted from the chemo-attractant reservoir. Similarly, cells that cross the channel to the chemo-attractant can be tracked by video. It would be possible to use this chemotaxis slide for examining the chemotaxis behaviour of *cj0700* mutant. The only possible drawbacks of this chemotaxis assay could be that non-chemotactic bacteria may diffuse through pores in the agarose in the channel connected between two reservoirs and thus would provide false positive results; however, if the placing of the agarose gel is carefully standardised it may provide true and reliable results.

Semisolid (soft) agar known as swarming assay is well established assay used for chemotactic investigation for chemotactic bacteria (Wolfe and Berg, 1989). Thus, in this experiment the swarming assay was used to assess chemotactic phenotype of *cj0700* mutants. Nevertheless, concentration of agar is critical of chemotaxis investigation, where less agar concentration enables fast migration, whereas high concentration reduces bacterial ability to migrate. Hence the optimum agar concentration has been suggested ranges between 0.2% to 0.4% agar concentration (Croze et al., 2011). Therefore, in this chemotaxis experiment, 0.3-0.4% agar concentration has been used for *cj0700* mutants. At the beginning, using 0.15% and 0.5% agar concentration brought difficulties, where 0.15% agar concentration was difficult to evaluate chemotactic spread on the plate, because the plate was difficult to handle due to the softness. Conversely, with 0.5% agar concentration, motile and chemotactic NCTC 11168 faced difficulties to migrate in denser agar and as a result, cells spread less on the plate. Taken together, swarming technique was assay of choice relative to the other two assays (Capillary and HAP assays), because unlike swarming assay, other assay were mainly used in attractant and repellent detection (Hartley-Tassell et al., 2010b, Baserisalehi and Bahador, 2011, Kanungpean et al., 2011a). However, swarming is to visualise and compare the diameter spread of non-chemotactic and chemotactic bacteria on the plate (Szurmant et al., 2004).

3.6.3. Complementation of *cj0700* mutants

Non-chemotaxis phenotype of *cj0700* observed in swarming was important for determining the role of *cj0700* in the chemotaxis signalling pathway in *C. jejuni*. Nevertheless, successfully restoration the wild type phenotype of *cj0700* mutants was also vital to prove the role of *cj0700* in chemotaxis signalling pathway.

Thus far, two complementation possibilities were available for *Campylobacter* sp. One of which is using pKmetK plasmid, where gene of interest was targeted to the *cj0046* pseudogene. Other approach for complementation is targeted to the space between the 16S and 23S locus in one of the three copies of the *C. jejuni* rRNA genes (Karlyshev and Wren, 2005). The only difficulty with this technique is the possibility of putting complementing locus into three rRNA alleles.

Complementation targeted into the *cj0046* pseudogene seemed easier and widely used (Kim et al., 2008, Rahman et al., 2014). Therefore, *cj0700* allele was targeted to *cj0046* pseudogene, whereby *metK* promoter is constitutively controlling *cj0700* expression. Nevertheless, phenotypes with and without *metK* promoter didn't demonstrate any phenotypic difference on semisolid agar plate. In addition, complementing the *cj0700* allele in to the *cj0046* pseudogene was successful and thus, putting *cj0700* allele *in trans* has successful restored wild type phenotype of *cj0700* mutants.

Chapter 4 : Expression, purification and phosphorylation

4. Introduction

The previous chapter described how the *cj0700* gene was mutated and its role in chemotaxis established. Hence it is worthwhile to determine the functional role of Cj0700 in the chemotaxis signalling pathway by examining whether Cj0700 has phosphatase activity and interacts with chemotaxis signalling proteins. Therefore in order to make an enzymatic assessment of phosphatase activity of Cj0700, it and other chemotaxis proteins need to be purfied using affinity tagged columns. The aim of this work was to express and purify the Cj0700 protein to enable the examination of the physical (pull-down) and chemical (phosphatase) interactions of Cj0700 with other chemotaxis proteins, specifically those with RR domains found in *C. jejuni* NCTC11168. As a first step, the expression and purification conditions of Cj0700 were optimised; thus making 100% pure of Cj0700 protein would enable me to study the structure and function of the protein. In *E. coli*, when attractant or repellent is attached to the chemo-receptors of the cell a signal is transferred to CheA which modulates its kinase activity and thus the autophosphoylation state of the histidine residue. Subsequently, the phosphate is transferred to the CheY RR at an aspartate residue. In normal conditions, the flagella is in anticlockwise rotation and the phosphorylation of CheY-P results in a switch of flagellar rotation to the clockwise direction (Young et al., 2007). In this situation, in order for a chemotactic cell to deactivate the signal cascade, CheY autodephosphorylates at a slow rate, however this results in a slow response to environmental signals (Terry et al., 2006). For that reason, CheZ protein plays an important role for chemotaxis, where the cell responds rapidly to the stimuli, by removing phosphate from CheY-P (Zhao et al., 2002).

The genome of *C. jejuni* was first believed to lack a CheZ homologue and instead CheV was suggested to operate as a phosphate sink (Terry et al., 2006). Hence, *C. jejuni* was thought similar to *Sinorhizobium meliloti* and *Rhodobacter sphaeroides* which both lack CheZ, and instead have evolved a phosphate sink mechanism in order to redirect phosphate from RRs such as CheY. Consequently, *C. jejuni* was suggested to use CheV to sequester phosphate in the chemotaxis pathway (Terry et al., 2006). However, the recently identified *hp0170* gene from *H. pylori* was confirmed to be a distant orthologue of *cheZ* in *E. coli*. Furthermore, amino acid alignment has shown that Cj0700 from *C. jejuni* shares about 50% identity with the Hp0170 protein. In addition, the residues in the active site of CheZ and Hp0170 protein are also conserved in the Cj0700 protein (Terry et al., 2006).

It is important to briefly introduce the background of the CheV protein in *C. jejuni*, because that will give a better understanding of its role in the chemotactic pathway. In the genomic sequence of *C. jejuni* it was identified that a CheZ homologue was missing (J. Parkhill et al., 2000, Young et al., 2007) and as result of that it was hypothesised that CheV could act as a phosphate sink for CheY-P (Young et al., 2007). Additionally, the CheV sequence comprises of a hybrid of CheW at the N-terminal and a RR at the C-terminal (Young et al., 2007). CheV homologues were first identified in *Bacillus subtilis* and then later in *Helicobacter pylori* (Helmann, 1994, Wadhams and Armitage, 2004). In *B. subtilis* CheV has been found to play an adaptation role for attractants (Karatan et al., 2001). In addition, a report has suggested that CheV in *H. pylori* contributes a role similr to CheW in *E. coli* for stabilising the chemoreceptor complex and enhancing adaptation through desensitising the CheW-like domain of the CheV (Alexander et al., 2010, Lowenthal et al., 2009b). Taken together a role for CheV in *C. jejuni* is still elusive; however, it is worthwhile to determine the role of the CheV in the chemotaxis pathway. Since the CheV protein is a structural

hybrid of RR and has a CheW domain, we want to examine if Cj0700 has a phosphatase role on phosphorylated CheV-P.

It is worth mentioning here that proteins used in the phosphorylation, such as CheY, CheA-HK, CheA-RR and Cj0700, occasionally will be designated $CheY_{cj}$, CheA-HK_{cj}, CheA-RR_{cj}, $CheV_{cj}$ and $CheZ_{cj,}$ this it is to avoid confusion with other chemotaxis proteins found in the other bacteria such as *E. coli*, thus they are assigned the name of bacteria from which they were purified, i.e.*C. jejuni* (cj).

The purification and expression efficiency of proteins was optimised by selecting the appropriate purification methods and also the optimal concentration of the inducer. In this work, IPTG was utilized to induce expression of His_6-tagged proteins.

Purification of His tagged proteins is based on the strong affinity with a nickel that the His-tag has in the affinity column incontrast the untagged whole cell proteins can pass through the affinity column without binding. Also the elution of the His_6-tagged proteins from immobilisation column was achieved by an increasing concentration gradient of imidazole. The elution of His tagged proteins in this experiment was the modification of the earlier protocol (Crowe et al., 1994). Alternatively, the His_6-tagged fusion proteins carry either enterokinase or TEV (Tobacco Etch Virus) cleavage site, where His tags can be excised to elute them.

4.1. Constructing His_6-tagged *cj0700* expression plasmid

The *cj0700* gene was amplified from genomic DNA of NCTC11168 using primers (cj0700F-pleics03 and cj0700R-pleics03) designed in accordance (Chapter 2; section 2.9.1.1) with guidelines provided by PROTEX (Biochemistry, University of Leicester) and then *cj0700* was inserted into a pLeics03 expression vector. The reason for using this vector rather than other expression vectors available was that the pLeics03 vector has a TEV protease cleavage

site which was needed to be able to remove the His tag site for the later Cj0700 structure study (Chapter 6) whereas other available expression vectors had an enterokinase protease cleavage site. The TEV protease protein was produced in the Biochemistry Department (University of Leicester) whereas enterokinase was only commercially available making it expensive in comparison to TEV. In brief, a *cj0700* gene fragment 696 bp long was amplified using cj0700R-pleics03 and cj0700F-pleics03 primers and cloned into pLeices-03 at the 3' end of the sequence encoding six histidine residue. Phusion polymerase was used to ensure that the amplified *cj0700* sequence was likely to be error free.

PCR products (Figure 4.1) were amplified from chromosomal DNA of *C. jejuni* NCTC 11168 using cj0700F-pleics03 and cj0700R-pleics03 primers which contain *cj0700* sequence at the 3' end and pLeics03 at the 5' end. These three amplicons migrated to a position on an agarose gel that corresponds with the predicted size of 696 bp fragments long. After that these PCR products were cleaned with PCR purification kit (Chapter 2; section 2.4.4) and they were sequenced using cj0700F-pleics03 and cj0700R-pleics03 primers in order to confirm that the fragment sequences were correct. Subsequently, the Cj0700 PCR product was given to PROTEX to construct the *cj0700* (pLeics03::*cj0700*) recombinant plasmid.

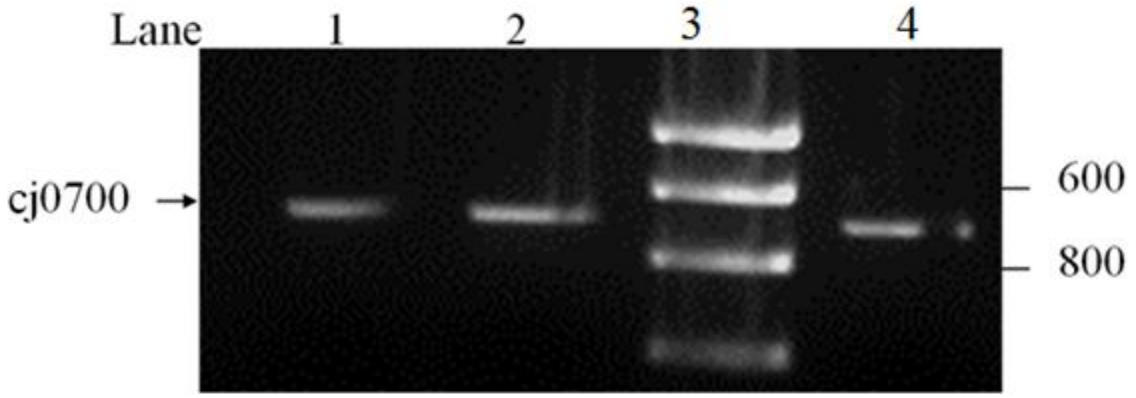

Figure 4.1.PCR product of *cj0700* amplified from NCTC 11168.

Three amplifications resulting in *cj0700* amplified from chromosomal DNA using cj0700F-pleics03 and cj0700R-pleics03 primers. Lanes: 1 = *cj0700*PCR product, 2 = *cj0700*PCR product, 3 = Hyper-ladder I marker with fragment sizes shown in bp on the right, 4 = *cj0700*PCR product. A fragment size of 696 bp was expected. PCR product was electrophoresed on 1% TAE agarose gel stained with ethidium bromide.

The *cj0700* allele was cloned into the expression vector, pLeics03 by Dr. X. Yang (PROTEX, department, University of Leicester). Three pLeics03:*cj0700* constructs were obtained from PROTEX. Again, presence of the *cj0700* allele in recombinant (pLeices03::cj0700) plasmid was confirmed by doing PCR using cj0700F-pleics03 and cj0700R-pleics03. PCR products of the *cj0700* constructs were shown to migrate to a position that corresponded with the predicted size of 696 bp (Figure 4.2) in comparison to PCR amplified from chromosomal DNA. Hence PCR product of *cj0700* amplified from pLeices03::*cj0700* plasmid (Figure 4.2, lanes 2, 3 and 4) and shows *cj0700* amplified from chromosomal DNA (Figure 4.2, lane 5) illustrate the same molecular size. In addition, *cj0700* insert from clones 2 and 3 were sequenced using cj0700F-pleics03 and cj0700R-pleics03. All were shown to migrate to a position that corresponds with the predicted size of *cj0700* and were error-free.

Once the *cj0700* amplicon showed the correct size and had been verified by sequencing to be error free then two clones (Figure 4.2, lane 2 and 3) were transformed into DH5αE competent cells by heat shock and these were stored. Again, *cj0700* was amplified from pLeics03:*cj0700* plasmid in DH5αE transformats with a predicted size 696 bp long (lane 4, Figure 4.2). Once again, *cj0700* sequence in clone 4 was proved to be correct and was

designated pAJ8 (Figure 4.3). For expression, pAJ8 was transformed into competent cells of the *E. coli* BL21 expression strain via heat shock. *Cj0700* was amplified from pAJ8 plasmid transformant cell (lane 6, Figure 4.2) by colony PCR (Chapter 2; section 2.4.1. 1) using cj0700F-pleics03 and cj0700R-pleics03 primers. Furthermore, NCTC 11168 was used as a control using cj0700F-pleics03 and cj0700R-pleics03 primers, which shows a *cj0700* PCR amplicon with the predicted size of 696 bp (Figure 4.2, lane 5). Once again *cj0700* sequence (pAJ8 plasmid) in *E. coli* BL21 expression strain (Figure 4.2, lane 6) was confirmed to be correct.

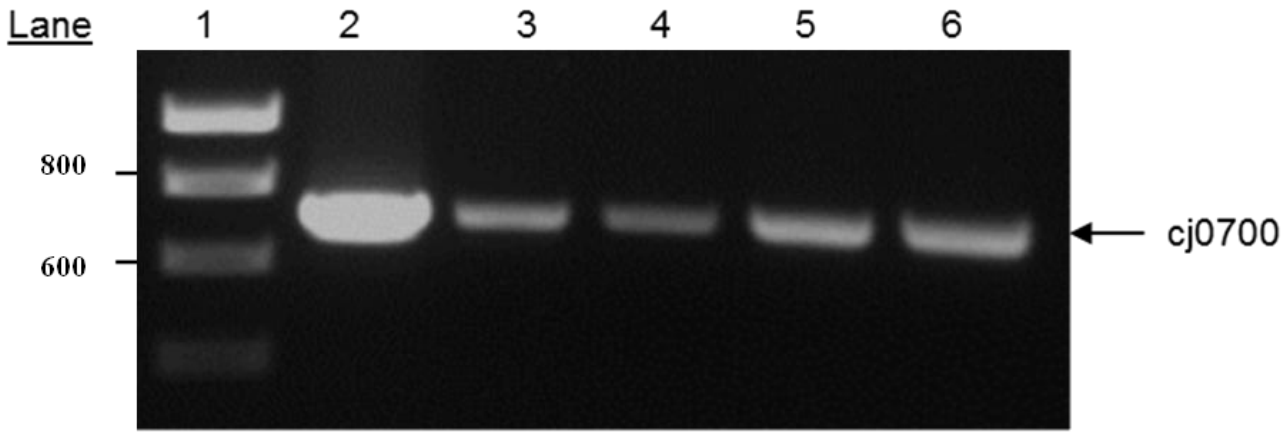

Figure 4.2.Verification of the presence of *cj0700* in the pLeics03:cj0700 construct.

The *cj0700* gene was amplified from pLeics03:cj0700 plasmid using cj0700F-pleics03 and cj0700R-pleics03 primers. Lane 1= hyper-ladder I marker with relevant fragment sizes shown in bp on the left. Lanes 2, 3 and 4= pLeics03::*cj0700* plasmid; lane 5= *cj0700* from chromosomal DNA of *C. jejuni*; Lane 6 =*cj0700* from pAJ8. PCR product was electrophoresed on a 1% TAE agarose gel and visualised by staining with ethidium bromide.

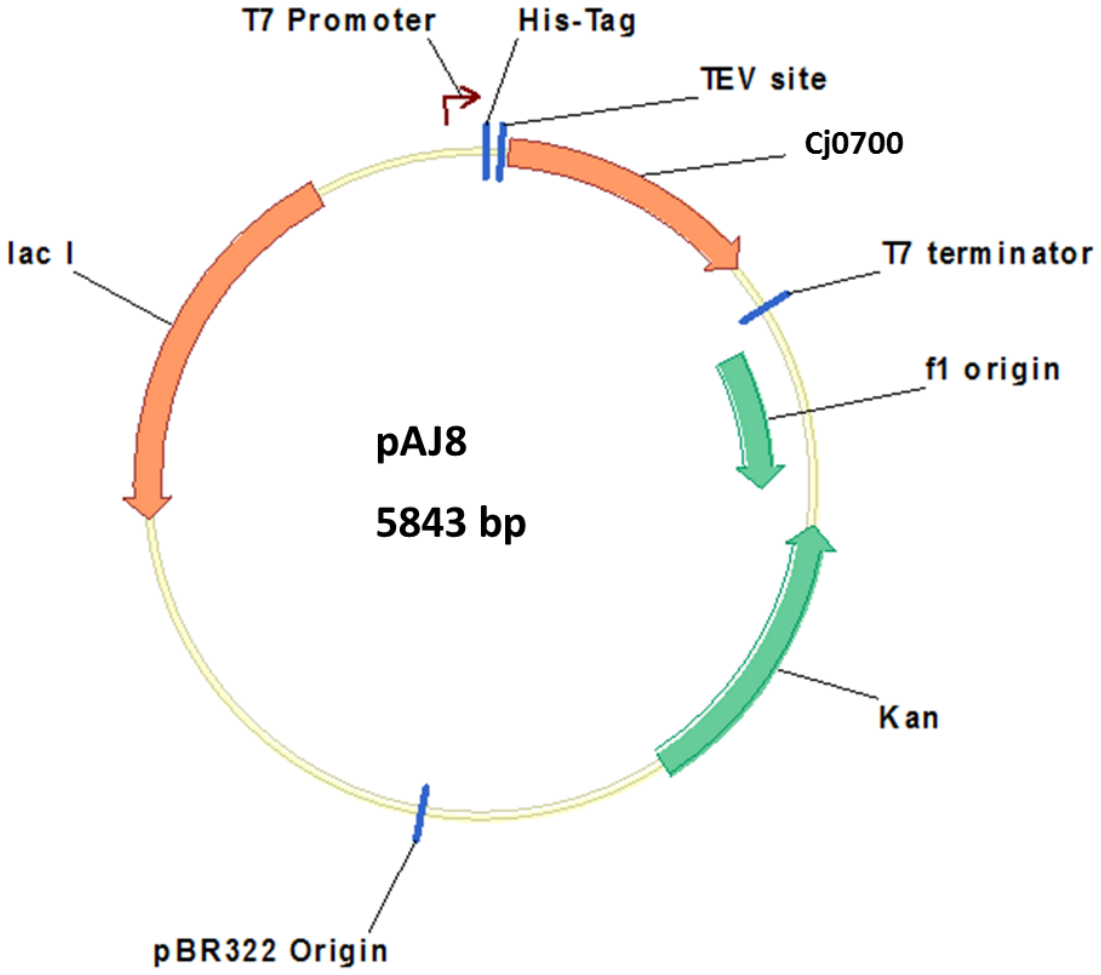

Figure 4.3. Schematic map of the *cj0700* gene fused into His-tagged plasmid.
The new pAJ8 plasmid was derived from pleics03 plasmid. Plasmid carries 6xhistine residues and TEV site for excising histidine from *cj0700* (orange) fusion protein. pAJ8 carries: *lacI* gene (orange), kanamycin resistance (green), *f1* origin of replication (green).

4.2. Optimization of His_6-tagged *cj0700* expression and purification

Expression of pAJ8 plasmid was optimised using different IPTG concentrations. Equally, the temperature at which to express was optimised as well. Visualisation of His_6-tagged Cj0700 protein was recognised by 10%-15% Tris-Glycine SDS-PAGE. Results were visualised either by staining gels with Commassie Brilliant Blue stain or Western blotting with anti-His antibody.

For protein production optimisation the IPTG concentration was tested at 0.5, 0.8, 1.0, 1.2 and 1.4 mM. Likewise, recombinant cells induced with IPTG were incubated at room temperature, 30°C or 37°C with the purpose of optimizing the expression condition in order to maximise the protein quality and yield.

At the beginning, overnight cultures of *E. coli* BL21 cells were diluted 1/100 with Luria broth and grown shaking at same temperature until cell concentration reached to 0.5 OD at A600. Then cells were induced with 0.5 mM and 0.8 mM concentration of IPTG and incubated at room temperature, 30 °C or 37 °C for 3 or 4 hours. In 0.5 mM and 0.8 mM of IPTG at 37 °C, protein was produced at low levels (or even not expressed at all) so that anti-His antibodies could not detect it in a Western blot (data not shown). As a result of low level expression, cells were induced with 1 mM, 1.2 mM or 1.4 mM of IPTG at 30 °C for 3 hours. At 1 mM IPTG concentration, expression was saturated, because there is no difference in protein production levels above 1 mM IPTG (Figure 4.4). Protein bands indicate that there is no variation in terms of Cj0700 production with different IPTG concentrations (lanes, 2, 3 and 4, same figure). Therefore, Cj0700 was best produced using 1 mM of IPTG at 30 °C for 3 hours thus this IPTG and temperature condition was chosen for use in subsequent expression of *cj*0700.

After the expression conditions for Cj0700 were optimised, different purification conditions were also tried (data not shown). Finally, it was decided to establish Cj0700 purification with

a binding buffer containing 50 mM Tris-HCl, 0.5 NaCl, 20 mM imidazole adjusted to pH 7.6.

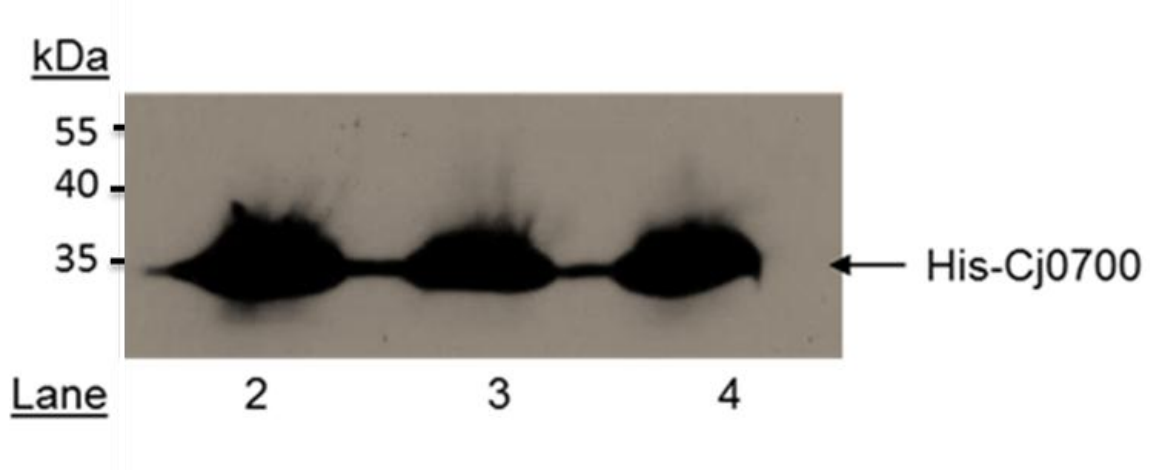

Figure 4.4. Optimising IPTG concentration to produce His tagged Cj0700.

His6 tagged Cj0700 stimulated at 1 mM (lane2), 1.2 mM (lane 3) and 1.4 mM (lane 3) of IPTG for 3 hours overexpression in BL21 cells at 30 $^{\circ}$C. Cj0700 was visualised by immunoblotting with anti-His6 (arrow). Sizes of the protein Protein ladder (are shown at the left) and Cj0700 was electrophoresed on 10% Tris-Glycine SDS-PAGE.

To create optimum conditions to remove Cj0700 protein from the His_6 affinity column the imidazole concentration was increased from 40 mM to 500 mM. Cj0700 was found to be released from the affinity column by using elution buffers containing 80 and 120 mM concentrations of imidazole. Each elution was compared to the supernatant of whole cell lysate. As shown in lane 4 (Figure 4.5) washing with 40 mM imidazole concentration didn't release Cj0700 from the His affinity column. Conversely after washing Cj0700 bound to the His affinity column with buffer containing 80 mM concentration of imidazole, Cj0700 was released from affinity column as shown in lane 3 (Figure 4.5). However, Cj0700 was not completely eluted from column, because in the second wash with 120 mM imidazole, there are still traces of Cj0700 released from the affinity column. Elution and purity level of Cj0700 protein using different concentrations of imidazole was compared to the supernatant of whole cell lysate shown in lane 5 (Figure 4.5). Since Cj0700 protein is an enzyme (some enzymes are unstable), it is more likely to be unstable in different conditions; hence protein is susceptible to degradation and often there is faint second band migrating below Cj0700.

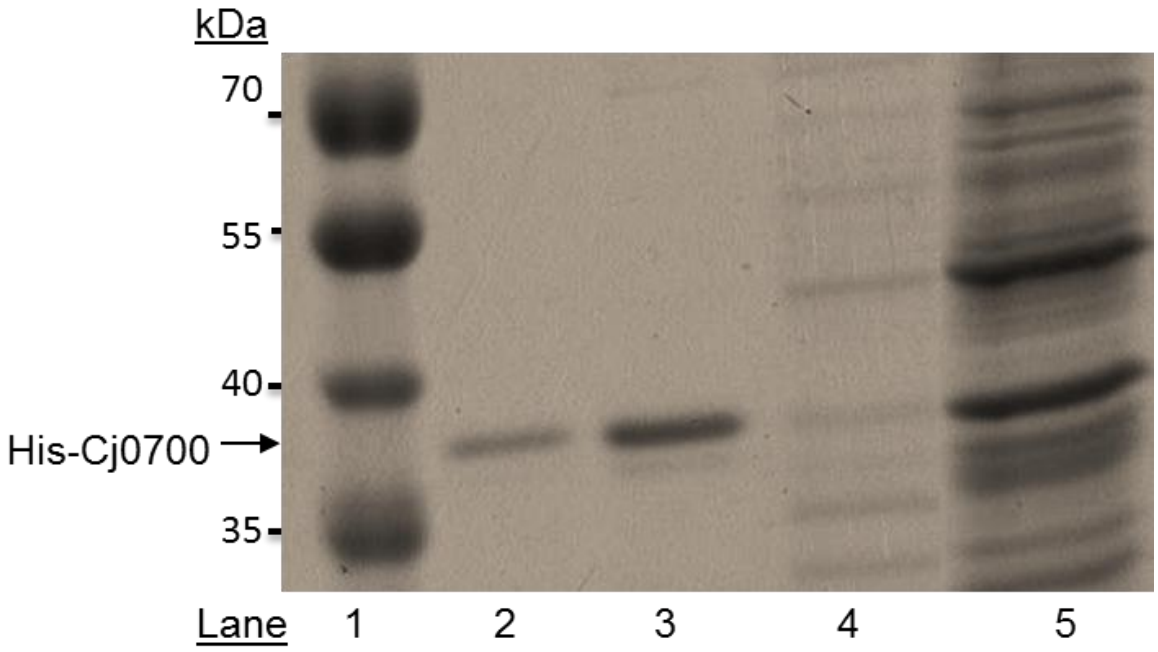

Figure 4.5. Optimising His tagged Cj0700 protein purification with different imidazole concentrations. The experiment was about producing uncontaminated Cj0700 protein**.** Lanes: 1= pre-stained protein ladder (10-250 kDa), 2= 120 mM imidazole wash, 3= 80 mM imidazole wash, 4= 40 mM imidazole wash and 5= whole cell lysate prior to column application. Lane 5 indicates Cj0700 was produced during induction with 1 mM IPTG (arrow point). Protein ladder and Cj0700 was electrophoresed on 10% Tris-Glycine SDS-PAGE gel and visualised by Coomassie Brilliant Blue stain.

It was found that at less than 80 mM imidazole concentration the His_6 Cj0700 protein was not released from immobilisation on the affinity column (Figure 4.5, lane 4). Nevertheless, 80 mM imidazole concentration was not enough to elute all Cj0700 bound to the affinity column (Figure 4.6, lane 3 and 4) and also as stated in Figure 4.5, when 120 mM wash was applied after 80 mM wash. As a result of removing the contaminants, Cj0700 purification conditions were established such that the His6 affinity column was washed with excess binding buffer containing 40 mM imidazole so that unbound cell lysate proteins would be removed. Then, to remove all Cj0700 protein from His affinity column, it was decided to use binding buffer containing 200 mM imidazole (Figure 4.7), in order to avoid any Cj0700 remaining in the affinity column after 120 mM imidazole wash. At an 80 imidazole the Cj0700 was judged, by eye, to be 95-100% pure (Figure 4.5 and Figure 4.6).

With regard to the observed molecular weight (MW) illustrated as kDa, the deduced amino acid sequence of Cj0700 indicates a predicted MW of 26 kDa, however when run on SDS-PAGE (Figure 4.4 and Figure 4.5) the His_6 tagged Cj0700 protein shows a mass of about 37.5 kDa relative to the pre-stained protein standards ruler. Despite the His_6 tag residue fused to protein, which has a size of 3 kDa, there is a notable shift in protein size in SDS-PAGE.

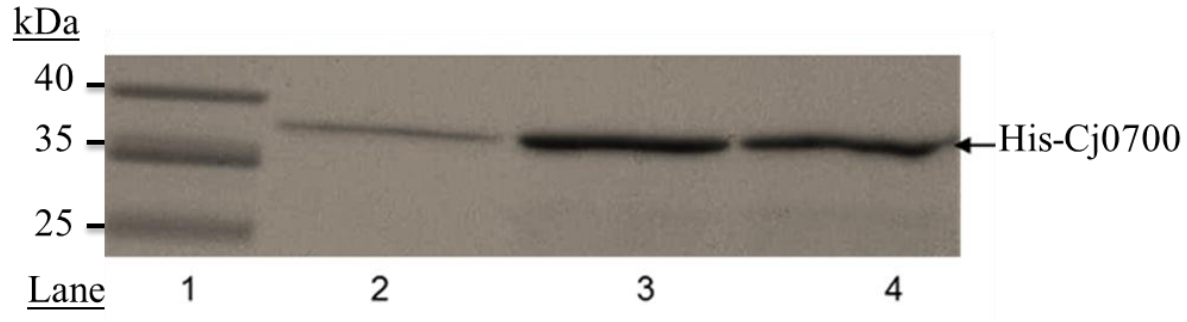

Figure 4.6. Optimising recombinant Cj0700 protein with elution buffer.

Eluting Cj0700 from His column by washing two imidazole concentrations. Lanes: 1= pre-stained protein ladder (10-250 kDa), 2 = 120 mM imidazole, 3 = 80 mM imidazole, 4 = 80 mM imidazole. 10% Tris-Glycine SDS-PAGE gel was visualised by Coomassie Brilliant Blue stain. Cells were induced to 1 mM concentration of IPTG for 3 hours at 30°C. MWs of the protein ladder separated beside Cj0700 are shown at the left.

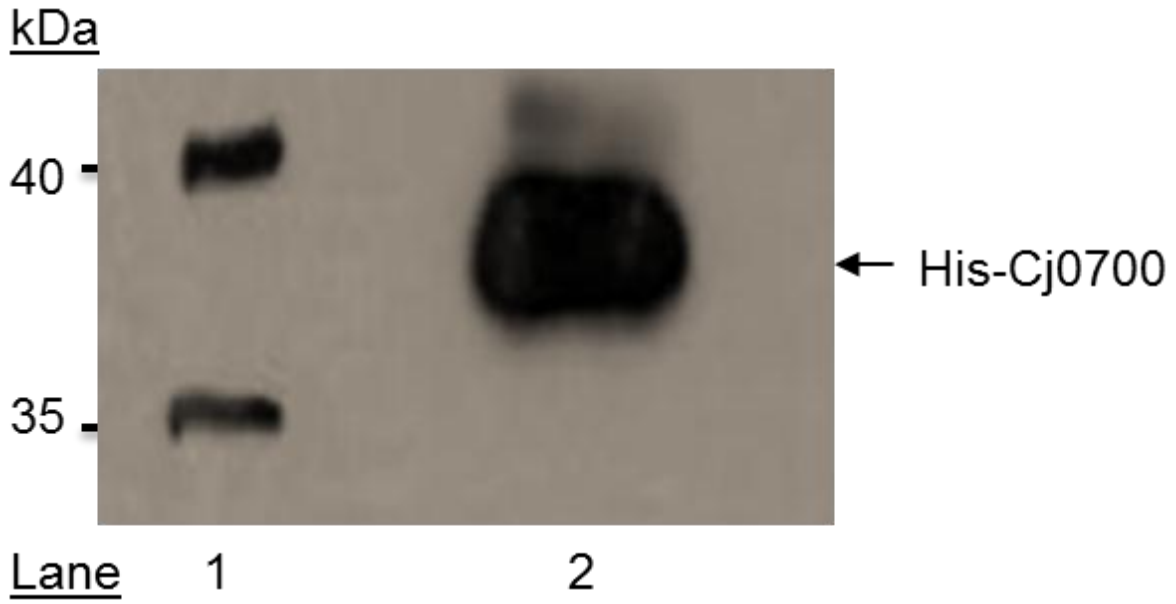

Figure 4.7. His_6-tagged Cj0700 protein released from affinity column.

Elution buffer containing 200 mM imidazole was adjusted pH at 7.6. Lanes: 1= pre-stained protein ladder (10-250 kDa), 2 = 200 mM imidazole. At the left is shown sizes of the protein ladder. Cj0700 was visualised by immunoblotting with antibody against His_6 residue in the fusion protein (arrow). Protein ladder and Cj0700 was electrophoresed on 10% Tris-Glycine SDS-PAGE gel.

4.3. Expression and purification of His_6-tagged CheY

The CheY RR of the chemotaxis signal pathway in *C. jejuni* was needed to be expressed and purified with the intention of probing for protein-protein interactions with Cj0700, and in addition to investigate any phosphatase effect of Cj0700 on CheY-P. Hence, the pPA021 plasmid containing His_6 tagged CheY protein was extracted and was transformed into the *E. coli* strain, Rosetta.

For production of the His_6 tagged CheY fusion protein 1 mM IPTG was used for induction and cells incubated at 37 $^{\circ}$C for 3 hours. Furthermore, the supernatant containing fusion protein was run through a His6 tagged affinity column so that CheY would selectively bind to the column. His6 tagged CheY protein (Figure 4.8, lanes 2 and 3) was separated on 10% SDS-PAGE and visualised by Coomassie Blue stain. Regarding the size of the protein, using Clone manager software the amino acid sequence of native CheY was predicted to be 13.2

kDa; however, as observed on SDS-PAGE using Coomassie Blue stain the fusion protein is shown to be about 19 kDa. Though 3 kDa of His tag is fused to the protein there is still a significant variation between the theoretical estimate and the experimentally observed size. Regardless of that, the His_6 tagged CheY fusion protein was successfully expressed and purified.

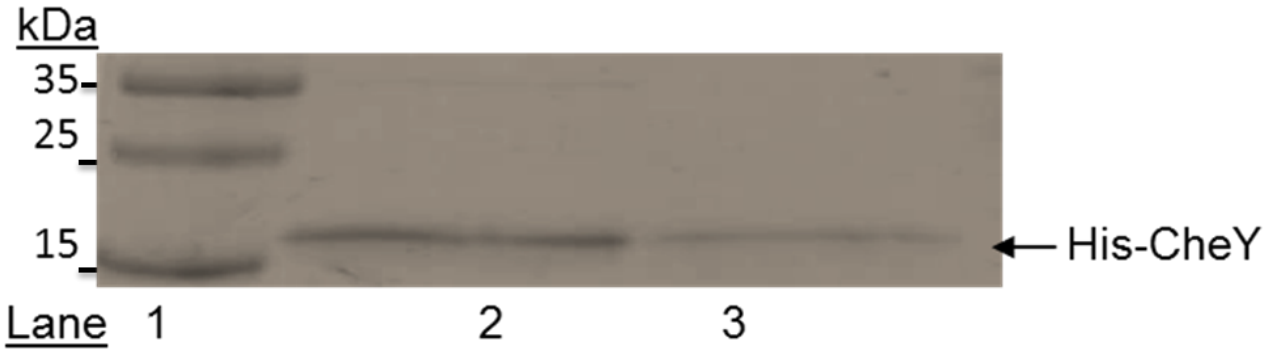

Figure 4.8. Expression and purification of His_6 tagged CheY.

CheY was eluted from His column using buffer containing 200 mM imidazole. Lanes: 1= pre-stained protein ladder (10-250 kDa), 2= contentrated His-CheY, 3= 1/2 diluted His-CheY. At the left is shown sizes of the protein ladder. Protein marker and fusion protein was electrophoresed on 15% Tris-Glycine SDS-PAGE gel and visualised by Coomassie Brilliant Blue.

4.4. Expression and purification of His_6 tagged CheV

The *cheV* gene was cloned by Answorth (2013) into the C-terminus of His_6 residue in the pTrcHisB vector and expressed in *E. coli* Rosetta. In this study the His_6 tagged CheV fusion protein was needed to examine protein-protein interactions (Chapter 5) with Cj0700, and in addition, since the chemotactic role of CheV in *C. jejuni* is still not elucidated, to investigate the phosphatase effect of Cj0700 on CheV-P.

His_6 tagged CheV was produced using a 1 mM IPTG concentration and cells incubated at 37°C for 3 hours. Cells were sonicated and chemically lysed with lysozyme then the lysate

was run through a His_6 tagged affinity column. Eventually, CheV fusion protein was released from the affinity column using elution buffer containing 200 mM imidazole. Purified protein was run on 10% SDS-PAGE gel and visualised using Coomassie Brilliant Blue stain. Assessment of the MW of the His_6 CheV fusion protein was made by comparing to the protein ladder migrating beside the SDS-PAGE (Figure 4.9, lane1 and lane 2). The size of the fusion protein is about 38 kDa, whilst native CheV was predicted to be about 36 kDa using Clone Manager software.

There are faint bands under the CheV protein that could be protein degradation which may have happened during expression, purification or the electrophoresis process. Besides that protein was produced successfully and purified about 90-100%.

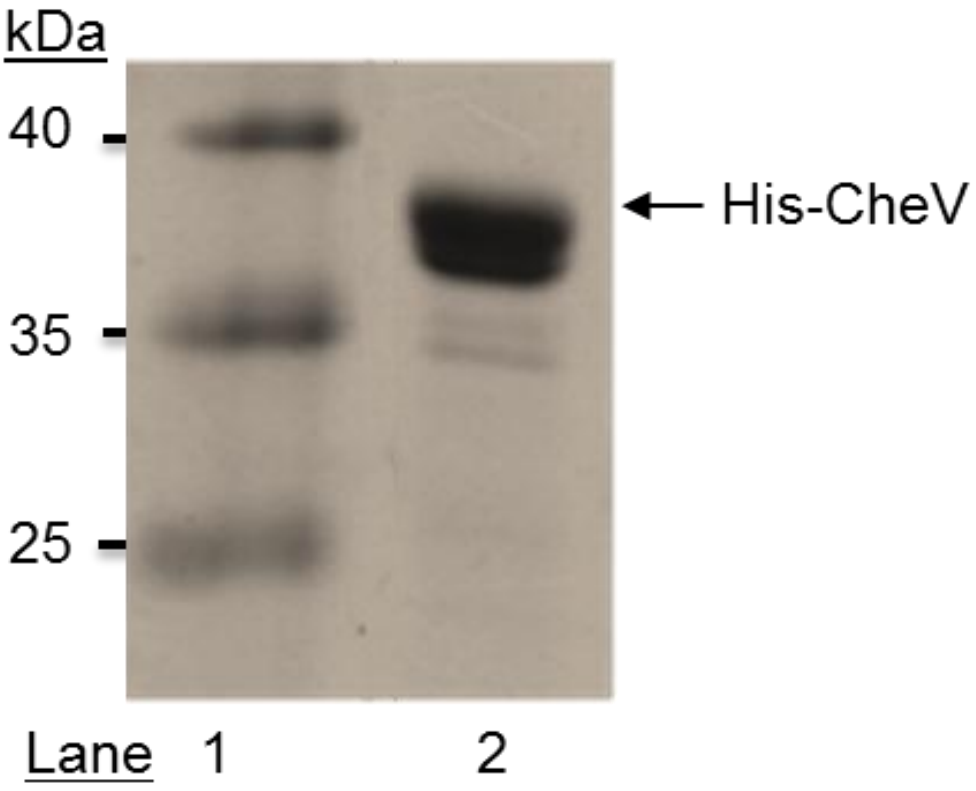

Figure 4.9. Screening expressed and purified His_6 tagged CheV on SDS-PAGE gel.

CheV was released from His column using buffer containing 200 mM imidazole. Lanes: 1= pre-stained protein ladder (10-250 kDa), 2 = His_6 tagged CheV (arrow). Protein ladder and His-CheV was ran on 10% Tris-Glycine SDS-PAGE gel and visualised by Coomassie Brilliant Blue stain. At the left is shown sizes of the protein ladder.

4.5. Expression of His_6 tagged CheA

Full CheA protein in *C. jejuni* comprises of a histidine kinase domain and a RR domain which is C-terminally connected to the histidine kinase domain (Marchant et al., 2002a). His_6 tagged *cheA* was cloned at the C-terminal of His_6 residue of pTrcHisB plasmid. In addition, CheA-HK domain, lacking the C-terminal RR domain, was cloned by Answorth (2013) into pTrcHisB plasmid. Likewise, the CheY-like RR domain was also cloned into the above mentioned plasmid. These recombinants were separately constructed by Ainsworth (2013). Expression and purification results for them will be explained in separate sections.

4.6.1. Full His_6-CheA expression

His_6 tagged *cheA* was cloned into pTrcHisB plasmid and expressed in *E. coli* Rosetta using a 1 mM IPTG concentration. After that cells were incubated at 37 $^{\circ}$C for 3 hours to overexpress CheA. Unbound proteins were removed by washing repeatedly with binding buffer. Eventually, the His_6 tagged CheA was eluted from the His tagged column with buffer containing 200 mM imidazole. Furthermore the purity of the His_6 tagged CheA protein was checked by running on a 10% SDS-PAGE gel (Figure 4.10). Pre-stained protein marker (10-250 kDa) was separated alongside the CheA so that the correct size of the fusion protein could be estimated. The full His_6 fusion CheA shows a size of about 110 kDa on SDS-PAGE gel. There are extra proteins above & below the CheA protein that could be protein degradation which may have happened during expression, purification or the electrophoresis process (Figure 4.10).

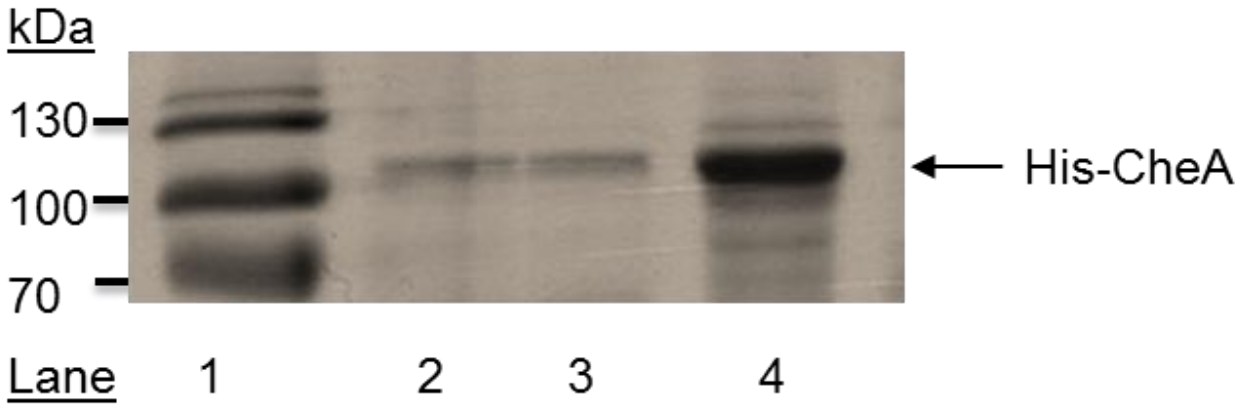

Figure 4.10. Expression and purification of H6 tagged CheA protein.

CheA was released affinity column elution buffer containing 200 mM imidazole. Lanes: 1= pre-stained protein ladder (10-250 kDa), 2 = 1/3 dilution of CheA, 3= 1/2 dilution of CheA, 4= concentrated CheA fusion protein. Proteins were separated on 10% SDS-PAGE gel and visualised by Coomassie Blue stain. At the left is shown sizes of the protein ladder.

4.6.2. Expression of His_6-CheA Histidine kinase

The *cheA-HK* (histidine kinase) lacking CheY like domain was cloned at the C-terminal of His_6 residues in pTrcHisB. Recombinant plasmid was received from Paul Ainsworth (2013). In addition, plasmids carrying *cheA-HK* were transformed and expressed in *E. coli* Rosetta. Expression of the His_6 tagged CheA-HK used a 1mM IPTG concentration and cells were incubated at 30°C for 3 hours. Purification used His_6 an affinity column, where supernatant was run through the column and washed repeatedly with binding buffer to wash out unbound cell lysate proteins. Eventually, His_6 CheA fusion was freed from immobilisation on the affinity column using elution buffer with 200 mM imidazole.

CheA-HK fusion protein was electrophoresed on 10% SDS-PAGE gel and visualised by Coomassie Brilliant Blue staining. The size of CheA-HK domain was predicted to be about 69 kDa, thus on the gel the size of the CheA-HK fusion protein shows the predicted size. Thin bands under the CheA-HK fusion (Figure 4.11, lane 2 and 3) might be related to degradation caused by elevated temperature during expression, purification or the

electrophoresis process. Despite these bands the experiment shows that the CheA-HK fusion protein was successfully produced and purified about 90%-100%.

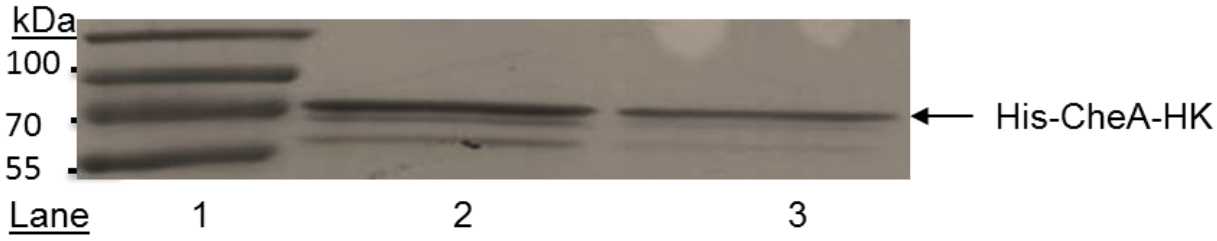

Figure 4.11. Expression and purification H_6 tagged CheA-HK.

CheA-HK domain lacking RR domain was released from affinity column elution buffer containing 200 mM imidazole. Lanes: 1= protein marker, 2= concentrated CheA-HK, 3= 1/2 diluted H_6 tagged CheA-HK domain. Protein marker and CheA-HK was run on 10 % SDS-PAGE. At left shows size of protein marker.

4.6.3. Expression of His_6-CheA response regulator

The CheY-like response regulator (RR) domain of *cheA-RR* was fused at the C-terminal of His_6 residues in pTrcHisB. In addition the fusion protein was overproduced in *E. coli* Rosetta. This recombinant plasmid was received from Ainsworth (2013). Expression of His_6 CheA-RR fusion protein used an IPTG concentration of 1 mM and incubation at 37°C for 3 hours. In addition, supernatant of whole cell lysate was run through His_6 affinity tag columns and excess washing with binding buffer (section 2.11.2, table 13) was utilised so that unbound protein was removed from affinity column. Finally, the His_6 CheA-RR was freed from immobilisation on the affinity column by using 200 mM imidazole in the binding buffer. Bands (Figure 4.12) indicate purified CheA-RR fusion protein separated beside the fusion protein (10-250 kDa) on 10% SDS-PAGE gel.The CheA-RR protein on 10% SDS-PAGE indicates a size of about 37 kDa. Regardless the faint bands under the CheA-R proteins that could be protein degradation, it shows that CheA-HK was successfully expressed and purified about 90%-100%.

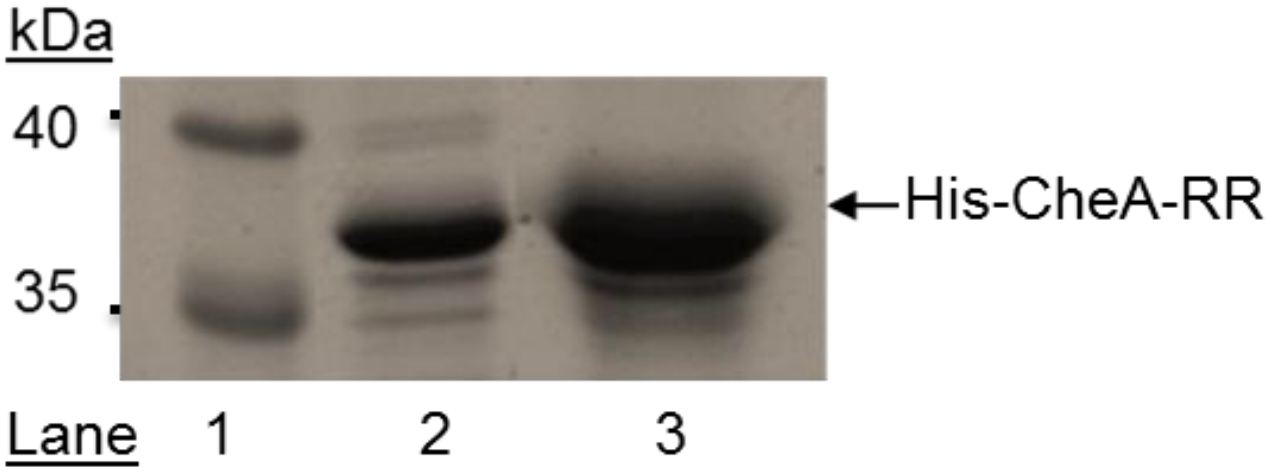

Figure 4.12. Expression and purification of H_6 tagged CheA-RR (response regulator) domain.
CheA-RR domain lacking HK domain was released from affinity column elution buffer containing 200 mM imidazole. Lanes: 1= protein marker (10-250 kDa), 2= 1/2 diluted His-CheA-RR, 3= concentrated H_6 tagged CheA-RR domain. Protein marker and CheA-RR was run on 10 % SDS-PAGE on 10% SDS-PAGE and visualised by Coomassie Brilliant Blue stain.

4.6. His_6-RacR and RacS

RacS and RacR are histidine kinase and RR proteins respectively from *C. jejuni* (Bras et al., 1999). Recombinant plasmids expressing *racR* and *racS* were made by cloning into the the pTrcHisB vector sequence encoding the His_6 residues. In addition, proteins were expressed in *E. coli* Rosetta. These recombinants were originally made by Ren (2011). Like the other His_6 tagged fusion proteins, RacS and RacR were expressed using a 1 mM IPTG concentration and incubated at 30°C and 37 °C respectively for 3 hours. Likewise, the His_6 affinity tag was used for purification and excess volume of binding buffer was washed through to remove unwanted cell lysate proteins. Furthermore, the His_6 tagged fusion proteins were freed from immobilisation on the affinity columns using binding buffer with 200 mM imidazole. Protein purity was checked on 10% SDS-PAGE and proteins visualised by Coomassie Brilliant Blue stain. Proteins migrating into the predicted size of RacR and RacS were observed 25.4 and 26 kDa respectively (Figure 4.13). Thus, these proteins were

successfully expressed and purified about 90%-100%. The purified RacR protein will be used to investigate if Cj0700 protein has a phosphatase effect on phosphorylated RacR.

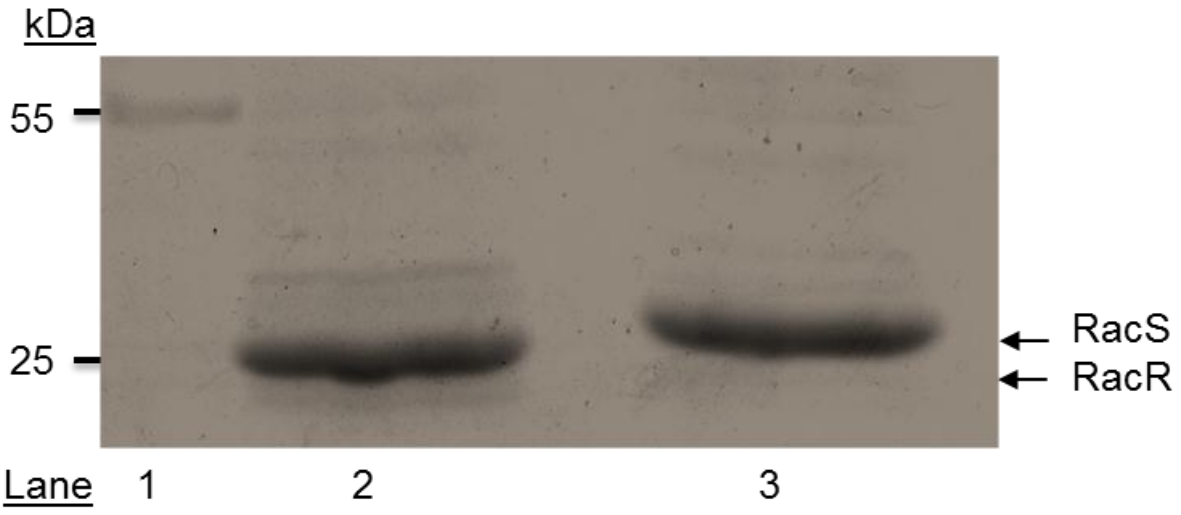

Figure 4.13. Expression and purification of H_6 tagged RacR and RacS fusion proteins.

RacR and RacS were released from affinity column elution buffer containing 200 mM imidazole Lanes: 1 = protein marker (10-250 kDA), 2= H_6 tagged RacR protein and 3= H_6 tagged RacS protein. Protein marker, RacR and RacS were run on 10% SDS-PAGE and visualised using Coomassie Brilliant Blue stain. The sizes of protein marker are shown on the left.

4.7. phosphorylation and dephosphorylation assay

In previous experiments (Chapter 3), Cj0700 was shown and confirmed to have a role in the chemotaxis pathway of *C .jejuni*. Likewise, Cj0700 was hypothesised to play a phosphatase role on RR domains in the chemotaxis pathway. To answer this question requires determining if Cj0700 has phosphatase activity that can act on CheY. Furthermore, it needs to be determined if there is any activity towards other RR domains associated with *C. jejuni* chemotaxis and if it will dephosphorylate RR domains from two component regulators not associated with chemotaxis.

4.8.1. Cj0700 dephosphorylation of CheY-P

This phosphorylation experiment was to investigate if Cj0700 removes phosphate from phosphorylated CheY-P *in vitro*. It is known that CheY is fundamental for the signal transduction pathway in *E. coli* chemotaxis, where CheY-P interacts with CheA, CheZ and FliM (flagella motor protein). CheY receives phosphate from CheA and in this phosphorylation state binds to FliM of the flagella and results in a clockwise rotational bias *E. coli* (Xiangyang Zhu, 1997).

In this *in vitro* phosphorylation assay only the CheA-HK domain was used because full CheA in *C. jejuni* consists both histidine kinase and RR domains where Ainsworth (2013) showed that the histidine domain can transfer phosphate to CheY and other RRs in chemotaxis pathway. Thus, in brief, CheA-HK (5 μM) was mixed with reaction buffer and radiolabelled (γ^{32}-P) phosphate (20 μCi) diluted with ATP (5mM) and incubated for 10 minutes at 30°C. In order to follow the phosphate transfer to CheY, a reaction containing the radiolabelled CheA-HK alone was transferred to a microcentrifuge tube containing 2xSDS sample loading buffer. The rest of the radiolabelled reaction mixture was aliquoted into two microcentrifuge tubes each containing CheY (15 μM) and Cj0700 was added to one of the tubes (15 μM). Reactions were carried out at ice cold conditions and samples inactivated every 30 seconds up to 90 seconds.

Results show the CheA-HK authophosphorylated (Figure 4.14, top left band) with radioactive Pi (γ^{32}-P) subsequently transferred as a phosphate to CheY (Figure 4.14, bottom band). Peak intensity increases with time, wherein CheY-P appears more intense at 90 seconds compared with 0 seconds. Conversely, the CheY-P reaction in the presence of Cj0700 (Figure 4.14, bottom, at right) shows phosphate is immediately stripped from CheY-P even at the zero time point when compared to the reaction where Cj0700 is absent. Increase of the radioactive signal of CheY (Figure 4.14, left bottom) shows that CheY takes phosphate from CheA-HK.

Hence, the absence of radioactive signal on CheY can be explained by Cj0700 removing the phosphate from CheY-P at a rate faster than CheY receives it from CheA-HK.

The peak intensity of the proteins was quantified using ImageQaunt TL software to show that Cj0700 immediately removes signal from CheY-P. The result of this CheY-P experiment indicates that Cj0700 removes 100% of phosphate from CheY-P immediately at 0 seconds when compared to a control reaction of CheY-P in the absence of Cj0700 where phosphate level increased 26% after 60 seconds of incubation (Figure 4.15). It is unlikely that Cj0700 can block transfer of phosphate from CheA-HK to CheY because in both the absence and the presence of Cj0700 the reaction shows that signal intensity of CheA-HK is at a constant level and that CheY strips phosphate from CheA-HK at the same rate in both reactions. Similar results were obtained when the CheY experiment was repeated six times. Thus Cj0700 protein appears to be acting in a fashion expected of a CheY-P phosphatase in the chemotaxis signalling pathway of *C.jejuni.*

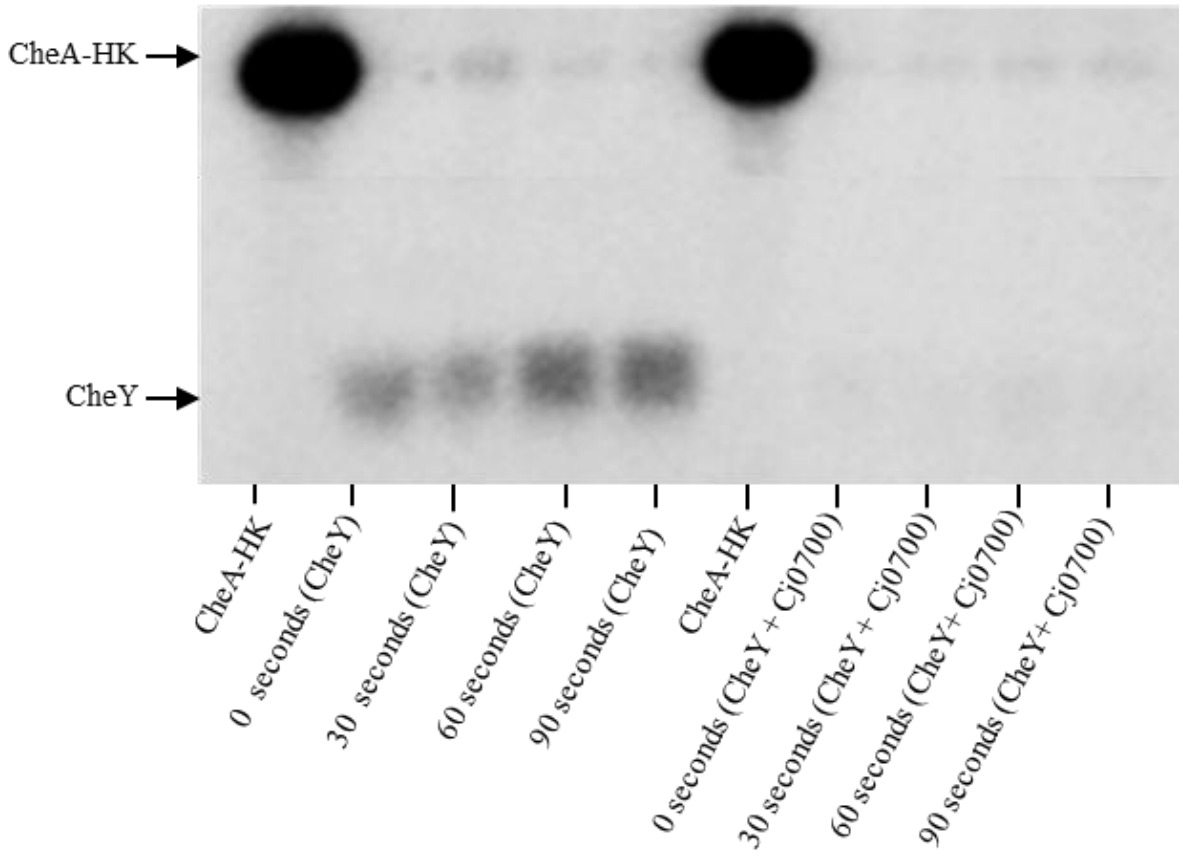

Figure 4.14. Phosphate release assay carried out on CheY and Cj0700 of NCTC 11168.

CheA-HK domain exposed [γ-^{32}P] ATP and incubated for 10 minutes at 30 ˚C (top labelled CheA-HK) and added to CheY to monitor phosphate transfer (left bottom bands). Similarly, Cj0700 added in CheA-HK/CheY mixture and monitored phosphate signal appearance/disappearance (right bottom). CheA-HK, CheY and Cj0700 mixture measured at 0, 30, 60 and 90 seconds. Samples were separated on 10% SDS-PAGE gel and visualised using a Typhoon 9400.

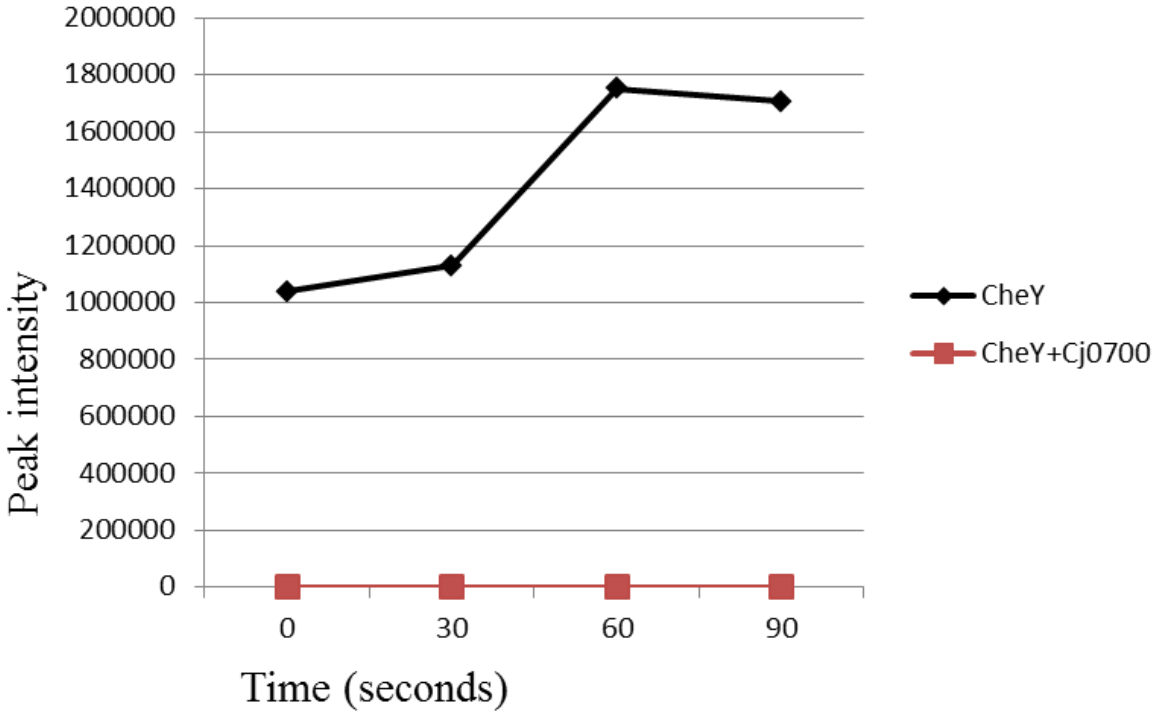

Figure 4.15. Quantification of peak from phosphorylated/dephosphorylated CheY on SDS-PAGE gel. Peak intensity as a function of labelled phosphate (γ-^{32}P) retained in time point by CheY-P. Black line illustrates phosphorylated CheY (CheY-P) with labelled ATP in the absence of Cj0700. Red line shows CheY-P with labelled ATP in the presence of Cj0700 protein. ImageQaunt TL software was employed for quantification of peak intensity.

4.8.2. Cj0700 dephosphorylation of CheA_RR-P

The sequence of CheA-HK, the histidine kinase domain from *C. jejuni*, has been shown to be functionally similar to one in *E. coli*. However, the RR domain attached at the C-terminal of CheA is specific to *C. jejuni* (Korolik, 2008). The additional RR on CheA was assumed to function as a phosphate sink in the absence of a phosphatase in *C .jejuni*. Besides that, the sequence of the CheA-RR domain indicates that it is not a CheY homologue (Marchant et al., 2002a). Therefore, this RR domain could have a chemotaxis function in *C .jejuni*, which needs to be elucidated. In a competion experiment carried out by Ainsworth (2013), where the reaction contained CheA (whole) and CheY it was demonstrated that, under the *in vitro* conditions used, CheA preferentially transferred phosphate to its own CheA-RR rather than CheY. Therefore, this assay is to determine if Cj0700 has phosphatase role on CheA-RR-P.

The CheA-RR phosphorylation is an *in vitro* SDS-PAGE based assay to determine the possible Cj0700-mediated loss of radioactive γ^{32}-Pi from CheA-RR-P. The CheA-HK concentration and the amount used for radioactive labelling were similar to that in previous reaction (section, 4.8.1). Then phosphorylation and dephosphorylation of the CheA-RR domain (5 μM) was monitored in the absence or presence of Cj0700 (15 μM) for 30 minutes at 30°C. In order to monitor CheA-HK autophosphorylation, a sample of the pre-exposed CheA-HK was stopped as previous (section, 4.8.1). Samples were separated on 10% SDS-PAGE and radioactivity was determined by Typhoon.

Result indicates that after 10 minutes CheA-HK was autophosphorylated (Figure 4.16, top middle band). Also in the same figure (left bottom band) it was observed that CheA-RR was phosphorylated by CheA-HK at 5, 10, 20, and 30 minutes in the absence of the Cj0700; it shows the ability of CheA-HK to pass Pi to CheA-RR. Similarly, it was shown CheA-RR radiolabelled phosphate transfer by CheA-HK in the presence of Cj0700 (Figure 4.16, at the right bottom band). In the absence of Cj0700 in the reaction containing only CheA-RR, strong bands are visible up to 10 minutes, but intensity starts gradually to disappear; this could be explained if CheA-RR has intrinsic autodephosphorylation so that it returns slowly to baseline state when there is no more Pi transfer from CheA-HK as auotphosphorylation is a one off event. Alternatively, CheA-RR could have a short life, where the phosphoryl residue site retains the phosphate for only a short time period; this can be explained if CheA-RR acts as a phosphate sink for the CheA-HK domain and in order to receive more phosphate it removes bound phosphate quickly or instead reverses phosphate back to CheA-HK, though this seems unlikely since signal intensity of CheA-Hk remains low.

Interestingly in the presence of Cj0700 the CheA-RR protein intensity is weak even at 5 minutes and at 30 minutes the band disappear (Figure 4.16, bottom right); these results demonstrate that Cj0700 may have weak phosphatase activity on CheA-RR-P and it is not as

effective as with CheY-P. On the other hand under the conditions used here the assay strongly indicates that CheA-HK passes Pi more efficiently to CheA-RR than it does to CheY. Four repeats of CheA-RR experiment were carried out and showed that similar results in each time.

Quantification of CheA-RR with labelled (γ^{32}-P) ATP was determined in the absence and presence of Cj0700 protein (Figure 4.17). The visualization and quantification of proteins was made using the ImageQaunt TL software. The intensity of each peak corresponds to the band on the SDS-PAGE gel. The phosphorylation level of CheA-RR in the absence of Cj0700 shows that after 30 minutes CheA-RR retains 30% of the phosphate, whereas in the presence of Cj0700, CheA-RR lost 88% of the phosphate. After 5 minutes in the presence of Cj0700, CheA-RR phosphate level dropped 14% comparing to the same time point in the absence of Cj0700(Figure 4.17). It can be concluded that Cj0700 may have weak a phosphatase effect on CheA-RR-P.

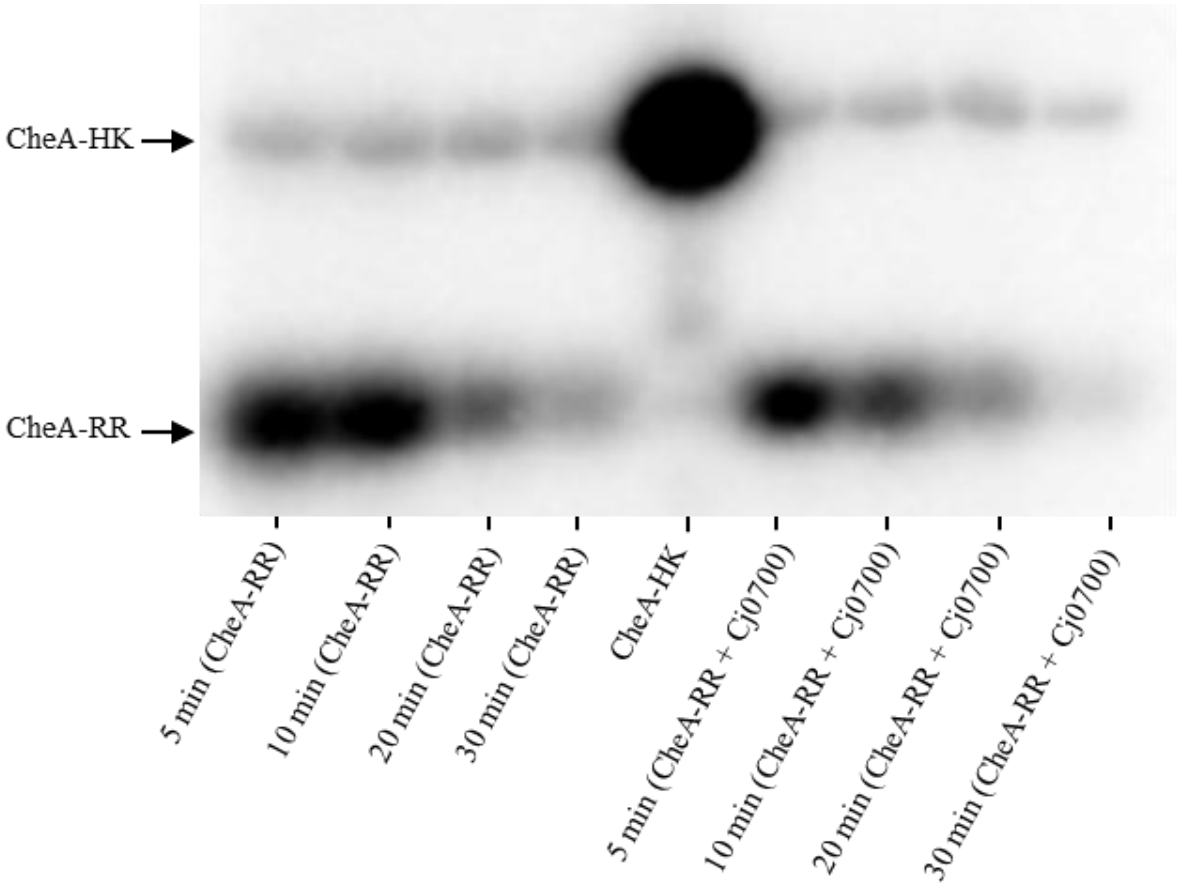

Figure 4.16. Phosphate removal assay carried out on CheA-RR and Cj0700 proteins.

CheA-HK domain exposed [γ-^{32}P] ATP for 10 minutes at 30°C (top, middle band) and added CheA-RR to monitor phosphate transfer (bottom bands). Similarly, Cj0700 added in CheA-HK/CheA-RR mixture (bottom right bands) to monitor phosphate signal appearance/disappearance. CheA-A/CheA-RR and Cj0700 mixture measured at 5, 10, 20 and 30 minutes. Samples were separated on 10% SDS-PAGE gel and visualised by Typhoon 9400 Variable Mode Imager.

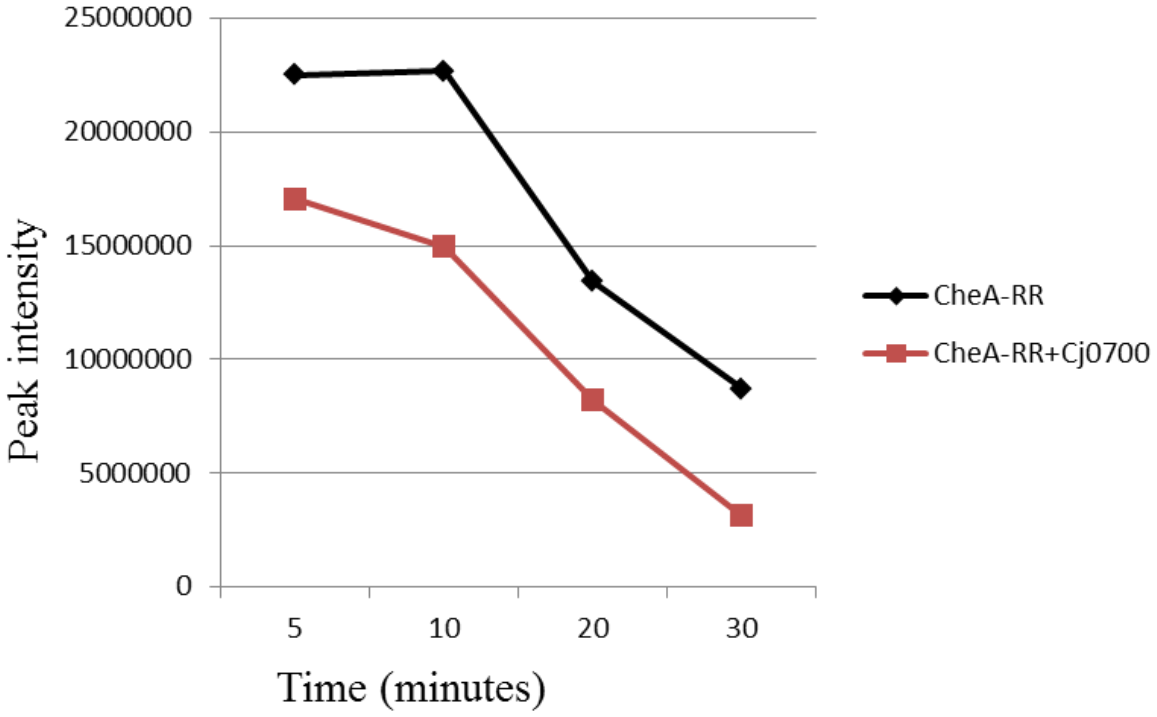

Figure 4.17. Quantification of protein intensity from phosphorylate/dephosphorylated CheA-RR on SDS-PAGE gel. Peak intensity as a function of phosphate release in time point from CheA-RR labelled (γ-^{32}P). Black line illustrates phosphorylated CheY (CheA-RR-P) with labelled ATP in the absence of Cj0700. Red line show CheA-RR-P with labelled ATP in the presence of Cj0700 protein. ImageQaunt TL software was employed for quantification of peak intensity.

4.8.3. Cj0700 dephosphorylation of CheV-P

Recent work carried out by Ainsworth (2013) has shown that CheA-HK passes Pi to CheV, in turn based upon that notion, our experiment was to investigate if Cj0700 could have phosphatase activity on CheY-P. Similar to the earlier experiments, the radiolabelled CheA-HK was intended to monitor the possible phosphorylation of CheV-P and then see if Cj0700 mediates loss of phosphate. Therefore, the CheA-HK concentration and amount of radiolabelled phosphate used was similar to the earlier experiment (section, 4.8.1). Prior to this optimization we had set up a CheV assay with very similar conditions to this assay except that it was at 30°C, however, in this attempt CheV didn't give visible bands. Failure to detect signal may have been because CheV-P loses Pi faster than at cooler conditions and hence this assay was afterwards carried out at ice cold conditions. Thus CheV (10 µM) was

mixed with reaction buffer containing Pi radiolabelled CheA-HK and monitored for phosphate loss in the absence and presence of Cj0700 (15 µM) for 90 seconds.

Results show that CheA-HK authophosphorylates (Figure 4.18, middle band) and transfers phosphate to CheV (Figure 4.18, bottom bands) in the presence and absence of Cj0700 of CheV. At each time point, CheV was more phosphorylated in both (Cj0700 absence/presence) reactions in comparison to the signal intensity at 0 seconds; the reduction of CheV-P intensity at the 60 second time point without Cj0700 may be due to technical reasons (Figure 4.18). When the CheV assay was repeated three times similar observations were seen with the CheV phosphorylation and dephosphorylation reactions.

The results demonstrate that CheA-HK passes phosphate to CheV in agreement with the findings of Ainsworth (2013), however, CheA-HK also retains phosphate which would suggest that CheA-HK may either lose less Pi or is able to re-autophosphorylate, or it may be less efficient in passing Pi to CheV in comparison to CheY and CheA-RR. Regardless, CheA-HK transfers phosphate to CheV. In addition the results show that Cj0700 doesn't detectably remove phosphate from CheV-P as was seen previously for CheY-P and CheA-RR-P (Figure 4.18). The corresponding SDS gel bands in figure 4.18 their peak intensity were quantified by using ImageQaunt TL softaware. The phosphorylation level of CheV in absence and presence of Cj0700 indicates that CheV phosphorylation increased 50% after 90 seconds (Figure 4.19). Thus, it shows that there is no difference in phosphorylation level of CheV in the absence and presence of Cj0700 after 90 seconds incubation.

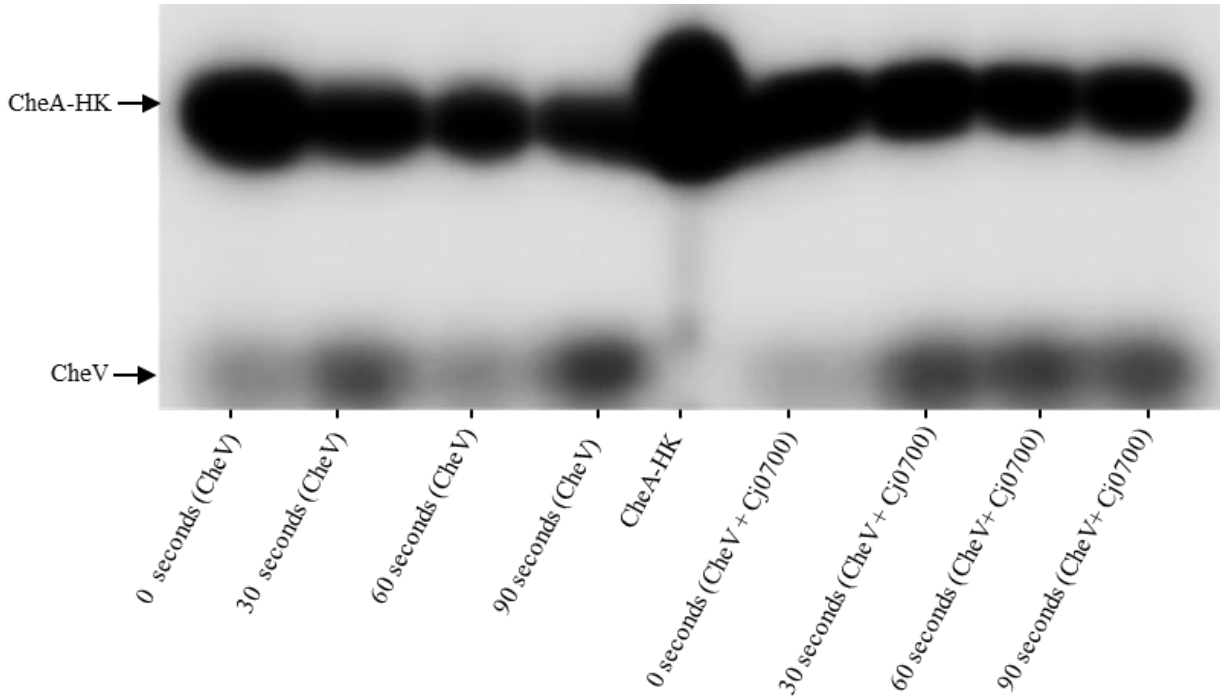

Figure 4.18. Phosphate release assay carried out on CheV and Cj0700 proteins.

CheA-HK domain exposed [γ-^{32}P] ATP for 10 minutes at 30 ˚C (top bands) and added CheV to monitor phosphate transfer (left bottom bands). Similarly, Cj0700 added in CheA-HK/CheV mixture (right bottom bands) to monitor phosphate signal appearance/disappearance. CheA-A/CheV and Cj0700 mixture carried out at 0, 30, 60 and 90 seconds. Samples were separated on 10% SDS-PAGE gel.

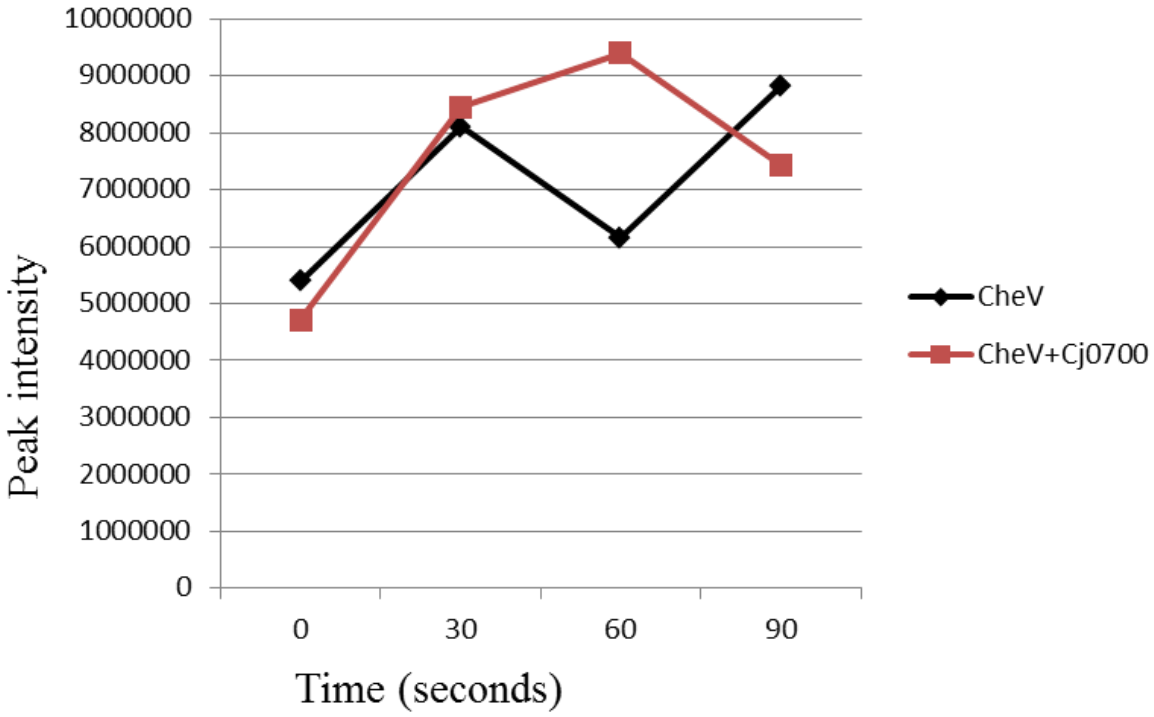

Figure 4.19. Quantification of protein intensity from phosphorylate/dephosphorylated CheV on SDS-PAGE gel. Peak intensity as a function of phosphate release in time point from CheV labelled (γ-^{32}P). Black line illustrates phosphorylated CheV-P with labelled ATP in the absence of Cj0700. Red line show CheV-P with labelled ATP in the presence of Cj0700 protein. ImageQaunt TL software was employed for quantification of peak intensity.

4.8.4. Cj0700 dephosphorylation of RacR-P

Here we want to investigate if Cj0700 had any non-specific phosphatase effect on the RacR RR; because it is hypothesised that Cj0700 is specific for the chemotaxis signalling system, where it dephosphorylates RRs notably CheY and CheA-RR.

RacS and RacR is a two component regulatory system identified in *C. jejuni* where RacS is a histidine kinase and RacR is a RR (Bras et al., 1999). It has been considered to be a temperature-dependent signalling system and required for colonising chicken intestine. Furthermore, RacS and RacR are shown to be highly conserved across the *C. jejuni* strains

(Fouts et al., 2005, Dasti et al., 2010). It has suggested *C. jejuni* utilises these proteins in adverse conditions (Apel et al., 2012).

The phosphorylation of RacR by the RacS was intended to monitor if Cj0700 mediates loss of phosphate. Therefore, RacS (10 µM) was pre-exposed and incubated 10 minutes at 30 $^{\circ}$C in a reaction buffer containing radiolabelled Pi (γ-^{32}P, 5µCi) diluted with unlabelled ATP (5 mM). RacR (20 µM) was mixed with reaction buffer containing the Pi radiolabelled RacS and monitored for phosphate gain/loss in the absence and presence of Cj0700 (15 µM) for 30 minutes. The reaction was carried out 5, 10, 20, and 30 minute time point at 30°C. Signals transferred from SDS-PAGE were scanned and analysed using the Typhoon 9400.

The results show that RacS was successfully radioactively phosphorylated with (γ-^{32}P) ATP (Figure 4.20, top left and top middle); in turn RacS transferred the labelled phosphate to RacR (Figure 4.20, bottom left) in the absence of Cj0700. In the presence of Cj0700 in the reaction mixture, there is no phosphatase effect on the RacR even at the 30 minute time point. Hence, the results demonstrate that there is no difference between absence and presence of Cj0700 on the RacR protein intensity. Therefore, it can be concluded that Cj0700 has no phosphatase effect on the RacR and suggests it is restricted to RRs found in chemotaxis such as the CheY and CheA-RR.

The quantification of RacR and RacS SDS gel bands in the presence and absence of Cj0700 (Figure 4.20) was quantified using ImageQaunt TL softaware. Results show that there is no difference in phosphorylation level of RacR after 30 minutes in the absence and presence of Cj0700, where RacR retains 99% of phosphate (Figure 4.21).

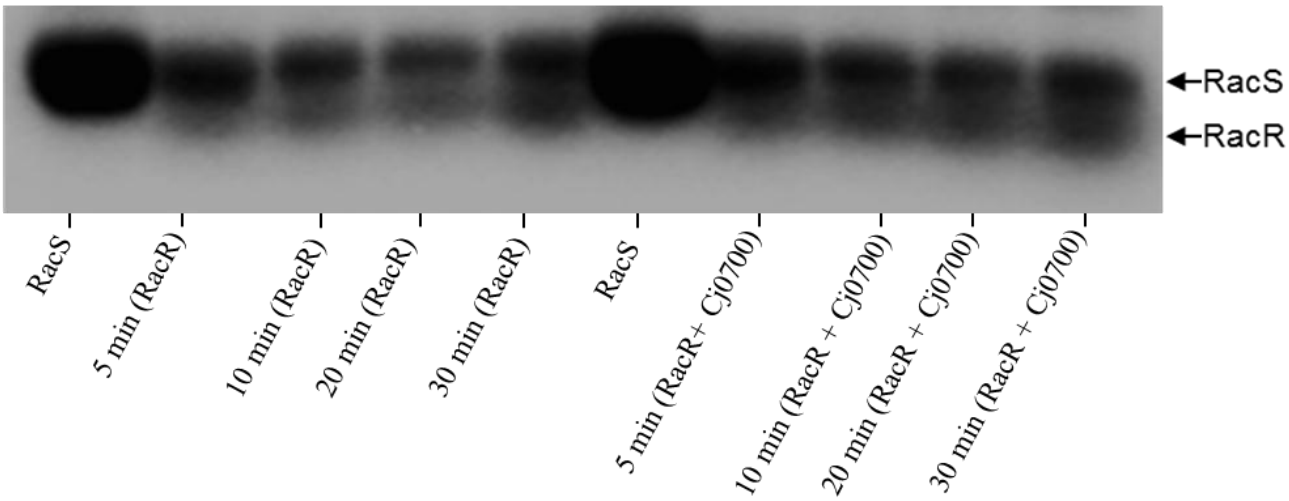

Figure 4.20. Phosphate release assay carried out on RacR and Cj0700 proteins.

RacS-HK exposed [γ-^{32}P] ATP for 10 minutes at 30 ˚C (top left and right bands) then added RacR to monitor phosphate transfer (bottom left bands). Similarly, Cj0700 added RacS-HK/RacR mixture (right bottom bands) to monitor phosphate appearance/disappearance. Experiment carried out at 5, 10, 20 and 30 minutes.

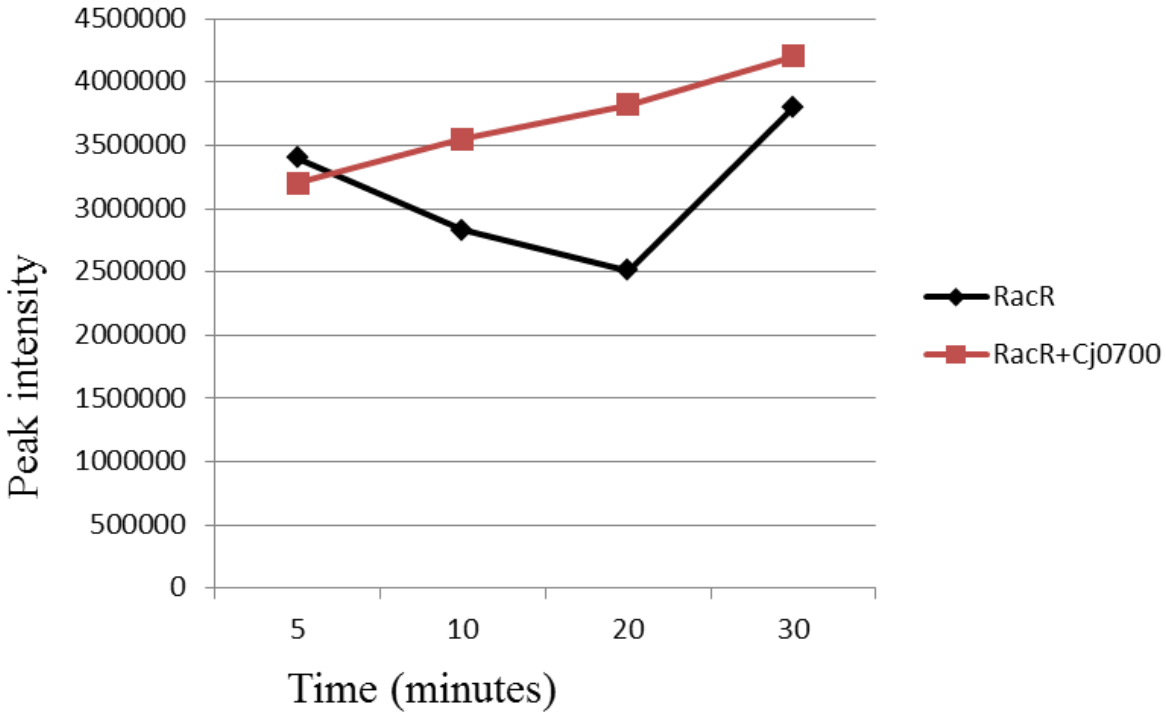

Figure 4.21. Quantification of protein intensity from phosphorylate/dephosphorylated RacR on SDS-PAGE gel. Peak intensity as a function of phosphate release in time point from RacR labelled (γ-^{32}P). Black line illustrates phosphorylated RacR-P with labelled ATP in the absence of Cj0700. Red red shows RacR-P with labelled ATP in the presence of Cj0700 protein. ImageQaunt TL software was employed for quantification of peak intensity.

4.8. Discussion

The challenges encountered during construction of expression plasmids, production of fusion proteins and purification of most of them were very time consuming. The construction of plasmids carrying proteins of interest fused with His_6 did not present any difficulties; however, expression of fused genes were tested number conditions for optimization in terms of concentration of IPTG, optimum temperature and finding the appropriate binding buffer for purification.

For the production of fused protein, IPTG was used to overexpress the chemotaxis target protein encoding genes so that unwanted genes remain unexpressed or in a low level. Therefore, in order to find optimum product level of the target protein the concentration of IPTG was steadily increased from 0.5 mM up to 1.4 mM. As a result of that all proteins in this experiment were expressed at 1 mM concentration of IPTG because at that concentration the optimun expression level of the proteins was observed.

The temperature used for gene expression was optimised at 30°C for enzymes such as Cj0700, RacS and CheA-HK (histidine kinase); this was because temperatures higher than 30°C were found to cause degradation of the protein. For instance, I attempted to express Cj0700 protein at room temperature, 30°C and 37 °C, but 30°C was the optimum in terms of protein quality such as purity and free from degration. Likewise, other His tagged proteins such as CheA-RR, CheY, CheV, and RacR were suited to be expressed at 37 °C.

Physically and chemically lysing expression cells using techniques such as sonication and lysozyme may have deleterious effect upon protein integrity and quality; however in order to maximise protein yield it was inevitable to employ these techniques. In spite of using the recommended steps for sonication and using anti-proteases (section 2.9.1.1) these still may be part of the reason the fusion protein could become degraded. Alternatively, to avoid excess sonication the cell lysis can be enhanced by storing the pelleted cells overnight at -80 °C and

prior to the column purification process DNAase can be used to treat samples to reduce viscosity.

Proteins were only kept at 4°C for short time periods; however most proteins were stable stored at this temperature for longer periods. With regard to losing activity, especially for enzymes, we saw that, for instance, newly expressed Cj0700 protein has a much more effective phosphatase activity than old Cj0700 protein on CheY phosphorylation. Regardless, of these problems encountered during expression and purification the production of each of the proteins was ultimately successful and enabled the project to progress to investigate the phospahatse activity of Cj0700 and its interaction with partner proteins (chapter 5).

In the *in vitro* CheY/Cj0700 assay, $CheY_{cj}$ was phosphorylated first by CheA-HK_{cj} with (γ-^{32}P)-ATP. In this radiolabelled phosphorylation experiment the reaction for the phosphatase activity of Cj0700 on $CheY_{cj}$ was carried out side by side, with a reaction which contained only phosphorylated $CheY_{cj}$-P. This is because CheY auto-dephosphorylates in the reaction with CheA-HK and CheY alone therefore it is required to determine the rate of phosphate removal of CheZ relative to the intrinsic phosphate release of $CheY_{cj}$-P (Zhao et al., 2002).

Results have shown rapid phosphate removal from CheY-P relative to the reaction where Cj0700 was absent. Similar results have been shown in *H. pylori*, when Hp0170, which is a remote CheZ homologue, was tested for a phosphatase effect on $CheY_{Hp}$ (Lertsethtakarn and Ottemann, 2010). However, what is not yet clear is whether this rapid removal of phosphate from CheY-P is because of using the CheA-HK and if that would have been different if full CheA was used. Maybe using full CheA would have shown different or similar phosphate removal rate from $CheY_{cj}$-P. A recent study showed that CheY phosphorylation bands were not detected in the reaction in which full CheA was used (Ainsworth, 2013) and hence using full $CheA_{cj}$ in a reaction containing $CheY_{cj}$ and $CheZ_{cj}$ may have given a false negative result. In a study to monitor the transfer rate using full $CheA_{hp}$ with $CheY_{hp}$ in the presence of

$CheZ_{hp}$ a delay of phosphate removal was shown compared to using CheA-HK_{Hp} with $CheZ_{Hp}$ (Lertsethtakarn and Ottemann, 2010). Nevertheless, the aim of this study was to find out whether $CheZ_{cj}$ could dephosphorylate $CheY_{cj,}$ and also if the manner of dephosphorylation is similar to its counterparts such as CheZ in *E. coli*. Results obtained from this assay show that $CheZ_{cj}$ removes phosphate in a similar manner to $CheZ_{ec}$ and hence supports the notion that $CheZ_{cj}$ protein is a remote orthologue of CheZ in *E. coli*. Other radiolabelled phosphorylation assays using other forms of CheZ-like phosphatases (CheX and CheC/D), found in *T. maritima* and *B. subtilis*, have also shown an acceleration of dephosphorylation of CheY (Park et al., 2004) as seen here with $CheZ_{cj}$ in *C. jejuni*. Likewise *H. pylori,* which is a close relative to *C. jejuni* (Young et al., 2007) has been found to encode a phosphatase (Terry et al., 2006) and which has shown a phosphatase effect on $CheY_{hp}$ in an *in vitro* phosphorylation assay (Lertsethtakarn and Ottemann, 2010) in a manner similar to the $CheZ_{cj}$ protein.

An amino acid alignment between Hp0170 and CheZ in *H. pylori* and *E. coli* show conserved amino acid residues. For instance the 143D/147Q residues of CheZ in *E. coli* which is the active site that interact with CheY were conserved. The corresponding 189D/193Q residues in Hp0170 of *H. pylori* are also shown to be conserved. Mutating these residues in both the CheZ and Hp0170 has demonstrated a non-dephosphorylation effect on CheY (Lertsethtakarn and Ottemann, 2010, Silversmith et al., 2003). This is evidence that the enzymatic reaction of $CheZ_{cj}$ in the presence of $CheY_{cj}$ supports that $CheZ_{cj}$ is a phosphatase in the chemotaxis pathway of *C. jejuni*.

It would have been useful to investigate the phosphatase phenotypes of $CheZ_{cj}$ mutants at the 167D/171Q residues upon $CheY_{cj}$, however due to the time limits of this project, it was not undertaken. To conclude, the first aim this project was to address role of the $CheZ_{cj}$ in *C. jejuni* chemotaxis, which was concluded to that $CheZ_{cj}$ has a role in the chemotactic pathway

in *C .jejuni* (refer to chapter 3). Here as well, it is concluded that $CheZ_{cj}$ is a phosphatase for $CheY_{cj}$-P. However, it is not yet known how well $CheZ_{cj}$ removes phosphate from $CheY_{cj}$; this can be achieved by measuring the phosphate removal rate of $CheZ_{cj}$. The phospatase reaction (kinetics) would determine the minimum concentration of $CheZ_{cj}$ needed to remove phosphate from $CheY_{cj}$ or the turnover rate of CheY.

Curiously, FLiY has been annotated in *B. subtilis*, *T. maritima* and *H. pylori*, which is a hybrid between FliN and CheC and CheX. The CheC and CheX proteins are phosphatases of CheY in *B. subtilis* and *T. maritima*. In addition, unlike in *H. pylori*, FliY has a CheY binding region in the aforementioned species (Szurmant et al., 2004, Muff and Ordal, 2007, Lowenthal et al., 2009b). In *H. pylori*, FliY has been suggested to be essential for flagellation (Lowenthal et al., 2009a) and not to be related to the dephosphorylation process. In *C. jejuni*, CheC and CheX have not been identified, but a FliY was found, which is not a homologue of FliY in *B. subtilis* (Korolik, 2008). In *C. jejuni*, the role that FliY plays in the chemotaxis signalling pathway still needs to be identified. It could be possible that FliY plays a role in flagellation but not in the chemotaxis signalling pathway as in *H. pylori*. Taken together, the phosphorylation experiment strongly indicates that $CheZ_{cj}$ is the sole phosphatase of $CheY_{cj}$.

In the experiments investigating if $CheZ_{cj}$ is a phosphatase of the CheA-RR domain the results have shown that phosphate was weakly removed from CheA-RR-P by $CheZ_{cj}$. Like CheY, the results show that CheA-RR possesses intrinsic autodephosphorylation, where radioactive bands disappeared at the end time point in the reaction in which $CheZ_{cj}$ was absent. Despite the fact that the $CheZ_{cj}$ phosphatase activity on CheA-RR is weaker than on CheY, this indicates that the phosphatase activity of $CheZ_{cj}$ is not restricted to $CheY_{cj}$ only but shows it to extend to CheA-RR.The weak phosphatase activity of $CheZ_{cj}$ on $CheA_{cj}$-RR is consistent with an earlier study where *in vitro* $CheZ_{hp}$ phosphatase activity was investigated

on $CheA_{hp}$-RR domain; this study showed that $CheZ_{hp}$ removed phosphate from $CheA_{hp}$-RR but was not as strong as on $CheY_{hp}$ (Lertsethtakarn and Ottemann, 2010).

Interestingly, CheA-HK_{cj} phosphorylates CheA-RR_{cj} similarly to $CheY_{cj}$. The question is, would this phenotype have been seen if full length CheA had been used to phosphorylate $CheY_{cj}$? The balance between phosphorylating CheY and the CheA-RR by full length CheA may be dependent on environmental conditions. For instance CheA under *in vitro* conditions preferentially passes phosphate to its own RR (Ainsworth, 2013) and other chemotaxis RRs in the presence of attractant for adaptation. The notion that the full $CheA_{cj}$ preferentially transfers phosphate to its own RR domain is supported by the multiple turnover reactions in which full length $CheA_{hp}$ of *H. pylori* was phosphorylated first with radiolabelled ^{32}P and subsequently $CheY_{hp}$ protein intensity have increased (Lertsethtakarn and Ottemann, 2010). $CheY_{hp}$ bands only appeared after 10 minutes which is evidence that $CheA_{cj}$ RR is prefentially phosphorylated prior to $CheY_{cj}$. Conversely, in a hostile environment, CheA rapidly passes phosphate onto $CheY_{cj}$ to counteract the stimulus and quickly respond. Therefore the rate of phospho-transfer is state dependent, where in an attractive environment the phospho-transfer rate to CheA-RR exceeds that of $CheY_{cj}$, and where, in a hostile environment, CheY phosphate uptake exceeds that of CheA-RR; in other words, it is a balance between these two conditions.

M. xanthus has been observed to desensitize the target protein by diverting signals to DifD (CheY-Like) which functions as a phosphate sink. The DifD functions together with DifG (CheC-like) to inactivate the signalling pathway (Black et al., 2010). It is possible that CheZcj phosphatase activity may be is regulated for instance in hostile conditions $CheZ_{cj}$ preferentially removes more phosphate from $CheA_{cj}$-RR-P than $CheY_{cj}$-P. Alternatively, depending on the environmental conditions, the binding between $CheZ_{cj}$ and CheY-like RR

domains is structurally selective whereby the conformational changes of RR domains enhance or reduce CheZ affinity with RR (Zhao et al., 2002, Black et al., 2010).

A CheV phosphorylation assay has apparently indicated that under the conditions used in the assay $CheZ_{cj}$ doesn't remove phosphate from $CheV_{cj}$-P. Reasons for this may be that $CheZ_{cj}$ is restricted to $CheY_{cj}$ and $CheA_{cj}$-RR dephospharylation or alternatively, $CheZ_{cj}$ may only have a phosphatase effect on $CheV_{cj}$-RR domain, since CheV is a hybrid of CheW and RR in C. *jejuni, B. subtilis* and *H. pylori* (Helmann, 1994, Hartley-Tassell et al., 2010a, Alexander et al., 2010). Hence if the $CheV_W$ domain was separated from the $CheV_{RR}$ domain, it may have been possible to observe the phosphatase activity on $CheV_{RR}$. It has been suggested by Alexander et al. (2010) that the CheVw domain may be an anti-phosphatase so that the $CheV_{RR}$ domain is constitutively phosphorylated. In *H. pylori* it has been shown that there is reduced dephosphorylation of CheA-P by CheV1 and CheV2 under single and multiple turnover conditions (Jimenez-Pearson et al., 2005), which is consistent with our findings that CheV in *C. jejuni* shows weak phospho-transfer from CheA-P relative to other RRs. Thus $CheZ_{cj}$ doesn't have phosphatase effect on $CheV_{cj}$ and therefore this needs more work in order to be elucidated. In addition, in the future the $CheV_{RR}$ domain alone needs to be overexpressed and assayed against $CheZ_{cj}$ in order to prove whether the $CheV_W$ domain may be involved in prevention of $CheZ_{cj}$ removing phosphate from the $CheV_{RR}$ domain. It is also possible that CheV in *C. jejuni* acts differently to other species.

RacR and RacS is a two component regulator found in *C. jejuni*. Proteomic analysis has shown that RacR regulates expression of more than 10 genes in temperature dependent and independent manners. In addition, *C. jejuni* with an intact RacR has been shown to colonise chicken optimally at 42°C temperature whereas a RacR mutant strains exhibited growth defects at 42°C and reduced chicken colonization (Young et al., 2007, MacKichan et al., 2004, Apel et al., 2012, Bras et al., 1999). An *in vitro* phosphorylation assay was designed to

examine whether $CheZ_{cj}$ has any phosphatase effect on phosphorylated RacR; the primary aim of this assay was to test if $CheZ_{cj}$ dephosphorylation extends across to other RRs found in two component systems in *C. jejuni* and is not restricted to $CheY_{cj}$. An *in vitro* phosphorylation assay of RacS and RacR was first carried out by Ren (2011), where he demonstrated that RacS could transfer phosphate to RacR. Here Ren's experimental work was modified and $CheZ_{cj}$ was included in the reaction. The RacS and RacR picture presented in this study was the best possible separation achieved in this assay using 15% SDS-PAGE gel, because molecular sizes of both fusion proteins were very close to each other, therefore it was difficult to separate them. This experiment has shown that $CheZ_{cj}$ doesn't remove phosphate from RacR protein; this result has confirmed that $CheZ_{cj}$ is specific to chemotaxis RRs, especially $CheY_{cj,}$ and hence is functionally similar to other CheZ phosphatases in *E. coli* and *H. pylori*.

To conclude the $CheZ_{cj}$ mutation has been shown to affect the chemotactic motility of *C. jejuni* and so has a role in chemotaxis signalling pathway. In addition, $CheZ_{cj}$ has shown to affect the phosphorylation of $CheY_{cj}$, CheA-RR_{cj}, but not that of $CheV_{cj}$or a TCR system (RacR/RacS) which is not associated with chemotaxis.

Chapter 5 : Protein-protein interaction

5. Introduction

These experiments are a complement to the phosphorylation assays where $CheZ_{cj}$ protein was confirmed to be a phosphatase of the $CheY_{cj}$ and $CheA\text{-}RR_{cj}$ RRs in the chemotaxis signalling pathway of *C. jejuni*. As it has been shown that Cj0700 promotes dephosphorylation of CheY and CheA-RR it would be predicted that Cj0700 will interact with RRs in the chemotaxis pathway. Therefore the aim of this study was to investigate if there is protein-protein interaction between $CheZ_{cj}$ and chemotaxis response regulator domains in the $CheY_{cj}$, $CheA_{cj}$ and $CheA\text{-}RR_{cj}$ and $CheV_{cj}$ proteins. These interactions may be enhanced by the phosphorylation status of the RRs. Also, interactions may reflect the specificity of dephosphorylation by Cj0700. In addition an *in vivo* assay with $CheB_{cj}$ protein was included as it would not be expected to interact with Cj0700. Because, in *C. jejuni*, $CheB_{cj}$ lacks a response regulator domain, it will be examined whether $CheZ_{cj}$ interacts with other proteins lacking a response regulator domain. In addition, results will support or reject the study hypothesis where $CheZ_{cj}$ was postulated to interact with chemotaxis RRs. The first experiments were to investigate *in vitro* protein-protein interaction between Cj0700 and CheY, CheA-RR, CheV and CheB proteins. The second series of experiments were to investigate protein-protein interaction *in vivo* using the bacterial two hybrid system.

There are several techniques to screen *in vitro* protein-protein interaction such as GST based pull-down experiments. Such protein pairs that are suspected to interact can be detected using affinity based columns or glutathione agarose beads. The physical interactions observed in *in vitro* experiments can be confirmed in *in vivo* experiments (Walhout et al., 2000) such as B2H or *vice versa*. In other words, *in vitro* and *in vivo* experiments are complementary to each other.

Two hybrid systems (TH) were initially developed to test protein-protein interactions; however when using these systems a number of drawbacks have been encountered, such as, producing false negatives where proteins failed to interact with each other due to steric hindrance. Also TH systems may produce false positives in which proteins that wouldn't otherwise interact would now interact (Walhout et al., 2000). One system of this is the yeast two hybrid system wherein protein interactions are assessed in a yeast cell background however prokaryotic proteins were inappropriate in yeast cell environment and hence were found to produce false negative results (Walhout et al., 2000). As a result of that a bacterial two hybrid system was developed which may be a better alternative for prokaryotic protein-protein investigations (Battesti and Bouveret, 2012a).

Principally, the technique of the bacterial two hybrid system is based upon utilising an *E. coli* strain that has a deleted adenylate cyclase gene (*cya*$^{-}$). Two catalytic domains of adenylate cyclases (CyaA) are cloned into two expression vectors under the control of the *lac UV5* promoter. In addition, the proteins of interest are genetically fused to the two complementing fragments of CyaA (T25 and T18). The pT25 plasmid encodes in frame 1-224 residues of CyaA whereas pT18 encodes the 225-399 catalytic residues of CyaA (Karimova et al., 1998). Interaction between two fused proteins results in complementation of two fragments of CyaA which in turn trigger synthesis of the cyclic AMP (cAMP). Subsequently newly synthesized cAMP binds to catabolite activator protein (CAP) (Figure 5.1). In turn the cAMP/CAP complex triggers transcriptional activation of catabolic operons, for instance lactose or maltose (Battesti and Bouveret, 2012b, Karimova et al., 1998). Therefore, the possible interaction between Cj0700 with CheY, CheA-RR, CheV and CheB can be screened using the functional complementation of the CyaA fragments to which they are fused. As a result cells with intact CyaA have the ability to ferment sugars (maltose) supplemented on the plate exhibiting red colour.

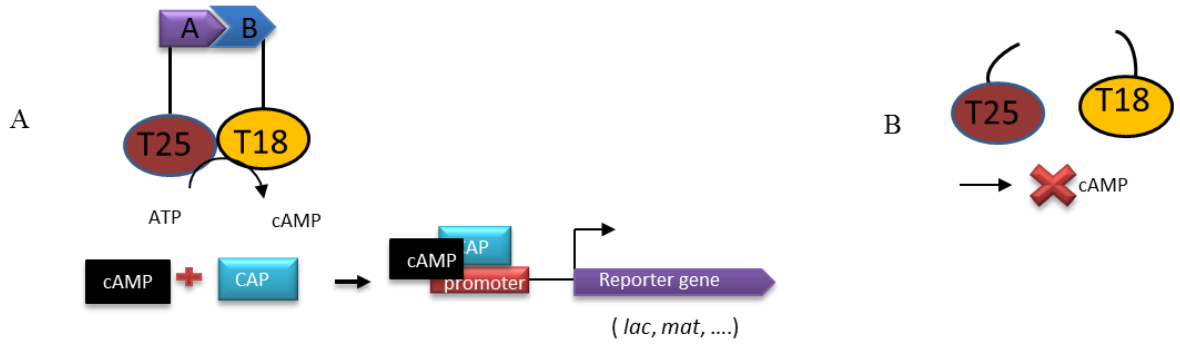

Figure 5.1. Principle of bacterial two hybrid system.

Function depends on interaction of two catalytic domain of adenylate cyclase fused in to T25 and T18 domains**.**Vector is fused to a T25 part of adenylate cyclase (panel A) to complement with the T18 domain carrying the other part of adenylate cyclase domain which activates cAMP production. Conversely, when two fragments of T25 and T18 do not complement, no cAMP is produced (panel B). In principle, A and B fusion proteins come to proximity to interact each other, cAMP is synthesised and hence with catabolite activator protein (CAP) complex enable to express corresponding reporter gene.

5.1. Protein production and purification

Fusion proteins used in the protein-protein interaction *in vitro* assay were tagged either with His_6 (see chapter 4), GST or Flag. The purity of the fused proteins is very important because contaminants may provide false results. Therefore, in order to maximise protein purity the fused proteins were immobilised on affinity columns and washed with excess binding buffer so that all unbound proteins were removed from the affinity columns.

5.1.1. Purification of GST tagged Cj0700 protein

Cj0700 was cloned in front of a C-terminal GST tag vector by E. Karunakaran (2007). For this experiment the GST-tagged Cj0700 was over-expressed in *E. coli* BL21. Like the His_6-tagged Cj0700 previously used in this study, the GST-tagged Cj0700 was induced with 1 mM IPTG for 3 hours at 30°C. In addition, purification was carried out using an immobilised glutathione affinity column, where unbound cell proteins were washed out with excess volumes of PBS binding buffer at pH 7.6 (Table 13). After that the GST-tagged Cj0700 was released from the immobilised glutathione affinity column using elution buffer (Table 13)

containing10 mM reduced glutathione. As shown in lane 2 (Figure 5.2) the molecular weight of the GST-tagged Cj0700 was about 52 kDa relative to the size of the protein ladder on an SDS-PAGE gel. The resultant 52 kDa protein comprises the GST protein with a predicted MW of 26 kDa and Cj0700 protein with a predicted size of 26 kDa; thus the GST-tagged Cj0700 observed at 52 kDa is the expected size. Purification and expression of GST-tagged Cj0700 showed a clean band (Figure 5.2, lane 2) on SDS-PAGE which illustrated that the GST-tagged Cj0700 protein was successfully expressed and purified about 100%

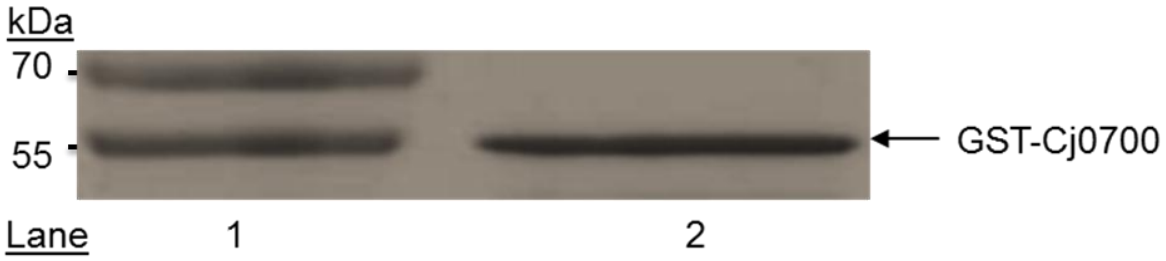

Figure 5.2. GST tagged Cj0700 production and purification.

Lanes: 1= protein ladder, 2= GST tagged Cj0700. At the left shows size of protein ladder ran parallel on gel. Cj0700 was expressed using 1 mM IPTG and eluted in PBS buffer containing10 mM reduced glutathione. Size of GST is 26 kDa, whereas Cj0700 is 26 kDa and thus fusion protein is estimated 52 kDa. GST-Cj0700 and Protein marker was run on 10% Tris-Glycine SDS-PAGE gel and visualised with Coomassie Brilliant Blue stain.

5.1.2. Purification of GST tagged CheV protein

CheV was also fused onto the C-terminus of the glutathione S-transferase protein in the pGex-4T-1 vector. The integrity and purity of the GST-tagged CheV fusion protein was assessed using SDS-PAGE. Hence, expression conditions such as concentration, temperature and time were optimised. Similarly, pH of PBS buffer was optimised so that to produce a 100% pure and good yield (2 mg/ml) of GST-CheV protein (Figure 5.3). The GST-tagged CheV protein was successfully expressed and purified with optimised conditions. The expected MW of GST-CheV is 62 kDa (Figure 5.3, lane 2). Similarly, the expected MW of GST is 25 kDa.

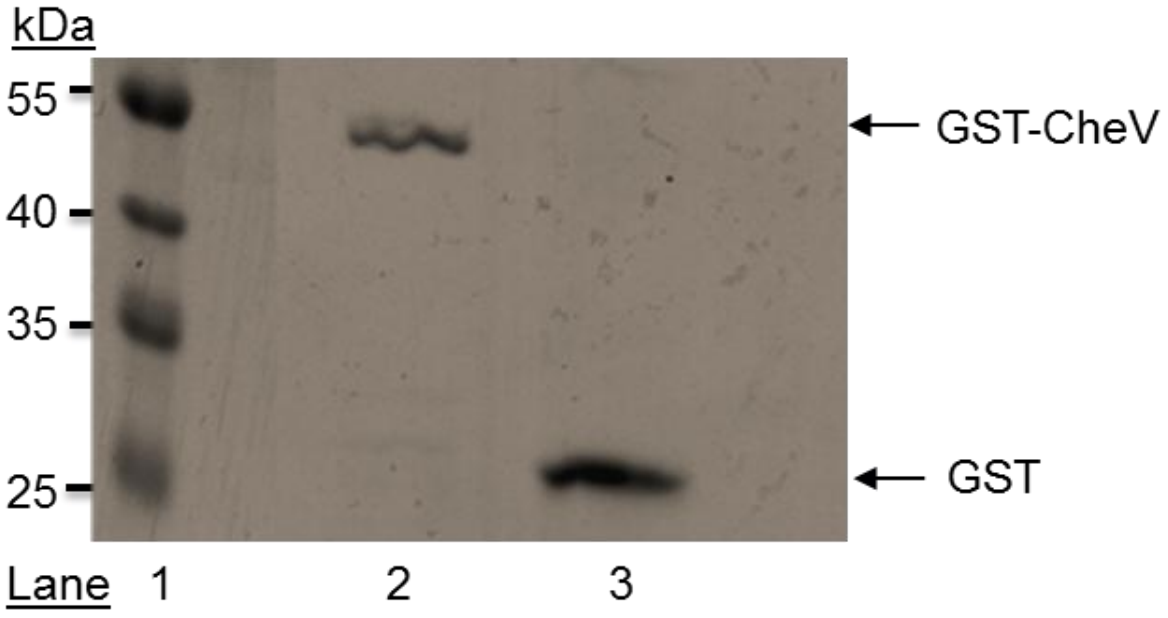

Figure 5.3. GST tagged CheV protein.

Lanes: 1 = protein marker, 2 = GST tagged CheV, 3= GST protein. Expression cells were induced 1 mM IPTG and incubated at 37 °C for 3 hours. Proteins were purified PBS buffer with pH at 7.3 and eluted from GST affinity column PBS buffer contained 10 mM reduced glutathione. Proteins were electrophoresed on 10% SDS-PAGE gel and visualised with Coomassie Brilliant Blue stain. Left is shown sizes of protein marker separated parallel to proteins.

5.1.3. Construction of a Flag-tagged expression plasmid

The main purpose for constructing the Flag-tag vector was to produce Flag-tagged CheV and CheA-RR fusion proteins to be used for protein–protein interaction assays. A problem was encountered in the protein pull down assay of His tagged Cj0700 with GST tagged CheV and CheA-RR wherein anti-his antibodies non-specifically cross-reacted with GST tagged protein; therefore, it was decided to construct and express Flag-tagged CheV and CheA-RR fusion proteins. Flag tag recombinant plasmid (Flag-*cheV* and Flag:*cheA-RR*) was derived from His tagged pTrcHisB (pTrcHisB:*cheV* and pTrcHisB:*cheA-RR*) plasmid and the construct was achieved by removing the His_6 sequence by site directed mutagenesis. An inverse PCR product was made using inverse primers each with a flag-tag sequence attached at the 5' end. Thus, Flag-tagged *cheV* and *cheA-RR* recombinant plasmids were amplified leaving out the His_6 sequence and creating a PCR product with *Not*I ends. The resultant PCR

products of pTrcFlag, pTrcFlag::cheV and pTrcFlag::cheA-RR (Figure 5.4, Figure 5.5) were digested with *Not*I restriction enzyme and then individually ligated.

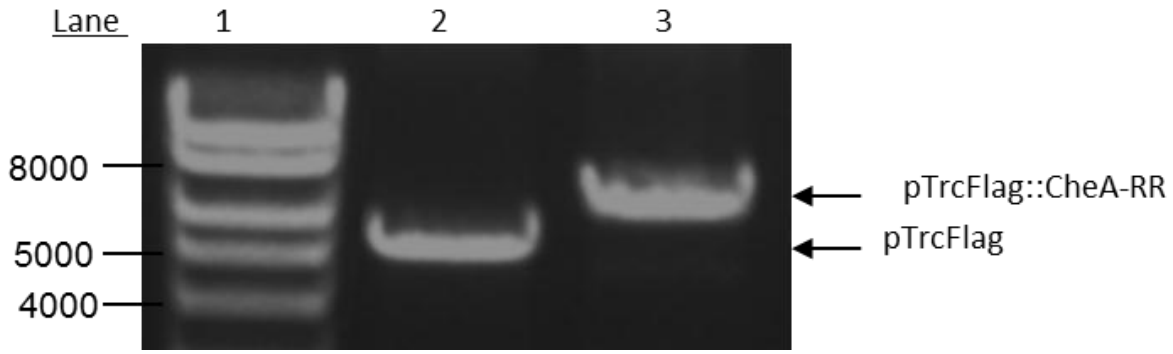

Figure 5.4. Inverse PCR product of pTrcFlag::CheA-RR and pTrcFlag using CheA-RR-flag-F/R and primers and pTrcflag-F/R primers. Lane 1 = hyper-ladder I marker with fragment sizes shown in bp on the left, lane 2= inverse PCR of pTrcFlag, lane =2 inverse PCR product of pTrcFlag::cheA-rr. PCR product was electrophoresed on 1% TAE agarose gel and visualised by staining with ethidium bromide.

Constructs containing the CheV and CheA-RR fusions were confirmed by PCR amplified from DH5αE clones and plasmids transformed into BL21 expression cells. These conjugate plasmids were designated pAJ9, for flag tag plasmid without insert (Figure 5.5), pAJ11 for CheA-RR (Figure 5.5) and pAJ10 for CheV (Figure 5.6). PCR products showed the predicted sizes for pAJ9 and pAJ11 (Figure 5.4, lane, 2 and 3 respectively). Similarly, CheV was amplified from the pAJ10 plasmid (Figure 5.6, lane 2) using specific primers (Chapter 2, table 8) and shows the predicted size of the *cheV* fragment.

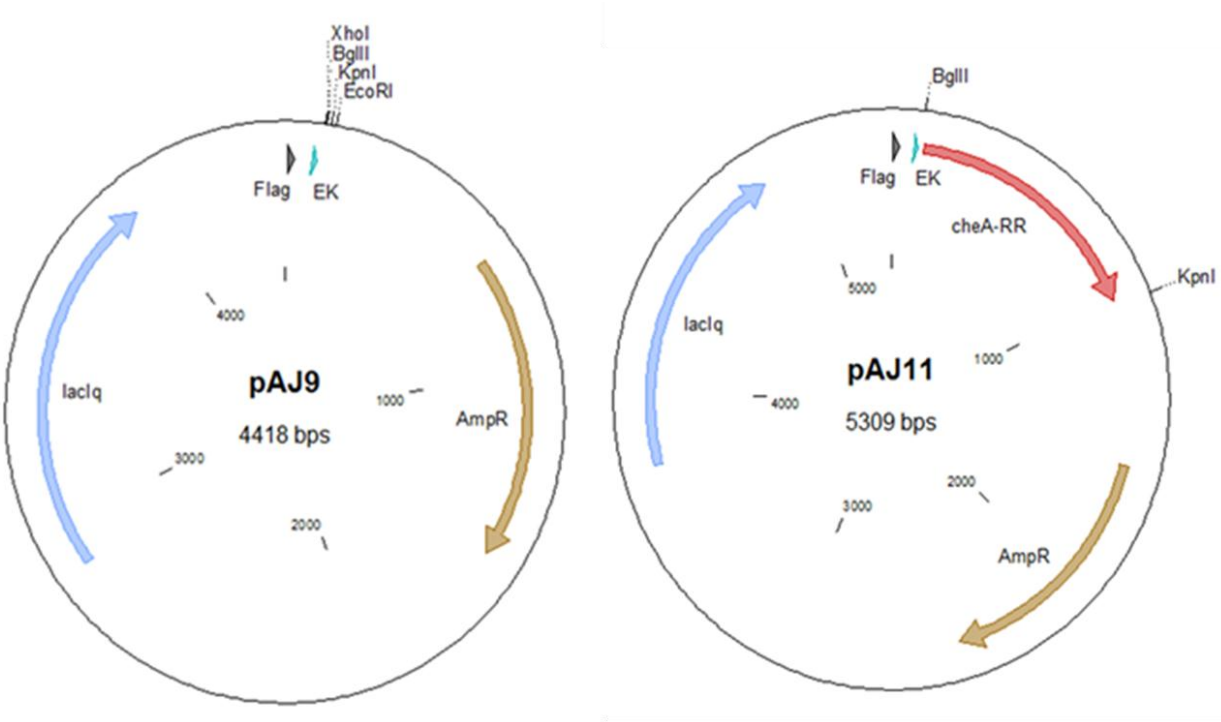

Figure 5.5. Diagram illustrates constructed pAJ9 and pAJ11 plasmids carrying Flag sequence.

At left is pAJ9 plasmid carrying flag tag sequence. At right is pAJ11 plasmid carrying CheA-RR protein fused into flag tag sequence. The pAJ9 plasmid is generated from pTrcHisB vector, whereas pAJ11 is constructed from pPA025. EK= enterokinase restriction site. *Bgl*II and *Kpn*I are restriction enzymes used for *cheA-rr* cloning.

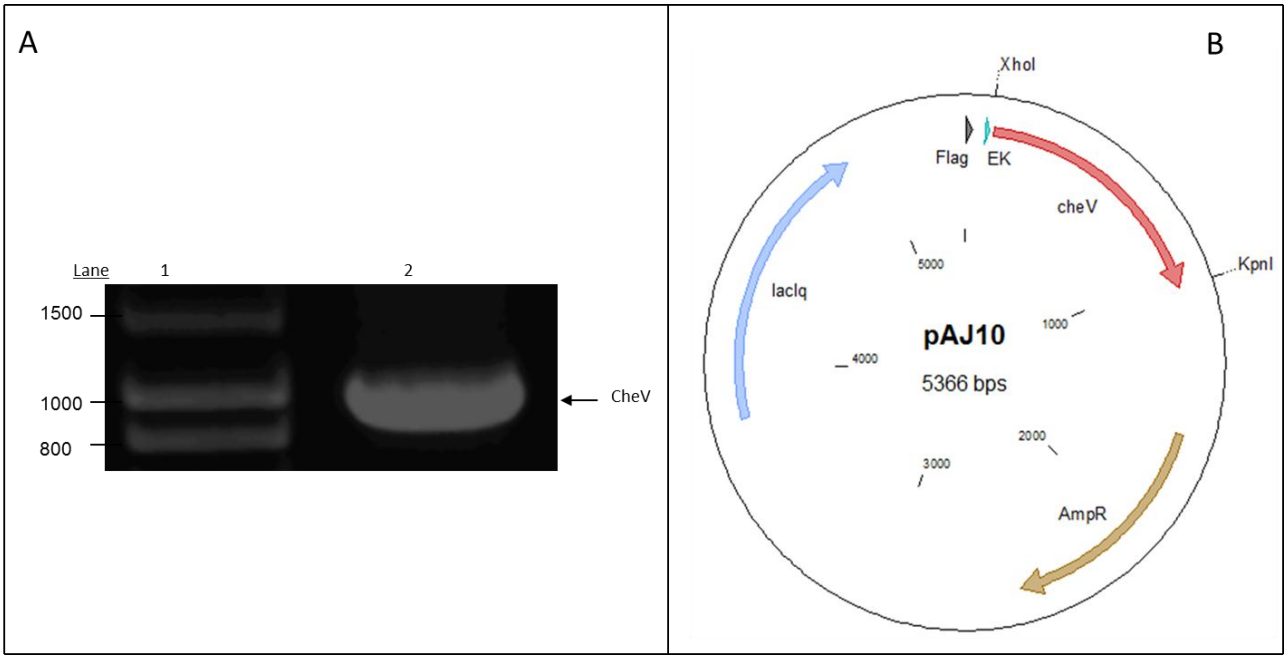

Figure 5.6. PCR for screening flag tagged *cheV* gene in the pTrcFlag recombinant plasmid.

Panel A: lane 1= hyper-ladder I marker with fragment sizes shown in bp on the left, lane 2= cheV PCR product amplified from pTrcFlag::cheV plasmid. PCR product was electrophoresed on 1% TAE agarose gel and visualised by staining with ethidium bromide. Panel B: pAJ10 is a plasmid carrying *cheA* gene fused into flag tag sequence. The pAJ10 plasmid was derived from pPA016 after removing His tag sequence. CheV amplification was used for cheV specific primers. EK= enterokinase restriction site. *Bgl*II and *Kpn*I are restriction enzymes used for *cheA-rr* cloning.

5.1.4. Purification of Flag-tagged CheV and CheA-RR proteins

Expression of the Flag-tag fused CheV and CheA-RR was induced with 1mM IPTG for 3 hours at 37°C with shaking. Subsequently the cells were sonicated, lysozyme added and centrifuged. 0.5 ml of supernatant was mixed with 0.5 ml of binding buffer and 0.2 ml of anti-Flag magnetic beads (Chapter 2, section 2.9.3).

Figure 5.7 shows that CheV and CheA-RR fused protein were successful produced and could be visualised on Western blot using anti-Flag antibodies. However, during purification, it was difficult to detect them on SDS-PAGE gel and in addition there is size shift of CheV and CheA-RR Flag-tagged proteins in comparison to His_6 tagged CheV and CheA-RR. The CheV and CheA-RR His tagged protein showed 38 and 36 kDa on 10% SDS-PAGE respectively whereas the Flag-tagged proteins were 30 and 29 kDa respectively. Nevertheless, CheV and

CheA-RR Flag-tagged proteins were successfully produced. The expression of CheV and CheA-RR Flag-tagged proteins was confirmed using anti-flag and anti-mouse conjugated with horseradish peroxidase (HRP). Results shown in Figure 5.7 are CheV (lane 1) and CheA-RR (lane 2) fusion proteins. Regardless of the size shift of both proteins showed in the Western (Figure 5.7) it can be concluded that construction and expression of Flag-tagged CheA-RR and CheV was successful. However, the expression levels were very low and hence it was difficult to produce a large amount of the protein (at least in this experiment) and as result of that I was unable to visualize them on SDS-PAGE using Coomassie Brilliant Blue stain.

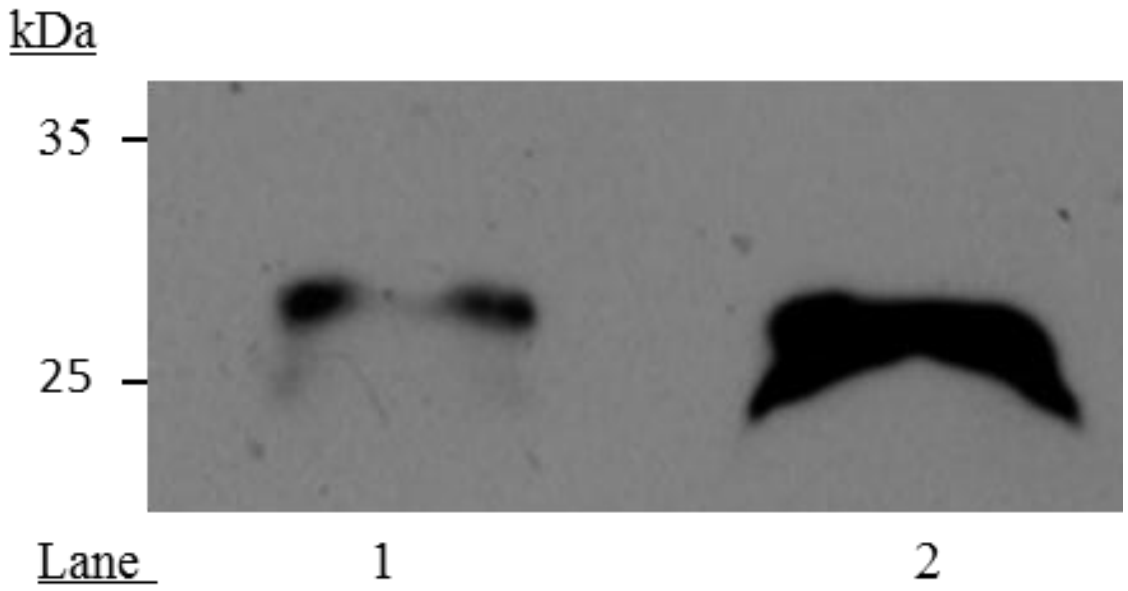

Figure 5.7. Expression and detection of CheA-RR and CheVproteins. Detection of CheV flag tagged protein by antiflag antibody. Lanes: 1= CheV flag tagged , 2= CheA-RR flag tagged.fused protein were electrophoresed on 10% Tris-Glycine SDS-PAGE gel and visualised by immunoblotting with antibody against flag tag sequence in the fusion protein. At left shows size of protein marker.

5.2. Protein pull-down assay

Generally proteins do not function independently, instead they accomplish their function through interacting with partners, hence knowing which proteins interact can provide important information about their biological function (Guo et al., 2013). In protein pull down *in vitro* assay, the purified chemotaxis proteins, $CheY_{cj}$, $CheA_{cj}$, $CheV_{cj}$ and $CheA_{cj}$-RR were used, all of which would be expected to interact with purified $CheZ_{cj}$. In order to avoid the necessity of producing specific antibodies against each of these proteins a tag based approach was used.

GST tagged fusion proteins were used to allow immobilisation on glutathione beads (section 2.9.2) and His tagged protein were added into the reaction as secondary protein in order for interaction between the two fusion proteins to take place. In addition, purified GST protein was used a negative control. Preliminary data indicated the need of phosphate donor to the RRs; therefore acetyl phosphate was added into the reaction mixture. Also Mg^{2+} was added into the reaction to facilitate $CheZ_{cj}$ binding to the active site of CheY (Zhao et al., 2002, Guhaniyogi et al., 2008b, Appleby and Bourret, 1998). The results for each fusion protein with its putative partner will be analysed separately in the following sections.

5.2.1. Interaction between purified Cj0700 and CheY proteins

The pull-down assay of Cj0700 with CheY was carried out on ice. 0.5 µg of GST-tagged CheY and GST protein was used and immobilised onto glutathione beads as the primary protein. Subsequently, to the binding reaction was added 0.5 µg of His tagged Cj0700 protein, acetyl-phosphate and Mg_2Cl to phosphorylate CheY and to enhance any binding reaction between CheY and Cj0700. Similarly, 0.5 µg of His-CheA protein was put into tubes containing phosphorylated GST-CheY protein. As a control, 0.5 µg of His-Cj0700 and CheA was put into tubes containing GST protein. The interaction was carried out by column-based

specific binding and elution and analysis was carried out on Western blot using anti-His-HRP (Horse Radish Peroxidase) conjugated antibody to detect His-CheA and His-Cj0700 tagged proteins bound on PVDF membrane.

Results indicate that the His_6 fused Cj0700 protein interacted with the GST fused CheY protein phosphorylated with acetyl-phosphate (lane 3, Figure 5.8). Likewise, His_6 tagged Cj0700 (D167N) was shown to interact with GST tagged CheY phosphorylated with acetyl-phosphate (lane 5, Figure 5.8). As a negative control Cj0700, Cj0700 (D167N) and CheY didn't show interaction with GST protein (lane 4 & 6, Figure 5.8). Native Cj0700 and Cj0700 (D167N) show similar molecular size (lane 8 & 9 and 3 & 5, Figure 5.8). Acetyl phosphate was used as a phosphate donor to CheY and Mg^{2+} was used because Mg^{2+}enhanced CheZ and CheY interaction in *E. coli* (section 5.2).

As a positive control, His-CheA protein was shown to have binding affinity with CheY as expected (lane 1, Figure 5.8); however, there is nonspecific interaction of His-CheA with GST protein which was used as a negative control (Lane 2, Figure 5.8). The predicted size of His-CheA is 89 kDA (Lane 7, Figure 5.8). In conclusion, purified Cj0700 protein can interact with the CheY-P.

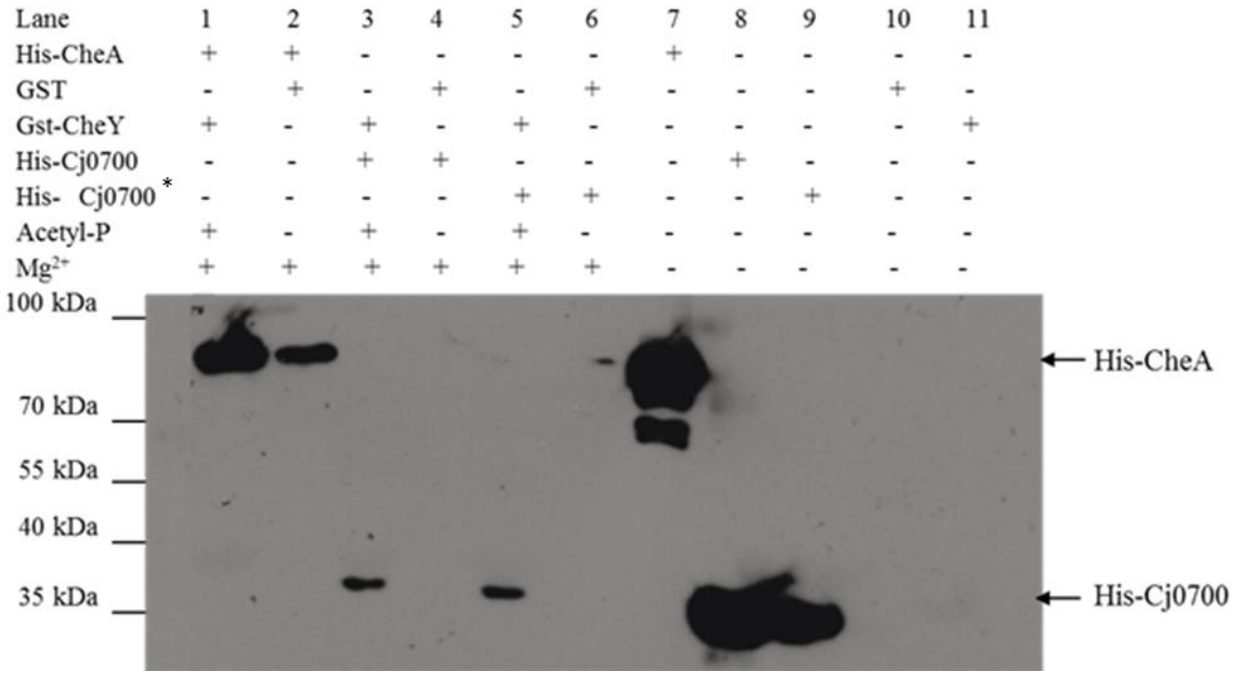

Figure 5.8. Western blot analysis of Cj0700 protein pull-down with GST-tagged CheY protein in the presence of magnesium and acetyl-phosphate. Detection of Cj0700 interaction with CheY protein by anti-His antibody. Laines: 1= GST-CheY+His-CheA, 2= His-CheA binds GST non-specifically, 3 &5 = His-Cj0700 + GST-CheY, 4= His-Cj0700 + GST, 7= Native His-CheA (control), 8&9= Native His-Cj0700 (control), 10= Native GST-CheY (control), 11= Native GST. + = presence. - = absence.* = Cj0700 (D167N). His tagged proteins were detected using anti-His-HRP conjugated antibodies and captured on Fuji X-ray film.

5.2.2. Interaction between purified Cj0700 and CheA-RR proteins

Cj0700 is able to dephosphorylate the RR domain of CheA (section 4.8.2) and therefore the ability of purified His-Cj0700 to interact with GST-CheA-RR was investigated *in vitro*. In this in *vitro* assay, GST-CheA-RR as a primary protein was immobilised into glutathione beads; subsequently acetyl-phosphate and His-Cj0700 as the secondary protein was added in order to determine if any interaction occurs between Cj0700 and CheA-RR-P. The CheA-RR-Cj0700 interaction was visualised on Western blot using anti-His-HRP conjugated antibody to detect His-Cj0700 tagged proteins bound on PVDF membrane.

C. jejuni encodes an additional RR at the C-terminal of CheA which is not homologous to that of CheY (Marchant et al., 2002b, Fahmy et al., 2012, Korolik, 2010b). The CheA-RR

domain was expressed separately from CheA and it was then investigated if Cj0700 could possibly interact with CheY-like response regulator. The results indicate that Cj0700 does have binding affinity for the CheA-RR domain (lane 1, Figure 5.9) as detected by anti-His antibody against the His-Cj0700 fusion protein. In addition, His-Cj0700 did not non-specifically interact with GST (lane 2, Figure 5.9), nor did anti-His conjugated antibodies non-specifically detect native GST-CheA-RR used as a control (lane 3, Figure 5.9). Equally, using native His-Cj0700 fusion protein (lane 5 & 6, Figure 5.9) as a size marker showed similar kDA size as Cj0700 interacted with GST-CheA-RR (lane 1, Figure 5.9). Also, the His-CheA has shown that non-specifically binds to GST (Figure 5.8). To conclude, Cj0700 can bind to CheA-RR response regulator under these *in vitro* conditions.

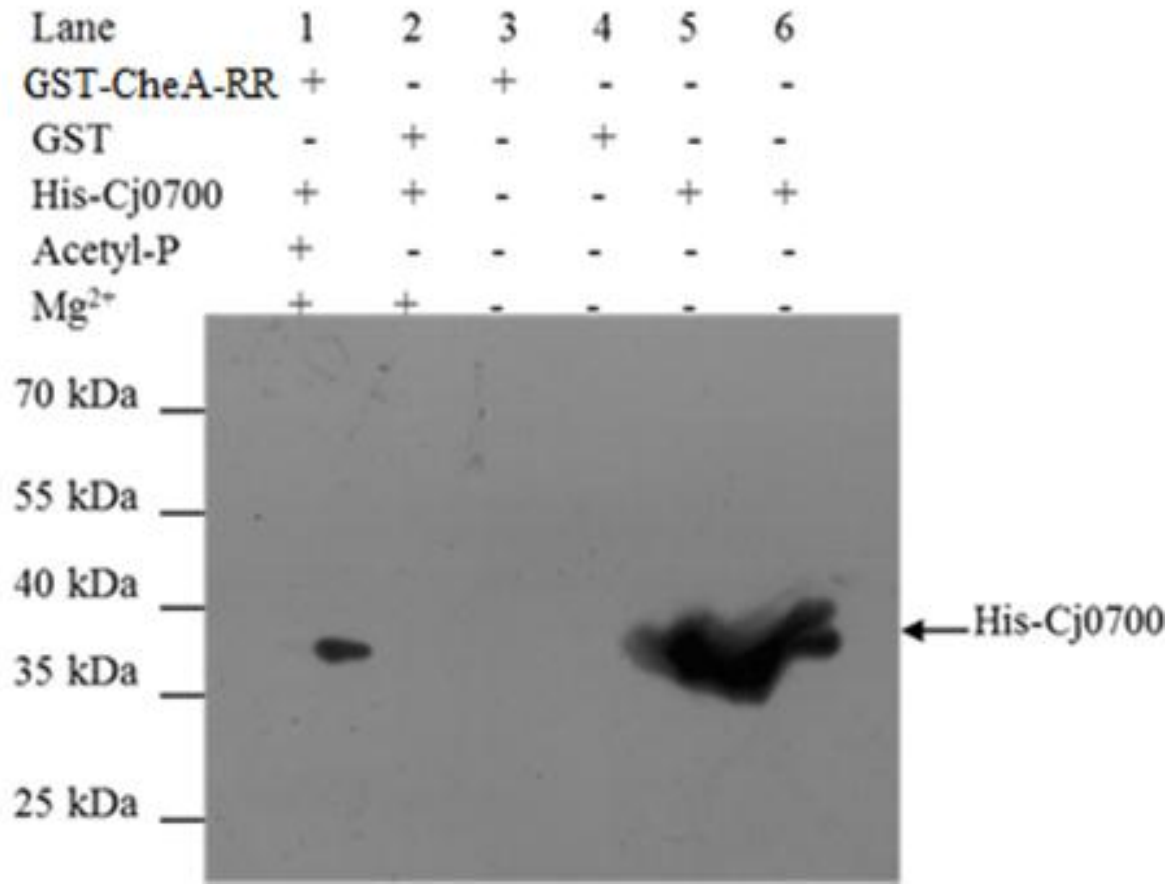

Figure 5.9. Western blot analysis of Cj0700 protein pull-down with GST-tagged CheA-RR protein in the presence of magnesium and acetyl-phosphate. Detection of Cj0700 interaction with CheA-RR protein by anti-His antibody. Lanes: 1= His-Cj0700 + GST-CheA-RR, 2= Cj0700 + GST, 3= Native GST-CheA, 4= Native GST, 5&6= Native His-Cj0700. At left side is molecular size of pre-stained protein marker. + = presence. - = absence. His-proteins were detected using anti-His-HRP conjugated antibodies and capture on Fuji X-ray film.

The interaction assay between Cj0700 and CheA-RR was also reversed such that GST-Cj0700 was immobilised into glutathione beads as primary protein, followed by incubation with His-CheA-RR and added acetyl phosphate and Mg^{2+}. The aim of the test was to investigate if Cj0700 could still interact with CheA-RR response regulator of His-CheA-RR with acetyl phosphate and Mg^{2+} added. Analysis of the results was carried out on 10% SDS-PAGE and visualised using Coomassie Blue stain to detect possible protein-protein interaction of Cj0700 with CheA-RR.

Results illustrate that the Cj0700 protein interacted with the CheA response regulator domain (lane 1, Figure 5.10). In addition, the His tagged CheA-RR non-specifically bound to the GST protein (lane 2, same figure). Also, the CheA-RR shows correct molecular size at 36 kDA (lane 1, same figure). This interaction is confirmed by the presence of a GST-Cj0700 protein at the top of CheA-RR protein (lane 1, at same figure) which shows similar size to the native GST-Cj0700 protein (lane 5, at same figure). Estimated molecular weight of the GST-Cj0700 is 52 kDa. Hence, to conclude, regardless of the nonspecific interactions seen with CheA-RR andGST, Cj0700 can bind to CheA-RR, which is consistent with the previous results shown in figure 5.9.

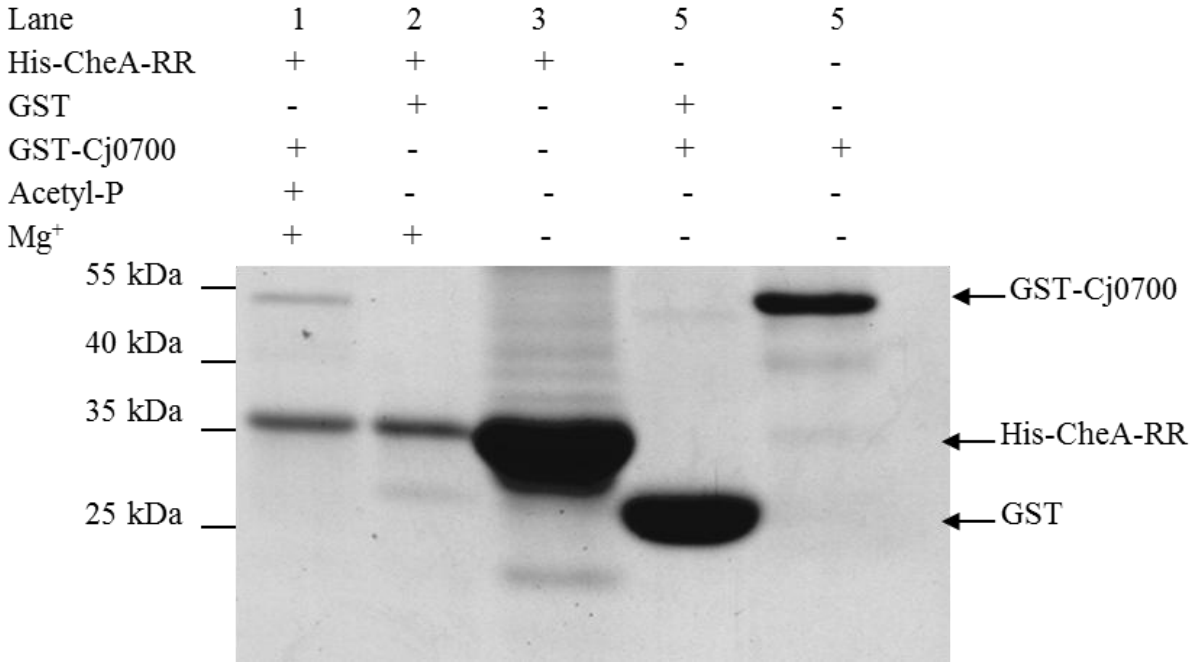

Figure 5.10. Coomassie stained SDS-PAGE analysis of GST-Cj0700 protein pull-down with His-tagged CheA-RR protein in the presence of magnesium and acetyl-phosphate.

Interaction between His-CheA-RR and GST-Cj0700 fusion proteins. Lanes: 1= His-CheA-RR + GST-Cj0700, 2= His-CheA-RR + GST, 3= Native His-CheA-RR, 4= Native GST, 5= Native GST-Cj0700. At left side is molecular size of pre-stained protein marker. + = presence. - = absence. Image visualised on 10% SDS-PAGE stained with Coomassie Brilliant Blue stain.

5.2.3. Interaction between purified Cj0700 and CheV proteins

Cj0700 is unable to dephosphorylate the CheV (section 4.8.3) and therefore the ability of purified His-Cj0700 to interact with GST-CheV was investigated *in vitro*. In this CheV and Cj0700 pull-down assay, GST tagged Cj0700 was used as the primary protein and immobilised on glutathione beads, followed by incubation with His-tagged CheV as the secondary protein. Furthermore, the binding reaction was supplemented with acetyl phosphate to phosphorylate CheV and Mg^{2+} was added to enhance any protein-protein interaction. Hence, like the other RRs, it was investigated if CheV phosphorylated at the response regulator domain could interact with Cj0700 protein. In an earlier dephosphorylation assay Cj0700 had not shown any removal of phosphate from phosphorylated CheV. Thus, the experiment was carried out on 10% SDS-PAGE and visualised using Coomassie Blue stain to detect possible protein-protein interaction of Cj0700 to CheA-RR.

The results illustrate that the GST-Cj0700 shows only a weak interaction with the His-CheV protein (lane 1, Figure 5.11), and also shows that CheV interacts non-specifically with GST protein (lane 2, Figure 5.11). This non-specific interaction between RR domains and GST control was also been observed in CheA-RR reaction.

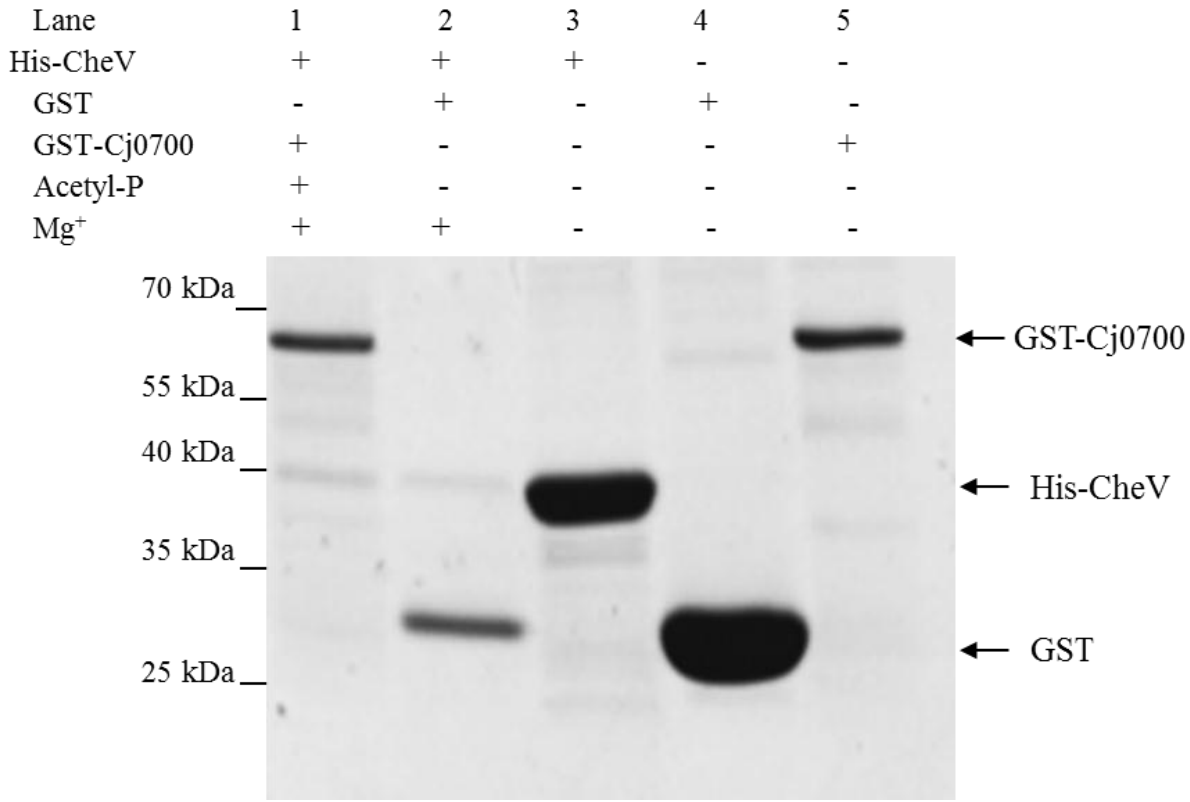

Figure 5.11. Coomassie stained SDS-PAGE analysis of GST-Cj0700 protein pull-down with His-tagged CheV protein in the presence of magnesium and acetyl-phosphate.

Interaction between His-CheV and GST-Cj0700 fusion proteins. Lanes: 1= His-CheV (prey) + GST-Cj0700 (bait), 2= His-CheV + GST (control), 3= Native His-CheV, 4= GST, 5= Native GST-Cj0700.At left side is molecular size of pre-stained protein marker. + = presence. - = absence. Image visualised on 10% SDS-PAGE stained with Coomassie Blue.

In conclusion, this experiment indicates that Cj0700 protein interacts with CheV phosphorylated by the acetyl phosphate donor. Taken together, this research has demonstrated that Cj0700 protein can form interactions *in vitro* with each of the chemotactic RRs of CheY, CheA-RR and CheV from *C. jejuni*. The next aim of this study was to investigate whether similar results of protein-protein interaction using purified proteins in an *in vitro* assay could be seen when the interactions occur in a bacterial cell. Hence, the expected Cj0700 pull down in a cell of CheY, CheA-RR and CheV were analysed in bacterial two hybrid system.

5.3. Bacterial two hybrids

The bacterial two hybrid assay (B2H) was designed to screen the *in vivo* protein–protein interaction of Cj0700 protein with the *C. jejuni* chemotactic RRs CheY, CheA-RR and CheV. The B2H assay is based on restoring adenylate cyclase activity of the cell when two fragments of CyaA are brought together.

CheB was used as a negative control, because it lacks a response regulator domain. The earlier *in vitro* protein-protein interaction experiment indicated that Cj0700 interacted with each RR thus B2H experiment was to screen if it is consistent with the results observed in protein-protein interaction using purified His and GST tagged proteins. Furthermore, using B2H system is to investigate if interactions seen *in vitro* of His/GST –tagged CheV and CheA-RR proteins are an artefact. Bridle (2007) previously made the plasmids used for the B2H and did some initial interaction studies. An aim was also to correlate the intensity of B2H interactions with pull down efficiency and level of dephosphorylation of Cj0700 on chemotaxis RRs.

5.3.1. Preparation of recombinant plasmids

The two domain sub-unit of adenylate cyclase, T25 and T18, were reconstituted into vectors at N- and C-terminal ends respectively. The *cj0700* gene was fused at N-terminal end of T18 sub-unit. Also, *cheY, cheA-rr*, *cheV* and *cheB* proteins were fused at C-terminal end of T25 sub-unit. The recombinant plasmids for this assay had been constructed previously by Bridle (2007) and Cj0700 interaction with CheY, CheA-RR, CheV and CheB had previously been analysed.

Preliminary work had indicated that Cj0700 interacted with all aforementioned tested proteins except CheB (Bridle, 2007). Hence, the aim was to reconfirm the protein-protein interaction between Cj0700 and other chemotactic RRs in the context of the *in vitro*

interaction studies and dephosphorylation assay data. Therefore, in this two hybrid assay, recombinant plasmids of pU18::*cj0700*, pKT25::*cheY*, pKT25::*cheA*, pKT25::*cheV* and pKT25::*cheB* were used. In addition, schematic illustration of the site of these genes fused into the vectors is shown in Figure 5.12.

In order to confirm the presence of insert, plasmids of these constructs were extracted from transformed cells and screened for the presence of insert by PCR, and those positive for inserts were sequenced (section 2.4.2). PCR products for Cj0700 (lane 2) CheA-RR (lane 3), CheB (lane 4), CheV (lane 5) and CheY (lane 6) are shown in figure 5.12 and give the expected size; these were sequenced to confirm they were correct (data not shown).

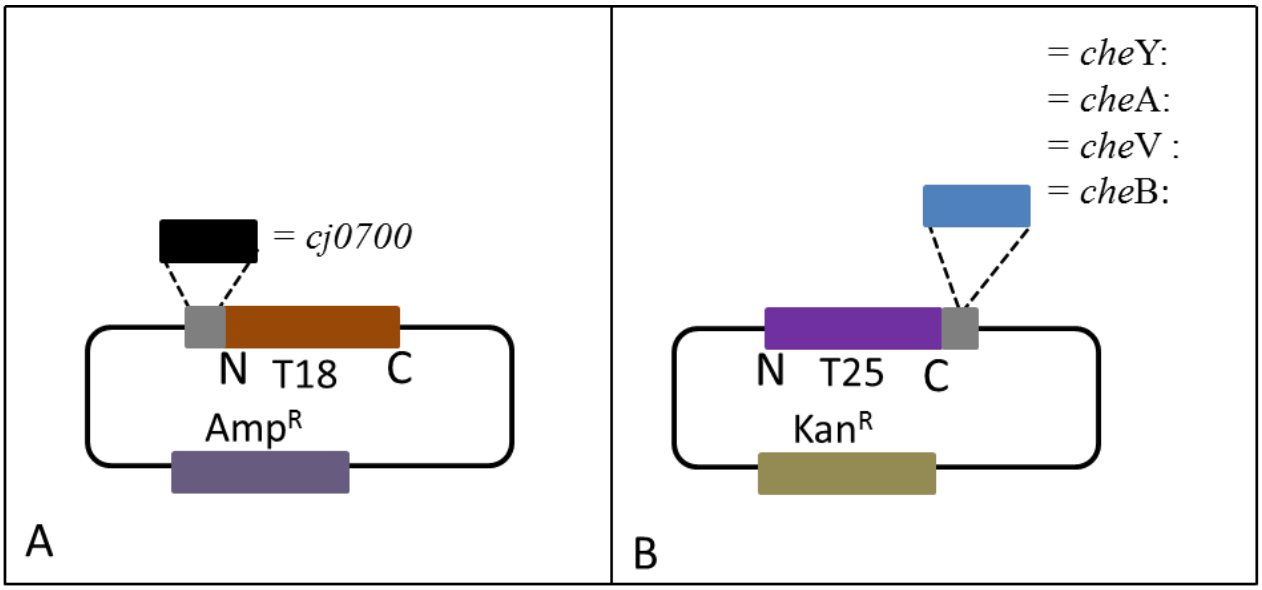

Figure 5.12. Schematic illustration of sites of chemotaxis genes in pUT18 and pKT25 plasmids. Chemotaxis proteins cloned into two domains of adenylate cyclase. Cj0700 gene cloned into N-terminal of adenylate cyclase of pUT18 plasmid (panel A), which carries ampicillin antibiotic resistance cassette. Positions cloned into chemotaxis genes (*che*V, *che*A, *che*B) into C-terminal of adenylate cyclase domain of pKT25 plasmid carrying kanamycin antibiotic R cassette (panel B).

Pairs of recombinant plasmids were co-transformed into competent cells of *E. coli* (cya$^-$) strain BTH101 and grown on selective LA-plates overnight at 37°C. Subsequently, the presence of the correct recombinant plasmids was confirmed by colony PCR using specific

primers (2.4.1.1, table 8). Furthermore, the transformants were assayed for their metabolic phenotype using MacConkey plates supplemented with 1% glucose-free maltose and incubation of the plates at 30°C for 48 hours. Positive and negative controls were included into experiment.

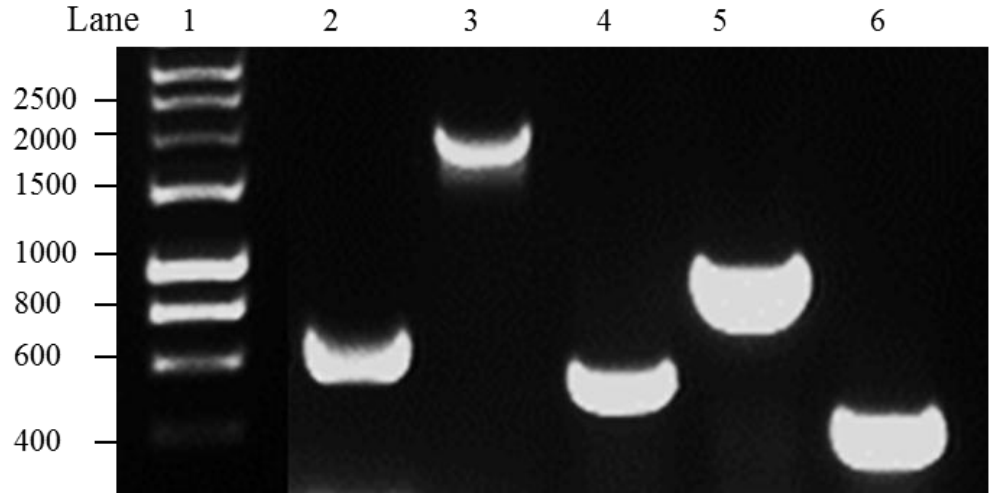

Figure 5.13 . Screening present of inserts in the recombinant plasmids.

PCR products of CheA, CheY, CheV, CheB and Cj0700**.** *cj0700* (lane 2), *cheA* (lane 3), *cheB* (lane 4), *cheV* (lane 5) and *cheY* (lane 6). The predicted PCR product of: *cj0700*= 721 bp **(**Cj0700-F/ Cj0700-R primer**),** *cheA*= 1972 bp **(**CheA_pKT25F/ CheA_pKT25R primer)**,** *cheB*= 575 bp **(**CheB_pKT25F/ CheB_pKT25R primer), *cheV*= 968 bp **(**CheV_pKT25F/ CheV_pKT25R primer **)** and *cheY*= 417 bp **(**CheY_pKT25F /CheY_pKT25R primer**).** Lanes: 1= hyper-ladder I marker. PCR product was electrophoresed on 1% TAE agarose gel and visualised by staining with ethidium bromide.

The recombinant plasmids co-transformed into BTH101 cells were screened by colony PCR. PCR product of CheA shows predicted size with length of 1972 bp (Figure 5.14, panel A, lane 2), similarly, CheV PCR product shows predicted fragment length of 967 bp (Figure 5.14, B, lane 2). The PCR product of CheB also shows the expected size with fragment length of 575 bp (Figure 5.14, B, lane 3). Also CheY PCR product shows predicted fragment size of 417 bp (Figure 5.14, B, lane 4). The PCR product of Cj0700 was confirmed in co-transformed BTH101 cells having a predicted fragment size of 721 bp (Figure 5.15, lanes 2,

3, 4 and 5). All inserts showed the expected molecular size and their DNA sequences confirmed that there were no spontaneous errors created during cloning (data not shown).

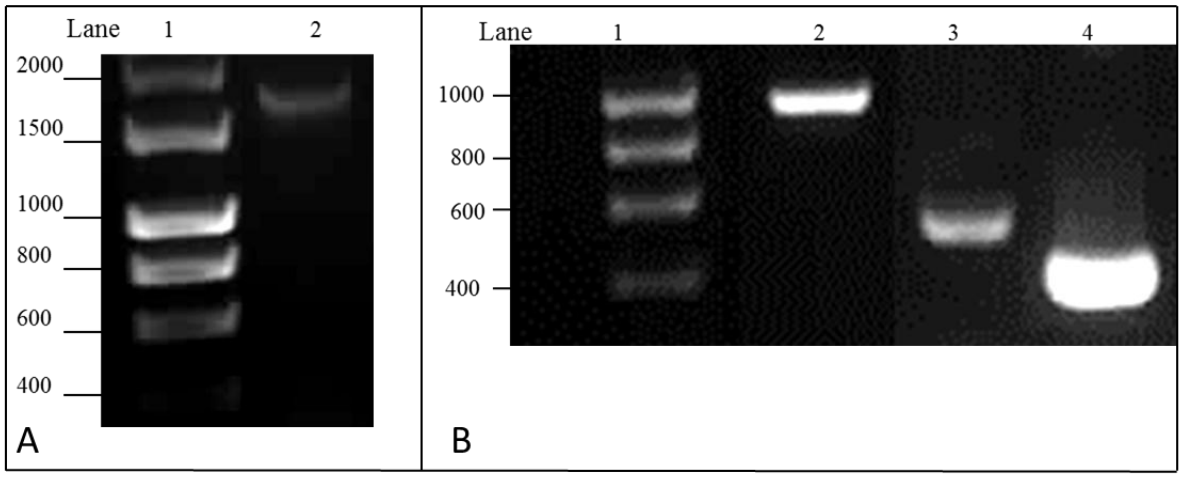

Figure 5.14. PCR product confirming presence of fusion inserts from extracted plasmids.

Colony PCR products of CheA, CheV, CheB and CheY from sectored B2H cells. *cheA* (lane 2, A), *cheV* (lane 2, B), *cheB* (lane 3, B) and *cheY* (lane 4, B). 1= hyper-ladder I marker. PCR product was electrophoresed on 1% TAE agarose gel and visualised by staining with ethidium bromide.

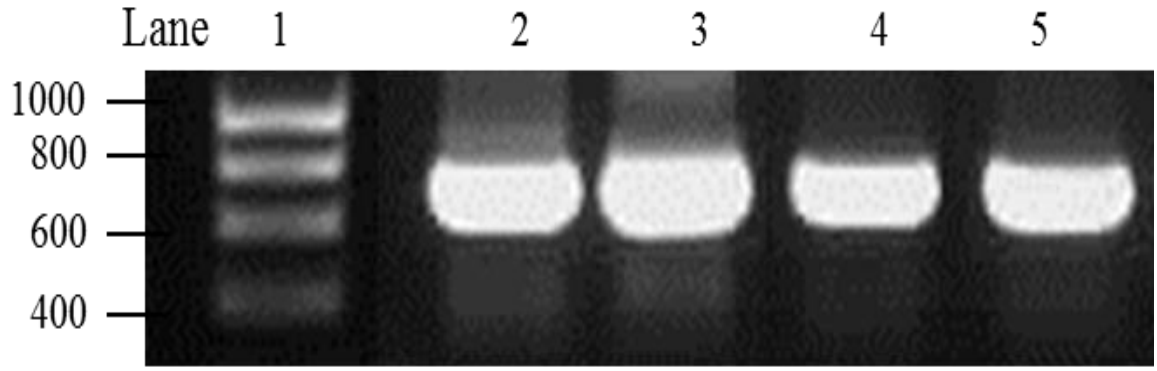

Figure 5.15. PCR product to confirm presence of cj0700 insert in recombinant plasmid.

Amplification of cj0700 from 4 strains co-transformed with cj0700 and CheA, CheV, CheB or CheY plasmids separately using Cj0700-F/ Cj0700-R primers. Cj0700 (lane 2) amplified from transformant carrying CheA (lane 2, Figure 5.14A), Cj0700 (lane 3) amplified from *E. coli* transformant carrying CheV (lane 2, Figure 5.14 B), Cj0700 (lane 4) amplified from *E. coli* transformantCheB (lane 3, Figure 5.14 B) and Cj0700 (lane 5) amplified from *E. coli* transformant CheY (lane 4, Figure 5.14B).1= hyper-ladder I marker. PCR product was electrophoresed on 1% TAE agarose gel and visualised by staining with ethidium bromide.

5.3.2. CheY and Cj0700 protein-protein interaction

The two hybrid experiment was to screen for possible protein-protein interaction of Cj0700 with CheY *in vivo* in *E. coli* lacking adenylate cyclase. Thus the interaction of Cj0700 with CheY was visualised on MacConkey plates, where an interaction of these proteins would allow complementation by the two adenylate cyclase fragments and would transform the colour of the bacterial growth into red. Conversely, if two fusion proteins did not interact the plate would turn a yellow colour.

The level of interaction was estimated semi-qualitatively based on the red colour on the plate with designations of higher (++), moderate (+) and no interaction when compared to positive control of BTH101 cells containing pT25: Zip/p18: Zip plasmids co-transformed. As the positive control pT25:Zip/p18:Zip plasmids carry a leucine zipper region which was fused with the two fragments of adenylate cyclase and hence active adenylate cyclase is formed, increasing levels of cAMP in the cell.

The results of the metabolic screen of CheY/Cj0700 transformant cells, show there is strong interaction phenotype between the Cj0700 protein and the CheY fusion protein (section 3, Figure 5.16) when comparing to cells transformed with the positive control (plate section 1, Figure 5.16). In contrast, the CheB/Cj0700 strain shows a yellow colour indicating that there is no interaction between them (plate section 2, Figure 5.16).

To conclude, Cj0700 protein interacts with CheY protein and is consistent with results of the purified protein pull down of Cj0700 and CheY. In addition, CheB was shown not to interact with Cj0700 protein, which is consistent with previous result of Bridle (2007).

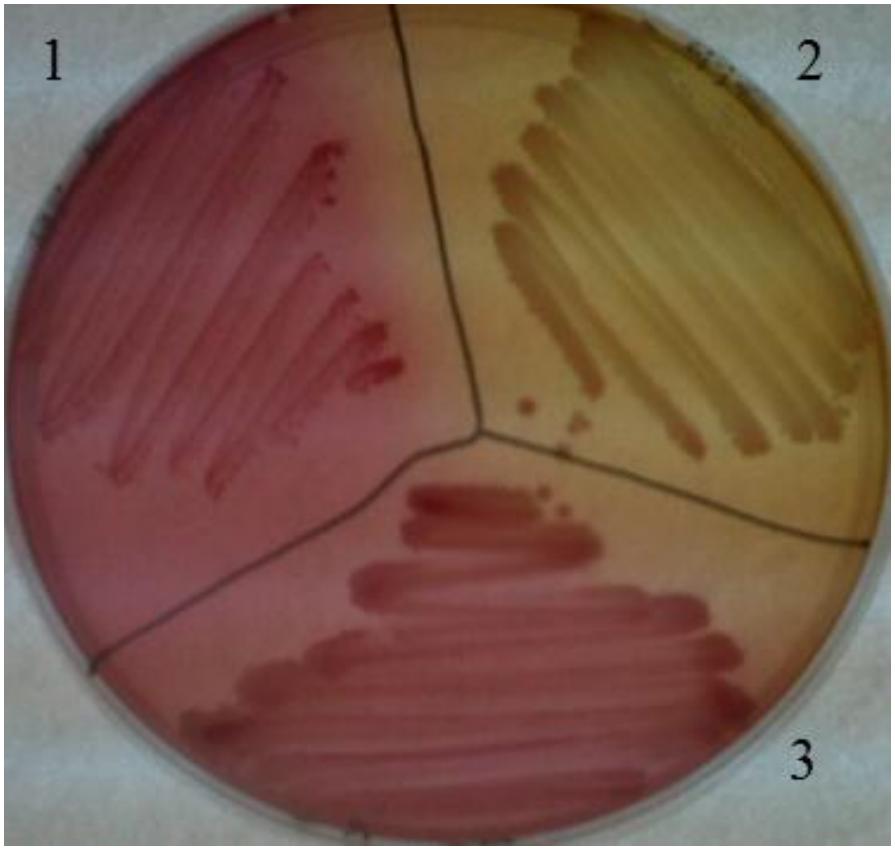

Figure 5.16. Bacterial two hybrid system screening for interaction of Cj0700 with CheY and CheB.
1: Positive control (pT25::Zip and pT18: Zip, ++ interaction), 2: CheB / Cj0700 (no interaction), 3: CheY /Cj0700 (++ interaction). *E. coli cya* strain screened on glucose-free MacConkey agar plates with added 1% maltose and incubated at 30 °C for 48 hours.

5.3.3. CheV and Cj0700 protein-protein interaction

The protein-protein interaction experiment was to screen the possible interaction between Cj0700 and CheV proteins in the cell. The CheB protein was included in the pull-down assay, because it was not expected to interact with Cj0700. Conversely, BTH101 cell with pT25: Zip/p18: Zip plasmids co-transformed to show that their strong interaction. Cells carrying co-transformed recombinant plasmids to express Cj0700 and CheV protein were incubated for 48 hours at 30°C. Consequently, cells with active adenylate cyclase by the result of Cj0700 and CheV interaction will exhibit a red colour, whilst there is no between interaction Cj0700 and CheV as a result of lacking an active adenylate cyclase cells will display yellow colour on MacConkey plates.

Results show that Cj0700 interacts with CheV (+) (section 3, Figure 5.17), however this interaction is not as strong as that of Cj0700 with CheY (++) (Figure 5.16) as can be seen by comparison with the control (++) of pT25: Zip/p18: Zip (plate section 2, Figure 5.17). Equally, Cj0700/CheB (plate section 1, same figure) as negative control demonstrate the level of no interaction between two proteins. The *in vivo* protein pull-down experiment was carried out five times and consistent results were obtained. To conclude, Cj0700 protein interacts moderately with CheV protein.

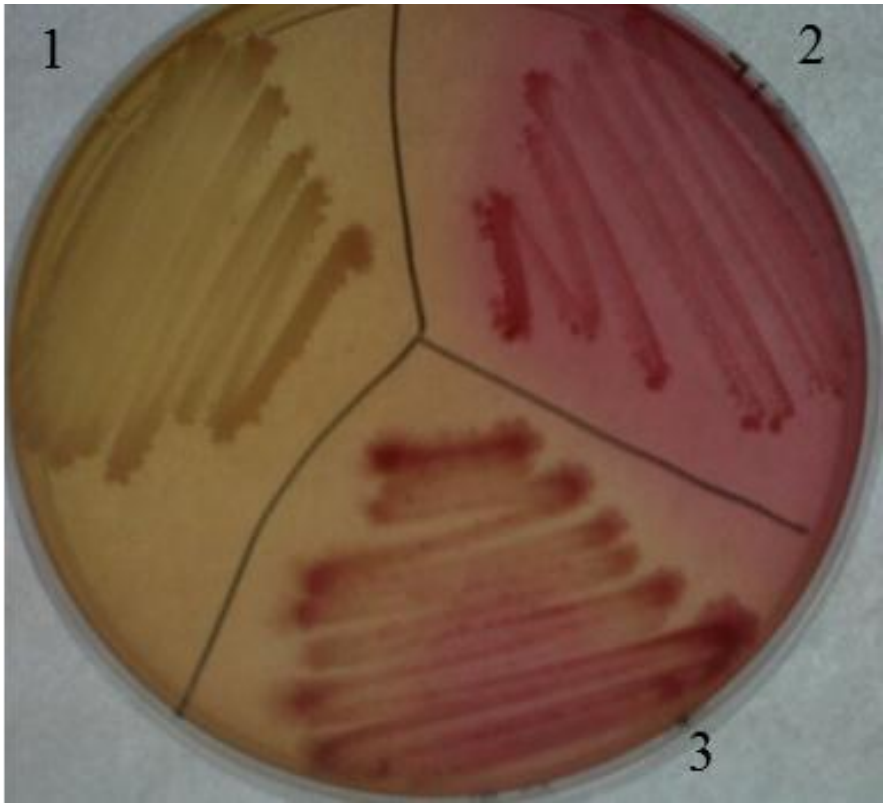

Figure 5.17. Bacterial two hybrid system screening for interaction of Cj0700 with CheV and CheB.
Each section illustrates interaction of Cj0700 with target proteins and Zip/ Zip (control).1: CheB/Cj0700 (no interaction), 2: positive control (++ interaction), 3: CheV/Cj0700 (+ interaction). *E. coli cya* strain screened on glucose-free MacConkey agar plates with added 1% maltose and incubated at 30 °Cfor 48 hours.

5.3.4. CheA-RR and Cj0700 protein-protein interaction

This assay screened for possible *in vivo* interaction between Cj0700 and CheA-RR each fused into at the end of complementary adenylate cyclase fragments. If Cj0700 interacts with CheA-RR colonies will show a red colour MacConkey plate.

The results demonstrate that the Cj0700 protein interacts with the CheA-RR protein (plate section 2, Figure 5.18).The interaction between these proteins appears to be moderate (+) when compared to the pT25: Zip/p18: Zip (plate section 2, same figure) interaction (++) used as a positive control. In contrast, Cj0700 displays no interaction with CheB, thus, this was used as negative control. To conclude, Cj0700 interacts weakly with the CheA-RR response regulator domain. Also, CheA-RR has shown to interact with Cj0700 protein in B2H system. In addition, this finding supports the observation of purified Cj0700 pull down with CheV.

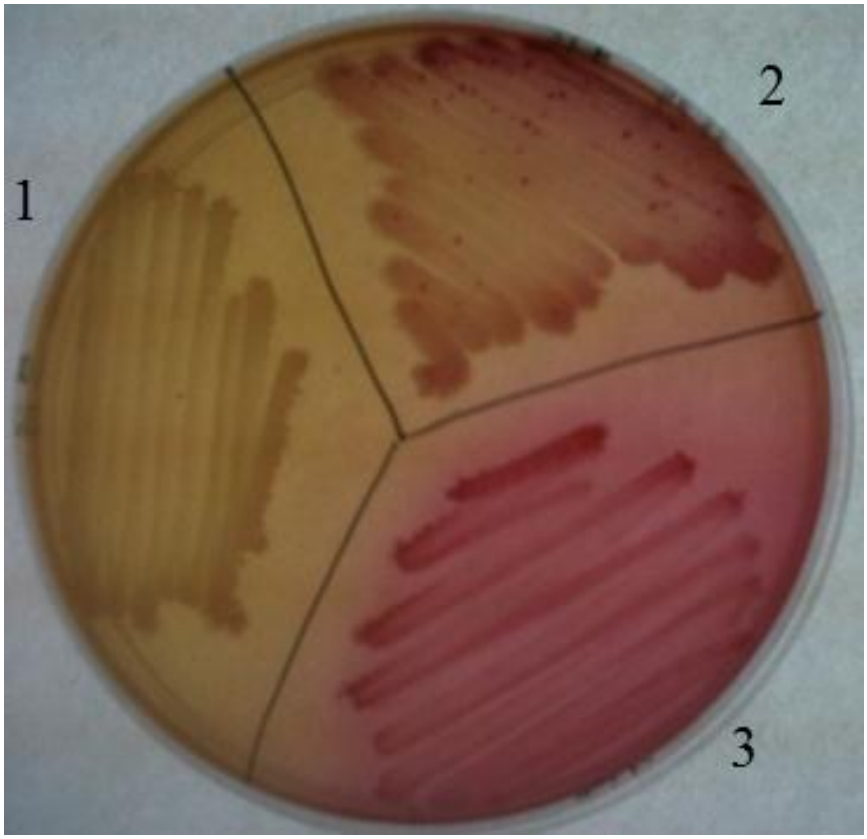

Figure 5.18. Bacterial two hybrid system screening for interaction of Cj0700 with CheY, CheA-RR and CheB. Each section is designated interaction of Cj0700 with target proteins and Zip/ Zip (control). 1: CheB /Cj0700 (no interaction), 2: CheA-RR/Cj0700 (+ interaction), 3: positive control (++ interaction). *E. coli cya* strain screened on glucose-free MacConkey agar plates with added 1% maltose and incubated at 30°Cfor 48 hours.

In order to confirm the validity and reliability of the assay; the possible interaction between the proteins encoded by pT25: CheA-RR/p18CheA-RR, pT25: Zip/p18: Zip and pT25: CheA-RR/p18: Zip recombinant plasmids were examined. The predicted outcome of these interactions was that the CheA-RR/CheA-RR proteins would interact; likewise the Zip/Zip would interact. However the CheA-RR and Zip proteins were not expected to interact with each other. Cells containing these plasmid pairs were co-transformed and were then streaked onto MacConkey plates and incubated at 30 °C for 48 hours.

The results show that CheA-RR interacted (++) strongly with CheA-RR (plate section 3, Figure 5.19). Similarly, the control Zip interacted (++) strongly with the Zip protein (plate section 3, Figure 5.19). However, as expected, CheA-RR didn't interact with Zip protein.

Conversely, as expected CheA-RR/CheA-RR showed strong interaction. Hence this shows that the results are genuine and that the results observed using this method are a true representation of the interactions between the tested proteins. Therefore, from these results it can be concluded that Cj0700 protein interacts with CheY, CheA-RR and CheV proteins, but that it doesn't interact with the CheB protein.

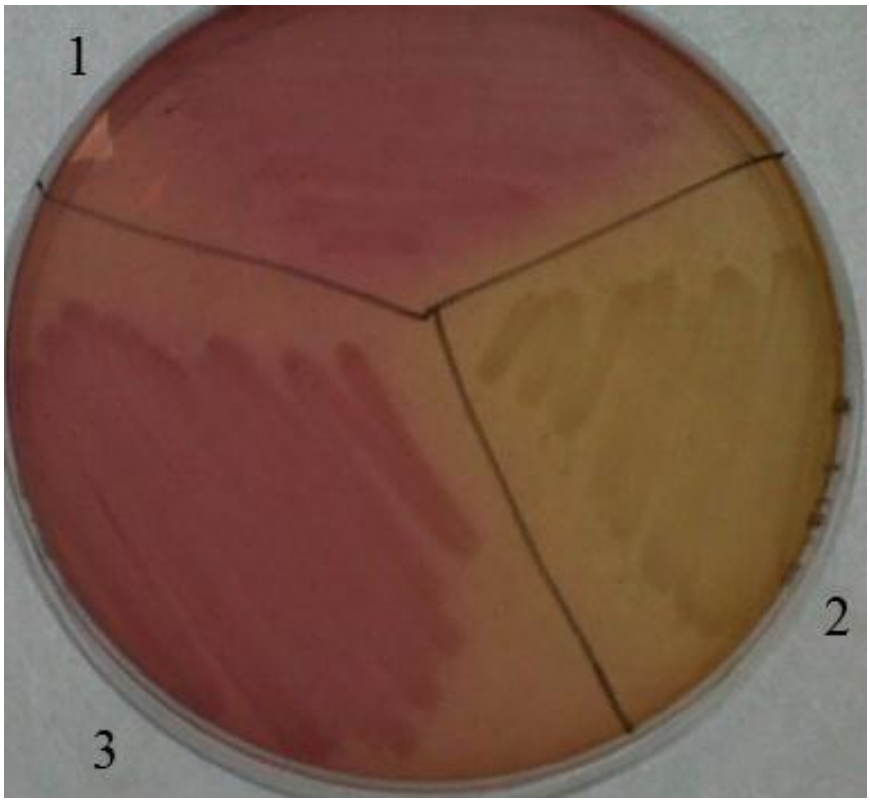

Figure 5.19. Bacterial two hybrid system screening for interaction of cheA-RR with CheA-RR and Zip. Each section is for interaction of Cj0700 with target proteins and Zip/ Zip (control).1: positive control of Zip /Zip (++ interaction), 2: negative control of ChA-RR/Zip (no interaction), 3: positive control of CheA-RR and CheA-RR (++ interaction). *E. coli cya* strain screened on glucose-free MacConkey agar plates with added 1% maltose and incubated at 30 °Cfor 48 hours.

5.4. Discussion

The purpose of the work described in this chapter was that given CheZcj has been shown to be able to specifically dephosphorylate RR associated with chemotaxis then it would be expected that CheZcj would be able to physically interact with response regulators in chemotaxis signalling pathway. Hence the first aim of the experiments was to investigate possible protein-protein interactions *in vitro* using purified Cj0700 protein with other purified chemotaxis proteins such as CheY, CheA-RR and CheV. The second aim of the experiment was to carry out B2H to test the binding between Cj0700 and CheY, CheA-RR, CheV and CheB proteins in whole cells. The reason for the B2H experiment was to confirm the *in vitro* results and to examine if the interactions seen *in vitro* of His/GST –tagged CheV and CheA-RR proteins are an artefact. In addition, in order to confirm the results were genuine in the *in vivo* assay, a Zip/Zip reporter was also included as a positive control. In the cloning protocol, *cj*0700 was fused at the N-terminal of the T18 fragment, whereas *cheY*, *cheA*-RR, *cheV* and *cheB* were fused at the C-terminal of the T25 fragment of adenylate cyclase. Interaction of the proteins would cause complementation of these fragments which would restore enzymatic activity of the adenylate cyclase, which subsequently would increase cAMP level in the BHT101 cells.

The *in vitro* pull-down assay indicated that Cj0700 interacted with CheY, CheA-RR and CheV proteins. In addition, protein-protein interaction of Cj0700 with response regulator proteins was supported by the B2H protein-protein interaction of Cj0700 protein with same proteins. In B2H and pull down assays CheA-HK was not investigated, assuming that Cj0700 may interact with only RR and thus only RR domain of CheA was used for protein-protein interaction assay. The idea that Cj0700 may be specific to bind only with chemotaxis RRs may be supported by non-binding observed in testing Cj0700 protein interaction with CheB protein, which lacks RR domain and also Cj0700 may interact only with RRs. In

addition to this, similar results using B2H has been demonstrated by Bridle (2007), where Cj0700 interacted with CheY, CheA, CheV and didn't interact with CheB. Therefore, these results confirmed that Cj0700 interacts with the annotated response regulator proteins in *C. jejuni*. Bacterial two hybrid experiment has shown that Cj0700 interacts with all known RRs in the chemotaxis pathway. This was observed in the B2H which supports results obtained from the protein pull down and dephosphorylation experiments in which it was demonstrated that Cj0700 interacts and removes phosphate from the same RRs.

A similar experiment using a similar B2H method and purified proteins have also demonstrated the interaction between CheZ and CheY in *E. coli* which is remote homologue of Cj0700. This study using purified proteins in an *in vitro* assay showed that CheY/CheZ complex formation is achieved, phosphorylating CheY by using acetyl phosphate as phosphate donor (Silversmith et al., 2001). Further study of *E. coli* chemotaxis proteins has shown that CheZ interacts with CheY by using Renila Luciferase complementation assay, which is technically similar to the adenylate cyclase method. In this assay the N- and C-terminals of the luciferase enzyme were fused to CheY and CheZ respectively, and as a result of the interaction between the two proteins the luciferase enzyme activity was restored (Hatzios et al., 2012).

Use of Flag tagged proteins was more difficult in terms of purification, because the reagent (beads) used for purification was not suitable for large scale purification; hence less volume (0.2 ml) was used for the purification which meant this was not enough for large scale purification in comparison to the His_6 and GST tagged proteins. Therefore, it was difficult to visualise the proteins using Coomassie Brilliant Blue on SDS-PAGE gel; in that case it was helpful to use Western blot technique using anti-Flag antibody.

Anomalous SDS-PAGE mobility observed with Flag tagged CheV and CheA-RR fusion proteins relative to their predicted molecular mass, may have been the result of the intrinsic

behaviour of the proteins. These abnormalities may be explained as a result of changes in the overall charge of the amino acid residues in the proteins because with Flag proteins the net amino acid charges have increased. Another explanation maybe that due to the modification resulting from Flag tag amino residues there may be a conformational change in the proteins. Previous studies have also shown these phenomena have an effect on protein mobility on SDS-PAGE gel (Carlotti et al., 2008, Rath et al., 2009, Georgieva and Sendra, 1999). As the result of these difficulties we were not able to use purified Flag-tagged CheV and CheA-RR proteins in the protein-protein interaction experiments.

The non-specific interactions observed between GST and the CheA-RR and CheV proteins may have been mediated by contamination with negatively charged DNA that binds to the surface of proteins. Hence, treatment with micrococcal nuclease in the *in vitro* pull-down assay might have prohibited the non-specific protein-protein interactions observed in immobilised GST (Nguyen and Goodrich, 2006). The GST blank showed a non-specific interaction and it was attempted to eliminate this using excess washing with buffer. Neither using different buffers nor adding BSA to the column based binding reaction improved the results especially in CheA-RR and CheV pull-down assays. However, treating with micrococcal nuclease in these reactions may have eliminated non-specific binding. Nevertheless, the *in vivo* protein-protein interaction using the B2H assay supports the hypothesis that Cj0700 interacts with CheY, CheA, CheA-RR and CheV.

Interaction of the Cj0700 with phosphorylated response regulator (CheY-P) is transient (milliseconds) (Wadhams and Armitage, 2004) which makes it difficult to detect easily in an *in vitro* assay using Western-blot and SDS-PAGE electrophoresis, so that may be one reason why weak bands were seen. It would have been better to look at whether interaction between Cj0700 and CheV without the W domain in both *in vitro* and *vivo* experiments. Similarly, it would have better to check the interaction between RRs and Cj0700 with mutated the

important residues (167D/171Q). Taken together, the B2H, dephosphorylation and pull down experiments supported each other well and have shown that Cj0700 interacts with the chemotactic RRs of *C. jejuni*. Therefore, both interactions are evidence and supports the hypothesis that Cj0700 is remote homologue of CheZ in *E. coli*.

The advantage of using GST fused proteins is because they are widely used method for prediction of possible protein-protein interactions between novel proteins with GST-fused proteins. The costs of glutathione resins are much more reasonable relative to anti-Flag tagged resins. In addition, GST tagged proteins are highly expressed and easily immobilised on bead particles containing reduced glutathione. However, because of the size of the GST-tag *per se* false positives may occur, and also steric hindrance may cause the bait protein not to interact with the prey protein (Sandoz and Lesage, 2008, Ueki et al., 2011, Phillips-Mason et al., 2006). Regardless of the non-specific interaction between GST and test proteins, the existence of Cj0700 protein-protein interaction is supported by other complementary assays such as the B2H and the phosphorylation assay, where both assays demonstrated Cj0700 interacts with the RRs. Therefore, the experiment demonstrated successfully the answer of the stated hypothesis and in addition assays are reproducible.

In the future other B2H systems, such as the luciferase-based system, could be used to investigate Cj0700 and other interesting response regulator proteins. The advantages of luciferase-based system experiment would be that the fluorescence reactions can be directly monitored in complementation of Che mutants of *C. jejuni*. Alternatively, using a cross linking agents such as 1-ethyl-3-(dimethylaminopropyl) carbodiimide hydrochloride and N-hydroxysuccinimide agents may enable to show Cj0700 and CheY similar interactions as observed *in vivo* and *in vitro* reactions . This agent has established the interaction between the purified CheZ and CheY of *E. coli*. Results have shown that CheZ and CheY have formed interaction using chemical cross-linking agent (Blat and Eisenbach, 1996b). May be the

interaction between the Cj0700 and RRs can be achieved also using chemical cross-linking agents, where only transient/weak interactions can be easily detected.

Using cross-linking agents has been suggested in conditions where it is difficult to obtain detectable protein interactions such as having low affinity interaction and because protein is intrinsically disordered (Pham et al., 2013).

Chapter 6 : Structural characterisation of Cj0700

6. Introduction

The three dimensional structure of Cj0700 would possibly provide insight into its catalytic function on the chemotaxis response regulator proteins. Thus the aim of the study was to determine the crystal structure of Cj0700, since it has been demonstrated in the previous assays of swarming, phosphorylation and protein-protein interaction assays that Cj0700 is a remote orthologue of CheZ in *E. coli*. Therefore, it is worth introducing a brief background to the terms used in relation to structurally folded and unfolded proteins in a biological perspective.

A precondition of crystallization is getting the protein under study into a crystal lattice. During crystallization the solubility of the protein is reduced by adding a high concentration of salts or polymers, however the major bottle neck is still to get the protein aggregated (Bukowska and Gruetter, 2013). Proteins which are, for instance, intrinsically disordered are difficult to be crystalized (Dyson and Wright, 2005). In addition, studies suggest that natively unfolded proteins can form a complex with their target proteins, so they are in-between a disordered and ordered transition. Consequently, the transition of the protein from disorder to order has been explained to be a desirable state for the protein to increase its binding affinity with substrate. Furthermore, it has been demonstrated that disordered regions of the protein play a crucial role in cell signalling pathways (Dyson and Wright, 2005). Therefore, it has been hypothesised that disordered regions found in proteins allow them to get access to target sequences in order to regulate conformation and activity of the protein (Collins et al., 2008).

As mentioned above the disordered regions of the protein may affect its folding, thus the disordered regions of Cj0700 was investigated using bioinformatics programmes. Also the secondary structure of Cj0700 was studied directly by Circular Dichroism (CD), and in addition, the tertiary structure of the protein was investigated by exposing it to a different

concentration of guanidine hydrochloride. Furthermore, nuclear magnetic resonance (NMR) was used to investigate Cj0700 folding in solution

6.1. Expression and purification of Cj0700 for structural characterization

For the crystallization experiment the His tagged Cj0700 fusion protein was used (Chapter 4, Figure 4.3). The His-Cj0700 fusion protein has a TEV protease recognition site so that the His tag can be excised from the Cj0700 protein; however, attempts to remove the His tag from the Cj0700 protein using the TEV protease were unsuccessful because the TEV caused degradation of the protein (data not shown). Thus the attempt at crystallization was carried out using His tagged Cj0700 protein.

Expression and purification of the Cj0700 protein used the same expression method and conditions as described before (chapter 4), however, for crystallization, it was necessary to express a large amount (>10 mg) of good quality Cj0700 protein, free from contamination and not degraded. Thus, a high yield of Cj0700 was produced14 mg/ml, and in addition successfully was purified 100% (Figure 6.1). Figure 6.1 shows purified His-Cj0700 protein. Theoretically the predicted size of Cj0700 is 26 kDa, whereas the His tagged Cj0700 protein visualised by Coomassie blue and Western blot using 10% SDS-PAGE electrophoresis shows a band of 38 kDa (Figure 6.1).

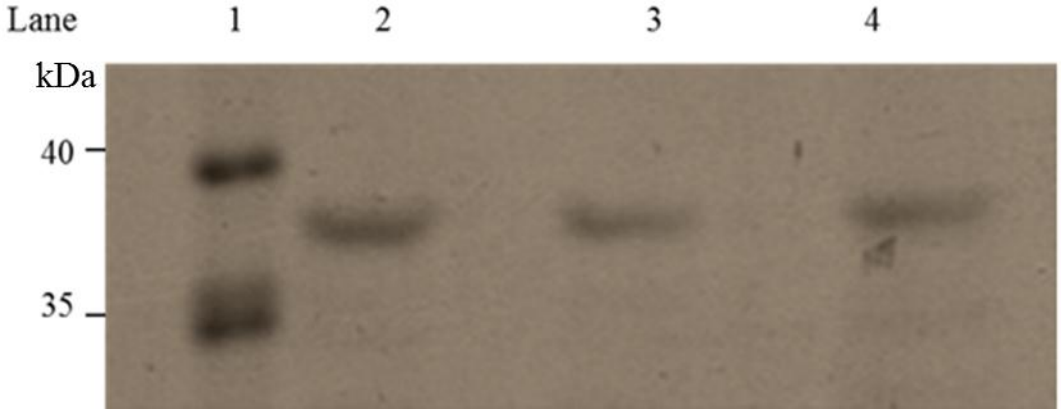

Figure 6.1. Purification of His tagged Cj0700 protein.

Lanes: 1 = pre-stained protein ladder, 2, 3 and 3 = His-Cj0700 protein from separate batches. Protein ladder and Cj0700 was electrophoresed on 10% Tris-Glycine SDS-PAGE gel and visualised by staining Coomassie Brilliant Blue stain.

6.2. Disorder prediction of Cj0700 by bioinformatics

Prior to predicting the level of disorder in the folding of Cj0700 protein, attempts were made to determine the three dimensional structure of Cj0700. To estimate the purity of Cj0700 protein that there were minimal degradation samples were analysed by SDS-PAGE. In order to maximise the chances of achieving Cj0700 crystal formation using the sitting drop diffusion method I used three different screens, JCSG, Cryo I&II, and Proplex (section 2.13); these contained buffers with different salts and with different pHs both of which can affect protein solubility. The crystallization of $CheZ_{cj}$ was unsuccessful despite many attempts using different screens with optimised conditions.

In order to establish if Cj0700 is folded correctly when column purified from *E. coli*, computer based software was used to predict the disordered regions of Cj0700. Using this analysis, Cj0700 was compared to the Hp0170 and CheZ phosphatases; these proteins are functionally similar to Cj0700 in that they remove phosphate from CheY-P response regulators in *H. pylori* and *E. coli* respectively. In addition the CheZ structure in *E. coli* has

been identified when it was co-crystallized with the CheY response regulator. In order to predict the disordered regions of Cj0700, which may affect its crystallization, it was analysed by the RONN (**R**egional **O**rder **N**eural **N**etwork) software technique. The parameters of analysis were set that regions above a threshold 0.5 are considered to be disordered (Ferron et al., 2006). Using this software, Cj0700 was compared to CheZ and Hp0170 proteins (Figure 6.2, 6.3 and 6.4).

6.2.1. Probability of disorder for CheZ in *E. coli*

The CheZ protein, which is a phosphatase to the CheY response regulator in *E. coli*, was shown to have disordered regions in its amino acid sequences using RONN software. The CheZ protein comprises 214 amino acids of which 75 are shown to be disordered (panel A&B,).

The results show that the disordered areas of CheZ are mostly at the N- terminal or C-terminal with 47 out of 75 disordered amino acids being C-terminal. In comparison to the disordered areas of both $CheZ_{hp}$ and $CheZ_{cj}$, the $CheZ_{ec}$ sequence has less disordered areas. Despite its more ordered structure, crystallization of CheZ was only achieved through co-crystallizing with CheY; hence, it seems probable that $CheZ_{cj}$ crystallization may also only be achieved through CheY co-crystallization.

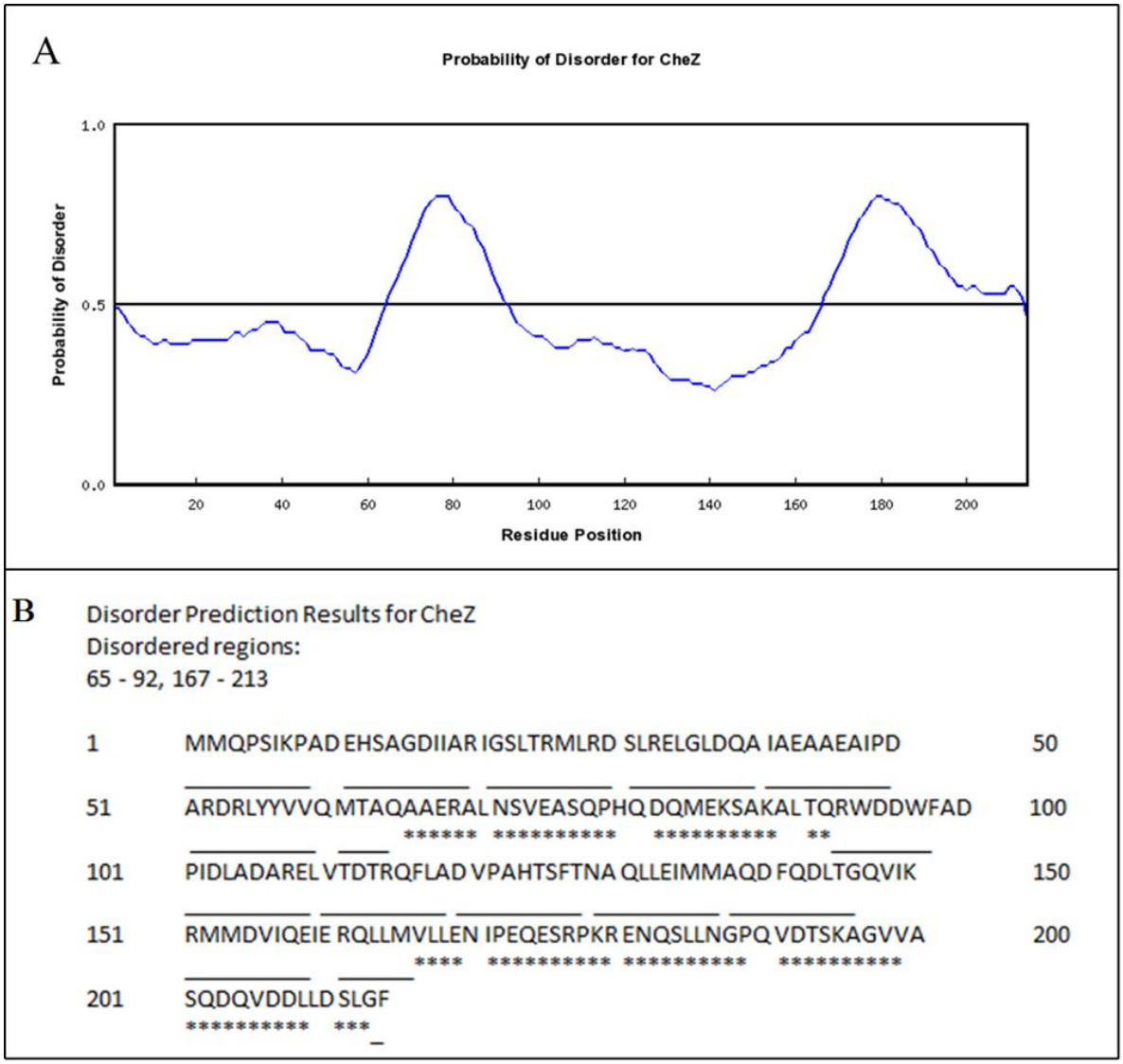

Figure 6.2 . Predicted disorder regions of CheZ protein using RONN software.

Amino acids above/under (0.5) threshold are disordered and ordered respectively (panel A). Regions locate disordered amino acids are: 63-92 and 167-21 (panel B).). Underlined amino acid sequences are ordered, whereas asterisk (*) represents disordered amino acid sequences. 75out of 214 amino acids are disordered in CheZ protein from *E. coli*.

6.2.2. Probability of disorder for Hp0170 of *Helicobacter pylori*

Analysis of the probability of disorder of Hp0170 shows that the disordered regions of Hp0170 are scattered across the protein, but mostly in the N-terminal region. Amino acids above the 0.5 threshold, according to RONN interpretation, are considered to be disordered. Conversely, amino acids which fall under the 0.5 threshold are said to be ordered (panel A,

Figure 6.3). According to results for the predicted disorderedness of Hp0170 protein, 154 of the 253 amino acids are considered to be disordered. Based on the prediction of disordered areas seen in the Hp0170 protein, it shows that Hp0170 is more disordered than CheZ (Figure 6.2) and that may have an effect upon its crystallization.

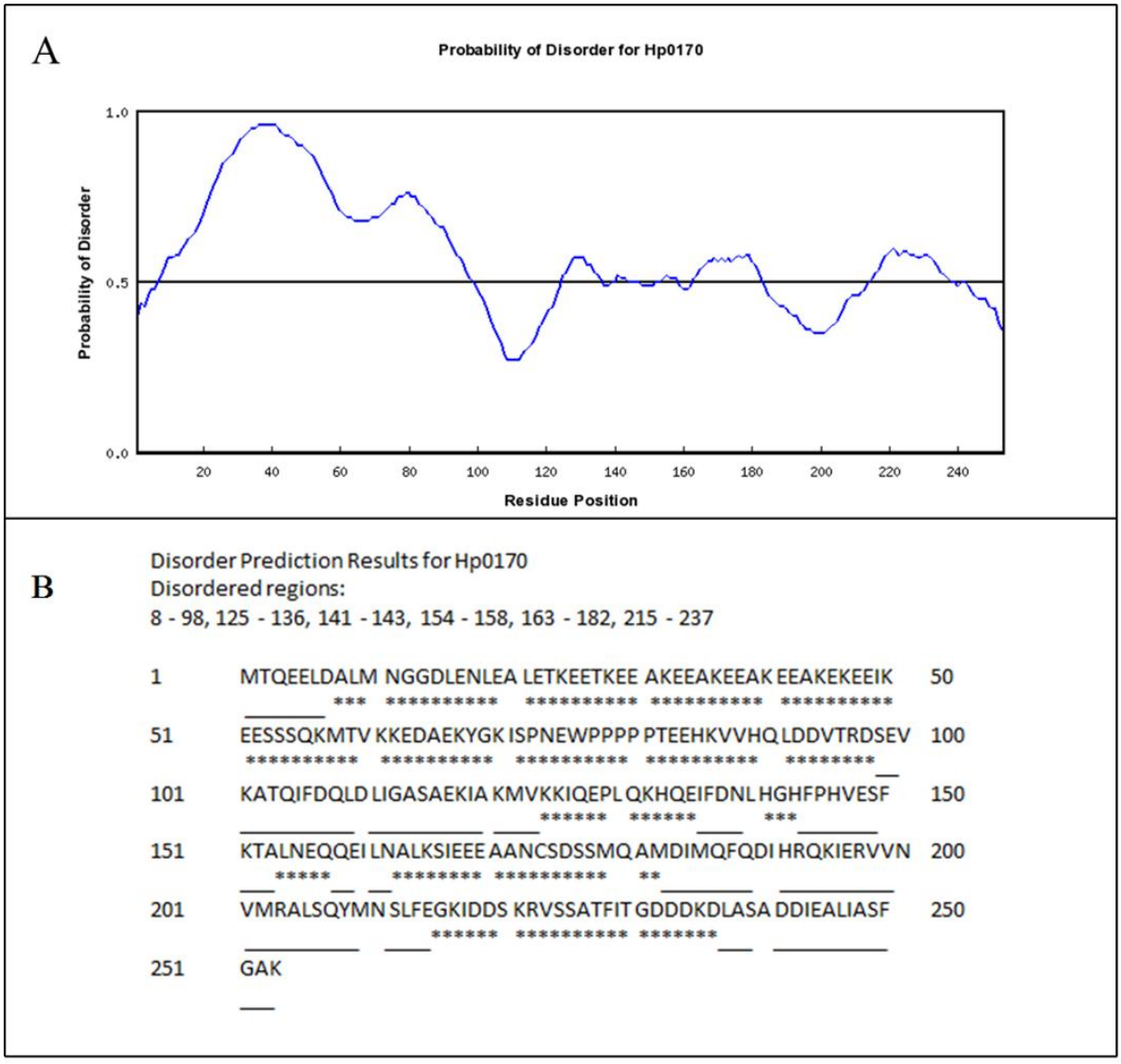

Figure 6.3. Predicted disorder regions of Hp0170 protein using RONN software.

Amino acids above/under (0.5) threshold are disordered and ordered respectively (panel A). Regions with disordered amino acids are: 8-98, 125-136,141-143, 154-158, 163-182, 215-237 (panel B), equivalent to amino acids with an asterisk (*) under them. Amino acids underlined are ordered amino acids (panel B). 154 out of 253 amino acids are disordered in Hp0170 from *H. pylori*.

6.2.3. Probability of disorder for Cj0700 of *Campylobacter jejuni*

Cj0700 protein was analysed using the same computer based software (RONN), in order to predict protein folding. The results show that 120 amino acids out of 231 amino acids of the Cj0700 protein are disordered (panel A & B, Figure 6.4). As with Hp0170 the disordered areas are found throughout the amino acid sequences in Cj0700 protein. Comparing the disordered areas of amino sequences in Cj0700 protein (Figure 6.4) to the disordered areas in Hp0170 protein indicates that Cj0700 has less disordered areas than Hp0170 protein (Figure 6.3). Interestingly the amino acid residues of Hp0170 which have been suggested to have a catalytic role on CheY (189D/193Q) are shown to be in ordered areas (Figure 6.2, B). In comparison to Hp0170, the amino acid residues in Cj0700 which are the potential catalytic site (167D/171Q) are shown to be ordered (Figure 6.4, B). In addition, the disordered areas of the two proteins Hp0170 and Cj0700 are spread throughout the sequences whereas the CheZ disordered areas are found at the N-terminal and C-terminal of the sequences (Figure 6.2). It is therefore possible that the disordered areas found in the amino acid sequence of Cj0700 may have been the reason for the failure to form crystals

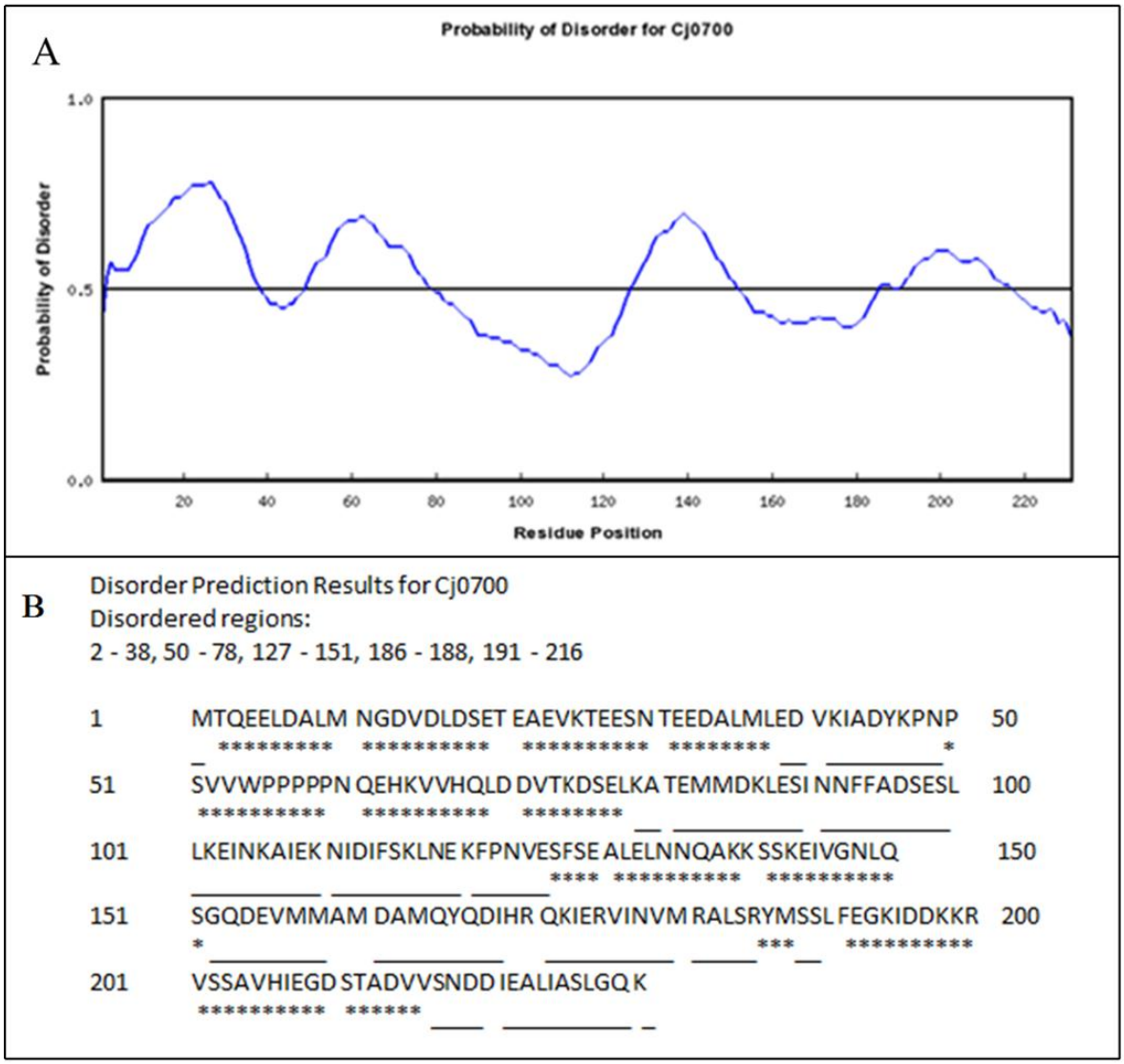

Figure 6.4. Predicted disorder regions of Cj0700 protein using RONN software.

Amino acids above/under (0.5) threshold are disordered and ordered respectively (panel A). Regions locate disordered amino acids are: 2-38, 50-78, 127-151, 186-188, 191-216 (panel B). Underlined amino acid sequences are ordered, whereas asterisk **(*)** represents disordered amino acid sequences. 120 out of 231 amino acids are disordered in Cj0700 protein from *C. jejuni*.

6.2.4. Predicting three dimensional structure of Cj0700

Predicting the secondary structure of Cj0700 was also undertaken using computer based software. The output 3-D structure of Cj0700 is based on the Cj0700 amino acid alignment to the CheZ as a template. Therefore, results shown in figures 6.5, 6.6 and 6.7 are complementary to each other.

Phyre^2 (**P**rotein **H**omology/Analog**Y** **R**ecognition **Engine**) is an algorithm-based software which predicts the structure of a query protein using the structural data from known proteins in the protein database/bank (PDB) as a template. The amino acid sequence of the query protein is processed by scanning with PSI-BLAST against the database searching for homologues so as to create an evolutionary relationship. Then the identified homologous sequences are converted into a Hidden Markov Model (HMM). This HMM creates an evolutionary fingerprint of the protein relative to the proteins. After that the created HMM sequence of query protein aligns against the HMM sequences of other known structures in the protein database. This alignment of the query protein to the known proteins allows it to build a 3-D model of the query protein. The accuracy of the query protein structure depends on the sequence similarity within the database where a more than 30% of confidence of similarity is required to consider that a model is accurate and reliable (Kelley and Sternberg, 2009).

The three dimensional protein structure of Cj0700 was predicted using the Phyre^2 server for predicting protein folding and disorder. The model construction of Cj0700 was based upon the selected sequence with maximum coverage and confidence. Hence, the CheZ model structure in *E. coli* was the only template having a high score of coverage (63%) and confidence (100%) with the Cj0700 alignment. Using CheZ as a model, Phyre2 generated 146 amino acids out of the 231 amino acids of Cj0700 to predict the three dimensional structure of the Cj0700 (Figure 6.5). Primary amino acid sequence modelled in 3-D structure (Figure 6.5) of Cj0700 indicated it to have 16% identity with the template of the CheZ amino acid sequence. Based on this model the 3-D structure of Cj0700 is predicted to contain α helices and coils. Equally, the 3-D structure of CheZ indicates to contain α-helices (Figure 6.5)

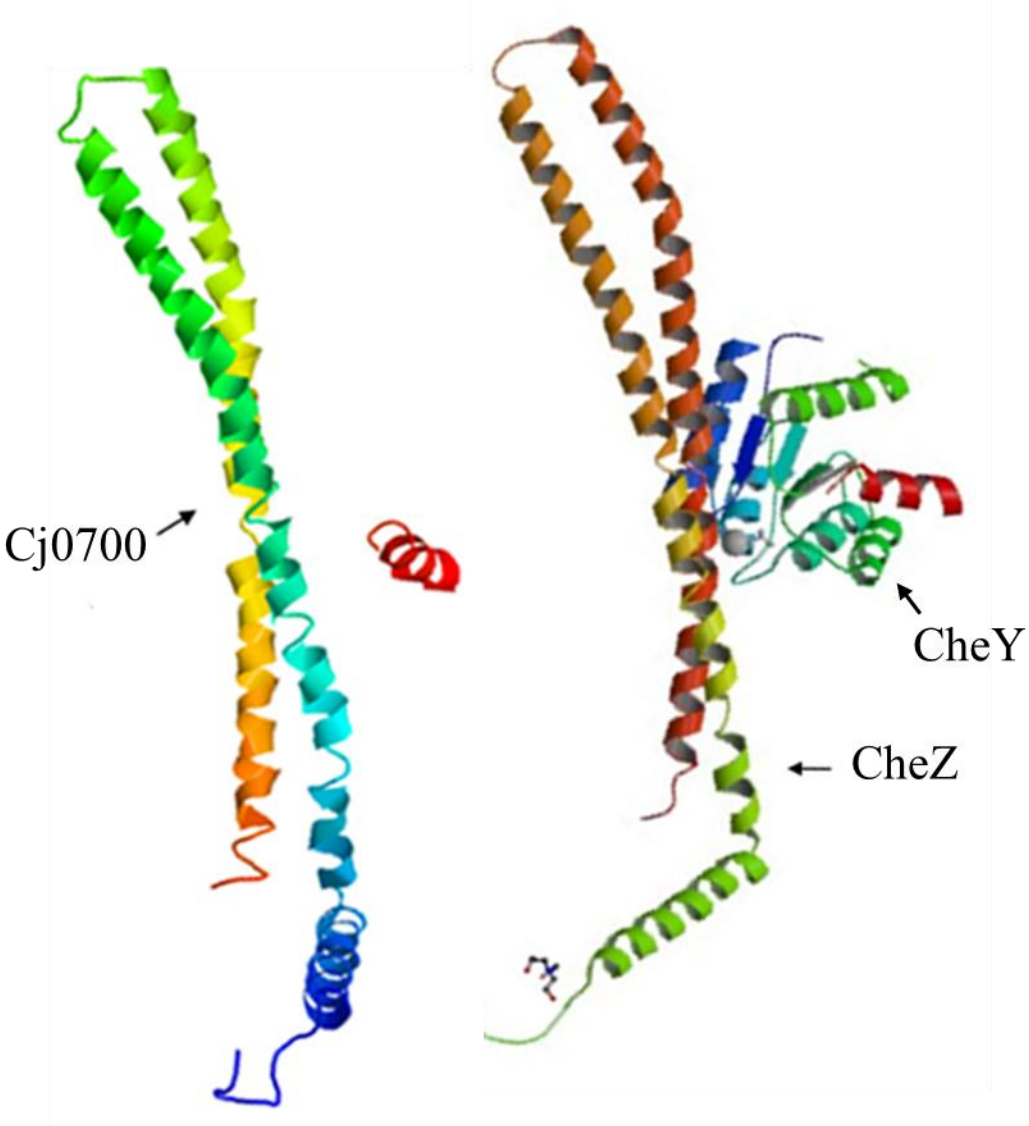

Figure 6.5. Comparing the 3-D structure of the Cj0700 and CheZ.

The model structure is based on the CheZ structure used as template using Phyre[2]program.The left structure is built of 146 amino acids out of 231 of Cj0700 with 63% coverage and 100% of confidence similarity. Image coloured by rainbow colour gradient N → C terminus. The right diagram shows CheZ-CheY co-crystal - arrows indicate CheZ and CheY. CheZ-CheY crystal structure was taken from PDB with ID 1KMI.

The primary amino acid sequence of Cj0700 protein (Figure 6.6) illustrates the disordered regions found in the Cj0700. Results are based on the alignment against CheZ amino acid sequences as a template. The predicted structure of Cj0700 is built upon amino residues added together from all parts of sequences to a total of 146 amino acids that formed helices and coils in Cj0700 relative to the model template of CheZ from *E. coli*. The CheZ used to model the structure of Cj0700 is the only distant homologue of Cj0700 that so far has a structure in the Protein Data Bank (PDB). The structure of CheZ was not successfully determined independently until its partner, CheY, has been co-crystallized. In addition to that, the whole of CheZ was not crystallized, suggesting there are disordered regions that hinder the determination of the structure of the entire CheZ protein (Silversmith et al., 2008, Guhaniyogi et al., 2006, Guhaniyogi et al., 2008a).

Using Phyre[2] software, Cj0700 has been analysed to predict possible disorder within its primary amino acid sequences. The results of the structure and disorder predictions indicate that Cj0700 comprises 82% α-helices, that no beta strands are found, and that 34% of Cj0700 is disordered (Figure 6.7).

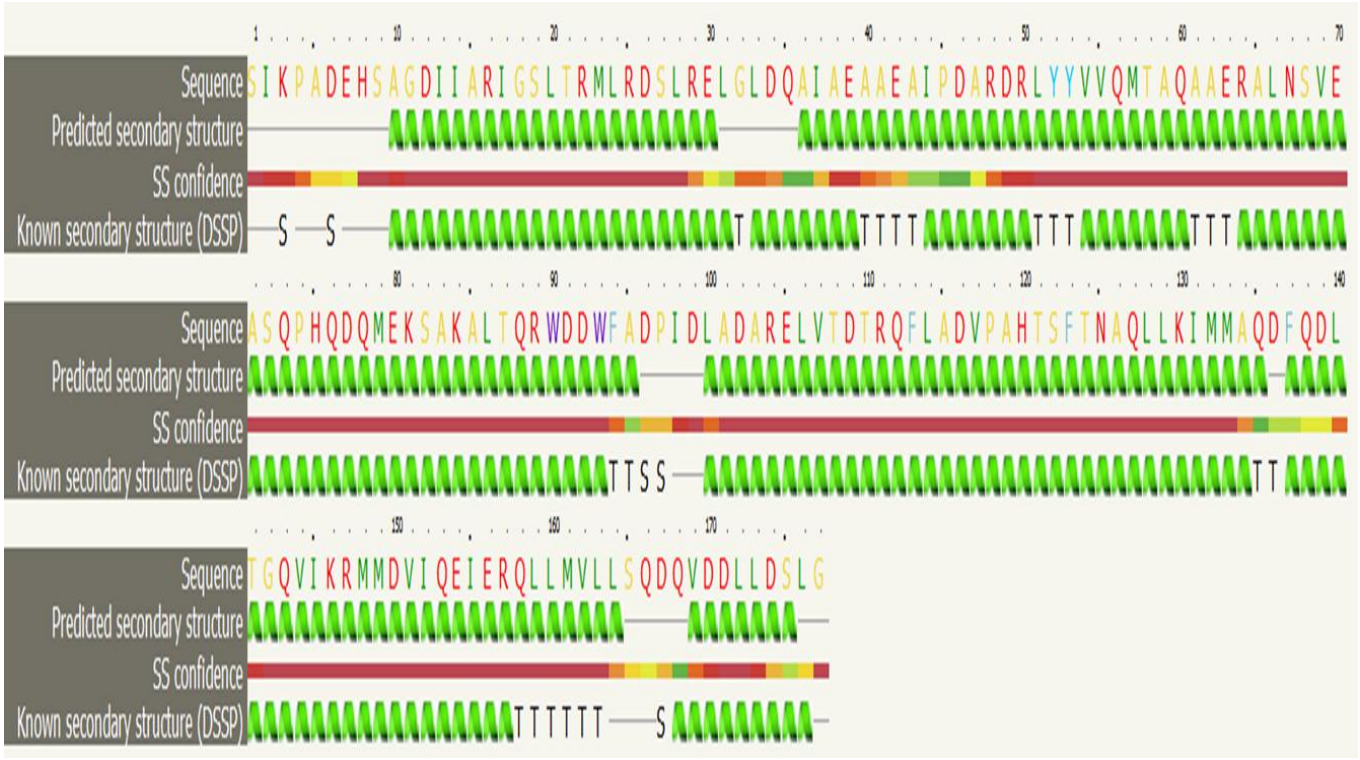

Figure 6.6. **Amino acid sequence used to predicted secondary structure of Cj0700 protein**.

Alignment of Cj0700 with CheZ amino acid sequence for predicting 3-D structure modelled in figure 6.5. Green represents α-helix. Faint lines between helices represent coil. T = hydrogen bond, S = bend. Secondary structure confidence: red = highest and black is the lowest. Predicting Cj0700 structure was used by Phyre[2] program.

The prediction of disordered regions in the sequence of primary Cj0700 protein structure is based upon comparing to the CheZ amino acid sequence. Thus overall the results indicate that disordered regions are spread throughout Cj0700 protein, which is consistent to the previous disorder prediction using the RONN software. To conclude, the RONN and Phyre[2] have indicated that Cj0700 is structurally disordered. In order to investigate the prediction that Cj0700 is disordered, the Cj0700 protein was further analysed using CD, to predict secondary structure composition, and NMR to analyse disorder.

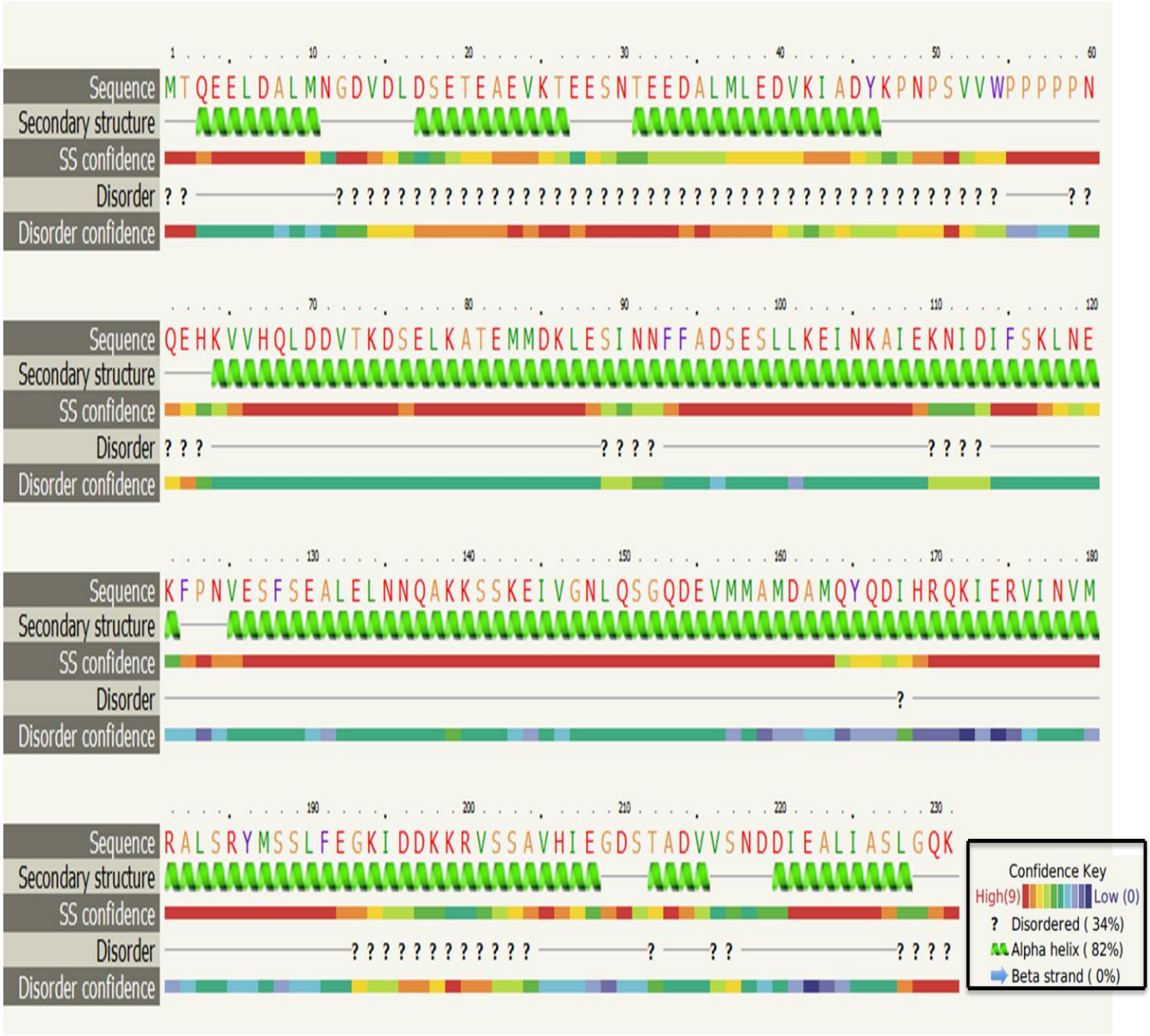

Figure 6.7. Secondary structure and disorder prediction of Cj0700 protein.

The secondary structure of Cj0700 and disorder regions were predicted using by Phyre[2] program. Green coils represent amino acids formed α-helices, faint grey lines between helices illustrate amino acids form coil, question marks (?) shows disorder regions. Confidence (0-9) highest 9 and lowest is 0. Estimated 34% is disordered, 82% α-helices and none of beta strands.

6.3. Far ultraviolet (UV) circular dichroism (CD) spectrum of Cj0700

Circular dichroism is a technique used to measure secondary or tertiary protein structure at different wavelengths. A CD spectrum is obtained as a function of wavelength and is reported in millidegrees (mdeg). The CD spectrum is calculated by subtracting the absorbance generated from counter-clockwise (L) and clockwise (R) rotating circularly polarized light. Based upon the CD signals the secondary and tertiary structure of a protein can be predicted. Absorption at wavelengths between 160- 250 nm is used for secondary structure composition whilst readings at wavelength range 260 to 320 nm are used for tertiary protein structure (Kelley and Sternberg, 2009).

The *in vitro* assay of secondary structure of Cj0700 was examined using a Chirascan-Plus CD spectrometer (Applied PhotoPhysics, UK); signals from peptide bonds of the protein in a form CD spectrum were obtained as a function of wavelength. A 20 µM concentration of purified Cj0700 was used in a buffer (20 mM Tris-buffer, pH, 7.6) solution to predict secondary structure using wavelengths with a range between 185-260 nm.

The CD spectra obtained for the Cj0700 structure are consistent with the previous predictions of secondary structure made using RONN and Phyre^2 software programmes, because it shows that Cj0700 is structurally disordered. However, the existence of disordered regions or if the protein is partially disordered needs to be assessed via further analysis, such as, disruption of a protein's native structure with high temperature or the agent guanidine-HCl. Such temperature increases will examine the protein's sensitivity to heat and in addition, determine the stability of the protein in the folded state. Also, use of different concentrations of the guanidine hydrochloride denaturing agent will allow assessment of the tertiary structure of Cj0700.

The CD spectra acquired from the measurement of Cj0700 secondary structure composition indicates that there are two bands; one of them is positive and the other is negative. The

positive band is in the wavelength range 190-200 nm, whereas the negative band is at the 208-222 nm wavelengths (Figure 6.8). The positive peak at 195 nm and the negative peaks at about 208 and 222 nm are characteristic of a α-helical protein. In addition, the CD spectrum has shown that the secondary structure of Cj0700 is 89% α-helices, 9.1% β-turn, 3.3% random coil and just 1.3%/0.1% of parallel/antiparallel β-sheets (Table 15).

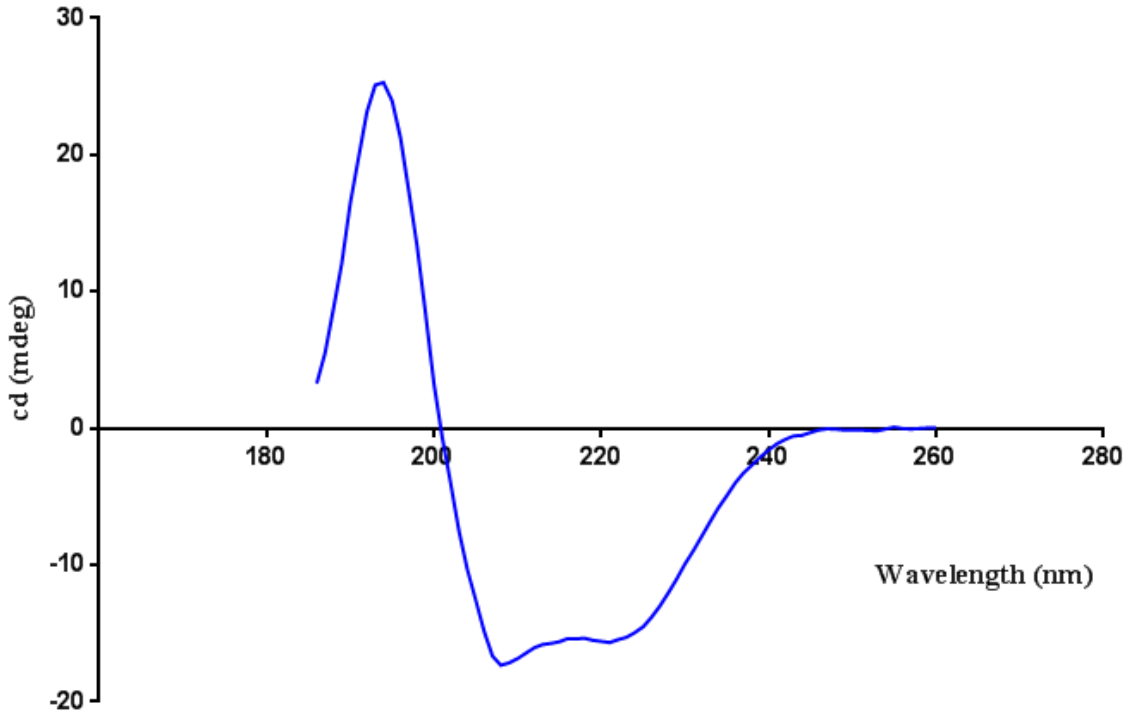

Figure 6.8. Far-UV CD spectra of Cj0700 protein.

A α-helix structure of Cj0700. 20 µM concentration of Cj0700 at 20 °C was used to predict secondary structure composition. Wavelength used is range between 185 to 260 nm.

Table 15. Far-UV CD spectra of predicted secondary structure composition of Cj0700.

Struct.	185-260 nm	190-260 nm	195-260 nm	200-260 nm	205-260 nm	210-260 nm
Helix	**88.8%**	90.9%	93.0%	94.8%	96.5%	96.0%
Antipar.	**0.1%**	0.0%	0.2%	0.5%	0.6%	0.4%
Parallel	**1.3%**	1.0%	0.7%	0.6%	0.4%	0.7%
B.Turn	**9.1%**	8.1%	7.2%	6.8%	6.4%	6.1%
R.Coil	**3.3%**	2.5%	2.6%	2.9%	2.7%	3.5%
Total Sum	**102.5%**	**102.5%**	**103.6%**	**105.6%**	**106.6%**	**106.8%**

6.3.1. Effect of temperature on Cj0700

CD analysis of native (unheated) Cj0700 in buffer (20 mMTris-Cl, pH 7.6) was measured at 20°C temperature. Then the effect on Cj0700 was measured in increments from 20 to 80°C. The results of post-melted folding and native folding of Cj0700 were examined using CD. The CD spectrum after heating indicates that Cj0700 folds back to its original secondary structure (Figure 6.9, red colour). Superimposing the folding of the post-melted structure to the folding of the unheated (native) Cj0700 demonstrates no structural differences between them (Figure 6.9, blue colour). Based upon the CD spectra, both show α-helical structure, i.e., a positive band at the 190-200 nm wavelength and negative bands between 208-222 nm which are characteristics of α-helical secondary structure.

The thermal treatment of Cj0700 indicated that the protein was stable until 35°C, where Cj0700 starts to melt (melting point) and reached midpoint at 46°C, where Cj0700 was completely melted. The semi-sigmoidal shape of the spectrum over the temperature range is characteristic of cooperative denaturation of unfolded protein (Figure 6.10. Since there are disordered/ordered regions predicted to exist in Cj0700, it can be concluded that Cj0700 protein is disordered/partially folded. Refolding Cj0700 protein after heat treatment may be explained by the fact that the protein folding is reversible with this temperature. Alternatively,

Cj0700 maybe partially folded, due to that it is temporarily resistant at this temperature to be fully denatured.

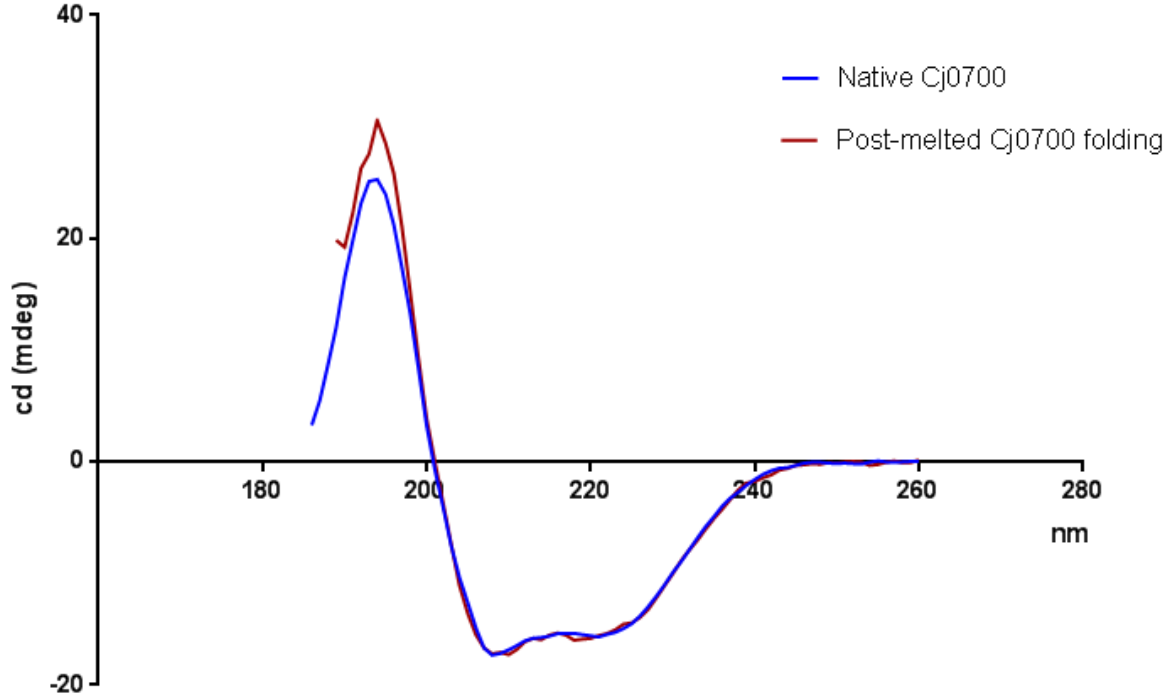

Figure 6.9. Far-UV CD spectra of Cj0700 protein.Cj0700 secondary structure was monitored using CD spectrum. Post-melted Cj0700 refolding. Native Cj0700 shows falling between 210 and 222 nm (blue). Cj0700 refolded into secondary structure after heat was treated (red). Characteristics of α-helices secondary structure protein falls between 208 and 222 nm wavelength. Cj0700 was heating ranged from 20 °C to 80 °C. CD spectra of Cj0700 show at the beginning positive and then negative CD over the range 190-200 nm and 201-260 nm respectively.

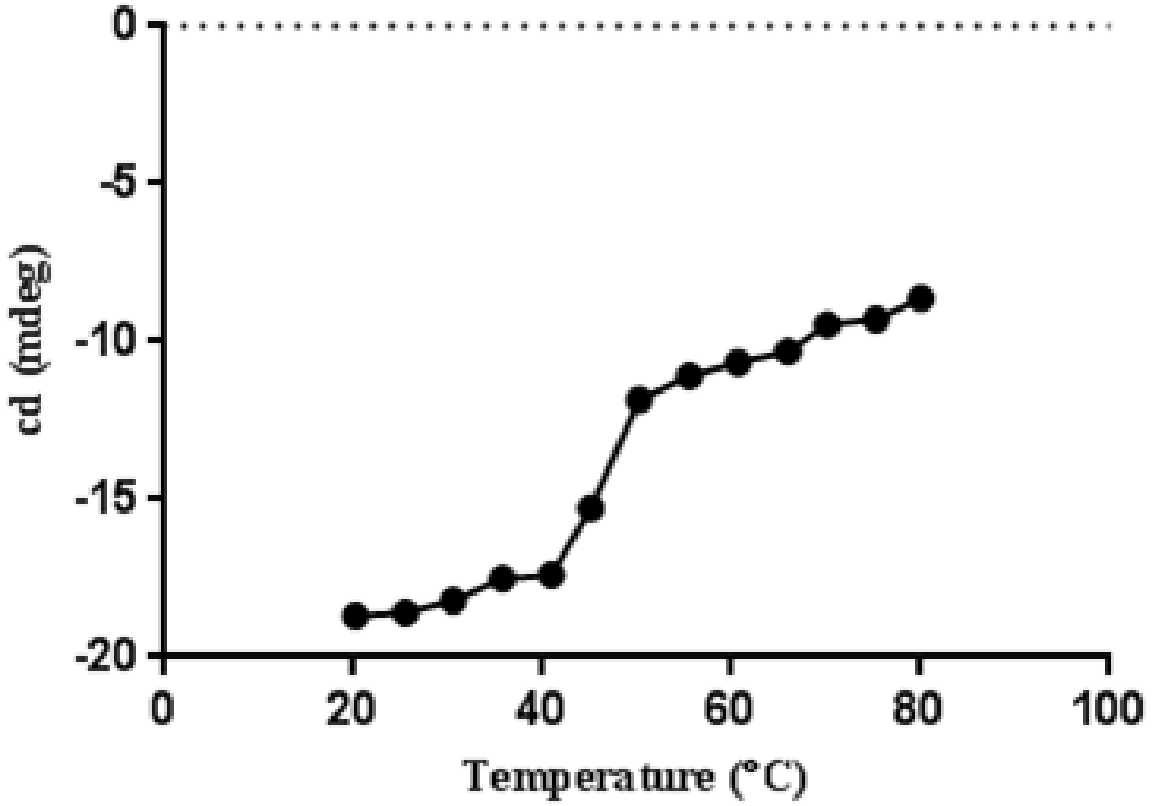

Figure 6.10. CD spectra of Cj0700 treated with heat.

20 µM Cj0700 treated heat ranging from 20 to 80 ^{o}C in (20 mM Tris, pH 7.6) buffer. Melting starts at 35 $^{\circ}$C and melting midpoint is 46 $^{\circ}$C.

6.3.2. Effect of chemical denaturation on Cj0700

The tertiary structure of Cj0700 was examined using different concentrations of guanidine hydrochloride. To monitor protein folding, 0.5 mg/ml of Cj0700 was dissolved in 20 mM Tris buffer, (pH 7.6) to produce a 20 µM concentration and was denatured using 0.5 M of guanidine hydrochloride up to 6M.

The graph shown in Figure 6.11 illustrates the denaturation effect of the guanidine hydrochloride on Cj0700 protein. As a control Cj0700 dissolved with Tris buffer was compared to Cj0700 with different concentration of guanidine hydrochloride in order to monitor the change of light intensity. To predict Cj0700 folding, measurement is based upon the fluorescence that Cj0700 emits at maximum wavelength as its intrinsic tryptophan is

exposed to the solvent. Change of fluorescence emission of each guanidine hydrochloride concentration (0.5 M to 6M) was recorded and compared to the fluorescence light emitted by native Cj0700 (Tris buffer). Interestingly Cj0700 shows slight cooperative unfolding, which does not follow a sigmoidal curve. This is a property of unfolded or partially folded proteins. Thus, Cj0700 lacks a complete tertiary structure.

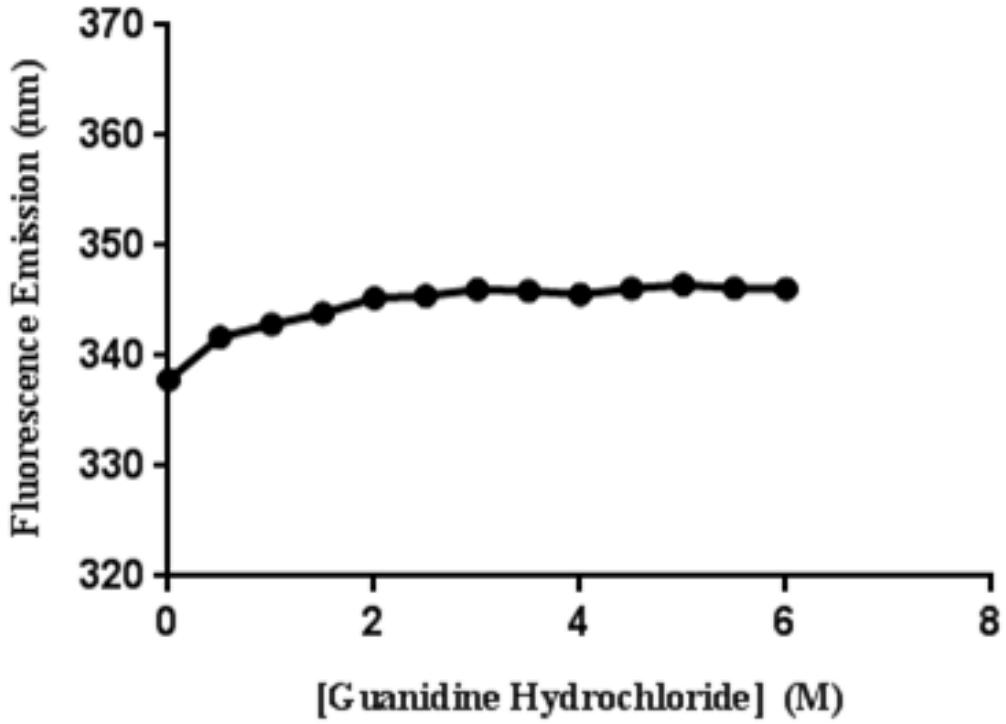

Figure 6.11. Intrinsic fluorescence of Cj0700 exposed with guanidine hydrochloride.
The denaturation of Cj0700 with Guanidine hydrochloride is to follow the fluorescence change as the increase of guanidine concentration. Coordinates: X = increasing guanidine HCl concentration, Y= fluorescence emitted by tryptophan.

The results presented in Figure 6.11 shows the wavelength of maximum fluorescence (nm). In the native structure at 20°C the tryptophan (Tyr-53) residue is buried and not exposed to aqueous solution (Tris buffer); here the wavelength of maximum fluorescence emission intensity of Cj0700 is about 338 nm (Figure 6.12, A). However, gradual increases in guanidine hydrochloride concentration produced a slight shift of the wavelength of maximum

fluorescence (nm). At 6 M guanidine hydrochloride, where probably tryptophan is completely exposed to solvent, the wavelength of the maximum intensity is at about 345 nm. Cj0700 has only one tryptophan in its primary amino acid sequence which was, according to RONN software-based analysis, predicted to be amongst the disordered amino acids (Figure 6.3), however using the Phyr2 software the tryptophan in Cj0700 was predicted to be among the ordered amino acids (Figure 6.7). The results presented in both Figure 6.11 and Figure 6.12 indicate semi-sigmoidal and straight line and that Cj0700 may have partial tertiary structure (ordered and disordered folding) in this experimental condition.

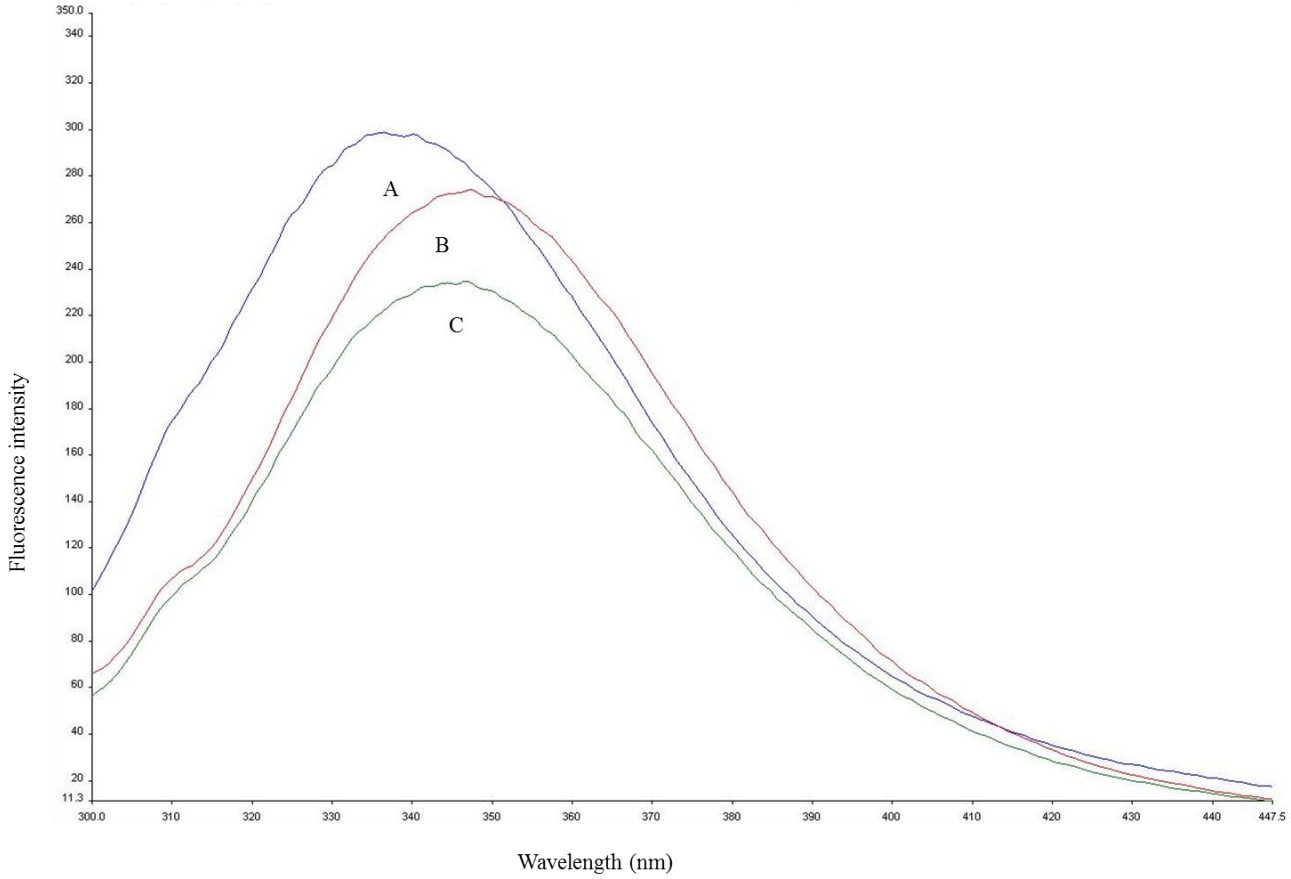

Figure 6.12.Tryptophan fluorescence emitted from Cj0700 protein.

Predicting tertiary structure of Cj0700. Cj0700 was measured all the time at 20^{o}C. Cj0700 (Tris buffer) fluorescence wavelength obtained at about 338 (A, blue), 6 M at about 345 nm (B, red), 2 M at about 341 (C, green).

6.4. Analysis of Cj0700 using one dimensional ^{1}H nuclear magnetic resonance (NMR)

One dimensional H nuclear magnetic resonance is the basic spectrum of NMR spectroscopy. It has been routinely used to characterize folding behaviour of a protein in terms of signal dispersion and peak intensity of NMR spectra. Protein folding behaviour can be assessed by the chemical shift of the NMR spectral regions. There are three chemical shifts observed from NMR spectra methyl proton at -0.5 to 1.5 ppm, α-protons at 3.5 to 6 and amide backbone protons at 6 to 10 ppm regions (Rehm et al., 2002, Page et al., 2005). A typical unfolded protein shows narrow chemical shift dispersions throughout the spectra. Particularly unfolded proteins show the amide backbone chemical shift at about 8.5 ppm with small signal dispersions (Rehm et al., 2002).

This experiment aimed to investigate the order/disorder folding features of Cj0700, since the first attempt to crystalize the protein was not successful. A 100 µM concentration of Cj0700 was prepared in phosphate buffer and was analysed by using one dimensional ^{1}H NMR at 800 MHz.

One dimensional ^{1}H NMR spectra of Cj0700 shows that there is no chemical shift observed in the methyl (-Ch3) signals between 0 and -2 ppm (Figure 6.13, right). Also the undispersed short peaks seen (Figure 6.13) at the left (downfield) of the NMR spectra (6.25 to 8.25 ppm) are formed from backbone amide (-NH). All of the peaks for the Cj0700 spectra are broad rather than sharp and they are not dispersed. All of these features indicate characteristics of a protein which is structurally unfolded (Figure 6.13). In conclusion, the analysis from bioinformatics and CD indicate that Cj0700 structurally is partially disordered and according to the NMR spectra, Cj0700 appears to be unfolded; these data are all consistent with the fact that Cj0700 failed to crystalize.

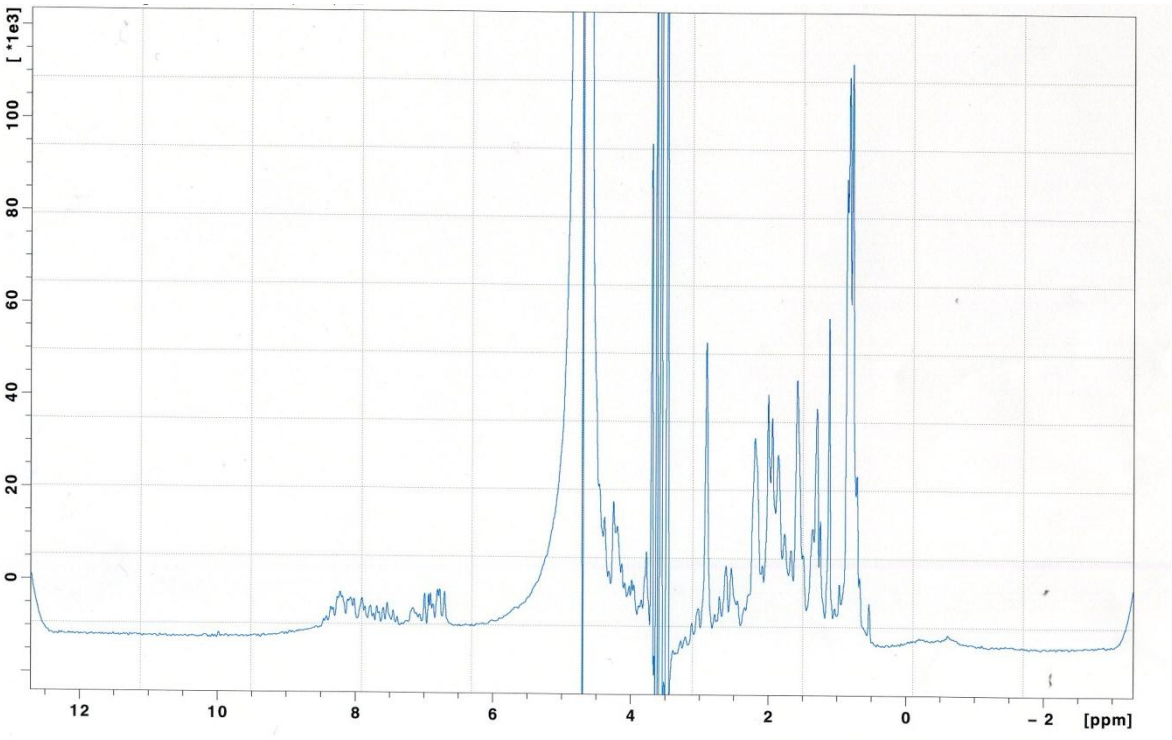

Figure 6.13.One dimensional ^{1}H NMR spectra recorded for Cj0700.

Predicting unfolded structure of Cj0700. The assay was carried out using 350µl of a 100 µM concentration Cj0700 dissolved in phosphate buffer (pH 7.3). NMR data was collected at 800 MHz at a temperature of 25°C. Coordinates: Y = peak height, X= chemical shift (dispersion) measured ppm.

6.5. Discussion

Determination of the structure of Cj0700 protein is important because understanding the molecular properties of the protein may provide better information about the active site and binding with response regulators. The crystallization process of Cj0700 was not easy because it required a high (100%) purity of the protein. In addition to that, the Cj0700 needed to be free from degradation so producing intact Cj0700 protein was extremely important for crystallization. During the purification it was attempted to remove the Histidine tag from the Cj0700 protein; however that resulted in the Cj0700 protein becoming degraded. Thus, in order to keep the protein intact it was decided to crystallize the His tagged Cj0700 protein.

The crystallization process involves an optimisation of all possible conditions where protein solubility can be reduced. Cj0700 was tested using three different screens which optimised across multiple different conditions. Also different temperatures and different Cj0700 concentrations were tried to form protein precipitation, however, none of these attempts were successful.

Failure to determine the crystal structure of Cj0700 could be explained if it contained disordered regions that could prevent the protein being crystallised. Absence of a stable conformation of Cj0700 protein *in vitro* was supported by the disorder prediction software. For instance CheZ, the phosphatase of CheY-P from *E. coli*, was demonstrated to have disordered regions in the protein using both RONN and Phyre^2 software. Equally, Hp0170, the phosphatase of CheY-P from *H. pylori,* also indicated that it had disordered regions. Interestingly, the disordered regions of CheZ are in the N- and C-terminus regions, whereas the C-terminus has been shown to interact with CheY response regulator in *E. coli* (Blat and Eisenbach, 1996a).

It may be possible that disorderedness is not the result of solvent exposure during the crystallization process, but that Cj0700 is *per se* disordered in the physiological environment.

This could be explained if there were flexible linkers in the protein, possibly related to the function of the protein so that it could interact with various targets. The failure of crystallization of Cj0700 was perhaps due to the fact that it is structurally disordered similar to the CheZ protein in *E. coli*; in which case the Cj0700 structure may only be achieved by co-crystallizing with the CheY response regulator.

Previous studies have shown that chemotaxis phosphatase CheZ from *E. coli* (Zhao et al., 2002) which is distant homologue of Cj0700, did not crystallise. The reason for this failure to crystallise was explained as being because of it containing disordered regions that would prevent protein folding into three dimensional structures (Guhaniyogi et al., 2006). This problem has been solved by co-crystallizing CheZ with the CheY response regulator (Silversmith et al., 2008). Unlike CheZ, the other chemotactic phosphatases, CheC, CheX and FliY, found in *B. subtilis* and *T. maritima* were crystallized without the presence of CheY (Sircar et al., 2013, Park et al., 2004). Maybe the reason for the success in crystallizing them can be explained in that these proteins are structurally ordered. The phosphatases CheC, CheX and FliY were studied to predict order/disorder properties using RONN software. Results showed (data not shown) that CheC and CheX were all ordered, however, FliY was shown to contain disordered regions. In *B. subtilis* FliY is different from other phosphatases such as CheC and CheX, as it is a hybrid of CheX and FliN (Szurmant and Ordal, 2004), thus this could also have its own effect for crystallization; because this hybrid form may influence protein conformation and it may be easier for the protein to form precipitates.

The predictions of Cj0700 disorder/order structure by the RONN and Phyre^2 were complementary to each other with both results indicating that there are disordered regions in the Cj0700 protein based on its primary amino acid sequence. In addition, using Phyre^2 software was more advantageous than the RONN, as it predicted Cj0700 to be disordered and most of the structure consisted of α-helices. These results were consistent with the previous

CheZ studies. Moreover, the results of CD spectra have demonstrated that Cj0700 is structurally α-helical and by temperature and guanidine hydrochloride denaturation that it is partially disordered. Also investigation of tertiary structure of the protein using guanidine hydrochloride indicates that there is a wavelength shift compared to control (native protein). This wavelength shift supports other experiments which concluded that Cj0700 is partially disordered and may therefore not crystallize. Similar characteristics of disordered proteins in CD and NMR spectra have been demonstrated (Renshaw et al., 2002), which are consistent to the results of Cj0700 spectra. Thus, the evidence supports the earlier conclusion that Cj0700 won't crystallise alone without finding another partner which may stabilize crystallization. In the future, it may be worth trying to co-crystallise with the CheY response regulator using beryllium fluoride as an analogue of a phosphate donor. The reason for this suggestion is because CheZ was successfully co-crystalize with CheY from *E. coli* (Silversmith et al., 2008)

The purpose of the experiment was to crystalize Cj0700, however it was found out that the 3-D structure of Cj0700 was difficult to achieve because of disordered regions in the protein. Therefore it is likely that Cj0700 needs the CheY partner protein and may be through co-crystallization that the obtained 3-D structure of Cj0700 can be obtained.

Chapter 7 : General Discussion

7. Summary of the project findings and conclusions

The findings in this study are based on the notion that motility and chemotaxis are believed to guide chemotactic bacteria to their preferred colonization site (Butler and Camilli, 2004). This is because chemotaxis signalling pathways together with motility (flagellum) can navigate the bacteria along a defined chemical gradient (Porter et al., 2008). At the present time *C. jejuni* is considered to be one of the major causes of human gastroenteritis in the world, where 400-500 million cases have been reported in a year (Fouts et al., 2005). In the UK alone in a year more than 371,000 cases of *Campylobacter jejuni* infection and more than 100 deaths were estimated by FSA (Wearne, 2013). Chemotaxis has been shown to be important for disease initiation (Fahmy et al., 2012) as previous studies have indicated that motility plays a pivotal role in intestinal colonization and invasion of epithelial cells (Poly and Guerry, 2008). The suggestion that chemotaxis is essential for virulent bacteria was supported by a study where a chemotaxis mutant of the medically important bacterium *H. pylori* was unable to colonize the mucosa and was not able to cause gastric cancer (Porter et al., 2008).

In order to understand the chemotaxis pathway employed by *C. jejuni*, the bacterial chemotaxis models of other bacteria were used to compare systems, such as the model system in *E. coli*. In *E. coli* the chemotaxis proteins consist of MCPs, CheA, CheW, CheY, CheB, CheR and CheZ proteins. CheA and CheY are the backbone of the chemotaxis and motility system which in *E. coli* regulates the direction of movement either toward an attractant or away from a repellent (MacKichan et al., 2004). However, the CheZ protein, which is the CheY phosphatase, is not conserved across bacterial species (Lertsethtakarn and Ottemann, 2010, Rao et al., 2005). For instance, in *H. pylori,* which is a close relative to *C. jejuni,*

Hp0170 has been identified to encode a protein that has been confirmed to be a remote homologue of CheZ (Silversmith et al., 2008); the homologue of the protein in *C. jejuni* is $CheZ_{cj}$. Hp0170 identification as a phosphatase has driven the hypothesis that Cj0700 has a role in the *C. jejuni* chemotaxis signalling pathway and may be is the remote homologue of $CheZ_{ec}$. Thus the aim of the work described here was to verify a role for Cj0700 in *C. jejuni* chemotaxis and determine the mechanism by which it acts.

7.1. Cj0700 has a role in the chemotaxis pathway of *C. jejuni*

Evidence supporting a role for Cj0700 in the chemotaxis signalling pathway has been established by creating mutants, and their respective complements, in three *C. jejuni* strains (NCTC11168, 81116 and 81176). The chemotactic behaviour of the *cj0700* mutants was tested using an established semisolid agar plate methodology referred to as swarming plates. The wild type phenotype of chemotaxis and motile *C. jejuni* is that it spreads equally to the edges of the plate. Conversely, non-motile and non-chemotactic bacteria have a much reduced diameter on the plate (Niu et al., 2005).

The chemotactic phenotype of *cj0700* mutant was shown to have a reduced diameter on semisolid plates relative to the wild-type. In addition the normal growth rate of the *cj0700* mutant relative to the *cheY* mutant and the wild-type has confirmed that the observed phenotype was due to a chemotactic defect of the $cheZ_{cj}$ mutant. Despite the clear non-chemotactic phenotype of the *cj0700* mutant it was speculated that this could be the result of a polar effect on genes downstream of *cj0700* due to the insertion of an antibiotic resistance cassette into the *cj0700* gene. It is possible that these downstream genes may be important for growth and survival and that disrupting the operon could affect the expression of the genes. In order to provide evidence that the *cj0700* gene really has a role in the chemotactic pathway and that the observed non-chemotactic phenotype is genuine was confirmed by

complementing with a copy of *cj0700 in trans*. The non-chemotactic *cj0700* mutant showed restoration of a chemotactic phenotype upon complementation thus it was concluded that the *cj0700* gene has a role in the chemotactic pathway of *C. jejuni*.

Generally speaking complementation of the *cj0700* mutant did not show a full return of the phenotype back to that of the wild-type, because inserting the *cj0700* gene into a new site may have influenced the expression level of the gene relative to the wild type. Thus, it was not anticipated that a complete phenotype restoration would be likely. Likewise, disrupting the genomic organization by the *cj0700* complement could influence the expression level due to the fact different places in the chromosome may be under regulation of many unknown factors. Therefore, to ensure at least a minimum level of expression of *cj0700* for complementation, the *metK* promoter, which is constitutively expressed in low level was put upstream of *cj0700* own promoter. As a result, for instance in strain NCTC11168 *cj0700* gene was put under the regulation of two promoters. However, when tested, the *cj0700* complement strains with or without *metK* promoter, both showed the same chemotactic phenotype.

Mutants of *cheZ* and *hp*0170 in *E. coli* and *H. pylori* respectively show a chemotactic defect on semisolid plates; however the chemotactic phenotype was restored when complementing copies of *cheZ* and *hp0170* were introduced into the mutant strains (Boesch et al., 2000, Terry et al., 2006). A similar result was seen in *B. subtilis* where a double mutant of *cheC* and *fliY* showed a chemotactic defect on semisolid plate when compared to wild-type (Szurmant et al., 2004). Based upon the results obtained from experiments in this study and knowledge of chemotactic defects previously shown in *E. coli*, *H. pylori* and *B. subtilis*, it was concluded that Cj0700 has a chemotaxis role in *C. jejuni*.

7.2. Cj0700 is a remote orthologue of $CheZ_{ec}$

The phosphorylation experiments were carried out in order to answer the question does Cj0700 have a phosphatase activity upon CheY. Genome analysis of *C. jejuni* had not identified a CheZ homologue (Parkhill et al., 2000) and thus it was proposed that CheV might act as phosphate sink for CheY. Results of dephosphorylation experiments have shown that Cj0700 has chemotaxis phosphatase activity on CheY.

Evidence to suggest that Cj0700 is a phosphatase is provided by the amino acid alignment of Cj0700 to the $CheZ_{ec}$ and $CheZ_{hp}$ phosphatases which have previously been identified to share conserved amino acid residues. Some of these conserved amino acid residues were identified, from the co-crystallization of CheZ with CheY from *E. coli*, to be in the active site and the binding site between CheZ and CheY proteins (Silversmith et al., 2003, Silversmith, 2010).

Other evidence that supports the hypothesis that Cj0700 is a phosphatase includes the results of the phosphorylation experiments which show a rapid phosphate removal from $CheY_{cj}$-P relative to a control reaction in which Cj0700 was absent. Similar results were previously shown in *H. pylori* where Hp0170, which is a remote homologue of CheZ, had a phosphatase activity upon $CheY_{hp}$ (Lertsethtakarn and Ottemann, 2010). Likewise, CheZ in *E. coli* has been shown to have a phosphatase effect on phosphorylated CheY-P (Silversmith et al., 2003). Similarly, other CheZ-like phosphatases, such as the CheX and CheC/D found in *T. maritima* and *B. subtilis* have been shown to accelerate the de-phosphorylation of CheY-P (Park et al., 2004). Thus, from this de-phosphorylation experiment it was concluded that Cj0700 has a phosphatase activity on CheY.

The results of the phosphorylation experiment showed that Cj0700 is also a phosphatase for the CheA-RR-P domain; however there was only weak phosphate removal and it is not as efficient as the reaction of Cj0700 with CheY-P. This weak phosphatase activity on CheA-

RR-P is consistent with a previous study where $CheZ_{hp}$ phosphatase activity has been investigated using $CheA_{hp}$-RR (Lertsethtakarn and Ottemann, 2010). This study showed that $CheZ_{hp}$ removed phosphate from CheA-RR-P; however the effect was not as strong as the $CheZ_{hp}$ removal of phosphate from CheY-P.

The phosphorylation experiments testing whether Cj0700 could remove phosphate from CheV-P indicated that, at least in the conditions tested, Cj0700 could not remove the phosphate. When comparing the RRs in the chemotaxis signalling pathway, the CheA-HK phosphor-transfer rate to CheV was not as efficient as that to CheY and CheA-RR. Similar effects have been seen in *H. pylori* in which CheV's phosphate uptake from $CheA_{hp}$-HK was reduced (Jimenez-Pearson et al., 2005). The reduction in phosphate transfer from CheA-HK to the CheV may be because Cj0700 couldn't remove phosphate from CheV-P. This is may be since CheV is a hybrid of CheW and a RR and in that case it was suggested that the CheW domain prevents the phosphatase from removing phosphate from the RR domain (Alexander et al., 2010). In conclusion, this research has shown that the role of Cj0700 protein in the chemotaxis signalling pathway is as a phosphatase, in which Cj0700 definitely removes phosphate from CheY-P and CheA-RR-P but may not have a phosphatase activity on CheV-P.

7.3. The predicted model for *C .jejuni* chemotaxis signalling pathway

This prediction of the chemotaxis signalling model is based upon evidence gathered from the results of previous work and from the experiments in this study. For instance, based upon the literature, *E. coli* has been used as the paradigm for predicting possible chemotaxis pathways that exist in other organisms, such as in *C. jejuni*. Furthermore, comparisons with the chemotaxis signalling pathway of *H. pylori* was also made in order to predict the chemotaxis signal transduction in *C. jejuni*. Likewise, results obtained from this research, such as

phenotypes shown by the *cj0700* mutant, the effect of phosphorylation and interaction of $CheZ_{cj}$ with chemotaxis proteins were also used to create a new model for *C. jejuni* chemotaxis.

The chemotaxis signal transduction model starts with the signal being detected by the transmembrane (Tlp) chemoreceptors and then is transferred to CheA via the CheW/CheV proteins. The activated CheA is autophosphorylated using ATP and in turn CheA transfers phosphate to CheY. The phosphorylated CheY diffuses through the cytoplasm and interacts with the flagellar motor switch FliM. The CheY/FLiM interaction results a rapid switch in the direction of rotation of the flagellum and thus *C. jejuni* moves in a new direction. The $CheZ_{cj}$ protein, which has been confirmed as a phosphatase in the chemotaxis signalling pathway of *C. jejuni*, terminates signal transduction at the CheY: FLiM interaction by removing the phosphate from CheY-P (Figure 7.1). Evidence for a physical interaction between $CheZ_{cj}$ and CheY has been provided by the protein pull-down and B2H experiments. In addition, CheA can pass phosphate to its own RR domain and to the CheV protein; the evidence for this phosphate exchange between CheA's own RR and CheV have been provided by the work of Paul Ainsworth (2013). It can be speculated that RR domains in CheA and CheV may play an important role in regulating chemotaxis signalling pathways in *C. jejuni*.

The protein-protein experiments have proved that there is an interaction between $CheZ_{cj}$ and CheA-RR, and in addition the phosphate exchange experiments have confirmed that $CheZ_{cj}$ can remove phosphate from the CheA-RR-P domain. Nevertheless, a role for the phosphorylated RR domain of CheA in the chemotaxis signalling pathway of *C. jejuni* still needs to be further investigated by e.g determining chemotaxis phenotypes of RR mutants. Furthermore, the protein-protein interaction experiments have confirmed the interaction between $CheZ_{cj}$ and CheV proteins; however, unlike with CheY and CheA-RR, in the phosphate exchange experiment it was shown that $CheZ_{cj}$ doesn't have a phosphatase activity

on CheV-P. It might be that CheV and $CheZ_{cj}$ can interact but the W domain may prevent the dephosphorylation activity. The exact role of CheV in *C. jejuni* has been debated in earlier work (Bridle, 2007, Ainsworth, 2013) where it was suggested that the phosphorylated CheV regulates the activity of CheB as it removes methyl groups from Tlp. The role of CheV in the chemotaxis pathway transduction still needs investigation. The arguments for CheV playing an adaption role are based upon previous work (Bridle, 2007) and in addition that the CheV homologues in *B. subtlis* and *H. pylori* were demonstrated to play adaption roles (Szurmant et al., 2004, Lam et al., 2010).

Homologues to *E. coli* CheR and CheW have been identified in *C. jejuni,* where CheW is a scaffolding protein connecting Tlps to CheA and where CheR adds methyl groups to Tlp when attractant (ligand) is bound to the receptor; however this has not still formally been proved (Figure 7.1). Therefore when ligand is bound on the receptor the phosphorylation activity of CheY and CheA is down regulated and *C. jejuni* swims smoothly up the gradient.

The phosphorylation *in vitro* experiments have shown that the HK domain can phosphorylate RRs and also it has been shown that the full CheA can preferentially phosphorylate the CheA-RR domain in the competition experiment with CheY (Ainsworth 2013). In addition, the HK domain can transfer phosphate to CheV (Ainsworth 2013). The B2H experiment has shown that CheV interacted with full CheA (Bridle 2007). It may be that the RR domain of full length CheA binds to the W of CheV to regulate activation of CheV. It was observed that the HK domain transferred phosphate to the RRs in the chemotaxis signalling pathway, but it is not known at what rate the full length CheA transfers phosphate to RRs. It is may be true CheA-RR regulates the autophosphorylation of its own HK domain in the presence of other RRs. A similar pathway has been proposed for the RR domain in *H. pylori* (Jimenez-Pearson et al., 2005*).*

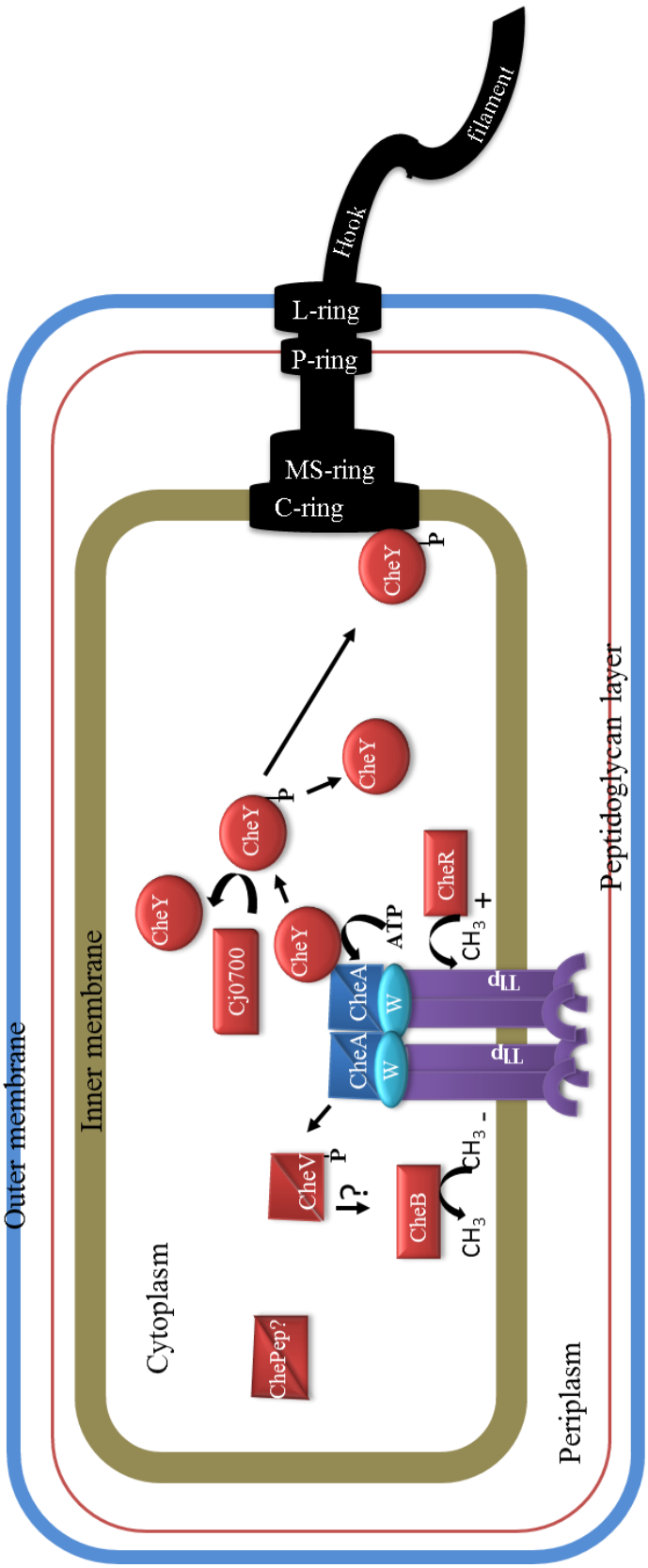

Figure 7.1. Schematic diagram illustrating predicted model of *C. jejuni* signalling pathway. Tlp receptors detect external repellent signal in the form of a ligand or in the absence of attractant. Conformational change of the transmembrane domain results in a ternary complex of the cytoplasmic domain forming receptor-CheW(CheV)-CheA. CheA can phosphorylate itself and transfer P to CheY or CheV. In turn, CheY-P binds to FliM of the flagellum motor and stops the flagellum in order to change the swimming direction. CheA, CheV and ChePep all have additional CheY-like RRs. = inner membrane, = peptidoglycan layer, = outer membrane.

7.4. Proposed future work and implications

Chemotaxis and motility in *C. jejuni* are considered factors that pathogenic and virulent strains employ for detection of attractant/repellent and in addition are used to escape the immune system and peristaltic clearance by the host. It is therefore important to have insights into the biological functions of factors such as flagella and chemotaxis components of *C. jejuni*. A large amount of work has already been carried out with regard to the chemotaxis signalling pathways (Bridle, 2007, Sandhu, 2011 and Ainsworth, 2013) however there still needs further elucidation. In this study much time and effort has been put in to characterise the novel phosphatase protein, $CheZ_{cj}$ in *C. jejuni*. Nevertheless, this work is still not complete and I will propose further investigation that may further improve our understanding of chemotaxis and motility in *C. jejuni*.

7.4.1. Proposed future work for $CheZ_{cj}$

The experiment to determine crystal structure of $CheZ_{cj}$ was unsuccessful and could be explained if it contained disordered regions that could prevent the protein being crystallized.

The predictions of $CheZ_{cj}$ disorder/order structure by the RONN and Phyre^2 software indicated that there are disordered regions in the $CheZ_{cj}$ protein. Failure to crystalize was supported by CD and NMR experiments which demonstrated that $CheZ_{cj}$ protein is structurally disordered which could prevent it being crystalized.

Previous studies have shown that CheZ in *E. coli,* which is a distant homologue of $CheZ_{cj}$, is a chemotaxis phosphatase. The initial attempt to crystallize CheZ of *E. coli* was unsuccessful (Zhao et al., 2002); it was suggested that the reason for this failure was that CheZ contains disordered regions which could have prevented it folding properly into three dimensional structures (Guhaniyogi et al., 2006). Nevertheless, co-crystallization with CheY was successful and showed the crystal structure of CheZ (Silversmith et al., 2008). Other CheZ

like phosphatases, such as CheC, CheX and FliY found in *B. subtilis* and *T. maritima*, have been shown to crystallize (Sircar et al., 2013, Park et al., 2004) without the need to co-crystallize with their RRs. When disorder/order properties were predicted for CheC and CheX, using RONN software, it showed that both proteins were structurally ordered.

The lack of proper folding may be partly explained by the structural similarity between $CheZ_{cj}$ and $CheZ_{ec}$ and supports the hypothesis that $CheZ_{cj}$ is a distant orthologue of CheZ from *E. coli*. Therefore, this study suggests that co-crystallization of $CheZ_{cj}$ with CheY may be possible and through that process the functional properties of $CheZ_{cj}$ may be better elucidated. A crystal structure for the $CheZ_{cj}$ protein is important in order to understand the atomic structure of $CheZ_{cj}$ and also to define the amino acids that interact with the CheY. To achieve a crystal structure of $CheZ_{cj}$ it is suggested that CheY should be phosphorylated by beryllium fluoride (BeF_3) without CheA-HK involvement. In addition, it has been suggested that the 167D/171Q residues of $CheZ_{cj}$ may have catalytic activity on CheY. If it is true mutating these 167D/171Q residues may affect the co-crystallization or the binding interaction between CheZ and CheY. Also, it may be possible that the 167D/171Q residues play catalytic activity in CheA-RR and CheV without W domain. It is very important to understand in detail the amino acid residues involved in interactions between CheZ and RRs, because knowing that would make possible the designed a small molecule inhibitors that would specifically disrupt *C. jejuni* chemotaxis and therefore colonisation.

Due to the time constraints during this work we were unable to do all of the desired complementation tests, such as putting copies of *hp0170* or *cheZ,* from *H. pylori* and *E .coli* respectively, *in trans* in a *C. jejuni* Δ$cheZ_{cj}$ strain. This complementation is to investigate if *cheZ* and *hp0170* could restore a wild type phenotype in a *C. jejuni* Δ*cj0700* strain. Equally, placing a complementing copy of *cj0700* into *E. coli* Δ*cheZ* would be a very worthwhile test. Restoration of wild type phenotypes of *cheZ*, *hp0170* and *cj0700* mutants by use of a foreign

phosphatase may be interpreted as demonstrating how well the chemotaxis phosphatases are functionally conserved cross the bacterial species.

The kinetic properties of $CheZ_{cj}$ such as the rate of phosphate release by $CheZ_{cj}$ can be visualized by employing the EnZChek® phosphate assay. With this assay CheY is steadily phosphorylated by a small phosphate donor, monophosphoimidazole (MPI). Subsequently the action of the $CheZ_{cj}$ will be assessed by the rate at which CheY-P is removed. This methodology has been used previously to investigate CheZ in *E. coli* and $CheZ_{hp}$ in *H. pylori* (Silversmith et al., 2001, Lertsethtakarn and Ottemann, 2010).

7.4.2. ChePep

The ChePep protein was originally identified in *H. pylori* and the identified *chePep* gene of *C. jejuni* has been shown to complement *H. pylori* Δ*chePep*. The *chePep* mutant strain showed a slight reduction in swarming (Howitt et al., 2011) however as yet its role in chemotaxis in *C. jejuni* has not been investigated. It has been speculated to be unique in *Epsilonproteobacteria* and is part of regulatory system in chemotaxis signalling pathway (Howitt et al., 2011). Thus an investigation of ChePep is required and this may provide information to aid a better modelling of the chemotaxis pathway of *C. jejuni*. This would be achieved by creating mutants, complementing these strains and subsequently testing their phenotype. In addition, protein-protein interaction of ChePep with the rest of the chemotactic proteins, flagella and Tlps can be investigated.

7.4.3. CheV and CheB

To date the role of CheB in the chemotaxis signalling system of *C. jejuni* is not clear. As was earlier identified by Parkhill et al. (2000) the *C. jejuni* CheB protein doesn't have an RR domain like the CheB in *E. coli*, but it has close homology with a methyl esterase. It has been

suggested that CheB could be part of an adaptation pathway in *C. jejuni* (Bridle, 2007, Sandhu, 2011 and Ainsworth, 2013) however how CheB and CheR are regulated in the chemotaxis pathway is important and needs to be elucidated. Equally, CheV in *C. jejuni* is the hybrid of a CheW domain and a RR domain however its role is also yet to be elucidated. It has been suggested that the additional CheW domain prevents phosphatase from removing phosphate from the RR domain (Alexander et al., 2010). In the future, it may be useful to express the RR domain of CheV separately and to investigate if $CheZ_{cj}$ has a phosphatase activity on CheV-RR-P not present with the intact CheV-P.

7.4.4. Implications of this investigation

In comparison to *E. coli* and the other model systems a great time and effort have been put into this research in order to explain and model the chemotaxis signalling pathway of *C. jejuni*. The worldwide public health burden related to *C. jejuni* infections is significant and in addition individuals diagnosed with post-infection symptoms are being increasingly identified. Prevention is better than cure for *C. jejuni* infections, thus understanding the sources of transmission is essential. In addition, in order to prevent *C. jejuni* infection, it is useful to understand the factors required by the *C. jejuni* to thrive and survive in the host's intestinal environment. Chemotaxis and motility have been implicated as virulence factors for *C. jejuni*. It was an important achievement confirming $CheZ_{cj}$ protein as a chemotaxis phosphatase because it may have an essential role for *C. jejuni* in colonization and invasion. Likewise, having insight into the biological functions of chemotaxis proteins will enable us to develop methods to reduce the potential risks of *C. jejuni*. For instance, by designing drugs that may block key chemotactic proteins such as CheA, CheY and $CheZ_{cj}$ it may be possible to reduce colonization and invasion in humans by *C. jejuni*. Impairment of the function of the chemotactic proteins may affect chemotaxis and therefore motility of *C. jejuni* in mucus layer

and then the host's immune system may be better capable to clear the organism from the system.

APPENDIX

Results of mass spectrometry against His-Cj0700

Q0PAH9, **Mass (M_r): 26007, Score: 2156, Sequence Coverage: 85%.**
Queries matched: 111. Matched peptides shown in Bold Red.

1 MTQEELDALM NGDVDLDSET EAEVK**TEESN TEEDALMLED VKIADYKPNP**
51 SVVWPPPPPN QEHKVVHQLD DVTKDSELKA TEMMDKLESI NNFFADSESL
101 LKEINKAIEK NIDIFSKLNE KFPNVESFSE ALELNNQAKK SSK**EIVGNLQ**
151 SGQDEVMMAM DAMQYQDIHR QKIERVINVM RALSR**YMSSL FEGKIDDK**KR
201 VSSAVHIEGD STADVVSNDD IEALIASLGQ K

Mr(expt)	Mr(calc)	ppm	Score	Peptide
672.3918	672.3918	-0.12	24	R.QKIER.V
730.4160	730.4160	0.02	50	R.VINVMR.A
746.4107	746.4109	-0.19	(45)	R.VINVMR.A
835.4439	835.4440	-0.01	38	K.NIDIFSK.L
943.5341	943.5338	0.31	1	K.EINKAIEK.N
1076.4846	1076.4848	-0.23	62	R.YMSSLFEGK.I
1152.6139	1152.6139	-0.00	53	K.VVHQLDDVTK.D
1428.6115	1428.6112	0.23	40	K.DSELKATEMMDK.L
1547.7186	1547.7177	0.56	12	R.YMSSLFEGKIDDK.K
1724.8941	1724.8945	-0.20	72	K.VVHQLDDVTKDSELK.A
1825.9106	1825.9098	0.48	70	K.LESINNFFADSESLLK.E
1951.8571	1951.8568	0.18	(38)	K.TEESNTEEDALMLEDVK.I
1967.8524	1967.8517	0.34	92	K.TEESNTEEDALMLEDVK.I
2035.9859	2035.9850	0.43	98	K.FPNVESFSEALELNNQAK.K
2164.0830	2164.0800	1.40	21	K.FPNVESFSEALELNNQAKK.S
2509.2769	2509.2754	0.62	33	K.IADYKPNPSVVWPPPPPNQEHK.V
2520.2514	2520.2496	0.71	77	K.LNEKFPNVESFSEALELNNQAK.K
2648.2348	2648.2349	-0.06	(8)	K.ATEMMDKLESINNFFADSESLLK.E
2664.2296	2664.2298	-0.10	96	K.ATEMMDKLESINNFFADSESLLK.E
3108.3466	3108.3773	-9.88	(10)	K.EIVGNLQSGQDEVMMAMDAMQYQDIHR.Q
3139.5532	3139.5521	0.37	51	R.VSSAVHIEGDSTADVVSNDDIEALIASLGQK.-
3156.3645	3156.3620	0.78	(8)	K.EIVGNLQSGQDEVMMAMDAMQYQDIHR.Q
3172.3605	3172.3570	1.13	31	K.EIVGNLQSGQDEVMMAMDAMQYQDIHR.Q
3236.5129	3236.5104	0.76	11	K.DSELKATEMMDKLESINNFFADSESLLK.E

REFERENCES

Ainsworth, P. 2013. Chemotaxis signal transduction in *Campylobacter jejuni*. PhD, University of Leicester.

Alexander, R. P., Lowenthal, A. C., Harshey, R. M. & Ottemann, K. M. 2010. CheV: CheW-like coupling proteins at the core of the chemotaxis signaling network. *Trends Microbiol,* 18**,** 494-503.

Altekruse, S. F., Stern, N. J., Fields, P. I. & Swerdlow, D. L. 1999. *Campylobacter jejuni*--an emerging foodborne pathogen. *Emerg Infect Dis,* 5**,** 28-35.

Ames, P., Studdert, C. A., Reiser, R. H. & Parkinson, J. S. 2002. Collaborative signaling by mixed chemoreceptor teams in *Escherichia coli*. *Proc Natl Acad Sci U S A,* 99**,** 7060-5.

Apel, D., Ellermeier, J., Pryjma, M., Dirita, V. J. & Gaynor, E. C. 2012. Characterization of *Campylobacter jejuni* RacRS reveals roles in the heat shock response, motility, and maintenance of cell length homogeneity. *J Bacteriol,* 194**,** 2342-54.

Appleby, J. L. & Bourret, R. B. 1998. Proposed signal transduction role for conserved CheY residue Thr87, a member of the response regulator active-site quintet. *Journal of Bacteriology,* 180**,** 3563-3569.

Backert, S. & Hofreuter, D. 2013. Molecular methods to investigate adhesion, transmigration, invasion and intracellular survival of the foodborne pathogen *Campylobacter jejuni*. *J Microbiol Methods,* 95**,** 8-23.

Baker, M. D., Wolanin, P. M. & Stock, J. B. 2006. Signal transduction in bacterial chemotaxis. *Bioessays,* 28**,** 9-22.

Balaban, M. & Hendrixson, D. R. 2011. Polar flagellar biosynthesis and a regulator of flagellar number influence spatial parameters of cell division in *Campylobacter jejuni*. *PLoS Pathog,* 7**,** e1002420.

Baserisalehi, M. & Bahador, N. 2011. Chemotactic behavior of *Campylobacter* spp. in function of different temperatures (37 degrees C and 42 degrees C). *Anaerobe,* 17**,** 459-62.

Battesti, A. & Bouveret, E. 2012a. The bacterial two-hybrid system based on adenylate cyclase reconstitution in *Escherichia coli*. *Methods,* 58**,** 325-34.

Battesti, A. & Bouveret, E. 2012b. The bacterial two-hybrid system based on adenylate cyclase reconstitution in *Escherichia coli*. *Methods,* 58**,** 325-334.

Bayliss, C. D., Bidmos, F. A., Anjum, A., Manchev, V. T., Richards, R. L., Grossier, J. P., Wooldridge, K. G., Ketley, J. M., Barrow, P. A., Jones, M. A. & Tretyakov, M. V. 2012. Phase variable genes of *Campylobacter jejuni* exhibit high mutation rates and specific mutational patterns but mutability is not the major determinant of population structure during host colonization. *Nucleic Acids Res,* 40**,** 5876-89.

Black, W. P., Schubot, F. D., Li, Z. & Yang, Z. 2010. Phosphorylation and dephosphorylation among Dif chemosensory proteins essential for exopolysaccharide regulation in *Myxococcus xanthus*. *J Bacteriol,* 192**,** 4267-74.

Blat, Y. & Eisenbach, M. 1996a. Conserved C-terminus of the phosphatase CheZ is a binding domain for the chemotactic response regulator CheY. *Biochemistry,* 35**,** 5679-5683.

Blat, Y. & Eisenbach, M. 1996b. Oligomerization of the phosphatase CheZ upon interaction with the phosphorylated form of CheY. The signal protein of bacterial chemotaxis. *J Biol Chem,* 271**,** 1226-31.

Boesch, K. C., Silversmith, R. E. & Bourret, R. B. 2000. Isolation and characterization of nonchemotactic CheZ mutants of *Escherichia coli*. *J Bacteriol,* 182**,** 3544-52.

Boin, M. A., Austin, M. J. & Hase, C. C. 2004. Chemotaxis in Vibrio cholerae. *FEMS Microbiol Lett,* 239**,** 1-8.

Bras, A. M., Chatterjee, S., Wren, B. W., Newell, D. G. & Ketley, J. M. 1999. A novel *Campylobacter jejuni* two-component regulatory system important for temperature-dependent growth and colonization. *J Bacteriol,* 181**,** 3298-302.

Bren, A. & Eisenbach, M. 2000. How signals are heard during bacterial chemotaxis: Protein-protein interactions in sensory signal propagation. *Journal of Bacteriology,* 182**,** 6865-6873.

Bren, A. & Eisenbach, M. 2001. Changing the direction of flagellar rotation in bacteria by modulating the ratio between the rotational states of the switch protein FliM. *J Mol Biol,* 312**,** 699-709.

Brondsted, L., Andersen, M. T., Parker, M., Jorgensen, K. & Ingmer, H. 2005. The HtrA protease of *Campylobacter jejuni* is required for heat and oxygen tolerance and for optimal interaction with human epithelial cells. *Appl Environ Microbiol,* 71**,** 3205-12.

Bui, X. T., Qvortrup, K., Wolff, A., Bang, D. D. & Creuzenet, C. 2012. Effect of environmental stress factors on the uptake and survival of *Campylobacter jejuni* in Acanthamoeba castellanii. *BMC Microbiol,* 12**,** 232.

Bukowska, M. A. & Gruetter, M. G. 2013. New concepts and aids to facilitate crystallization. *Current Opinion in Structural Biology,* 23**,** 409-416.

Burkart, M., Toguchi, A. & Harshey, R. M. 1998. The chemotaxis system, but not chemotaxis, is essential for swarming motility in *Escherichia coli*. *Proc Natl Acad Sci U S A,* 95**,** 2568-73.

Butcher, J. & Stintzi, A. 2013. The transcriptional landscape of *Campylobacter jejuni* under iron replete and iron limited growth conditions. *PLoS One,* 8**,** e79475.

Butler, S. M. & Camilli, A. 2004. Both chemotaxis and net motility greatly influence the infectivity of *Vibrio cholerae*. *Proc Natl Acad Sci U S A,* 101**,** 5018-23.

Butzler, J. P. 2004. *Campylobacter*, from obscurity to celebrity. *Clin Microbiol Infect,* 10**,** 868-76.

Capra, E. J. & Laub, M. T. 2012. Evolution of two-component signal transduction systems. *Annu Rev Microbiol,* 66**,** 325-47.

Chen, S., Beeby, M., Murphy, G. E., Leadbetter, J. R., Hendrixson, D. R., Briegel, A., Li, Z., Shi, J., Tocheva, E. I., Muller, A., Dobro, M. J. & Jensen, G. J. 2011. Structural diversity of bacterial flagellar motors. *Embo j,* 30**,** 2972-81.

Claudia Matz, A. H. M. v. V., Julian M. Ketley 2002. Mutational and transcriptional analysis of the *Campylobacter jejuni* flagellar biosynthesis gene flhB.

Clausznitzer, D., Oleksiuk, O., Lovdok, L., Sourjik, V. & Endres, R. G. 2010. Chemotactic response and adaptation dynamics in *Escherichia coli*. *PLoS Comput Biol,* 6**,** e1000784.

Collins, M. O., Yu, L., Campuzano, I., Grant, S. G. & Choudhary, J. S. 2008. Phosphoproteomic analysis of the mouse brain cytosol reveals a predominance of protein phosphorylation in regions of intrinsic sequence disorder. *Mol Cell Proteomics,* 7**,** 1331-48.

Crowe, J., Dobeli, H., Gentz, R., Hochuli, E., Stuber, D. & Henco, K. 1994. 6xHis-Ni-NTA chromatography as a superior technique in recombinant protein expression/purification. *Methods Mol Biol,* 31**,** 371-87.

Croze, O. A., Ferguson, G. P., Cates, M. E. & Poon, W. C. 2011. Migration of chemotactic bacteria in soft agar: role of gel concentration. *Biophys J,* 101**,** 525-34.

Dasti, J. I., Tareen, A. M., Lugert, R., Zautner, A. E. & Gross, U. 2010. *Campylobacter jejuni:* a brief overview on pathogenicity-associated factors and disease-mediating mechanisms. *Int J Med Microbiol,* 300**,** 205-11.

Day, C. J., Semchenko, E. A. & Korolik, V. 2012. Glycoconjugates play a key role in *Campylobacter jejuni* Infection: interactions between host and pathogen. *Front Cell Infect Microbiol,* 2**,** 9.

Day, C. J., Tiralongo, J., Hartnell, R. D., Logue, C. A., Wilson, J. C., Von Itzstein, M. & Korolik, V. 2009. Differential carbohydrate recognition by *Campylobacter jejuni* strain 11168: influences of temperature and growth conditions. *PLoS One,* 4**,** e4927.

Dyson, H. J. & Wright, P. E. 2005. Intrinsically unstructured proteins and their functions. *Nat Rev Mol Cell Biol,* 6**,** 197-208.

Eisenbach, M. 1996. Control of bacterial chemotaxis. *Mol Microbiol,* 20**,** 903-10.

Eisenbach, M. 2001. Bacterial Chemotaxis. *eLS.* John Wiley & Sons, Ltd.

Fahmy, D., Day, C. J. & Korolik, V. 2012. Comparative in silico analysis of chemotaxis system of *Campylobacter fetus*. *Arch Microbiol,* 194**,** 57-63.

Falke, J. J. 2002. Cooperativity between bacterial chemotaxis receptors. *Proc Natl Acad Sci U S A,* 99**,** 6530-2.

Falke, J. J., Bass, R. B., Butler, S. L., Chervitz, S. A. & Danielson, M. A. 1997. The two-component signaling pathway of bacterial chemotaxis: a molecular view of signal transduction by receptors, kinases, and adaptation enzymes. *Annu Rev Cell Dev Biol,* 13**,** 457-512.

Ferron, F., Longhi, S., Canard, B. & Karlin, D. 2006. A practical overview of protein disorder prediction methods. *Proteins,* 65**,** 1-14.

Flanagan, R. C., Neal-Mckinney, J. M., Dhillon, A. S., Miller, W. G. & Konkel, M. E. 2009. Examination of *Campylobacter jejuni* putative adhesins leads to the identification of a new protein, designated FlpA, required for chicken colonization. *Infect Immun,* 77**,** 2399-407.

Fouts, D. E., Mongodin, E. F., Mandrell, R. E., Miller, W. G., Rasko, D. A., Ravel, J., Brinkac, L. M., Deboy, R. T., Parker, C. T., Daugherty, S. C., Dodson, R. J., Durkin, A. S., Madupu, R., Sullivan, S. A., Shetty, J. U., Ayodeji, M. A., Shvartsbeyn, A., Schatz, M. C., Badger, J. H., Fraser, C. M. & Nelson, K. E. 2005. Major structural differences and novel potential virulence mechanisms from the genomes of multiple *Campylobacter* species. *PLoS Biol,* 3**,** e15.

Fredrick, K. L. & Helmann, J. D. 1994. Dual chemotaxis signaling pathways in *Bacillus subtilis:* a sigma D-dependent gene encodes a novel protein with both CheW and CheY homologous domains. *J Bacteriol,* 176**,** 2727-35.

Galindo, M. A., Day, W. A., Raphael, B. H. & Joens, L. A. 2001. Cloning and characterization of a *Campylobacter jejuni* iron-uptake operon. *Curr Microbiol,* 42**,** 139-43.

Garenaux, A., Jugiau, F., Rama, F., De Jonge, R., Denis, M., Federighi, M. & Ritz, M. 2008. Survival of *Campylobacter jejuni* strains from different origins under oxidative stress conditions: effect of temperature. *Curr Microbiol,* 56**,** 293-7.

Garrity, L. F. & Ordal, G. W. 1995. Chemotaxis in *Bacillus subtilis*: how bacteria monitor environmental signals. *Pharmacol Ther,* 68**,** 87-104.

Glekas, G. D., Plutz, M. J., Walukiewicz, H. E., Allen, G. M., Rao, C. V. & Ordal, G. W. 2012. Elucidation of the multiple roles of CheD in *Bacillus subtilis* chemotaxis. *Mol Microbiol,* 86**,** 743-56.

Guccione, E., Leon-Kempis Mdel, R., Pearson, B. M., Hitchin, E., Mulholland, F., Van Diemen, P. M., Stevens, M. P. & Kelly, D. J. 2008. Amino acid-dependent growth of *Campylobacter jejuni*: key roles for aspartase (AspA) under microaerobic and oxygen-limited conditions and identification of AspB (Cj0762), essential for growth on glutamate. *Mol Microbiol,* 69**,** 77-93.

Guerry, P. 2007. *Campylobacter* flagella: not just for motility. *Trends Microbiol,* 15**,** 456-61.

Guerry, P., Ewing, C. P., Schirm, M., Lorenzo, M., Kelly, J., Pattarini, D., Majam, G., Thibault, P. & Logan, S. 2006. Changes in flagellin glycosylation affect *Campylobacter* autoagglutination and virulence. *Mol Microbiol,* 60**,** 299-311.

Guhaniyogi, J., Robinson, V. L. & Stock, A. M. 2006. Crystal structures of beryllium fluoride-free and beryllium fluoride-bound CheY in complex with the conserved C-terminal peptide of CheZ reveal dual binding modes specific to CheY conformation. *J Mol Biol,* 359**,** 624-45.

Guhaniyogi, J., Wu, T., Patel, S. S. & Stock, A. M. 2008a. Interaction of CheY with the C-terminal peptide of CheZ. *Journal of Bacteriology,* 190**,** 1419-1428.

Guhaniyogi, J., Wu, T., Patel, S. S. & Stock, A. M. 2008b. Interaction of CheY with the C-terminal peptide of CheZ. *J Bacteriol,* 190**,** 1419-28.

Guo, J., Li, H., Chang, J.-W., Lei, Y., Li, S. & Chen, L.-L. 2013. Prediction and characterization of protein-protein interaction network in *Xanthomonas oryzae* pv. oryzae PXO99(A.). *Research in microbiology,* 164**,** 1035-44.

Hansen, C. H., Endres, R. G. & Wingreen, N. S. 2008. Chemotaxis in *Escherichia coli*: a molecular model for robust precise adaptation. *PLoS Comput Biol,* 4**,** e1.

Harrington, C. S., Thomson-Carter, F. M. & Carter, P. E. 1997. Evidence for recombination in the flagellin locus of *Campylobacter jejuni*: implications for the flagellin gene typing scheme. *J Clin Microbiol,* 35**,** 2386-92.

Harshey, R. M. 2003. Bacterial motility on a surface: many ways to a common goal. *Annu Rev Microbiol,* 57**,** 249-73.

Hartley-Tassell, L. E., Shewell, L. K., Day, C. J., Wilson, J. C., Sandhu, R., Ketley, J. M. & Korolik, V. 2010a. Identification and characterization of the aspartate chemosensory receptor of *Campylobacter jejuni*. *Mol Microbiol,* 75**,** 710-30.

Hartley-Tassell, L. E., Shewell, L. K., Day, C. J., Wilson, J. C., Sandhu, R., Ketley, J. M. & Korolik, V. 2010b. Identification and characterization of the aspartate chemosensory receptor of *Campylobacter jejuni*. *Molecular Microbiology,* 75**,** 710-730.

Hatzios, S. K., Ringgaard, S., Davis, B. M. & Waldor, M. K. 2012. Studies of Dynamic Protein-Protein Interactions in Bacteria Using Renilla Luciferase Complementation Are Undermined by Nonspecific Enzyme Inhibition. *Plos One,* 7.

Helmann, K. l. F. a. j. d. 1994. novel protein with both CheW and CheY subtilis: a sigma D-dependent gene encodes a Dual chemotaxis signaling pathways in *Bacillus* homologous domains. *Journal of bacteriology,* 176**.,** 2727-2735

Hermans, D., Van Deun, K., Martel, A., Van Immerseel, F., Messens, W., Heyndrickx, M., Haesebrouck, F. & Pasmans, F. 2011. Colonization factors of *Campylobacter jejuni* in the chicken gut. *Vet Res,* 42**,** 82.

Hofreuter, D., Tsai, J., Watson, R. O., Novik, V., Altman, B., Benitez, M., Clark, C., Perbost, C., Jarvie, T., Du, L. & Galan, J. E. 2006. Unique features of a highly pathogenic *Campylobacter jejuni* strain. *Infect Immun,* 74**,** 4694-707.

Howitt, M. R., Lee, J. Y., Lertsethtakarn, P., Vogelmann, R., Joubert, L. M., Ottemann, K. M. & Amieva, M. R. 2011. ChePep controls *Helicobacter pylori* Infection of the gastric glands and chemotaxis in the *Epsilonproteobacteria*. *MBio,* 2.

Inclan, Y. F., Laurent, S. & Zusman, D. R. 2008. The receiver domain of FrzE, a CheA-CheY fusion protein, regulates the CheA histidine kinase activity and downstream signalling to the A- and S-motility systems of *Myxococcus xanthus*. *Mol Microbiol,* 68**,** 1328-39.

Jackson, D. N., Davis, B., Tirado, S. M., Duggal, M., Van Frankenhuyzen, J. K., Deaville, D., Wijesinghe, M. A., Tessaro, M. & Trevors, J. T. 2009. Survival mechanisms and culturability of *Campylobacter jejuni* under stress conditions. *Antonie Van Leeuwenhoek,* 96**,** 377-94.

Javed, M. A., Cawthraw, S. A., Baig, A., Li, J., Mcnally, A., Oldfield, N. J., Newell, D. G. & Manning, G. 2012. Cj1136 is required for lipooligosaccharide biosynthesis, hyperinvasion, and chick colonization by *Campylobacter jejuni*. *Infect Immun,* 80**,** 2361-70.

Jimenez-Pearson, M. A., Delany, I., Scarlato, V. & Beier, D. 2005. Phosphate flow in the chemotactic response system of *Helicobacter pylori*. *Microbiology,* 151**,** 3299-311.

Josenhans, C. & Suerbaum, S. 2002. The role of motility as a virulence factor in bacteria. *Int J Med Microbiol,* 291**,** 605-14.

Kanungpean, D., Kakuda, T. & Takai, S. 2011a. False positive responses of *Campylobacter jejuni* when using the chemical-in-plug chemotaxis assay. *J Vet Med Sci,* 73**,** 389-91.

Kanungpean, D., Kakuda, T. & Takai, S. 2011b. Participation of CheR and CheB in the chemosensory response of *Campylobacter jejuni*. *Microbiology,* 157**,** 1279-89.

Karatan, E., Saulmon, M. M., Bunn, M. W. & Ordal, G. W. 2001. Phosphorylation of the response regulator CheV is required for adaptation to attractants during *Bacillus subtilis* chemotaxis. *J Biol Chem,* 276**,** 43618-26.

Karimova, G., Pidoux, J., Ullmann, A. & Ladant, D. 1998. A bacterial two-hybrid system based on a reconstituted signal transduction pathway. *Proc Natl Acad Sci U S A,* 95**,** 5752-6.

Karlyshev, A. V. & Wren, B. W. 2005. Development and application of an insertional system for gene delivery and expression in *Campylobacter jejuni*. *Appl Environ Microbiol,* 71**,** 4004-13.

Kelley, L. A. & Sternberg, M. J. 2009. Protein structure prediction on the Web: a case study using the Phyre server. *Nat Protoc,* 4**,** 363-71.

Kelly, D. J. 2001. The physiology and metabolism of *Campylobacter jejuni* and *Helicobacter pylori*. *Symp Ser Soc Appl Microbiol***,** 16S-24S.

Kentner, D. & Sourjik, V. 2006. Spatial organization of the bacterial chemotaxis system. *Curr Opin Microbiol,* 9**,** 619-24.

Ketley, J. M. 1997. Pathogenesis of enteric infection by *Campylobacter*. *Microbiology,* 143 (Pt 1)**,** 5-21.

Kim, J. S., Li, J., Barnes, I. H., Baltzegar, D. A., Pajaniappan, M., Cullen, T. W., Trent, M. S., Burns, C. M. & Thompson, S. A. 2008. Role of the *Campylobacter jejuni* Cj1461 DNA methyltransferase in regulating virulence characteristics. *J Bacteriol,* 190**,** 6524-9.

Kirby, J. R. 2009. Chemotaxis-like regulatory systems: unique roles in diverse bacteria. *Annu Rev Microbiol,* 63**,** 45-59.

Konkel, M. E., Christensen, J. E., Keech, A. M., Monteville, M. R., Klena, J. D. & Garvis, S. G. 2005. Identification of a fibronectin-binding domain within the *Campylobacter jejuni* CadF protein. *Mol Microbiol,* 57**,** 1022-35.

Konkel, M. E., Klena, J. D., Rivera-Amill, V., Monteville, M. R., Biswas, D., Raphael, B. & Mickelson, J. 2004. Secretion of virulence proteins from *Campylobacter jejuni* is dependent on a functional flagellar export apparatus. *J Bacteriol,* 186**,** 3296-303.

Konkel, M. E., Larson, C. L. & Flanagan, R. C. 2010. *Campylobacter jejuni* FlpA binds fibronectin and is required for maximal host cell adherence. *J Bacteriol,* 192**,** 68-76.

Korolik, V. 2010a. Aspartate chemosensory receptor signalling in *Campylobacter jejuni*. *Virulence,* 1**,** 414-7.

Korolik, V. 2010b. Aspartate chemosensory receptor signalling in *Campylobacter jejuni*. *Virulence,* 1**,** 414-417.

Korolik, V., Ketley , J. 2008. Chemosensory Singnal Transduction Pathway of *Campylobacter jejuni In:* I. Nachamkin (ed.) *Campylobacter (3rd Edition).* Washington, DC, USA: ASM Press.

Kumar-Phillips, G. S., Hanning, I. & Slavik, M. 2013. Influence of acid-adaptation of *Campylobacter jejuni* on adhesion and invasion of INT 407 cells. *Foodborne Pathog Dis,* 10**,** 1037-43.

Lam, K. H., Ling, T. K. & Au, S. W. 2010. Crystal structure of activated CheY1 from *Helicobacter pylori*. *J Bacteriol,* 192**,** 2324-34.

Lee, A., O'rourke, J. L., Barrington, P. J. & Trust, T. J. 1986. Mucus colonization as a determinant of pathogenicity in intestinal infection by *Campylobacter jejuni*: a mouse cecal model. *Infect Immun,* 51**,** 536-46.

Lertpiriyapong, K., Gamazon, E. R., Feng, Y., Park, D. S., Pang, J., Botka, G., Graffam, M. E., Ge, Z. & Fox, J. G. 2012. *Campylobacter jejuni* type VI secretion system:

roles in adaptation to deoxycholic acid, host cell adherence, invasion, and in vivo colonization. *PLoS One,* 7**,** e42842.

Lertsethtakarn, P. & Ottemann, K. M. 2010. A remote CheZ orthologue retains phosphatase function. *Mol Microbiol,* 77**,** 225-35.

Levit, M. N., Grebe, T. W. & Stock, J. B. 2002. Organization of the receptor-kinase signaling array that regulates *Escherichia coli* chemotaxis. *J Biol Chem,* 277**,** 36748-54.

Linton, D., Gilbert, M., Hitchen, P. G., Dell, A., Morris, H. R., Wakarchuk, W. W., Gregson, N. A. & Wren, B. W. 2000. Phase variation of a beta-1,3 galactosyltransferase involved in generation of the ganglioside GM1-like lipo-oligosaccharide of *Campylobacter jejuni*. *Mol Microbiol,* 37**,** 501-14.

Lipkow, K. 2006. Changing cellular location of CheZ predicted by molecular simulations. *PLoS Comput Biol,* 2**,** e39.

Louwen, R., Heikema, A., Van Belkum, A., Ott, A., Gilbert, M., Ang, W., Endtz, H. P., Bergman, M. P. & Nieuwenhuis, E. E. 2008. The sialylated lipooligosaccharide outer core in *Campylobacter jejuni* is an important determinant for epithelial cell invasion. *Infect Immun,* 76**,** 4431-8.

Louwen, R., Nieuwenhuis, E. E., Van Marrewijk, L., Horst-Kreft, D., De Ruiter, L., Heikema, A. P., Van Wamel, W. J., Wagenaar, J. A., Endtz, H. P., Samsom, J., Van Baarlen, P., Akhmanova, A. & Van Belkum, A. 2012. *Campylobacter jejuni* translocation across intestinal epithelial cells is facilitated by ganglioside-like lipooligosaccharide structures. *Infect Immun,* 80**,** 3307-18.

Lowenthal, A. C., Hill, M., Sycuro, L. K., Mehmood, K., Salama, N. R. & Ottemann, K. M. 2009a. Functional analysis of the *Helicobacter pylori* flagellar switch proteins. *J Bacteriol,* 191**,** 7147-56.

Lowenthal, A. C., Simon, C., Fair, A. S., Mehmood, K., Terry, K., Anastasia, S. & Ottemann, K. M. 2009b. A fixed-time diffusion analysis method determines that the three cheV genes of *Helicobacter pylori* differentially affect motility. *Microbiology,* 155**,** 1181-91.

Lux, R. & Shi, W. 2004. Chemotaxis-Guided Movements in Bacteria. *Critical Reviews in Oral Biology & Medicine,* 15**,** 207-220.

Mackichan, J. K., Gaynor, E. C., Chang, C., Cawthraw, S., Newell, D. G., Miller, J. F. & Falkow, S. 2004. The *Campylobacter jejuni* dccRS two-component system is required for optimal in vivo colonization but is dispensable for in vitro growth. *Mol Microbiol,* 54**,** 1269-86.

Marais, A., Mendz, G. L., Hazell, S. L. & Megraud, F. 1999. Metabolism and genetics of *Helicobacter pylori*: the genome era. *Microbiol Mol Biol Rev,* 63**,** 642-74.

Marchant, J., Wren, B. & Ketley, J. 2002a. Exploiting genome sequence: predictions for mechanisms of *Campylobacter* chemotaxis. *Trends Microbiol,* 10**,** 155-9.

Marchant, J., Wren, B. & Ketley, J. 2002b. Exploiting genome sequence: predictions for mechanisms of *Campylobacter* chemotaxis. *Trends in Microbiology,* 10**,** 155-159.

Mcnamara, B. P. & Wolfe, A. J. 1997. Coexpression of the long and short forms of CheA, the chemotaxis histidine kinase, by members of the family *Enterobacteriaceae*. *J Bacteriol,* 179**,** 1813-8.

Meier, V. M., Muschler, P. & Scharf, B. E. 2007. Functional analysis of nine putative chemoreceptor proteins in *Sinorhizobium meliloti*. *J Bacteriol,* 189**,** 1816-26.

Meier, V. M. & Scharf, B. E. 2009. Cellular localization of predicted transmembrane and soluble chemoreceptors in *Sinorhizobium meliloti*. *J Bacteriol,* 191**,** 5724-33.

Mendz, G. L., Ball, G. E. & Meek, D. J. 1997. Pyruvate metabolism in *Campylobacter* spp. *Biochim Biophys Acta,* 1334**,** 291-302.

Miller, C. E., Rock, J. D., Ridley, K. A., Williams, P. H. & Ketley, J. M. 2008. Utilization of lactoferrin-bound and transferrin-bound iron by *Campylobacter jejuni*. *J Bacteriol,* 190**,** 1900-11.

Morimoto, Y. V. & Minamino, T. 2014. Structure and function of the bi-directional bacterial flagellar motor. *Biomolecules,* 4**,** 217-34.

Muff, T. J. & Ordal, G. W. 2007. The CheC phosphatase regulates chemotactic adaptation through CheD. *J Biol Chem,* 282**,** 34120-8.

Muff, T. J. & Ordal, G. W. 2008. The diverse CheC-type phosphatases: chemotaxis and beyond. *Molecular Microbiology,* 70**,** 1054-1061.

Muller, J., Meyer, B., Hanel, I. & Hotzel, H. 2007. Comparison of lipooligosaccharide biosynthesis genes of *Campylobacter jejuni* strains with varying abilities to colonize the chicken gut and to invade Caco-2 cells. *J Med Microbiol,* 56**,** 1589-94.

Nachamkin, I., Liu, J., Li, M., Ung, H., Moran, A. P., Prendergast, M. M. & Sheikh, K. 2002. *Campylobacter jejuni* from Patients with Guillain-Barre Syndrome Preferentially Expresses a GD1a-Like Epitope. *Infection and Immunity,* 70**,** 5299-5303.

Neal-Mckinney, J. M., Christensen, J. E. & Konkel, M. E. 2010. Amino-terminal residues dictate the export efficiency of the *Campylobacter jejuni* filament proteins via the flagellum. *Mol Microbiol,* 76**,** 918-31.

Neal-Mckinney, J. M. & Konkel, M. E. 2012. The *Campylobacter jejuni* CiaC virulence protein is secreted from the flagellum and delivered to the cytosol of host cells. *Front Cell Infect Microbiol,* 2**,** 31.

Neumann, S., Hansen, C. H., Wingreen, N. S. & Sourjik, V. 2010. Differences in signalling by directly and indirectly binding ligands in bacterial chemotaxis. *Embo j,* 29**,** 3484-95.

Nguyen, T. N. & Goodrich, J. A. 2006. Protein-protein interaction assays: eliminating false positive interactions. *Nature Methods,* 3**,** 135-139.

Niu, C., Graves, J. D., Mokuolu, F. O., Gilbert, S. E. & Gilbert, E. S. 2005. Enhanced swarming of bacteria on agar plates containing the surfactant Tween 80. *J Microbiol Methods,* 62**,** 129-32.

Ottemann, K. M. & Miller, J. F. 1997. Roles for motility in bacterial-host interactions. *Mol Microbiol,* 24**,** 1109-17.

Page, R., Peti, W., Wilson, I. A., Stevens, R. C. & Wuthrich, K. 2005. NMR screening and crystal quality of bacterially expressed prokaryotic and eukaryotic proteins in a structural genomics pipeline. *Proc Natl Acad Sci U S A,* 102**,** 1901-5.

Park, S. F. 2002. The physiology of *Campylobacter* species and its relevance to their role as foodborne pathogens. *Int J Food Microbiol,* 74**,** 177-88.

Park, S. Y., Chao, X., Gonzalez-Bonet, G., Beel, B. D., Bilwes, A. M. & Crane, B. R. 2004. Structure and function of an unusual family of protein phosphatases: the bacterial chemotaxis proteins CheC and CheX. *Mol Cell,* 16**,** 563-74.

Parker, C. T., Quinones, B., Miller, W. G., Horn, S. T. & Mandrell, R. E. 2006. Comparative genomic analysis of *Campylobacter jejuni* strains reveals diversity due to genomic elements similar to those present in *C. jejuni* strain RM1221. *J Clin Microbiol,* 44**,** 4125-35.

Parkhill, J., Wren, B. W., Mungall, K., Ketley, J. M., Churcher, C., Basham, D., Chillingworth, T., Davies, R. M., Feltwell, T., Holroyd, S., Jagels, K., Karlyshev, A. V., Moule, S., Pallen, M. J., Penn, C. W., Quail, M. A., Rajandream, M. A., Rutherford, K. M., Van Vliet, A. H., Whitehead, S. & Barrell, B. G. 2000. The genome sequence of the food-borne pathogen *Campylobacter jejuni* reveals hypervariable sequences. *Nature,* 403**,** 665-8.

Pazy, Y., Motaleb, M. A., Guarnieri, M. T., Charon, N. W., Zhao, R. & Silversmith, R. E. 2010. Identical phosphatase mechanisms achieved through distinct modes of binding phosphoprotein substrate. *Proc Natl Acad Sci U S A,* 107**,** 1924-9.

Pazy, Y., Wollish, A. C., Thomas, S. A., Miller, P. J., Collins, E. J., Bourret, R. B. & Silversmith, R. E. 2009. Matching biochemical reaction kinetics to the timescales of life: structural determinants that influence the autodephosphorylation rate of response regulator proteins. *J Mol Biol,* 392**,** 1205-20.

Pham, N. D., Parker, R. B. & Kohler, J. J. 2013. Photocrosslinking approaches to interactome mapping. *Curr Opin Chem Biol,* 17**,** 90-101.

Phillips-Mason, P. J., Gates, T. J., Major, D. L., Sacks, D. B. & Brady-Kalnay, S. M. 2006. The receptor protein-tyrosine phosphatase PTP mu interacts with IQGAP1. *Journal of Biological Chemistry,* 281**,** 4903-4910.

Pittman, M. S., Goodwin, M. & Kelly, D. J. 2001. Chemotaxis in the human gastric pathogen *Helicobacter pylori*: different roles for CheW and the three CheV paralogues, and evidence for CheV2 phosphorylation. *Microbiology,* 147**,** 2493-504.

Poli, V. F., Thorsen, L., Olesen, I., Wik, M. T. & Jespersen, L. 2012. Differentiation of the virulence potential of *Campylobacter jejuni* strains by use of gene transcription analysis and a Caco-2 assay. *Int J Food Microbiol,* 155**,** 60-8.

Poly, F. & Guerry, P. 2008. Pathogenesis of *Campylobacter*. *Curr Opin Gastroenterol,* 24**,** 27-31.

Poly, F., Threadgill, D. & Stintzi, A. 2005. Genomic diversity in *Campylobacter jejuni*: identification of *C. jejuni* 81-176-specific genes. *J Clin Microbiol,* 43**,** 2330-8.

Porter, S. L., Wadhams, G. H. & Armitage, J. P. 2008. *Rhodobacter sphaeroides*: complexity in chemotactic signalling. *Trends Microbiol,* 16**,** 251-60.

Porter, S. L., Wadhams, G. H. & Armitage, J. P. 2011. Signal processing in complex chemotaxis pathways. *Nat Rev Microbiol,* 9**,** 153-65.

Rahman, H., King, R. M., Shewell, L. K., Semchenko, E. A., Hartley-Tassell, L. E., Wilson, J. C., Day, C. J. & Korolik, V. 2014. Characterisation of a Multi-ligand Binding Chemoreceptor CcmL (Tlp3) of *Campylobacter jejuni*. *PLoS Pathog,* 10**,** e1003822.

Rao, C. V., Kirby, J. R. & Arkin, A. P. 2005. Phosphatase localization in bacterial chemotaxis: divergent mechanisms, convergent principles. *Phys Biol,* 2**,** 148-58.

Rashid, M. H. & Kornberg, A. 2000. Inorganic polyphosphate is needed for swimming, swarming, and twitching motilities of *Pseudomonas aeruginosa*. *Proc Natl Acad Sci U S A,* 97**,** 4885-90.

Rehm, T., Huber, R. & Holak, T. A. 2002. Application of NMR in structural proteomics: screening for proteins amenable to structural analysis. *Structure,* 10**,** 1613-8.

Renshaw, P. S., Panagiotidou, P., Whelan, A., Gordon, S. V., Hewinson, R. G., Williamson, R. A. & Carr, M. D. 2002. Conclusive evidence that the major T-cell antigens of the *Mycobacterium tuberculosis* complex ESAT-6 and CFP-10 form a tight, 1:1 complex and characterization of the structural properties of ESAT-6, CFP-10, and the ESAT-6*CFP-10 complex. Implications for pathogenesis and virulence. *J Biol Chem,* 277**,** 21598-603.

Rubinchik, S., Seddon, A. & Karlyshev, A. V. 2012. Molecular mechanisms and biological role of attachment to host cells. *Eur J Microbiol Immunol (Bp),* 2**,** 32-40.

Samatey, F. A., Imada, K., Nagashima, S., Vonderviszt, F., Kumasaka, T., Yamamoto, M. & Namba, K. 2001. Structure of the bacterial flagellar protofilament and implications for a switch for supercoiling. *Nature,* 410**,** 331-7.

Sambrook, D. W. R. 2001. *Molecular cloning : a laboratory manual* 3rd ed ed. New York, USA: Cold Spring Harbor Laboratory Press.

Sanatinia, H., Kofoid, E. C., Morrison, T. B. & Parkinson, J. S. 1995. The smaller of two overlapping cheA gene products is not essential for chemotaxis in *Escherichia coli*. *J Bacteriol,* 177**,** 2713-20.

Sandoz, G. & Lesage, F. 2008. Protein complex analysis of native brain potassium channels by proteomics. *Methods in molecular biology (Clifton, N.J.),* 491**,** 113-23.

Schmitt, R. 2002. Sinorhizobial chemotaxis: a departure from the enterobacterial paradigm. *Microbiology,* 148**,** 627-31.

Sellars, M. J., Hall, S. J. & Kelly, D. J. 2002. Growth of *Campylobacter jejuni* supported by respiration of fumarate, nitrate, nitrite, trimethylamine-N-oxide, or dimethyl sulfoxide requires oxygen. *J Bacteriol,* 184**,** 4187-96.

Silversmith, R. E. 2010. Auxiliary phosphatases in two-component signal transduction. *Curr Opin Microbiol,* 13**,** 177-83.

Silversmith, R. E., Guanga, G. P., Betts, L., Chu, C., Zhao, R. & Bourret, R. B. 2003. CheZ-Mediated Dephosphorylation of the *Escherichia coli* Chemotaxis Response Regulator CheY: Role for CheY Glutamate 89. *Journal of Bacteriology,* 185**,** 1495-1502.

Silversmith, R. E., Levin, M. D., Schilling, E. & Bourret, R. B. 2008. Kinetic characterization of catalysis by the chemotaxis phosphatase CheZ. Modulation of activity by the phosphorylated CheY substrate. *J Biol Chem,* 283**,** 756-65.

Silversmith, R. E., Smith, J. G., Guanga, G. P., Les, J. T. & Bourret, R. B. 2001. Alteration of a nonconserved active site residue in the chemotaxis response regulator CheY affects phosphorylation and interaction with CheZ. *J Biol Chem,* 276**,** 18478-84.

Sircar, R., Greenswag, A. R., Bilwes, A. M., Gonzalez-Bonet, G. & Crane, B. R. 2013. Structure and Activity of the Flagellar Rotor Protein FliY A Member of the CheC Phosphatase Family. *Journal of Biological Chemistry,* 288**,** 13493-13502.

Skirrow, M. B. 1977. *Campylobacter enteritis*: a "new" disease. *Br Med J,* 2**,** 9-11.

Sourjik, V. 2004. Receptor clustering and signal processing in *E. coli* chemotaxis. *Trends Microbiol,* 12**,** 569-76.

Sourjik, V. & Schmitt, R. 1998. Phosphotransfer between CheA, CheY1, and CheY2 in the chemotaxis signal transduction chain of *Rhizobium meliloti*. *Biochemistry,* 37**,** 2327-35.

Stahl, M., Butcher, J. & Stintzi, A. 2012. Nutrient acquisition and metabolism by *Campylobacter jejuni*. *Front Cell Infect Microbiol,* 2**,** 5.

Stahl, M., Friis, L. M., Nothaft, H., Liu, X., Li, J., Szymanski, C. M. & Stintzi, A. 2011. L-fucose utilization provides *Campylobacter jejuni* with a competitive advantage. *Proc Natl Acad Sci U S A,* 108**,** 7194-9.

Stef, L., Cean, A., Vasile, A., Julean, C., Drinceanu, D. & Corcionivoschi, N. 2013. Virulence characteristics of five new *Campylobacter jejuni* chicken isolates. *Gut Pathog,* 5**,** 41.

Stock, A. M., Robinson, V. L. & Goudreau, P. N. 2000. Two-component signal transduction. *Annu Rev Biochem,* 69**,** 183-215.

Sweeney, E. G. & Guillemin, K. 2011. A gastric pathogen moves chemotaxis in a new direction. *MBio,* 2.

Szurmant, H., Muff, T. J. & Ordal, G. W. 2004. *Bacillus subtilis* CheC and FliY are members of a novel class of CheY-P-hydrolyzing proteins in the chemotactic signal transduction cascade. *J Biol Chem,* 279**,** 21787-92.

Szurmant, H. & Ordal, G. W. 2004. Diversity in chemotaxis mechanisms among the bacteria and archaea. *Microbiol Mol Biol Rev,* 68**,** 301-19.

Szymanski, C. M., King, M., Haardt, M. & Armstrong, G. D. 1995. *Campylobacter jejuni* motility and invasion of Caco-2 cells. *Infect Immun,* 63**,** 4295-300.

Terry, K., Go, A. C. & Ottemann, K. M. 2006. Proteomic mapping of a suppressor of non-chemotactic cheW mutants reveals that *Helicobacter pylori* contains a new chemotaxis protein. *Mol Microbiol,* 61**,** 871-82.

Thompson, S. A. & Gaynor, E. C. 2008. *Campylobacter jejuni* host tissue tropism: a consequence of its low-carb lifestyle? *Cell Host Microbe,* 4**,** 409-10.

Ueki, S., Lacroix, B. & Citovsky, V. 2011. Protein membrane overlay assay: a protocol to test interaction between soluble and insoluble proteins in vitro. *Journal of visualized experiments : JoVE*.

Van Putten, J. P., Van Alphen, L. B., Wosten, M. M. & De Zoete, M. R. 2009. Molecular mechanisms of *Campylobacter* infection. *Curr Top Microbiol Immunol,* 337**,** 197-229.

Van Vliet, A. H. M. & Ketley, J. M. 2001. Pathogenesis of enteric *Campylobacter* infection. *Journal of Applied Microbiology,* 90**,** 45S-56S.

Vater, S. M., Weisse, S., Maleschlijski, S., Lotz, C., Koschitzki, F., Schwartz, T., Obst, U. & Rosenhahn, A. 2014. Swimming behavior of *Pseudomonas aeruginosa* studied by holographic 3D tracking. *PLoS One,* 9**,** e87765.

Wadhams, G. H. & Armitage, J. P. 2004. Making sense of it all: bacterial chemotaxis. *Nat Rev Mol Cell Biol,* 5**,** 1024-37.

Walhout, A. J., Boulton, S. J. & Vidal, M. 2000. Yeast two-hybrid systems and protein interaction mapping projects for yeast and worm. *Yeast,* 17**,** 88-94.

Wang, X., Vu, A., Lee, K. & Dahlquist, F. W. 2012. CheA-receptor interaction sites in bacterial chemotaxis. *J Mol Biol,* 422**,** 282-90.

Wassenaar, T. M. 1997. Toxin production by *Campylobacter* spp. *Clin Microbiol Rev,* 10**,** 466-76.

Wearne, S. 2013. A refreshed strategy to reduce Campylobacteriosis from poultry.

Weerakoon, D. R., Borden, N. J., Goodson, C. M., Grimes, J. & Olson, J. W. 2009. The role of respiratory donor enzymes in *Campylobacter jejuni* host colonization and physiology. *Microb Pathog,* 47**,** 8-15.

Winer, J. B. 2014. An update in guillain-barre syndrome. *Autoimmune Dis,* 2014**,** 793024.

Wolfe, A. J. & Berg, H. C. 1989. Migration of bacteria in semisolid agar. *Proc Natl Acad Sci U S A,* 86**,** 6973-7.

Wu, Z., Sahin, O., Shen, Z., Liu, P., Miller, W. G. & Zhang, Q. 2013. Multi-omics approaches to deciphering a hypervirulent strain of *Campylobacter jejuni*. *Genome Biol Evol,* 5**,** 2217-30.

Xiangyang Zhu, K. V., and Philip Matsumura 1997. The CheZ-binding Surface of CheY Overlaps the CheA- and FliM-binding Surfaces. *The Journal of Biological Chemistry,* 272**,** 23758–23764.

Yi, T. M., Andrews, B. W. & Iglesias, P. A. 2007. Control analysis of bacterial chemotaxis signaling. *Methods Enzymol,* 422**,** 123-40.

Young, K. T., Davis, L. M. & Dirita, V. J. 2007. *Campylobacter jejuni*: molecular biology and pathogenesis. *Nat Rev Microbiol,* 5**,** 665-79.

Yuan, W., Glekas, G. D., Allen, G. M., Walukiewicz, H. E., Rao, C. V. & Ordal, G. W. 2012. The importance of the interaction of CheD with CheC and the chemoreceptors compared to its enzymatic activity during chemotaxis in *Bacillus subtilis*. *PLoS One,* 7**,** e50689.

Zhao, R., Collins, E. J., Bourret, R. B. & Silversmith, R. E. 2002. Structure and catalytic mechanism of the *E. coli* chemotaxis phosphatase CheZ. *Nat Struct Biol,* 9**,** 570-5.

Zhu, S., Kojima, S. & Homma, M. 2013. Structure, gene regulation and environmental response of flagella in Vibrio. *Front Microbiol,* 4**,** 410.

Zhu, X., Amsler, C. D., Volz, K. & Matsumura, P. 1996. Tyrosine 106 of CheY plays an important role in chemotaxis signal transduction in *Escherichia coli. J Bacteriol,* 178**,** 4208-15.

Zilbauer, M., Dorrell, N., Wren, B. W. & Bajaj-Elliott, M. 2008. *Campylobacter jejuni*-mediated disease pathogenesis: an update. *Trans R Soc Trop Med Hyg,* 102**,** 123-9.